AD-A087 856 SCIENCE APPLICATIONS INC MCLEAN VA F/G 19/4
MISERS BLUFF II CLOUD SAMPLING PROGRAM, DATA SUMMARY AND DUST C--ETC(U)
DEC 79 C R THOMAS, J E COCKAYNE DNA001-78-C-0217
UNCLASSIFIED SAI-80-118-WA DNA-5189F NL

1 OF 2
AD A087856

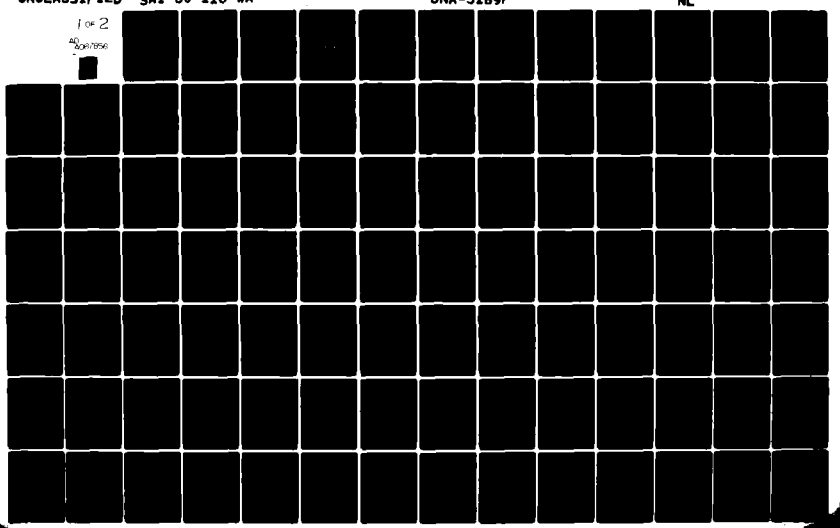

MISERS BLUFF II CLOUD SAMPLING PROGRAM

Data Summary and Dust Cloud Characterizations

Charles R. Thomas
John E. Cockayne
Science Applications, Inc.
8400 Westpark Drive
McLean, Virginia 22102

7 December 1979

Final Report for Period 2 April 1978—30 November 1979

CONTRACT No. DNA 001-78-C-0217

THIS WORK SPONSORED BY THE DEFENSE NUCLEAR AGENCY
UNDER RDT&E RMSS CODE B342079462 H35HAXYX95605 H2590D.

Prepared for
Director
DEFENSE NUCLEAR AGENCY
Washington, D. C. 20305

Destroy this report when it is no longer needed. Do not return to sender.

PLEASE NOTIFY THE DEFENSE NUCLEAR AGENCY, ATTN: TISI, WASHINGTON, D.C. 20305, IF YOUR ADDRESS IS INCORRECT, IF YOU WISH TO BE DELETED FROM THE DISTRIBUTION LIST, OR IF THE ADDRESSEE IS NO LONGER EMPLOYED BY YOUR ORGANIZATION.

UNCLASSIFIED

SECURITY CLASSIFICATION OF THIS PAGE (When Data Entered)

REPORT DOCUMENTATION PAGE

READ INSTRUCTIONS BEFORE COMPLETING FORM

1. REPORT NUMBER: DNA 5189F AD-E300 857
2. GOVT ACCESSION NO.: AD-A087856
3. RECIPIENT'S CATALOG NUMBER:
4. TITLE (and Subtitle): MISERS BLUFF II CLOUD SAMPLING PROGRAM, Data Summary and Dust Cloud Characterizations
5. TYPE OF REPORT & PERIOD COVERED: Final Report for Period 2 Apr 78—30 Nov 79
6. PERFORMING ORG. REPORT NUMBER: SAI-80-118-WA
7. AUTHOR(s): Charles R. Thomas, John E. Cockayne
8. CONTRACT OR GRANT NUMBER(s): DNA 001-78-C-0217
9. PERFORMING ORGANIZATION NAME AND ADDRESS: Science Applications, Inc., 8400 Westpark Drive, McLean, Virginia 22102
10. PROGRAM ELEMENT, PROJECT, TASK AREA & WORK UNIT NUMBERS: Subtask H35HAXYX956-05
11. CONTROLLING OFFICE NAME AND ADDRESS: Director, Defense Nuclear Agency, Washington, D.C. 20305
12. REPORT DATE: 7 December 1979
13. NUMBER OF PAGES: 180
14. MONITORING AGENCY NAME & ADDRESS (if different from Controlling Office):
15. SECURITY CLASS (of this report): UNCLASSIFIED
15a. DECLASSIFICATION DOWNGRADING SCHEDULE:

16. DISTRIBUTION STATEMENT (of this Report)

Approved for public release; distribution unlimited.

17. DISTRIBUTION STATEMENT (of the abstract entered in Block 20, if different from Report)

18. SUPPLEMENTARY NOTES

This work sponsored by the Defense Nuclear Agency under RDT&E RMSS Code B342079462 H35HAXYX95605 H2590D.

19. KEY WORDS (Continue on reverse side if necessary and identify by block number)

MISERS BLUFF II	Linear Superposition	Particle Concentration
Dust Clouds	Mass Loading	Spectrometers
Fallout Sampling	Size Distribution	Multiple Bursts
In-Situ Sampling	Mass Distribution	Knollenberg Probes

20. ABSTRACT (Continue on reverse side if necessary and identify by block number)

This report describes in detail the analysis of the MISERS BLUFF II dust cloud data base (in-situ particle size spectral data and fallout data) obtained during Phase 1 of the MISERS BLUFF II Cloud Sampling Program. The analysis indicates a mass loading ratio of 7 at cloud stabilization (T+10 minutes) between the multiple and single burst dust clouds. Although, within the range of measurement uncertainties, this value may be comparable to that value of six predicted by linear superposition, photographic evidence of the multiple burst event strongly suggests this 15 percent

DD FORM 1 JAN 73 1473 EDITION OF 1 NOV 65 IS OBSOLETE

UNCLASSIFIED

SECURITY CLASSIFICATION OF THIS PAGE (When Data Entered)

20. ABSTRACT (Continued)

"enhancement" in mass aloft may be real. Of greater importance, the analysis revealed that linearly superimposing six of the MBII single burst dust clouds resulted in a significant overestimation of average mass concentrations that were found in the multiple burst cloud. This overestimation appears to be due to the inability of linear superposition to treat the effects of the hydrodynamic and thermodynamic interactions occurring between closely spaced detonations.

PREFACE

The work presented in this report was performed under Contract DNA001-78-C-0217; the dust particle spectra data presented in the report were obtained from Dr. Robert G. Kollenberg of Particle Measuring Systems, Inc. who was under separate contract with DNA. Captain A. T. Hopkins, Jr., USAF of the Aerospace Systems Division was the contracting officer's representative for both contracts.

The authors would like to thank the Air Force Technical Applications Center (AFTAC) for furnishing SAI with filter paper samples obtained from the MISERS BLUFF II-2 dust cloud. We are especially grateful to Captain Tim Stanley (AFTAC/TNS) whose assistance was invaluable in helping us analyze the filters.

We are also grateful to Mr. W. (Wally) Boquist of Technology International Corporation who furnished SAI with his preliminary MISERS BLUFF II photographic data which was very useful in producing this document.

The authors would also like to thank the USAF 6th Weather Squadron Mobile Unit from Tinker AFB, Oklahoma, for their outstanding efforts in providing the much needed meteorological data.

A special thanks goes to the FCDNA Test Group Director for MISERS BLUFF, LCDR J.D. Strode, and his entire Test Group Staff. Their cooperation and assistance during the planning and experimental fielding phases of the MISERS BLUFF II Cloud Sampling Program proved to be invaluable in helping us meet the program objectives.

TABLE OF CONTENTS

TABLE OF CONTENTS (Continued)

TABLE OF CONTENTS (Continued)

LIST OF ILLUSTRATIONS

LIST OF ILLUSTRATIONS (Continued)

LIST OF ILLUSTRATIONS (Continued)

LIST OF ILLUSTRATIONS (Continued)

LIST OF ILLUSTRATIONS (Continued)

LIST OF TABLES

SECTION 1

INTRODUCTION

1-1. BACKGROUND

The MISERS BLUFF II (MBII) Cloud Sampling Program was initiated to provide the empirical data required to determine how dust cloud characteristics of single burst environments interact to form multiple burst environments. State-of-the-art dust cloud modeling relies on the principle of linear superposition in defining the flyout threats for advanced basing concepts, hence, validation of this hypothesis has become a very important consideration.

The high explosive (HE) tests in the MBII series (FY78) provided a unique opportunity to gather the dust particle environmental data from both a single burst dust cloud and a dust cloud generated by six, simultaneous, interacting bursts. Science Applications, Inc. (SAI), under the sponsorship of the Aerospace Systems Division of the Defense Nuclear Agency (DNA/SPAS), directed and performed extensive dust particle sampling experiments during both events in the MBII series. The experiment rationale and procedures utilized in sampling the dust clouds, along with the preliminary results, have been documented by SAI in DNA 4729F, "MISERS BLUFF II Cloud Sampling Program: Procedures and Preliminary Results" (Ref. 1). The purpose of this document is to summarize the extensive analysis that has been conducted with the empirical data gathered during the experimental phase of the program.

1-2. DATA BASE FOR THE MBII DUST CLOUD ANALYSIS

The majority of the dust cloud analyses focused on the in-situ dust particle spectral data obtained from both dust clouds by Particle Measuring Systems, Inc. (PMS). This data was gathered from an airborne platform (Cessna 206) as it penetrated the single and multiple burst dust clouds with approximately 20 sampling passes through each cloud. The PMS data consists of dust particle number concentrations for the size

range from ∿3-750 μm (single burst cloud) and from ∿0.1-3000 μm (multiple burst cloud) with ∿120 meter (400 foot) horizontal resolution within the clouds. The results of this effort and a description of the particle sizing spectrometers have been documented by PMS in DNA 4951F, "Results of the MISERS BLUFF II Aircraft Dust Particle Sampling Experiments" (Ref. 2).

Supplemental data sources utilized in this analysis includes data obtained by: (1) Science Applications, Inc. (SAI) - large particle fallout from the multiple burst cloud at times prior to, and coincident with, airborne sampling; (2) Air Force Technical Application Center (AFTAC) - filter paper samples containing dust from the top of the MBII multiple burst cloud;* (3) Technology International Corporation (TIC) - high resolution cloud photography for thirty minutes of both events in the MBII series; and (4) an Air Force 6th Weather Squadron (Mobil) Unit - detailed meteorological data from the surface to cloud top (approximately 4600 meters (15kft) above ground level (AGL)) for each event in the series.

In all, it is felt that the data base for the MISERS BLUFF II dust cloud analysis is the most extensive and complete that has been obtained to date during any dust cloud sampling program.

1-3 REPORT FORMAT

Due to the immense quantity of dust particle spectral data obtained from both MBII dust clouds, a major effort in producing this document was directed at formating the data in a manner such that little or no explanation would be required in interpreting the way the data has been presented or conclusions that have been drawn from it. Data sets from the single burst and multiple burst dust clouds have been made consistent with each other, i.e., the same

*AFTAC also fielded aerosol spectrometers which served as back-up instruments to the LAS-X instrument fielded by PMS for the multiple burst event. Since the LAS-X instrument functioned normally, the AFTAC spectral data have not been reduced or included in this analysis.

dust particle data has been presented for both clouds, in order to enable readers to make their own comparisons of the salient features of the single and multiple burst dust clouds. Further, the desire to have a "complete" document has led to the inclusion of several comprehensive appendices to supplement the material presented in the main body of the report.

Section 2 provides a detailed summary of the spectral data obtained from the single burst dust cloud (MBII-1) and also, describes the gross mass loading features of the cloud at ten and twenty minutes after detonation. Section 3 provides an identical description of the multiple burst dust cloud (MBII-2). Section 4 is devoted to detailed comparisons between the mass loading features of each cloud. Section 5 is included to discuss the significant uncertainties in calculating total mass lofted by each detonation and how these uncertainties would effect the calculations. Section 6 contains the conclusions and recommendations. Appendices A-D are included to provide the reader with detailed data on several other dust cloud parameters obtained from the measured spectral data and, also, to provide "back-up" material for Sections 2, 3, 4, and 5.

SECTION 2

THE MISERS BLUFF II SINGLE BURST DUST CLOUD

2-1 MBII-1 IN-SITU SAMPLING DATA SUMMARY

Although more than 20 sampling passes were flown at various altitudes through the MBII-1 dust cloud, only those passes that were made while the aircraft was ascending to the top of the cloud are included in the mass loading calculations. Further, sampling passes 1 and 2 were accomplished below the cloud cap and outside the visible stem, hence, data obtained from them have not been included in the calculations. Similarly, passes 10 and 11 were performed while the aircraft was maneuvering in and out of the cloud and they have also been excluded.

Table 2.1 summarizes and profiles the in-situ sampling mission accomplished within the MBII-1 dust cloud. Pass numbers, pass midpoint time-after-burst (TAB), and sampling altitude are tabulated at the top of the table. Pass numbers in parentheses and the altitudes of the top and bottom of the cloud layer they represent are enumerated on the left side of the table. Pass-averaged mass concentrations, as calculated from the measured particle number concentration (see Appendix B for details), are given for dust particle sizes $\cdot 47$ μm and $\cdot 47$ μm for each pass. The four columns on the right hand side of Table 2.1 contain calculated values of total pass-averaged mass concentration (all particle sizes), cloud volume represented by sample, mass in cloud layer sampled, and cumulative mass in cloud as measured from the cloud top. Volume calculations have been made assuming that the dust cloud is circular at each sampling level and that the length of the sampling pass represents the diameter of this circle (more will be said of this assumption in Section 5). All number entries in the Table are given in an abbreviated format, e.g., 7.94+8 = 7.94×10^8.

Several trends in the data become apparent in Table 2.1. First, the mass concentrations are generally decreasing with time (increasing altitude and pass number). This is due mainly to cloud diffusion under the influence of the significant wind shear aloft measured at detonation time. This wind induced cloud diffusion is also evidenced in the TIC

TABLE 2.1 MISERS BLUFF II-1 In-Situ Sampling Data Summary

Pass #		3	4	5	6	7	8	9	12	13	14	15				
TAB (Min)		4.03	4.63	5.87	6.77	8.73	10.43	11.30	16.30	19.23	24.15	26.15				
Altitude (m)		300	360	410	550	670	790	790	1280	1580	1890	1890				
Altitude (m) of Top and Bottom of Cloud Layer Sampled During Pass (meters)	Pass Number	Pass Averaged Mass Concentration (g/m^3) As Dust Cloud Was Sampled											Total Averaged Concentration (g/m^3)	Volume in Cloud Layer (m^3)	Mass in Cloud Layer (g)	Cumulative Cloud Mass (g)
		Particle Size (Spherical Particles)														
		< 47 μm	≥ 47 μm													
2500																
2045	(15)	2.75-2										5.13-3	3.27-2	4.79+9	1.57+8	1.57+8
	(14)	2.69-2									5.90-3		3.78-2			
1735	(13)	2.82-2								5.05-3			3.33-2	4.71+9	1.57+8	3.14+8
1430	(12)	2.95-2							7.89-3				3.74-2	6.19+9	2.29+8	5.43+8
1035	(9)	4.68-2						6.92-3					5.37-2			
	(8)	7.76-2					1.57-2						9.33-2	6.76+8	4.97+7	5.93+8
730	(7)	7.59-2				1.14-2							8.73-2	2.29+8	2.00+7	6.13+8
610	(6)	9.33-2			2.32-2								1.17-1	2.49+8	2.91+7	6.42+8
480	(5)	7.76-2		1.11-2									8.87-2	3.48+8	3.09+7	6.73+8
385	(4)	2.51-1	4.92-2										3.00-1	7.53+7	2.26+7	6.95+8
330	(3)	3.16-1	1.06-2										3.27-1	3.02+8	9.89+7	7.94+8
0																

photographic coverage of the MBII-1 dust cloud (Ref. 5). This fact is further supported by noting that although mass concentrations are decreasing with time, there is a corresponding increase in total mass at altitude; the maximum being found at 1280 m (Pass 12).

Another very interesting and important feature revealed by the data is that the mass contribution from dust particles $\geq$47 μm comprises only ∿15 percent of the total mass lofted. This fact was unexpected based on a preliminary analysis by PMS of subsurface soil samples taken from ground zero and sized by one of their probes (Ref. 2). That analysis indicated a mass peak at approximately 200-300 μm. It is apparent that either the flow fields generated by the MBII-1 fireball rise were not sufficient to keep many particles of this size aloft for sustained periods of time or that these larger particles were actually "silty" aggregates and were broken up by the high "pressures" from the cratering and particle ejection.

Based on the in-situ sampling data obtained from the MBII-1 dust cloud and assumptions concerning cloud geometry and soil density, the total mass lofted in the single burst event was 7.9×10^8 grams (highlighted value in Table 2.1). This number compares very favorably to that value calculated by PMS (8.0×10^8 g) in an independent analysis performed on the MBII-1 dust cloud. (Preliminary analysis of MBII-1 crater and ejecta measurements by AFWL and CERF have shown that approximately 10×10^8g of soil were unaccounted for after the burst.)

2-2 MBII-1 DETAILED SAMPLING PASS DATA

During each sampling pass through the MISERS BLUFF II-1 dust cloud, particle number concentrations were measured with two-second resolution (∿400 foot) within the cloud. From the measured number concentrations, it was possible to calculate mass concentrations every two seconds and plot time histories for each sampling pass considered in the analysis. Figures 2.1 through 2.13 contain the detailed sampling pass data derived from these measurements. With the exception of sampling passes 1 and 2 (data not included in the analysis), pass data are presented in pairs of figures; Figure 2.X (a) contains pass averaged particle size distributions (PSD) and cumulative mass plots while

Figure 2.X(b) depicts the time ("radial") dependence of mass concentration within the dust cloud.

In Figures 2.X(a), the particle size distributions of particles $\cdot 47$ μm are plotted with circles while the size distributions of particles $\cdot 47$ μm are plotted with squares. A straight line representing the "best fit" has been drawn through the large particle data so that the slope of the PSD can be easily determined. The dashed line at the bottom of each figure is merely the upper decade of the large particle PSD plotted on the same scale as the small particle PSD. The cumulative mass versus particle diameter plot is the curve that runs from the lower left to the upper right in Figures 2.X(a); values of cumulative mass (percent) are given on the inside right hand scale.

Figures 2.X(b) depict time histories of mass concentration within the MBII-1 dust cloud. Each figure contains the contribution to mass concentration from particles $\cdot 47$ μm (circles connected with solid line) and particles $\cdot 47$ μm (squares connected with dashed line). Values of total mass concentration can be obtained from Appendix B (Table B.1). The values of mass concentration in Figures 2.X(b) are logrithmic values and were plotted in this manner for scale compression. If values of mass concentration were calculated to be $\cdot 10^{-4.5}$ g/m^3, they have been plotted as $10^{-\infty}$, i.e., zero. Pass-averaged values of mass concentration ($\bar{e}$ in g/m^3) are represented by the horizontal lines drawn through the data ($\cdot 47$ μm - solid line; $\cdot 47$ μm - dashed line). To obtain pass time after detonation, subtract 13:05:00 from the pass start time.

2.3 GENERAL COMMENTS CONCERNING THE MBII-1 DUST CLOUD

Every attempt has been made to present the data in Figures 2.1 through 2.13 as unambiguous as possible, hence, only general comments concerning the sampling pass data will be made in this section of the report.

2-3.1 Particle Size Distributions

From the plotted particle size distributions depicted in Figures 2.X(a) it appears that, for particles $\cdot 47$ μm, the pass-averaged size distributions encountered in the MBII-1 dust cloud can be approximated by,

$$\frac{dN}{da} (\#/cm^3 \cdot \mu m) = kd^{-q}, \quad d \geq 47\ \mu m$$

where d is the particle diameter in microns and

$$3.5 \lesssim q \lesssim 4.0.$$

It should be reiterated that this range in q is for pass-averaged data - it would probably vary significantly within each two-second data acquisition interval in each pass. Further, poor counting statistics for particles $\gtrsim$ 200 μm lead to significant uncertainty in q for the tail of the distributions.

The size distribution of particles < 47 μm, however, appears to be approximately exponential in nature, i.e.,

$$\frac{dN}{da} (\#/cm^3 \cdot \mu m) = ke^{-pd}, \quad d < 47\ \mu m$$

The spectral data obtained from the multiple burst dust cloud for particle sizes 0.1-6 μm (see Appendix C) indicates a general increase in number concentration with decreasing particle diameter, hence, the possibility of the aerosol dust particles being distributed log-normally can be ruled out. This is mentioned because most current fallout models assume the radioactive dust particles are log normally distributed.

2-3.2 Cumulative Mass Distributions

With the exception of Pass 3, where only about 3 percent of the mass can be attributed to particles $\geq$ 47 μm, all subsequent sampling passes reveal that approximately 85 percent of the dust cloud's mass is attributed to particles < 47 μm. Further shown in Figures 2.x(a), is that the mass median diameter a-pears to lie between 25 μm and 30 μm.

2-3.3 Mass Concentration Time Histories

As might be expected, the highest mass concentrations encountered in the MBII-1 dust cloud were in the stem at 4-5 minutes after burst (Passes 3 and 4). Average concentrations in the stem were approximately 0.3 g/m^3 with the maximum mass concentration being

1.3 g/m^3 encountered during pass 3 (first pass in stem). For all passes made within the cloud cap (passes 6-15), maximum values of mass concentration are approximately 3-4 times the average concentration (see Appendix B, Table B.1 for maximum values).

Passes 1 and 2 were made below the cloud cap and to outside of the stem, therefore, the mass concentration time histories from these passes consist of dust particles falling out of the cloud cap. During both passes there appears to be an area near the cloud center that is nearly void of "fallout". This observation is also revealed in passes 4 (stem), 5 (stem), 7 (cloud cap), and 9 (cloud cap) where there are two areas of high mass concentration separated by a central region of low mass concentration. There is still some evidence of this feature in passes 14 and 15, however, at these late times this might be due to wind shear "pulling" the cloud into several pieces. The fact that this "hole" in the cloud is not evidenced in the mass concentration times histories from passes 6 and 8 is probably due to the aircraft not passing through the central region of the cloud. (A comparison of the sampling pass lengths of passes 6 and 8 with pass lengths of passes 5, 7 and 9 reveal that the maximum dimension of the dust cloud was not sampled during passes 6 and 8.) Hydrocode (HULL) flow field calculations that were performed in support of the DICE THROW HE detonation (600 ton ANFO - hemispherically capped cylinder charge configuration) predict a reverse flow or downdraft in the center of the cloud at 5 seconds after detonation that persists for approximately 10 seconds. This downdraft could prevent soil from initially flowing into the central core region of the cloud. (Overhead photography of the DICE THROW cloud (Ref. 4) did reveal this mass loading phenomena at T+15 seconds.) Further, the lack of any evidence indicating any toroidal flow in the MBII-1 dust cloud as it rose, would suggest that any flow field(s) surrounding the early time toroidal ring of dust were probably too weak to replenish this central core region with dust as the cloud was rising. This would account for the low mass concentration in this region at later times.

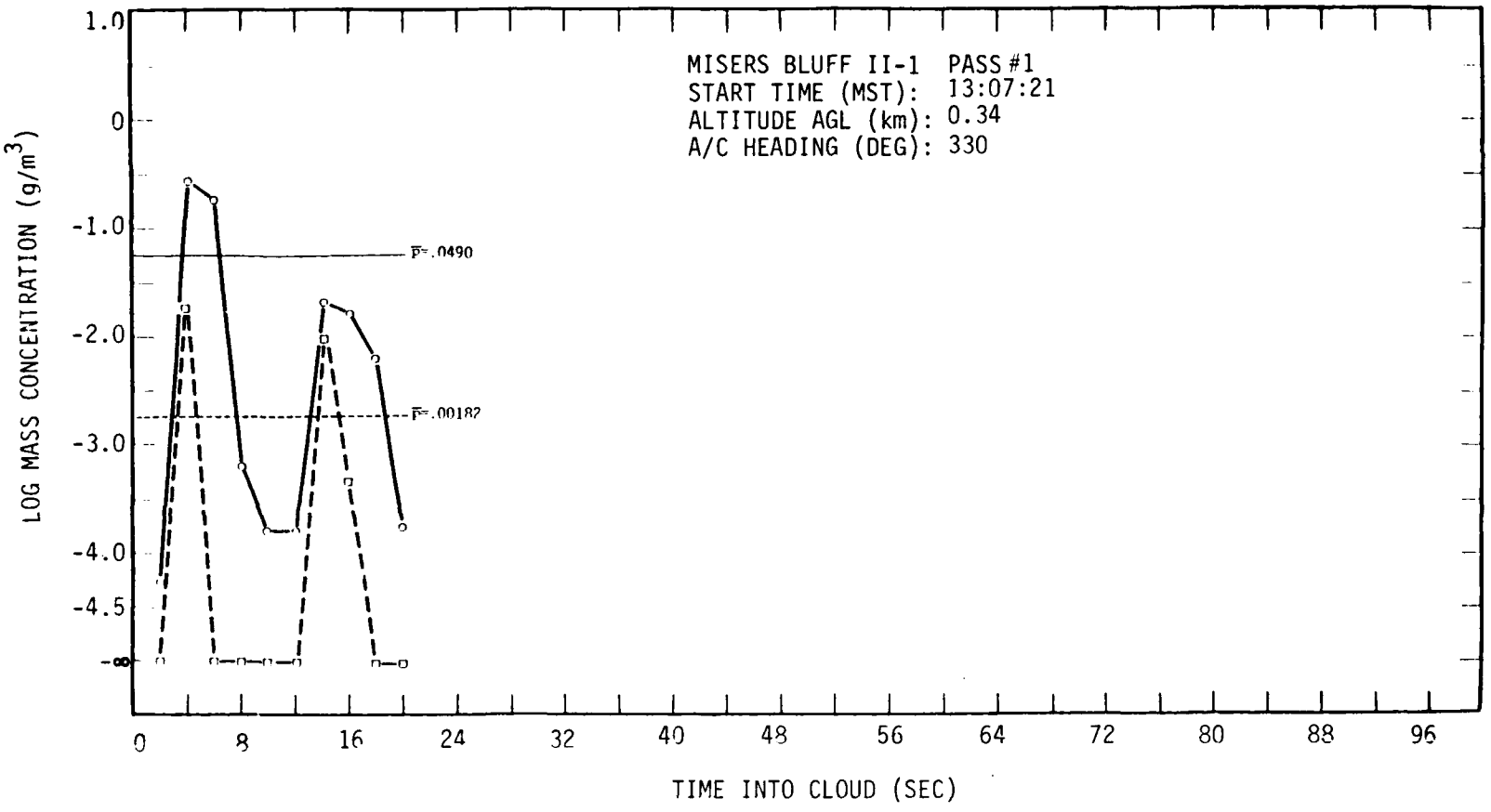

Figure 2.1. MISERS BLUFF II-1, Pass 1, Mass Concentration Time History

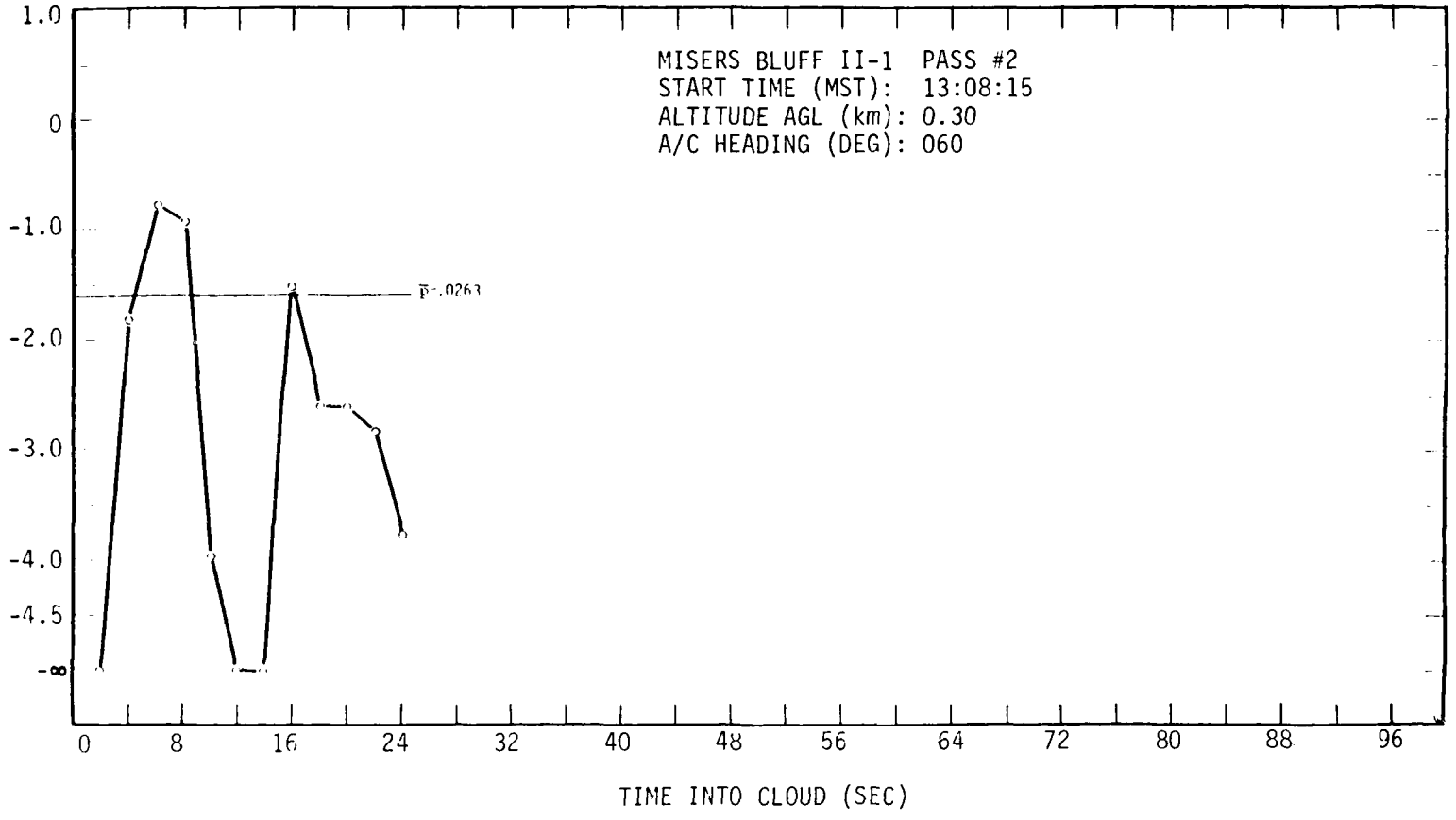

Figure 2.2. MISERS BLUFF II-1, Pass 2, Mass Concentration Time History

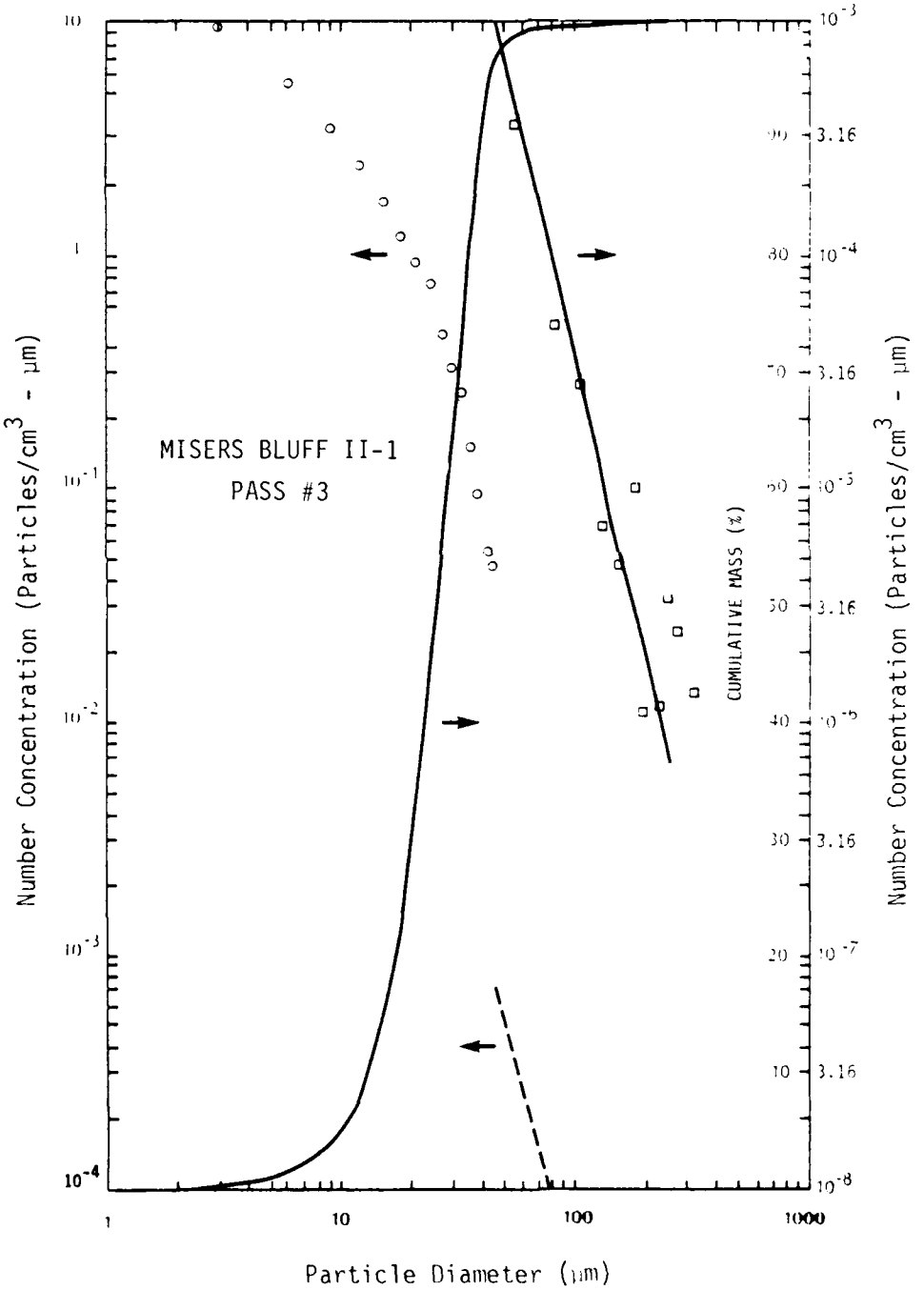

Figure 2.3(a) MISERS BLUFF II-1, Pass 3, Particle Size and Cumulative Mass Distributions

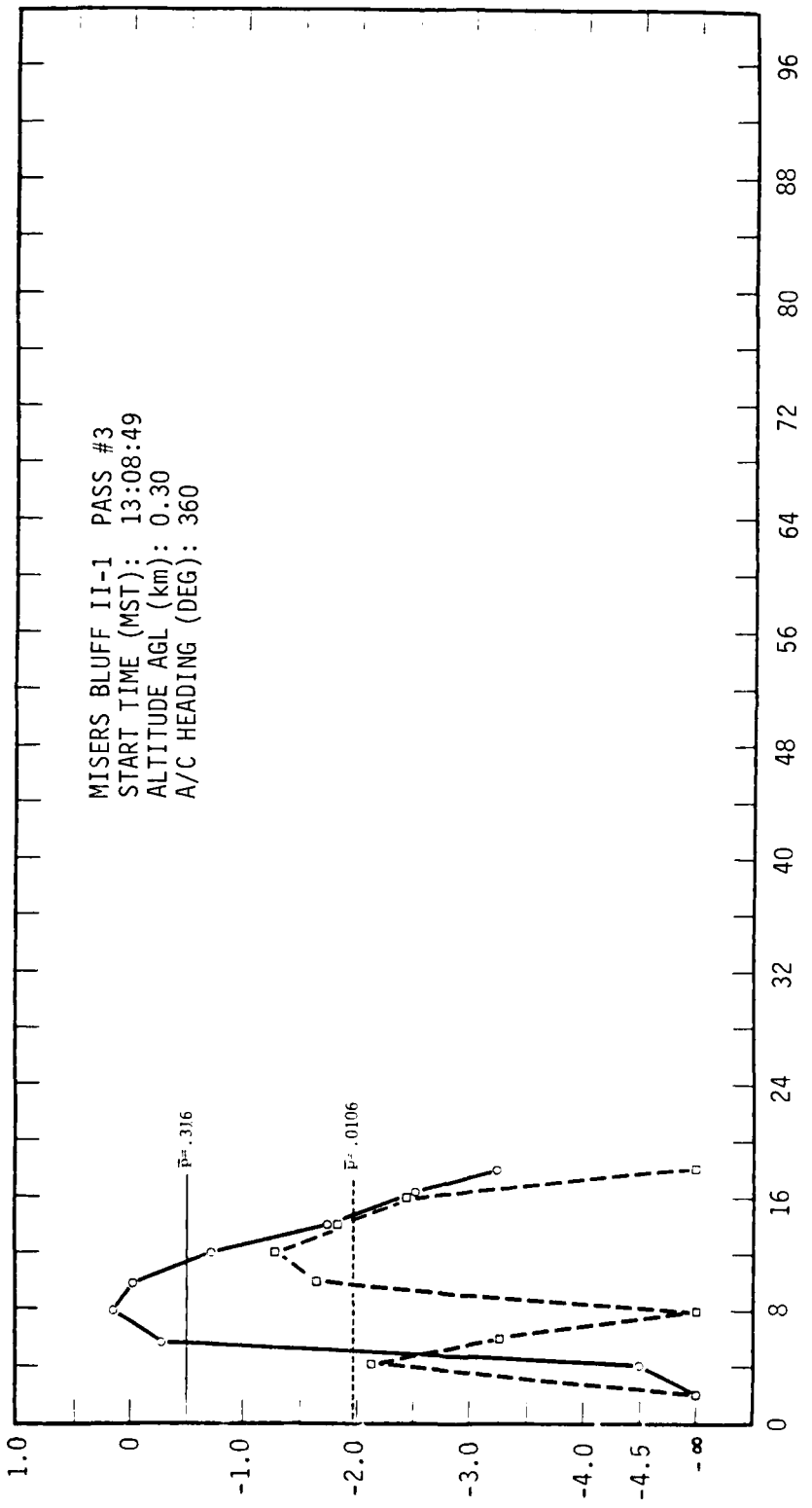

Figure 2.3(b) MISERS BLUFF II-1, Pass 3, Mass Concentration Time History

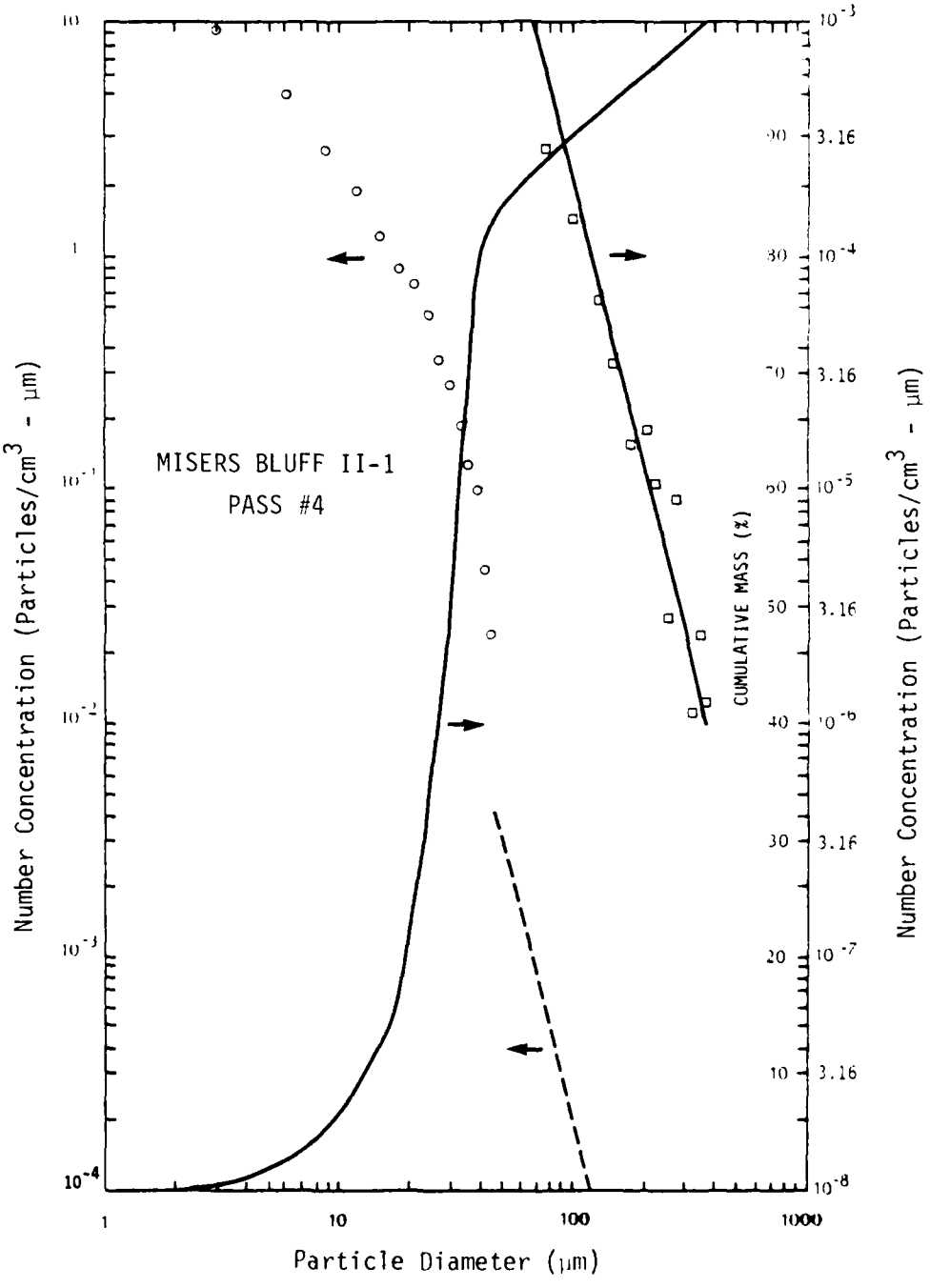

Figure 2.4(a) MISERS BLUFF II-1, Pass 4, Particle Size and Cumulative Mass Distributions

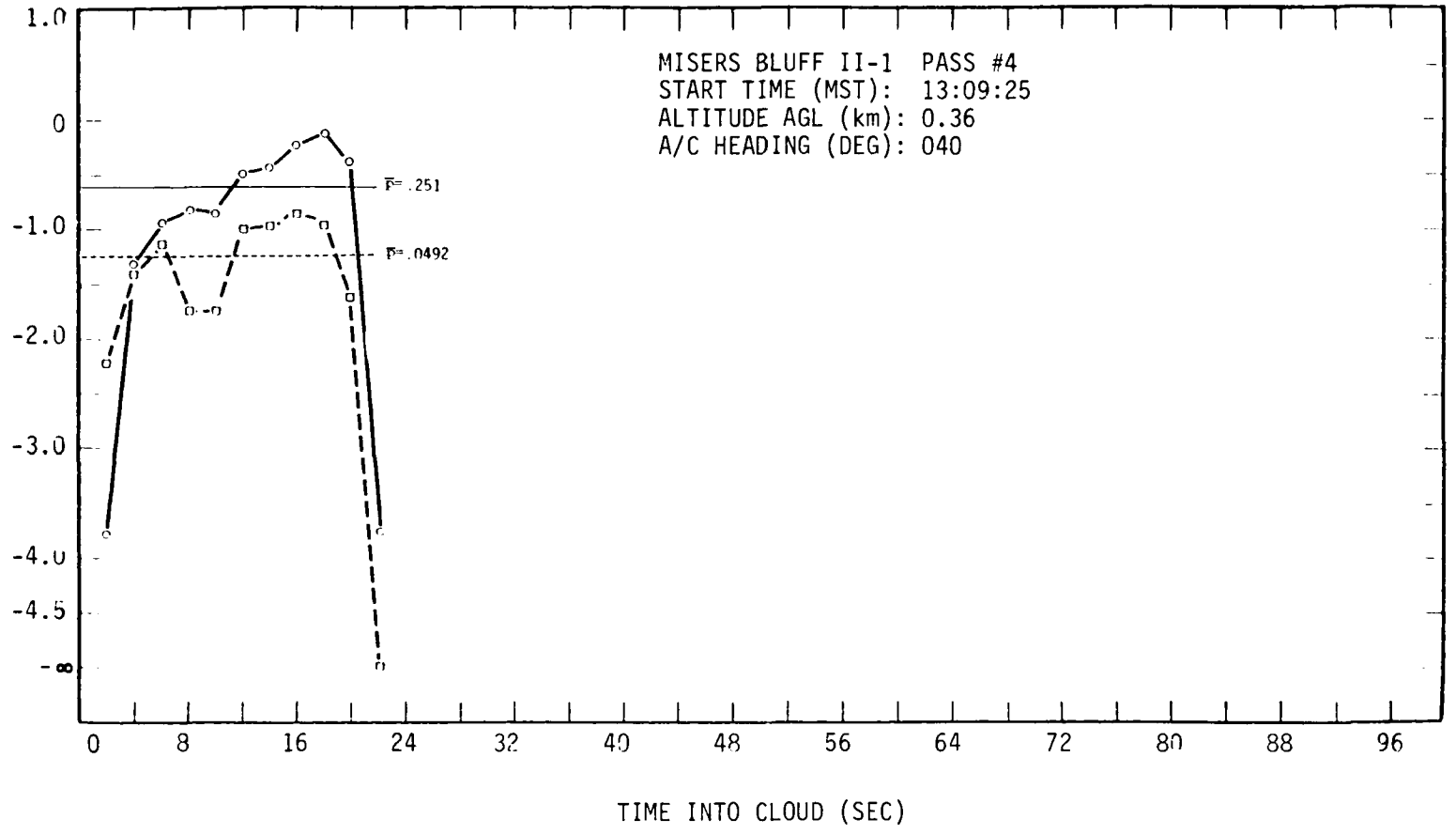

Figure 2.4(b) MISERS BLUFF II-1, Pass 4, Mass Concentration Time History

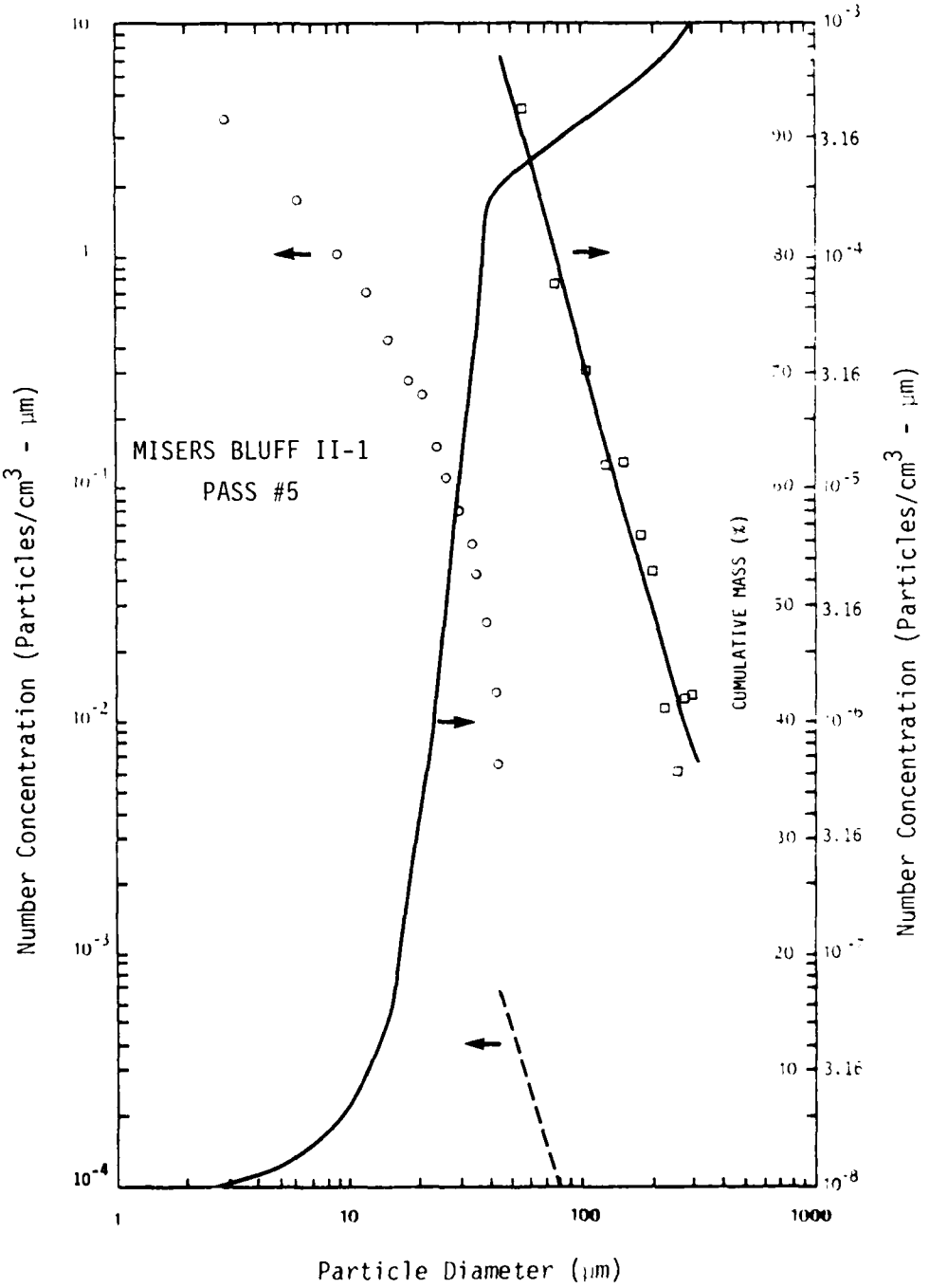

Figure 2.5(a) MISERS BLUFF II-1, Pass 5, Particle Size and Cumulative Mass Distributions

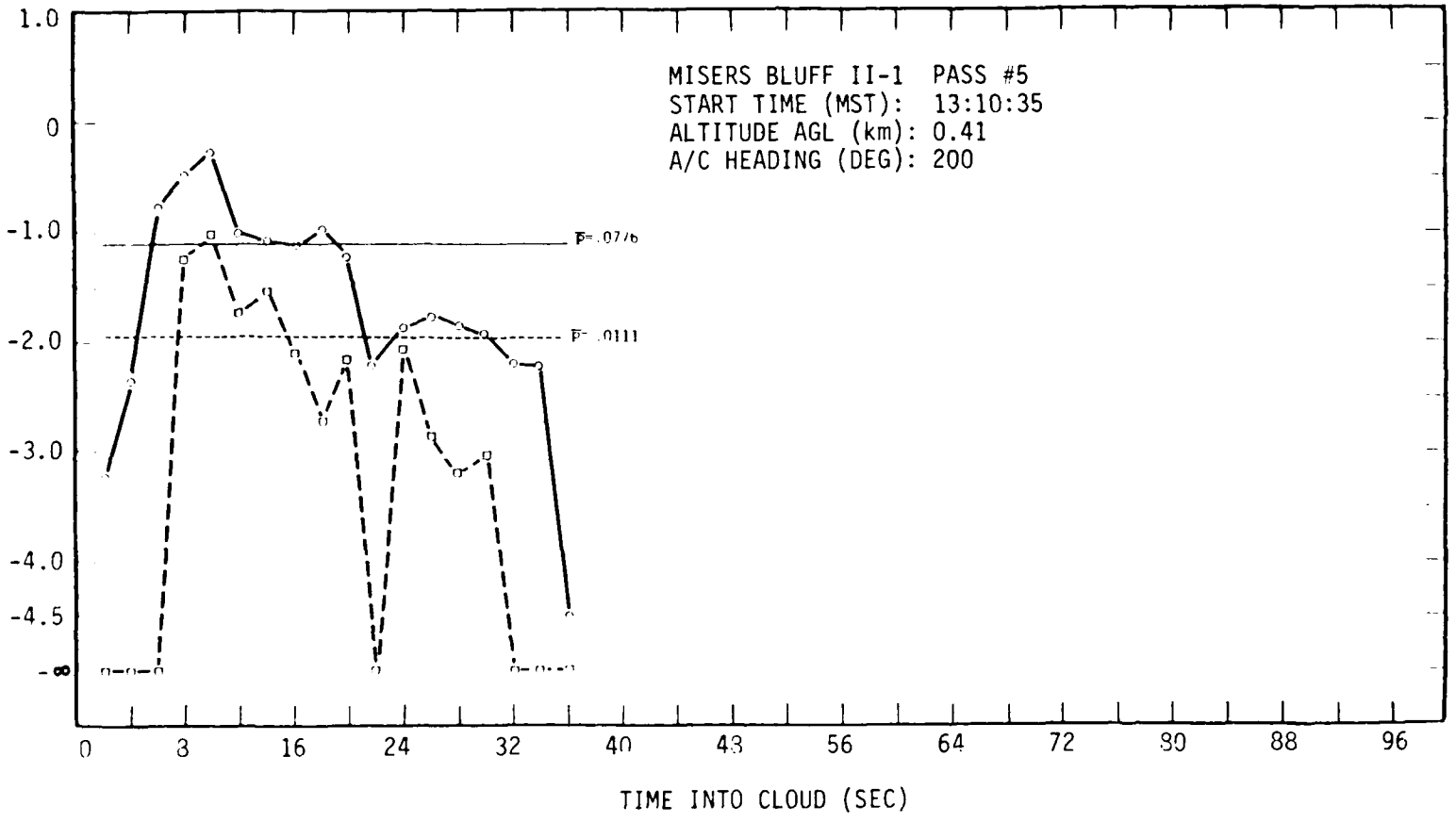

Figure 2.5(b) MISERS BLUFF II-1, Pass 5, Mass Concentration Time History

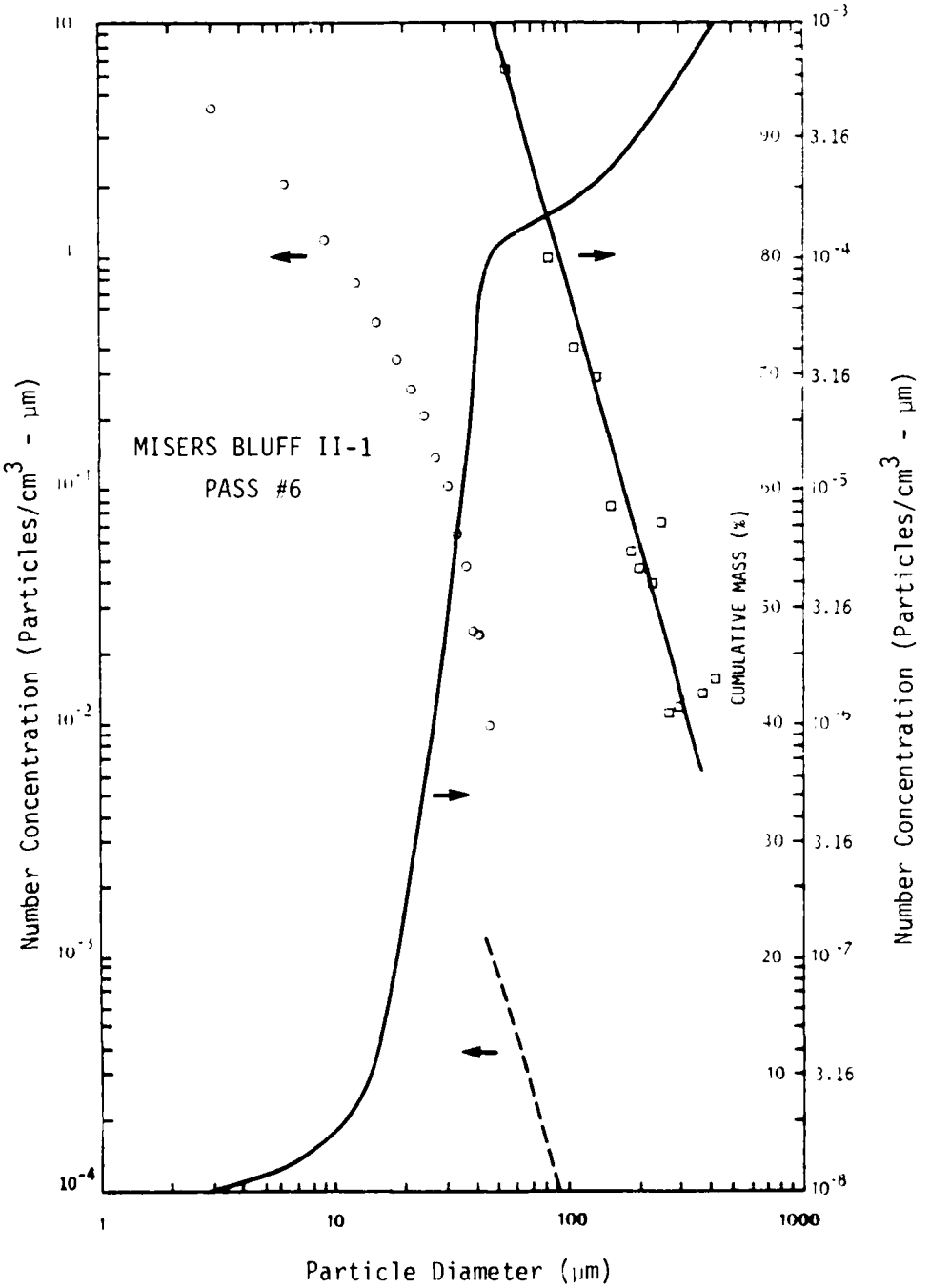

Figure 2.6(a) MISERS BLUFF II, Pass 6, Particle Size and Cumulative Mass Distributions

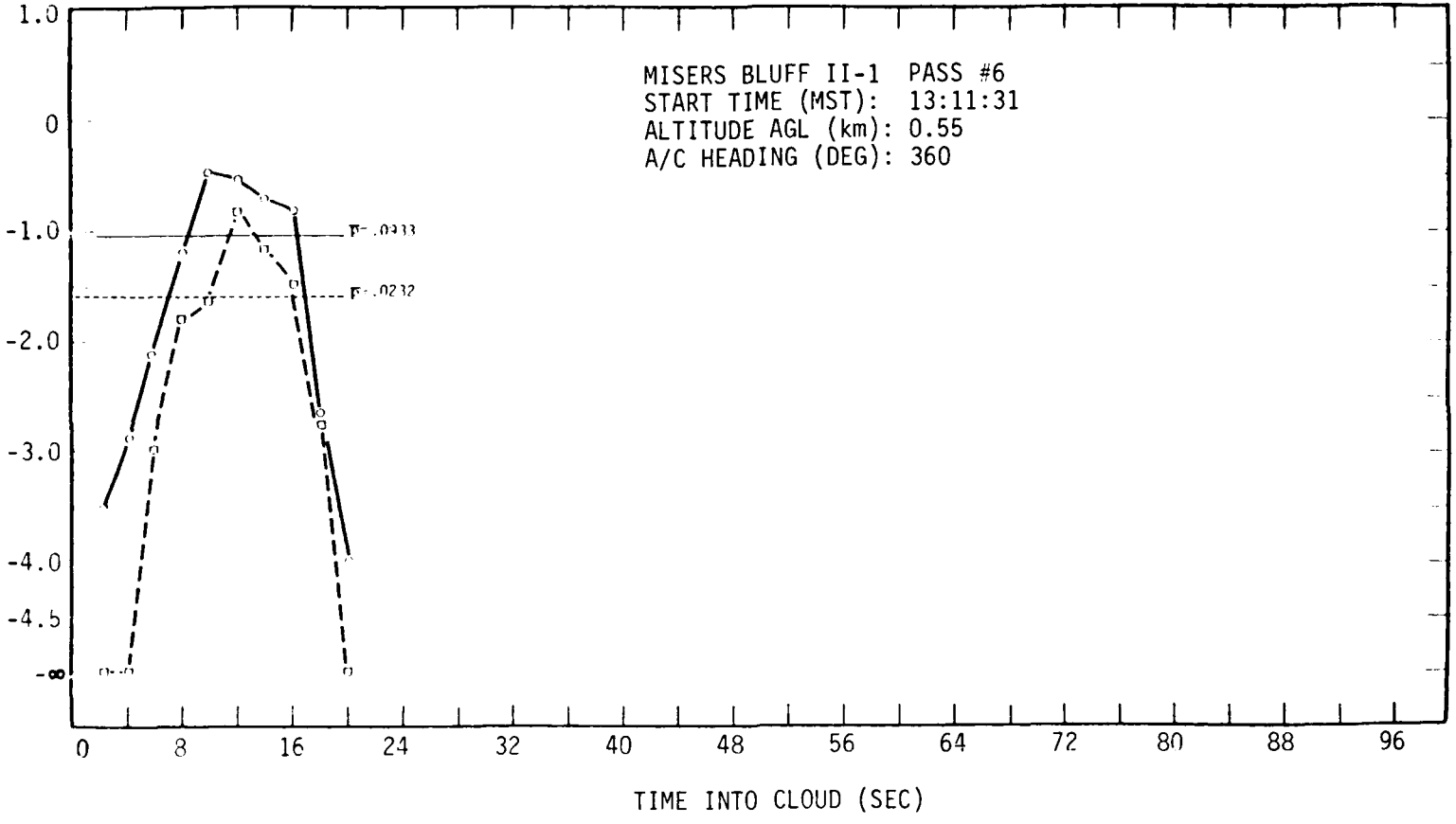

Figure 2.6(b) MISERS BLUFF II-1, Pass 6, Mass Concentration Time History

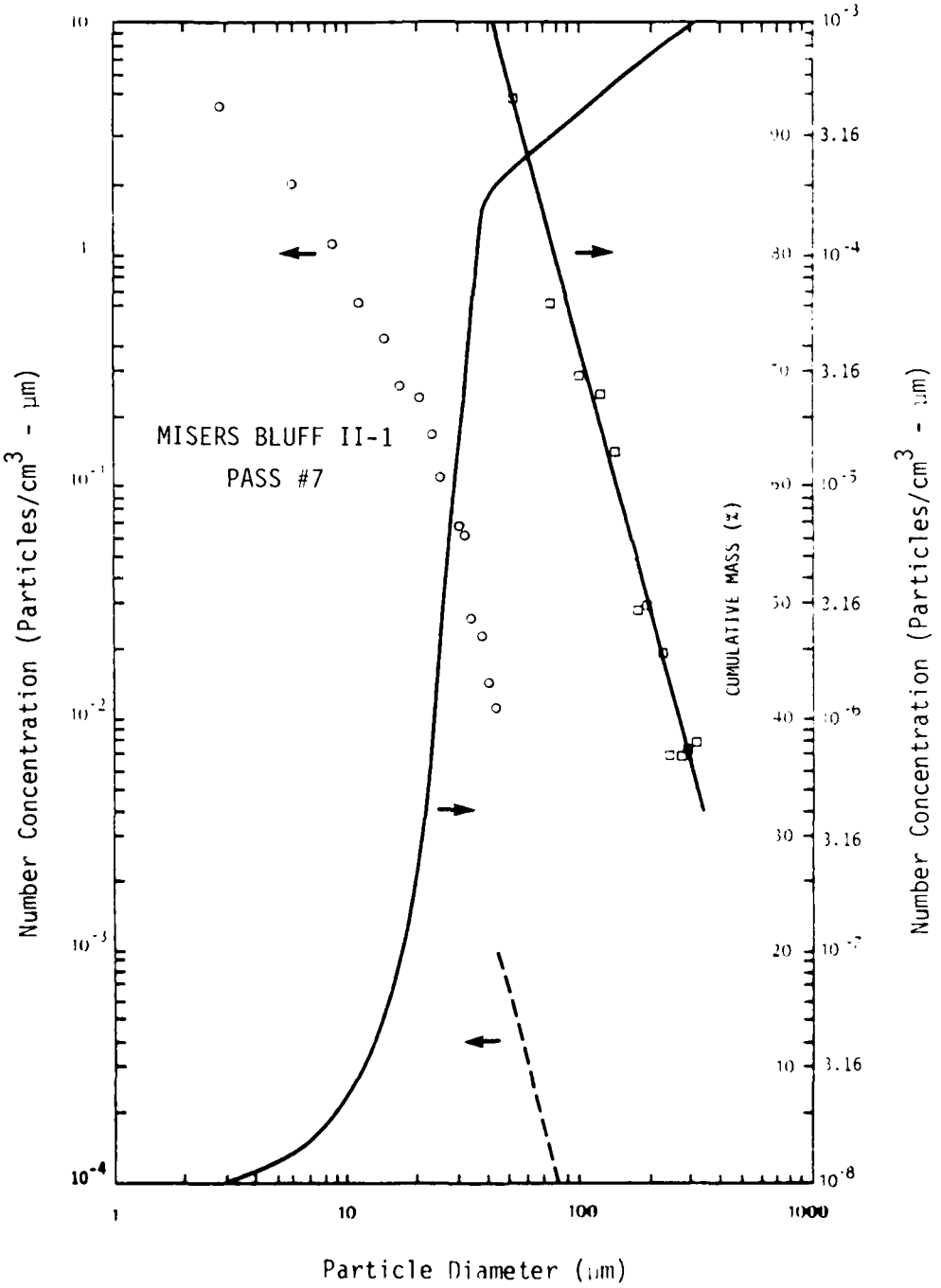

Figure 2.7(a) MISERS BLUFF II-1, Pass 7, Particle Size and Cumulative Mass Distributions

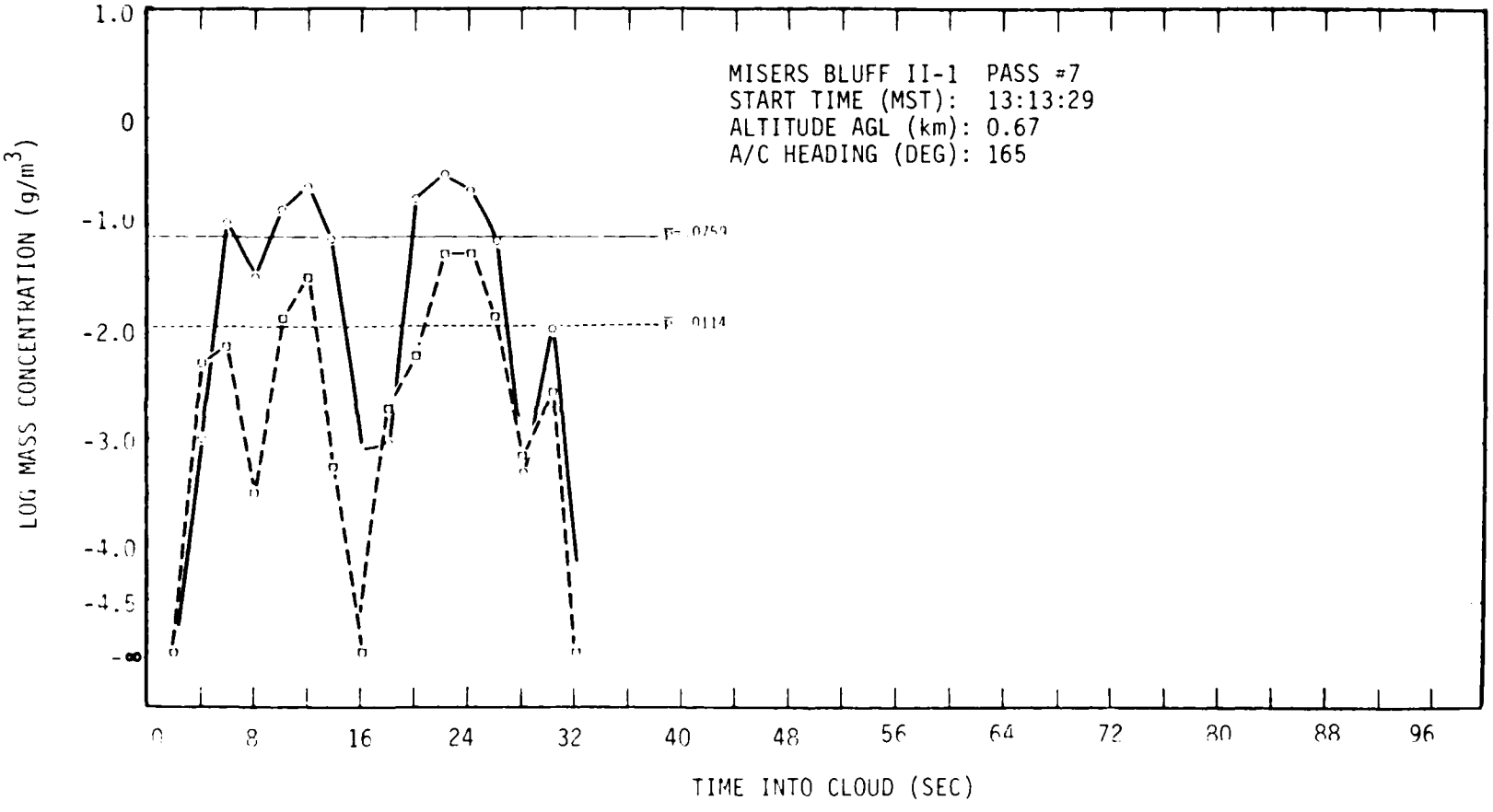

Figure 2.7(b) MISERS BLUFF II-1, Pass 7, Mass Concentration Time History

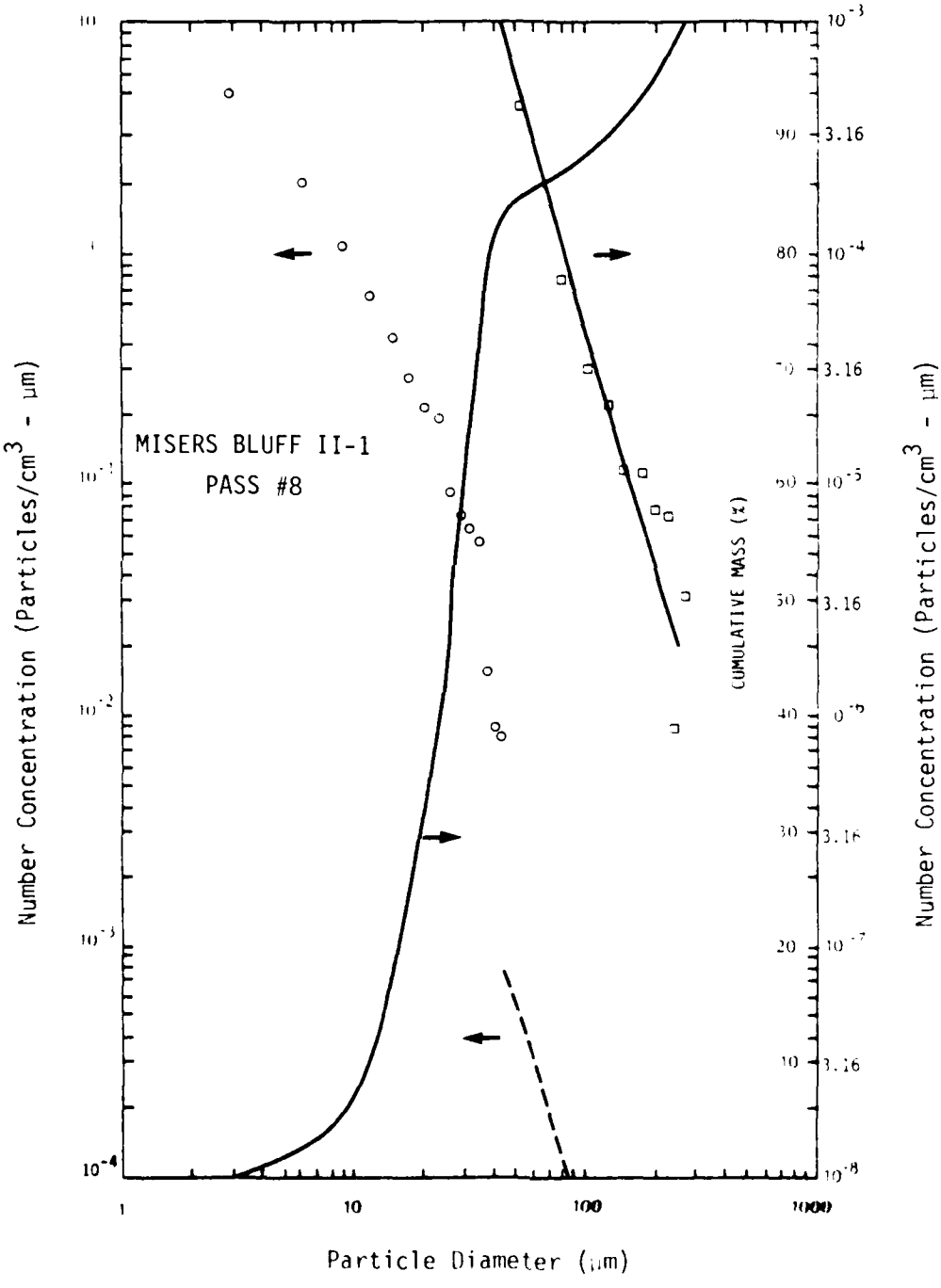

Figure 2.8(a) MISERS BLUFF II-1, Pass 3, Particle Size and Cumulative Mass Distributions

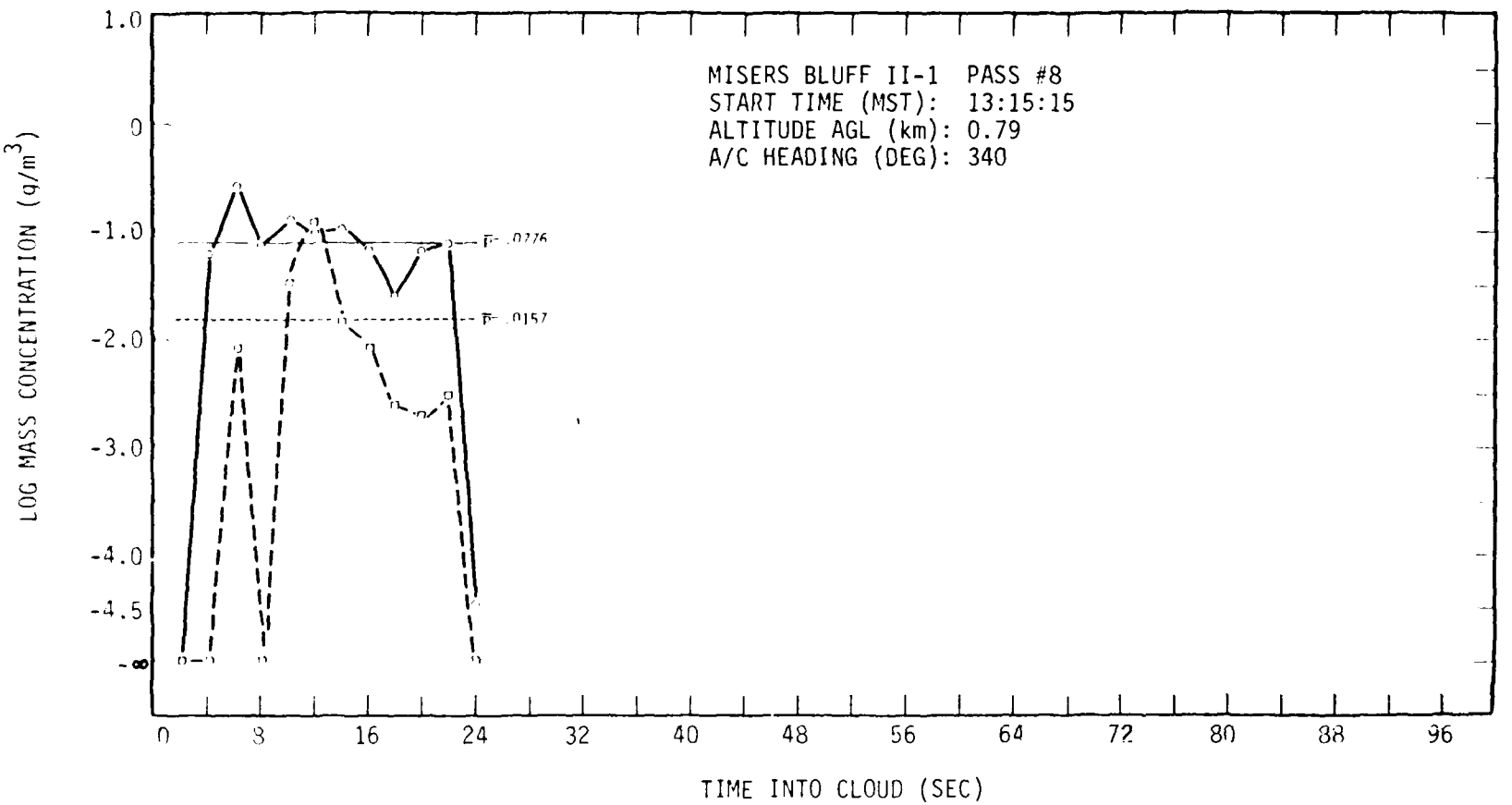

Figure 2.8(b) MISERS BLUFF II-1, Pass 8, Mass Concentration Time History

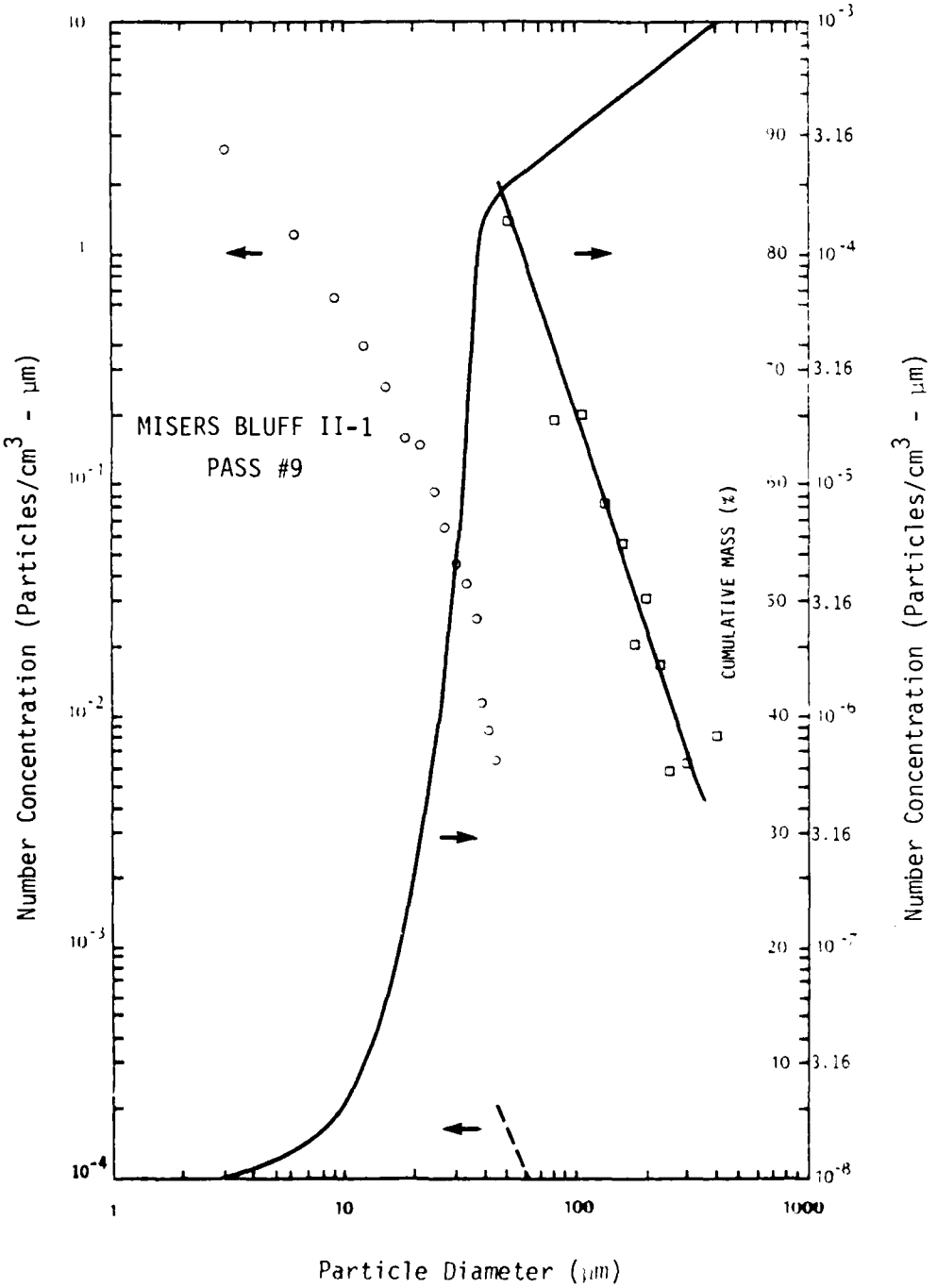

Figure 2.9(a) MISERS BLUFF II-1, Pass 9, Particle Size and Cumulative Mass Distributions

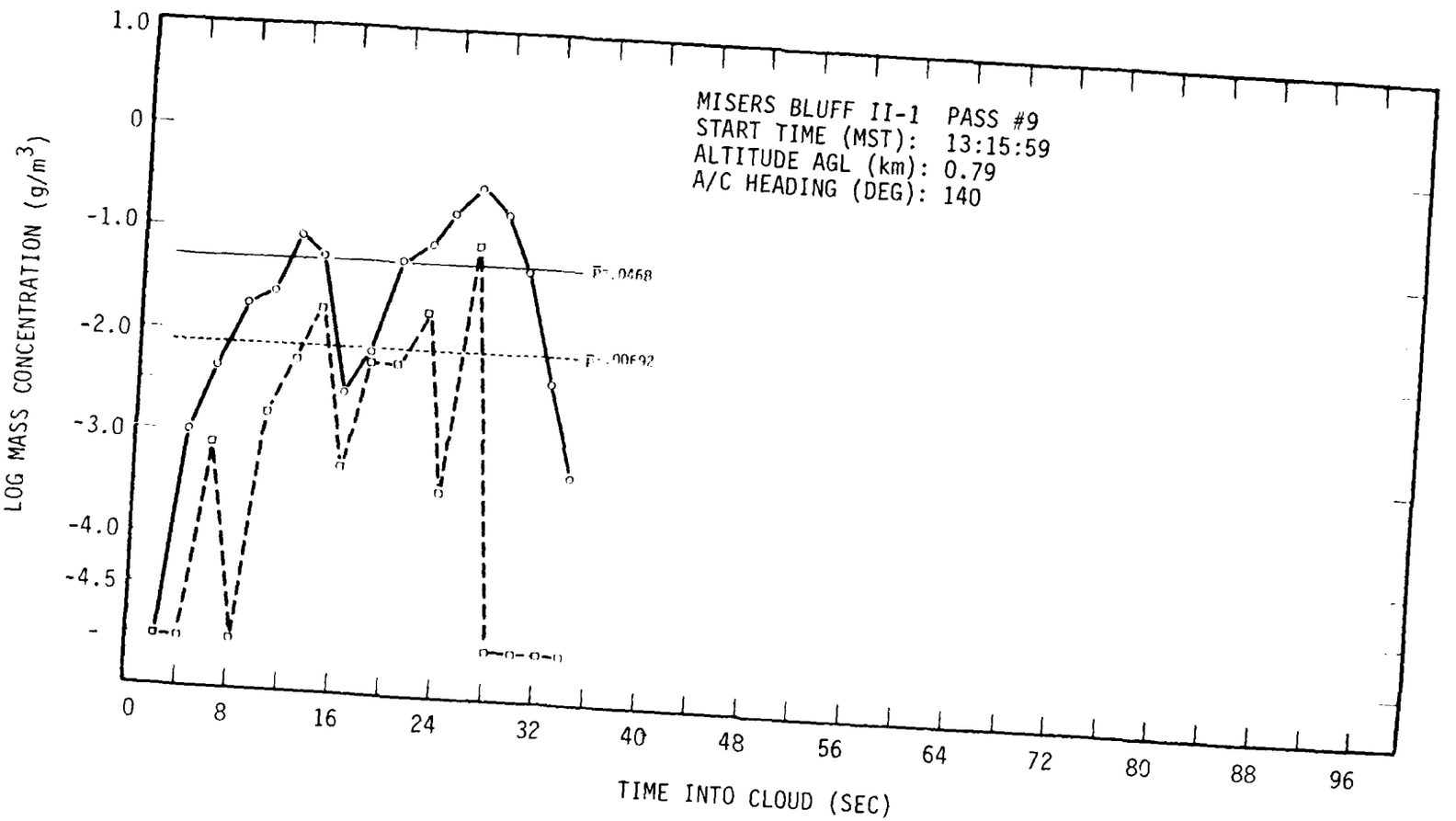

Figure 2.9(b) MISERS BLUFF II-1, Pass 9, Mass Concentration Time History

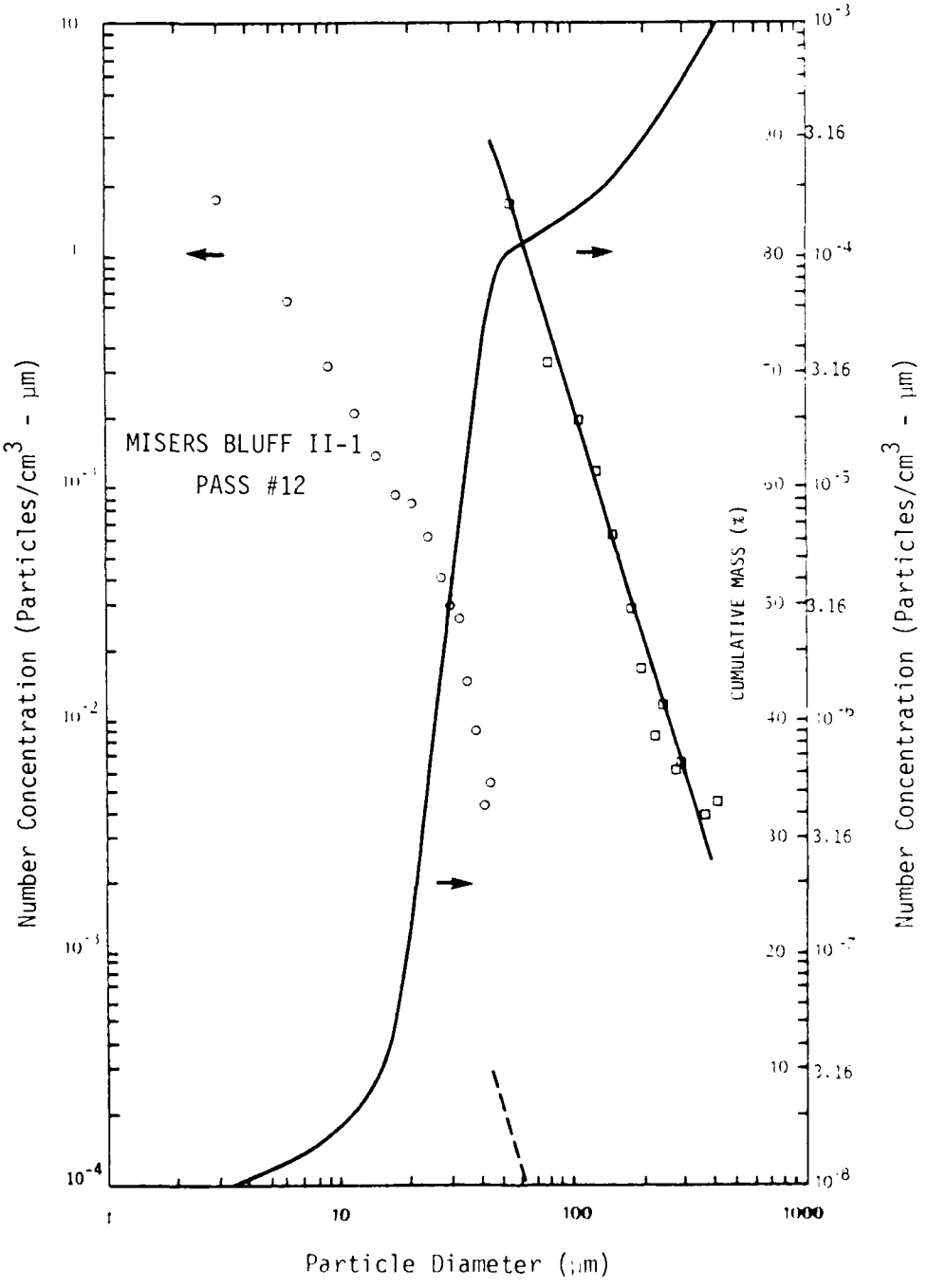

Figure 2.10(a) MISERS BLUFF II-1, Pass 12, Particle Size and Cumulative Mass Distributions

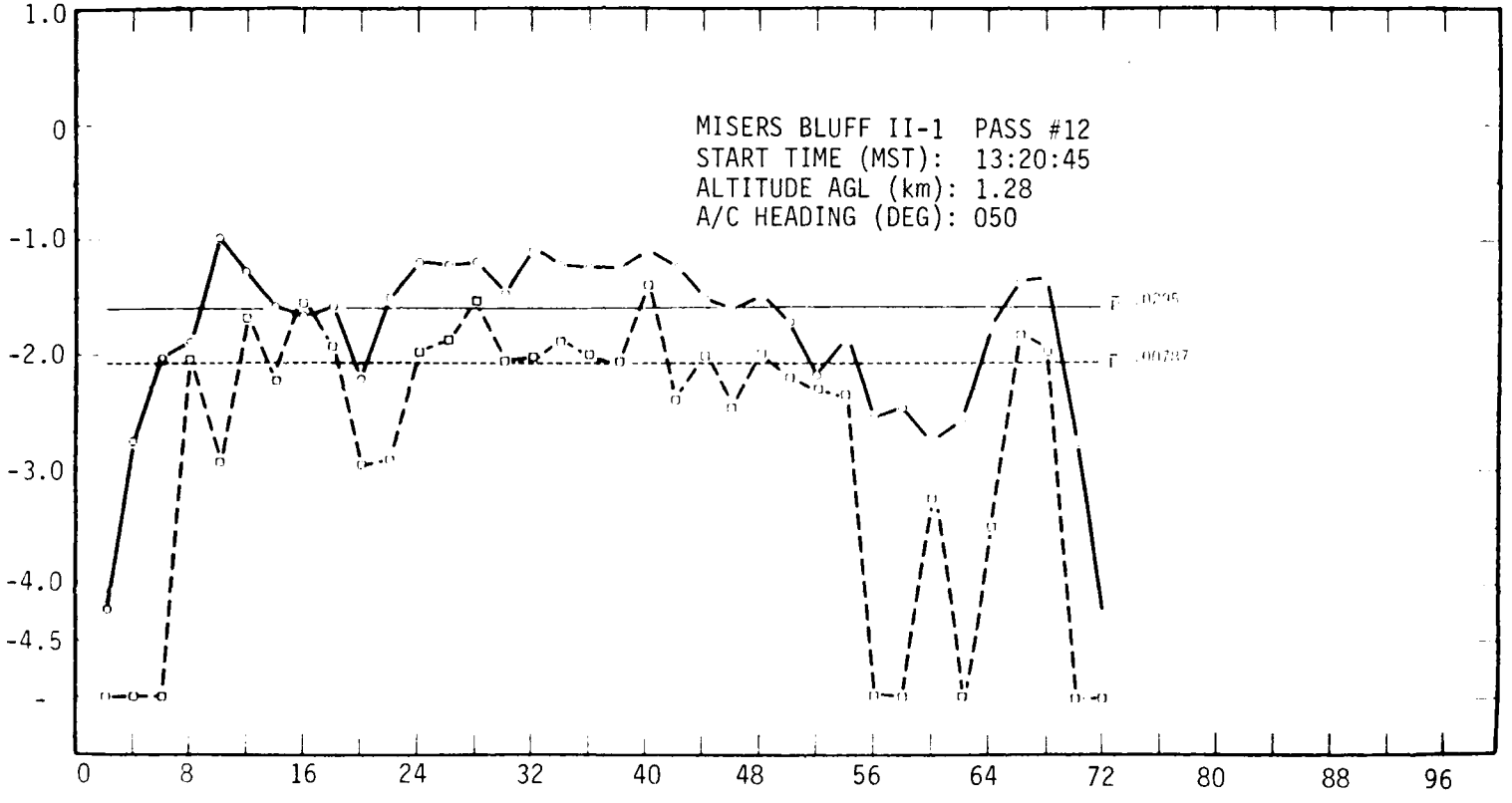

Figure 2.10(b) MISERS BLUFF II-1, Pass 12, Mass Concentration Time History

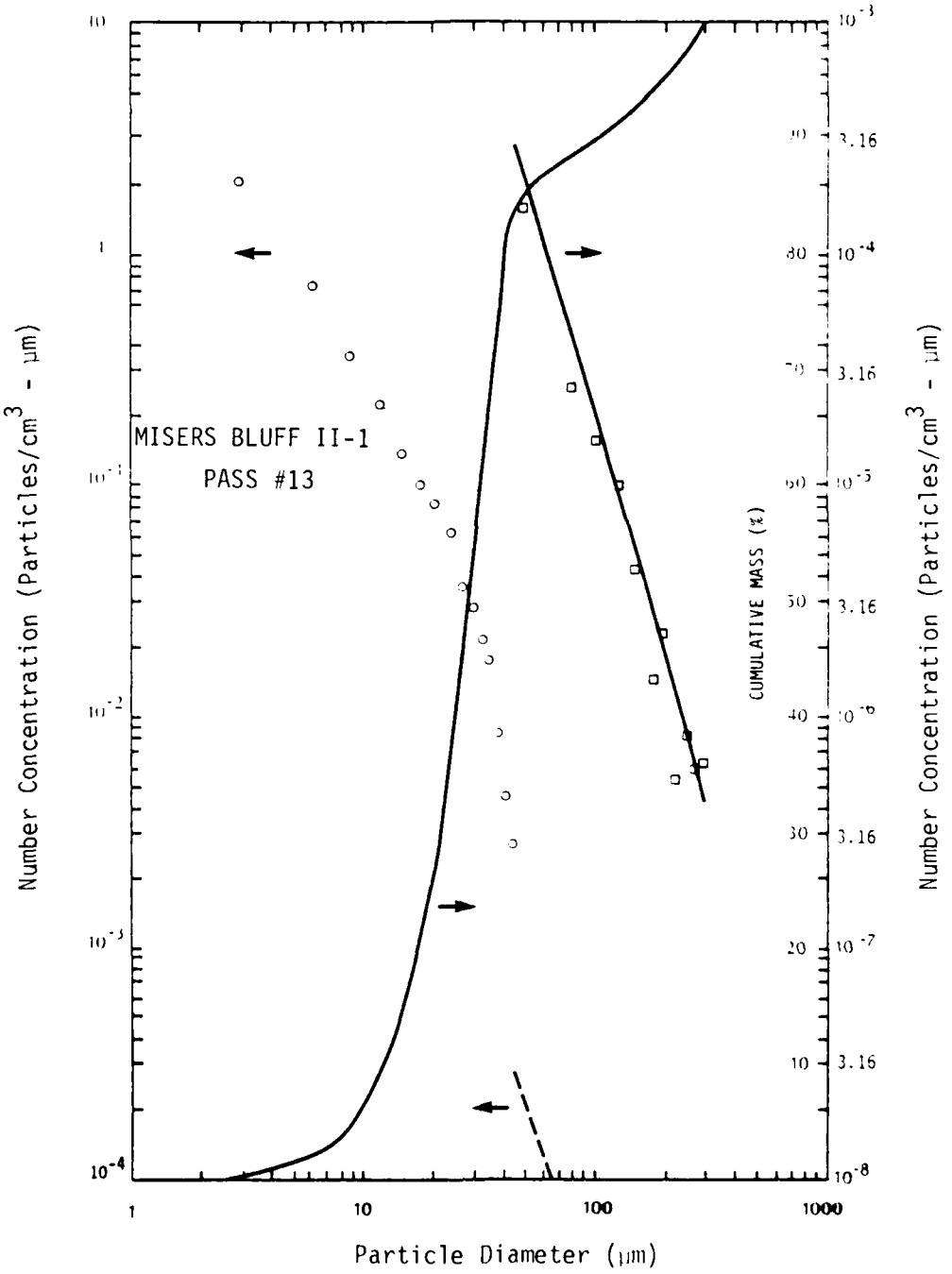

Figure 2.11(a) MISERS BLUFF II-1, Pass 13, Particle Size and Cumulative Mass Distributions

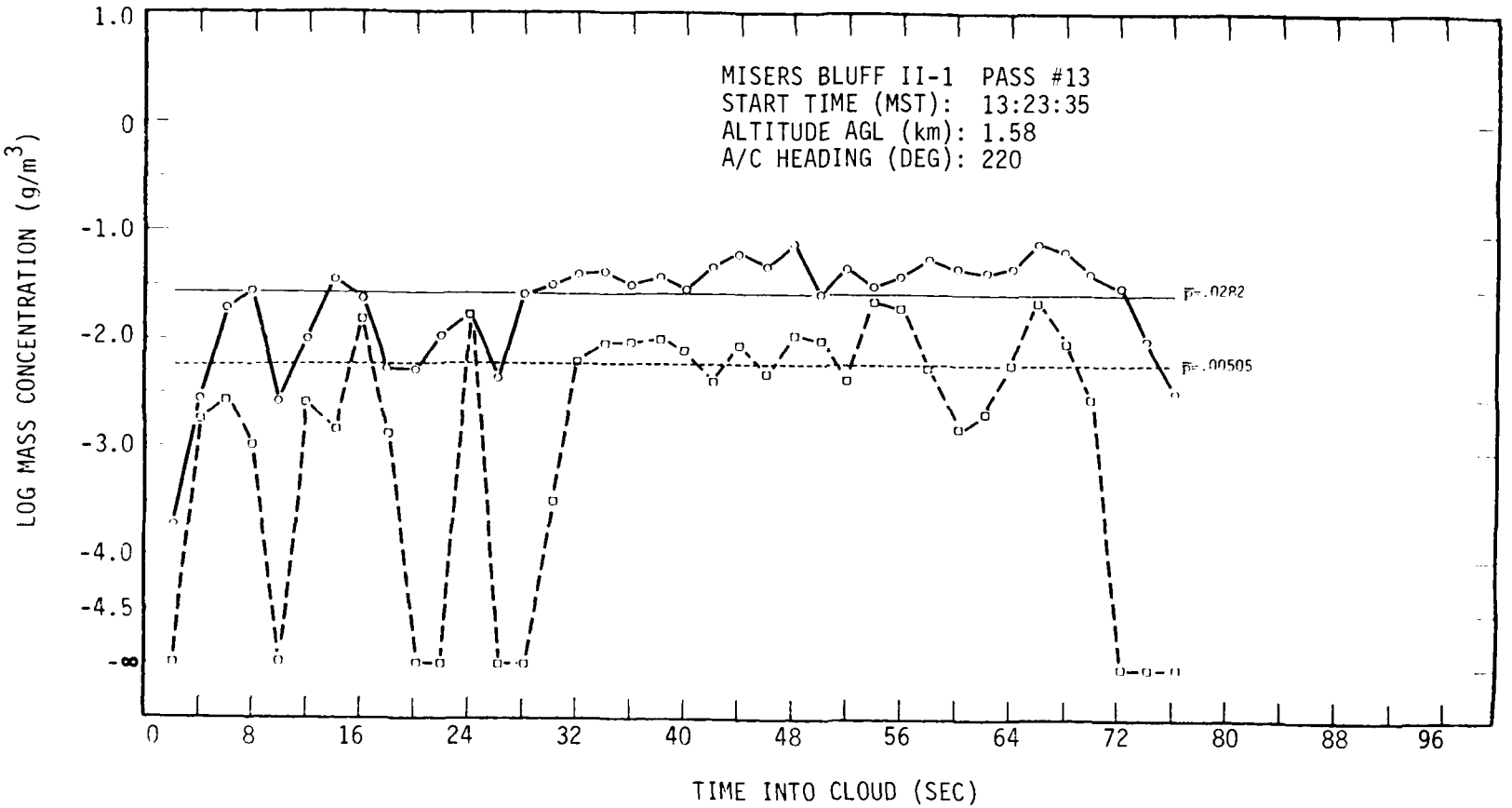

Figure 2-11(b) MISERS BLUFF II-1, Pass 13, Mass Concentration Time History

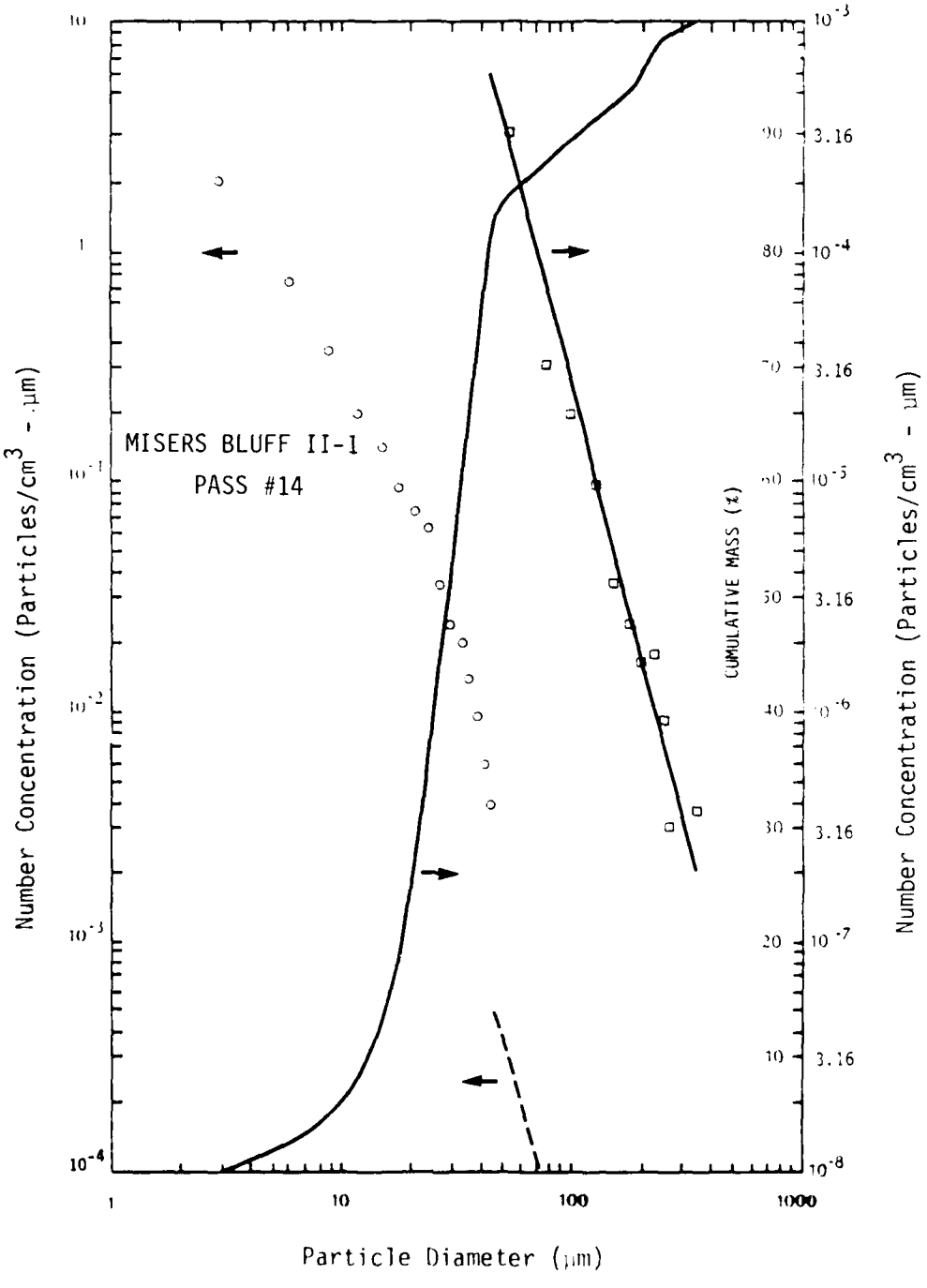

Figure 2.12(a) MISERS BLUFF II-1, Pass 14, Particle Size and Cumulative Mass Distributions

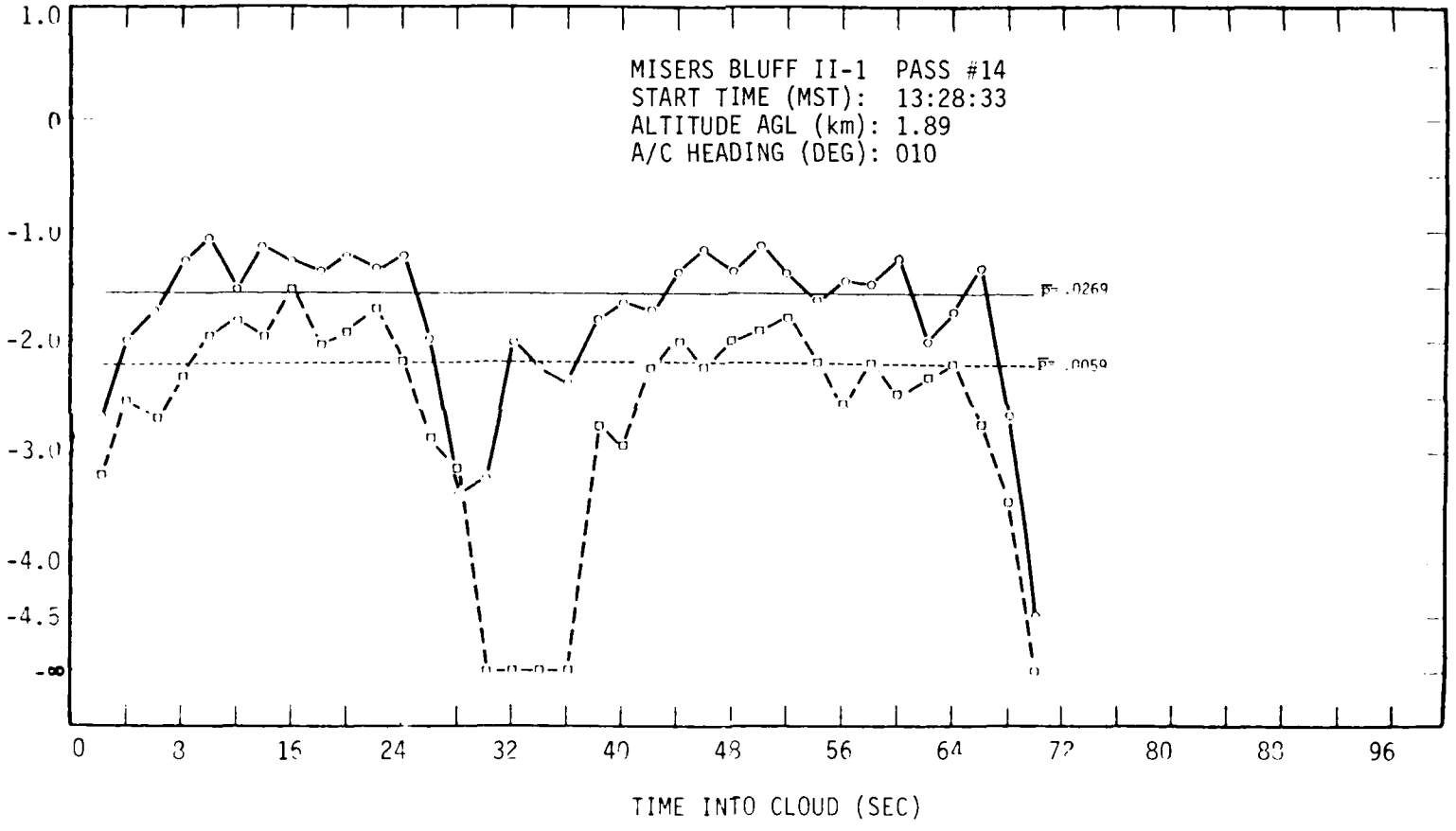

Figure 2.12(b) MISERS BLUFF II-1, Pass 14, Mass Concentration Time History

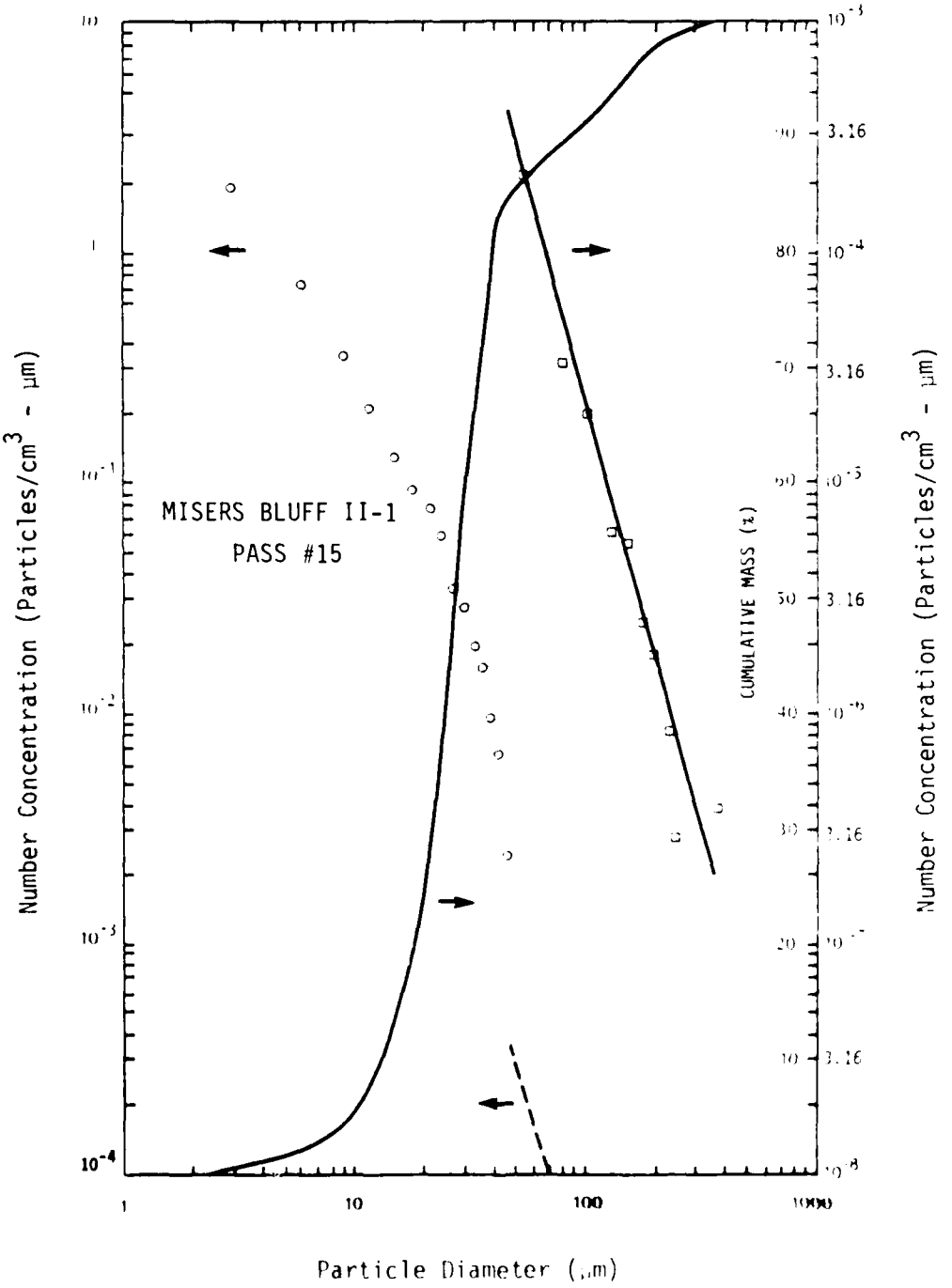

Figure 2.13(a) MISERS BLUFF II-1, Pass 15, Particle Size and Cumulative Mass Distributions

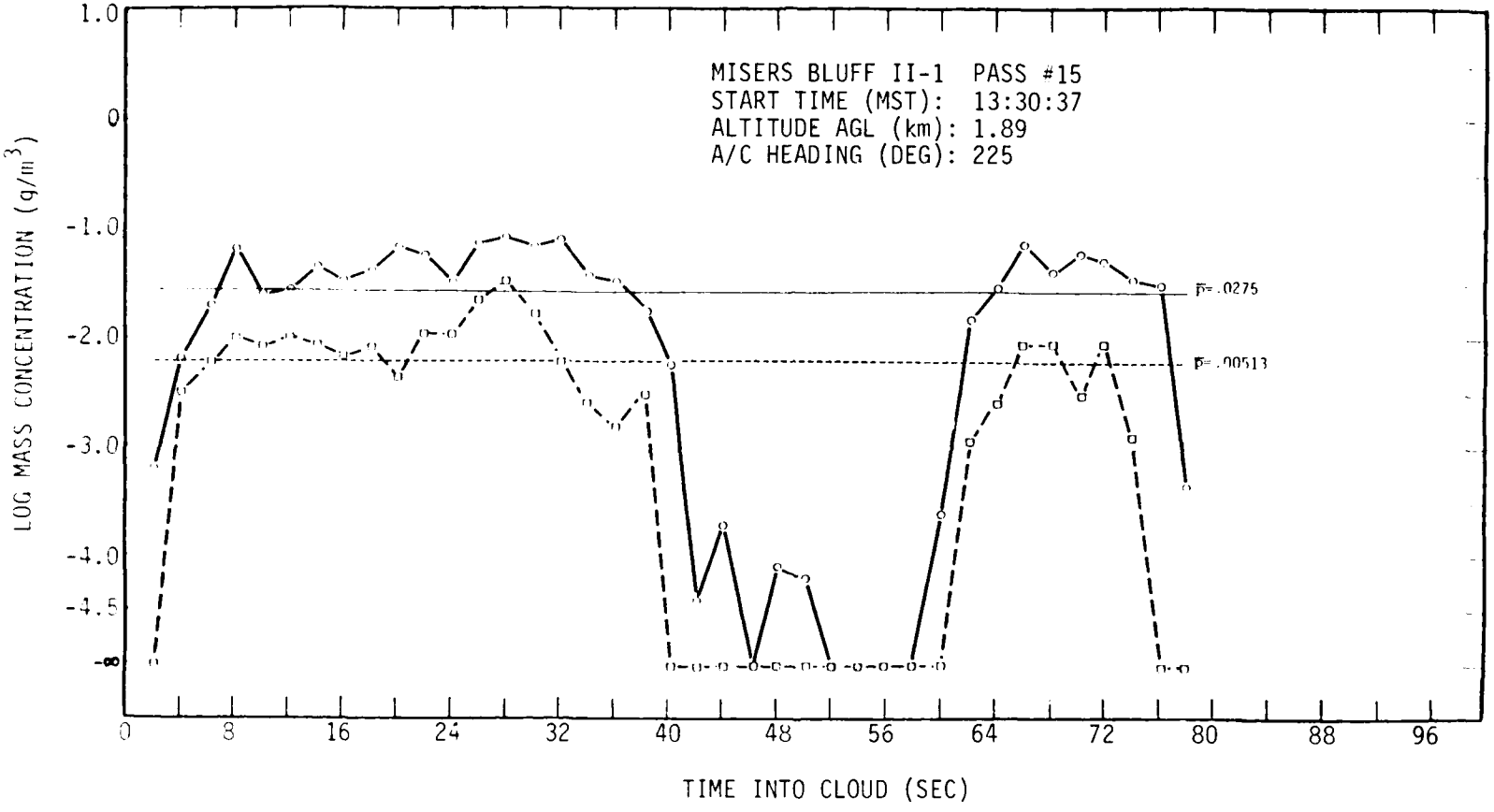

Figure 2.13(b) MISERS BLUFF II-1, Pass 15, Mass Concentration Time History

2-4 RECONSTRUCTING THE MISERS BLUFF II-1 DUST CLOUD

In order to gain more insight into the gross mass loading features of the MBII dust clouds, it was necessary to reconstruct the clouds at various times after burst. Although the measured mass concentrations are very useful in identifying radial variations in dust densities at one altitude and one time, they do not give the reader "snapshots" of both clouds at any given time for comparison purposes.

Based on cloud dimensions at a specified time after burst, particle fall velocities, and in-situ sampling data, it is possible to approximate the mass concentrations within various layers of the cloud at any specified time after burst. The times selected for the MBII dust cloud analysis were ten (T+10) and twenty (T+20) minutes after detonation. At times prior to this (pre-stabilization) it was felt that flow fields within the dust clouds (cloud buoyancy and ambient lapse rate operate interactively) would be so uncertain that any analysis based on them would not be meaningful.

The basic methodology followed in reconstructing the dust clouds was to take pass totalled mass spectral data and, depending on what time the data was acquired with reference to the specified cloud reconstruction time (either before or after), raise or lower the particles to the cloud layer in which they would be at the specified time. For instance, if the cloud was to be reconstructed at T+10 minutes, some particles that were sampled at T+5 minutes may be on the ground at T+10 minutes. Similarly, particles sampled at T+15 minutes would have to have been in cloud layers above the sampling altitude at T+10 minutes.

The distance that the various sized particles were raised or lowered depended only on when they were sampled and their terminal fall velocities. Pass mid-point times were used to specify the times when the pass totalled mass spectral data were acquired. A further simplification to the calculations was made possible by assuming that dust particles 47 μm sampled in a cloud layer would remain in that same cloud layer over the periods of time considered in

reconstructing the clouds. This assumption is acceptable when one realizes the terminal fall velocity of a 47 μm particle is only ~7 m/min and, at most, twenty minutes of dust particle vertical motion has been considered in the analysis. (See Appendix D for assumptions concerning particle terminal fall velocities used in this analysis). The final variable, dust cloud dimensional data at various times-after-burst, was obtained from either photographic documentation of the MBII dust clouds (Ref. 5) or from the sampling pass lengths at times near cloud reconstruction times.

2-4.1 The MBII-1 Dust Cloud at Ten Minutes After Detonation

Based on the methodology and assumptions outlined in the previous paragraphs, the MBII single burst dust cloud was reconstructed at ten minutes after detonation; the resulting mass loading (g/m^3) calculations as a function of altitude are presented in Table 2.2. The format for Table 2.2 is almost identical to that used in Table 2.1. Pass numbers, times-after-burst, and sampling altitudes are presented on the top of the table, while the top and bottom of cloud layers sampled in a particular pass are located on the left-hand side of the table. Tabulated values in Table 2.2 for particles ~47 μm and ~47 μm at the various cloud layers are now mass values (g) as opposed to values of mass concentrations (g/m^3) in Table 2.1. The four columns on the right-hand side of Table 2.2 yield values of total mass at altitude (obtained by summing mass contributions from all particle sizes at a given altitude), cumulative mass as measured from the cloud top, volume in cloud layer at T+10 minutes (calculated based on the estimated T+10 minute cloud diameter of ~1700 m), and calculated values of average mass concentrations at altitude.

Several features of the tabulated data should be pointed out. As previously mentioned, the mass contribution from particles with diameters ~47 μm was not moved out of the cloud layer where the particles were sampled; hence, it is not "spread out" by time into other cloud layers. Further, the mass spectral data obtained during sampling

Table 2.2 MISERS BLUFF II-1 Dust Cloud Reconstructed at Ten Minutes After Detonation

Pass #		3	4	5	6	7	8	9	12	13	14	15	Total Mass at Altitude (g)	Cumulative Mass (g)	Volume in Cloud Layer At T+10 Minutes (m^3)	Average Mass Concentration At T+10 Minutes (g/m^3)	
TAB (Min)		4.03	4.63	5.87	6.77	8.73	10.43	11.30	16.30	19.23	24.15	26.15					
Altitude (m)		300	360	410	550	670	790	790	1280	1580	1890	1890					
Distribution of Mass (g) With Altitude at 10 Minutes After Detonation																	
Particle Size (Spherical Particles)		< 2.37 μm	2.37 μm														
									6.17+6	6.90+6	8.50+6	6.88+6	2.85+7	2.85+7	Above Cloud		
	2500								9.17+6	6.00+6	1.65+6	2.85+6	1.97+7	4.82+7	1.02+9	1.93-2	
	2045 (15)	6.61+7							5.47+6	3.68+6	4.01+6	2.45+6	1.55+8	2.03+8	6.94+8	2.23-1	
	(14)	6.45+7							5.47+6	3.68+6							
	1735 (13)	1.33+8							1.25+7	3.77+6			1.49+8	3.52+8	6.83+8	2.18-1	
	1430 (12)	1.81+8						5.23+5	8.02+6				1.90+8	5.42+8	8.85+8	2.15-1	
	1045 (9)	1.58+7						1.80+6					4.93+7	5.92+8	6.83+8	7.22-2	
	(8)	2.62+7					5.31+6										
	730 (7)	1.74+7				1.32+6							1.87+7	6.10+8	2.69+8	6.96-2	
	610 (6)	2.32+7			1.13+6	9.61+5							2.53+7	6.36+8	2.91+8	8.69-2	
	480 (5)	2.71+7			8.14+5	3.09+5							2.82+7	6.64+8	2.13+8	1.33-1	STEM AVG .141
	365 (4)	1.36+7		1.11+6	2.34+5								2.01+7	6.84+8	1.23+8	1.63-1	
	330 (3)	9.56+7	1.09+6	1.89+6	1.87+6	2.15+6							1.03+8	7.86+8	7.39+8	1.39-1	
	0		1.25+6	1.80+6	8.70+5	1.44+6							6.30+6	7.94+8	On Ground		

pass 8 from particles >47 μm is not "spread-out" into other cloud layers due to the proximity of the data acquisition time and cloud reconstruction time. For mass spectral data obtained in subsequent sampling passes, the mass is distributed in and above the sampling altitude while, for sampling passes made prior to pass 8, the mass is distributed in and below the sampling altitude. Finally, pass data from passes 3, 4, and 5 have been averaged in calculating the average stem mass concentration.

One apparent contradiction does exist in the data in Table 2.2 and that is, starting with pass 12, the distribution of mass extends above the visible, MBII-1 cloud top (2500m). There are two possible explanations for this inconsistency in the data: (1) the larger dust particles are probably not spherical in shape and, hence, their terminal fall velocities have been overestimated by the assumptions made in this analysis (see Appendix D); and (2) the larger particles may be organics (low specific gravity) whose mass contribution could be ignored. Whatever the reason, the mass lofted to altitudes greater than the visible cloud top comprises only 3.6 percent of the total cloud mass; therefore, it is not felt that this inconsistency creates a significant perturbation in the analysis.

2-4.2 The MBII-1 Dust Cloud at Twenty Minutes After Detonation

Following an analysis identical to that used in reconstructing the MBII-1 cloud at T+10 minutes, the dust cloud was also reconstructed at twenty minutes after detonation. Table 2.3 presents the mass loading calculations for the T+20 minute cloud and is identical in format to Table 2.2; the observed cloud diameter is now 4400m.

Due to the relatively late time of this reconstructed cloud with respect to aircraft sampling time, it can be seen from Table 2.3 that the calculated mass in all passes made prior to pass 13 is now "falling out" of the cloud. Further, the "late time" fallout (on ground) accounts for only ~2.2 percent of the total mass lofted (7.9×10^8g) which supports the observation that only approximately

Table 3.3 MISERS BLUFF II-1 Dust Cloud Reconstructed at Twenty Minutes After Detonation

Pass # TAR (Min) Altitude (m)		3 4.03 300	4 4.63 360	5 5.87 410	6 6.77 550	7 8.73 670	8 10.43 790	9 11.30 790	12 16.30 1280	13 19.23 1580	14 24.15 1890	15 26.15 1890	Total Mass at Altitude (g)	Cumulative Mass (g)	Volume in Cloud Layer At T+20 Minutes (m^3)	Average Mass Concentration At T+20 Minutes (g/m^3)	
		Distribution of Mass (g) With Altitude at 20 Minutes After Detonation															
		Particle Size (Spherical Particles)															
		< 22 μm	> 22 μm														
	2500											1.27+6	8.51+6	9.78+6	9.78+6	Above Cloud	
	2045											7.28+6	3.63+6	1.09+7	2.07+7	6.81+9	1.59-3
	(15)	6.61+7															
	(14)	6.45+7										5.66+6		1.36+8	1.57+8	4.66+9	2.92-2
	1735																
	(13)	1.33+8									2.40+7			1.57+8	3.14+8	4.59+9	3.42-2
	1430																
	(12)	1.81+8								2.04+7				2.01+8	5.15+8	5.94+9	3.38-2
	1035																
	(9)	1.58+7								1.33+7				5.53+7	5.70+8	4.59+9	1.21-2
	(8)	2.63+7															
	730																
	(7)	1.74+7						1.10+6	3.53+5	3.15+6				2.20+7	5.92+8	1.81+9	1.22-2
	610																
	(6)	2.32+7					5.21+5	3.44+5	2.56+5	9.88+6				3.42+7	6.26+8	1.96+9	1.75-2
	480																
	(5)	2.71+7				7.58+5	2.00+5		1.98+5					2.83+7	6.54+8	1.43+9	1.98-2
	385																
	(4)	1.88+7					2.21+5	4.78+5						1.95+7	6.74+8	8.27+8	2.36-2
	310																
	(3)	9.56+7	6.31+5	3.42+5	1.11+6	7.30+5	3.90+5	1.04+6	3.51+5					1.01+8	7.75+8	4.96+9	2.03-2
	0																
			1.66+6	2.22+6	2.76+6	4.23+6	1.27+6	2.36+6	1.39+6					1.75+7	7.93+8	On Ground	

STEM AVG 2.06-2

15 percent of the cloud's mass (as sampled) could be attributed to particles ≥47 μm. Also note that the mass lofted above the visible cloud top now accounts for only ~1 percent of the total mass lofted.

2-4.3 Comparisons of the MBII-1 Dust Cloud at T+10 and T+20 Minutes

Figure 2.14 summarizes the effects of reconstructing the MBII-1 dust cloud by graphically revealing how several mass loading parameters are changing with time and altitude. Figure 2.14(a) depicts the dust cloud mass contribution from particles ≥47 μm and shows where this mass contribution is distributed at T+10 and T+20 minutes within the cloud. As would be expected, much of the mass contribution from these particles in the upper layers of the cloud at T+10 minutes is being depleted with time and redistributed throughout the lower regions of the cloud at T+20 minutes.

Figure 2.14(b) (plotted on same altitude scale as Figure 2.14(a)) depicts how the average mass concentration (all particle sizes) is changing with time and altitude. From Tables 2.2 and 2.3 we can see that the mass aloft at T+10 and T+20 is nearly the same. However, due to cloud diffusion (cloud radius has increased by a factor of ~2.6), Figure 2.14(b) reveals an approximate factor of 7 decrease in average mass concentration with time. The similarity of the average mass concentration profiles at T+10 and T+20 minutes, as opposed to a "non-linear" difference between the curves in Figure 2.14(b), points out the fact that the MBII-1 dust cloud mass loading is being governed by the smaller particles aloft, i.e., 47 μm particles. Average mass concentrations from Table 2.1 (as sampled) have been included in Figure 2.14(b) to show how the cloud reconstruction processes have drastically modified the vertical distribution of the measured spectral data.

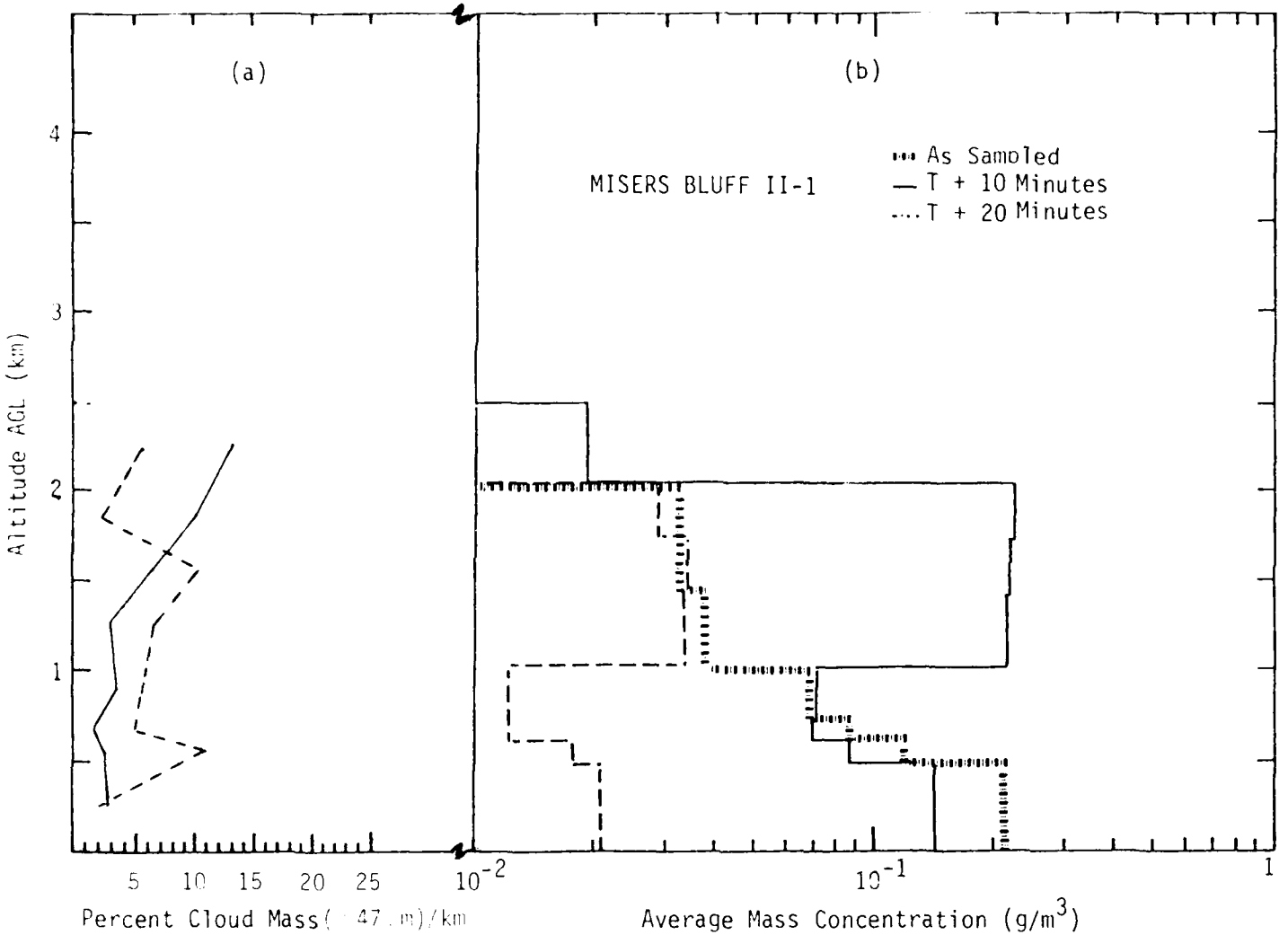

Figure 2.14. MISERS BLUFF II-1: Percent of Cloud Mass $\geq$ 47 μm and Average Mass Concentration As a Function of Altitude and Time After Detonation.

SECTION 3
THE MISERS BLUFF II MULTIPLE BURST DUST CLOUD

3-1 MBII-2 IN-SITU SAMPLING DATA SUMMARY

Twenty two in-situ sampling passes were accomplished by PMS in the MBII multiple burst dust cloud. Of these, sampling passes 2-11 were flown through the cloud as the aircraft ascended to the cloud top and are included in the multiple burst data cloud analysis.

Table 3.1 summarizes and profiles the MBII-2 sampling mission (note that the format is identical to Table 2.1). Pass-averaged mass concentrations (g/m^3) have been calculated from the measured particle number concentrations for each pass and are tabulated as a function of particle size, sampling altitude, and time of acquisition. The size range of particles contributing to the total mass concentration is consistent with the size ranges used in the MBII-1 dust cloud analysis so that mass loading comparisons can be readily made.

Passes 2, 3 and 4 were made through the cloud stem while the remaining passes were flown through the cloud cap. An interesting phenomena to note in Table 3.1 is that, unlike the MBII-1 cloud cap, mass concentrations are not systematically decreasing with time and altitude but seem to flucuate randomly throughout the sampling mission. Further, the calculated values of mass in each cloud layer are relatively uniform throughout the cloud cap as opposed to those calculated for the single burst cloud. The most probable reason for these two observations is that, while under the influence of generally light winds and little shear, wind induced diffusion did not play as great a role in "pulling" the MBII-2 dust cloud apart as was evidenced in the single burst dust cloud (see section 2-4.3).

Another intrinsic feature of the multiple burst dust cloud is the larger percentage of mass being contributed to the total mass lofted by particles >47 μm - approximately 25-35 percent in most passes as opposed to 15 percent in the single burst cloud. There are probably

Table 3.1 MISERS BLUFF II-2 In-Situ Sampling Data Summary

Pass #	2	3	4	5	6	7	8	9	10	11		Total Averaged Concentration (g/m^3)	Volume In Cloud Layer (m^3)	Mass In Cloud Layer (g)	Cumulative Cloud Mass (g)
TAB (Min)	6.31	8.0	10.08	12.31	15.06	17.84	20.44	23.96	26.48	30.64					
Altitude (m)	670	730	1130	1490	1890	2310	2500	2740	3020	3260					
Pass Averaged Mass Concentration (g/m^3) As Dust Cloud Was Sampled															
Particle Size (Spherical Particles)															
Pass Number	<.45 μm	>.45 μm													
3700															
3480															
(11)	6.12-2										9.90-3	7.16-2	7.11+9	5.09+8	5.09+8
3110															
(10)	9.55-2									4.46-2		1.40-1	6.77+9	9.48+8	1.46+9
2880															
(9)	4.57-2								2.31-2			6.88-2	5.96+9	4.10+8	1.87+9
2620															
(8)	1.35-1							4.54-2				1.80-1	3.51+9	6.32+8	2.50+9
2405															
(7)	1.02-1						2.55-2					1.27-1	2.70+9	3.43+8	2.84+9
2100															
(6)	2.14-1					1.11-1						3.25-1	2.90+9	9.42+8	3.78+9
1690															
(5)	7.21-2				4.57-2							1.18-1	6.20+9	7.32+8	4.52+9
1310															
(4)	1.07-1			6.03-2								1.67-1	1.58+9	2.64+8	4.78+9
960															
(3)	3.21-2		3.60-2									6.81-2	1.38+9	9.41+7	4.87+9
730															
(2)	1.23-1	1.16-1										2.39-1	1.00+9	2.39+8	5.11+9
0															

two contributing factors influencing this observation: (1) MBII-2 flow fields were sufficient to keep these larger particles aloft for sustained periods of time and; (2) the MBII-2 ANFO stack site geologies varied somewhat from the single burst GZ site geology.

The MBII-2 dust cloud mass loading analysis, based on the same assumptions made for the single burst cloud analysis (Section 2-1), revealed that the total mass lofted in the multiple burst dust cloud was 5.1×10^9 grams. Again, this value compares favorably with 5.2×10^9 grams determined by PMS in their independent analysis.

3-2 MBII-2 DETAILED SAMPLING PASS DATA

Figures 3.1-3.11 in this section are identical in format to those presented in Section 2-2. For each sampling pass used in the analysis, pass-averaged particle size and cumulative mass distributions have been plotted (Figures 3.X(a)) along with calculated mass concentrations within the cloud (Figures 3.X(b)); except sampling Pass 1 which was flown below the cloud cap and outside the visible stem. In the particle size distributions, circles represent particles · 47 μm, squares represent particles 47-470 μm, and triangles depict the size distribution of particles · 470 μm. For the mass concentration plots, the contribution from particles · 47 μm are plotted with circles (solid line) and that from particles · 47 are plotted with squares (dashed line).

3-3 GENERAL COMMENTS CONCERNING THE MBII-2 DUST CLOUD

3-3.1 Particle Size Distributions

As in the MBII-1 dust cloud, particle sizes ·47 μm are approximately distributed according to a power law (see Section 2-3.1), however, there appears to be more variation of the power "q" in the multiple burst dust cloud. For the particle size range 47-470 μm,

$$3.0 \cdot q \cdot 5.0$$

while for particles ·470 μm (except passes 3 and 9),

$$q \cdot 5.0$$

Again, it should be mentioned that the size distribution depicted in Figures 3.X(a) are based on pass-averaged data and significant variation in "q" will exist from point to point within a given pass and in the tail end of the distributions due to poor counting statistics.

3-3.2 Cumulative Mass Distributions

Passes 2 and 3 were flown through the visible stem of the cloud and the cumulative mass distributions show that the dust mass is fairly evenly distributed between particles less than and greater than 47 μm. At later sampling times, the major contribution to mass loading shifts toward the smaller particles where approximately 65-75 percent of the mass is found (except passes 9 and 11 where the contribution from particles <47 μm is 80-85 percent).

3-3.3 Mass Concentration Time Histories

Unlike the MBII-1 cloud penetrations, the highest mass concentration encountered in the MBII-2 cloud was in the cloud cap (pass 6) and not in the cloud stem. One reason for this is that because of operational problems, cloud penetrations in the single burst cloud began approximately two minutes before entry into the multiple burst cloud was possible, i.e., when stem mass concentrations were much higher. Another possibility is that flow fields within the multiple burst dust cloud were sufficient to keep those portions of the cloud containing the higher mass concentrations aloft for a sustained period of time, whereas, the mass in the MBII-1 dust cloud was rapidly being depleted by fallout through the stem region at very early times. Peak mass concentrations in the MBII-2 cloud were generally 3-4 times the average values; pass 5 had a peak value slightly 5 times the average mass concentration.

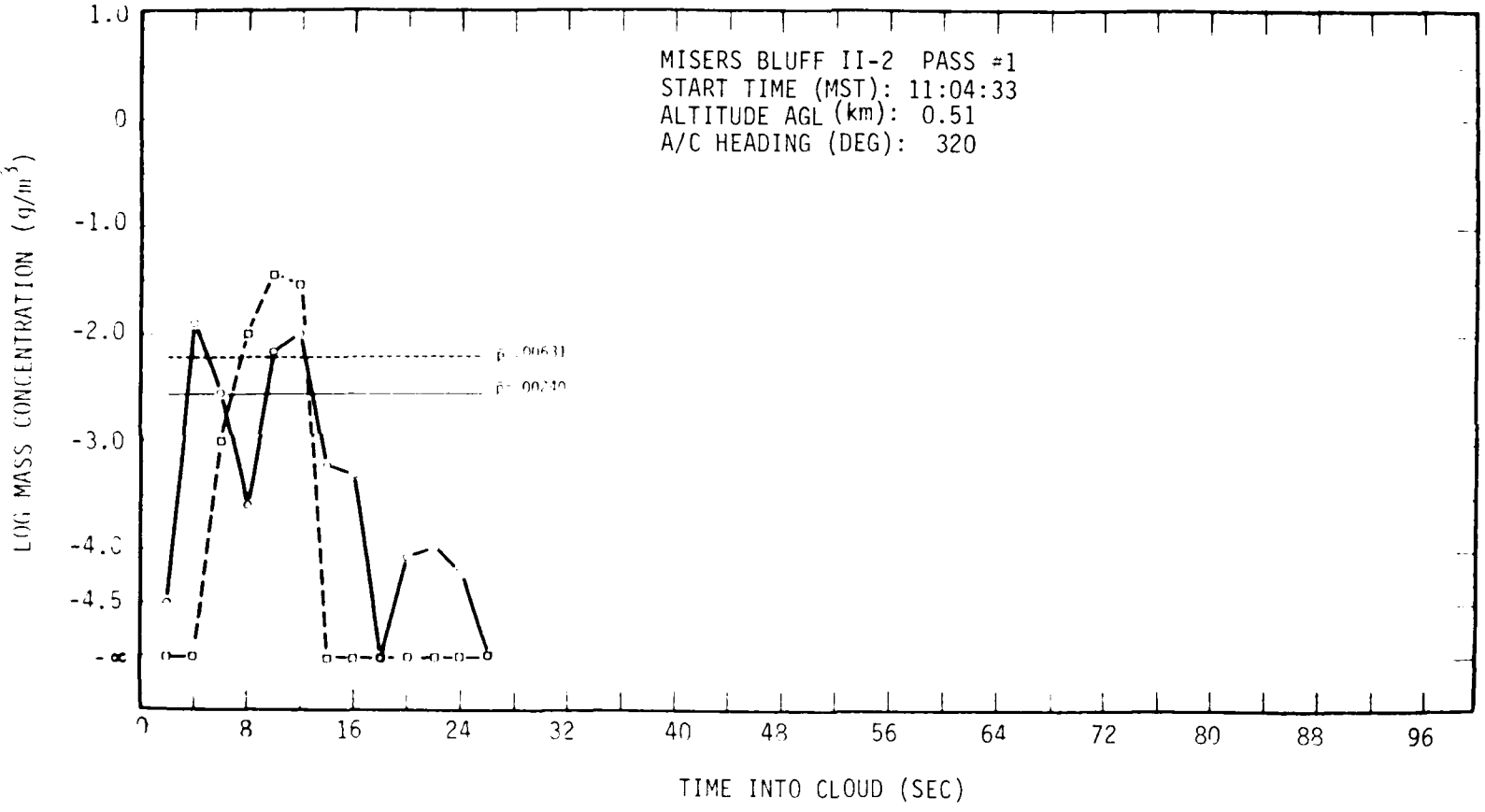

Figure 3.1. MISERS BLUFF II-2, Pass 1, Mass Concentration Time History

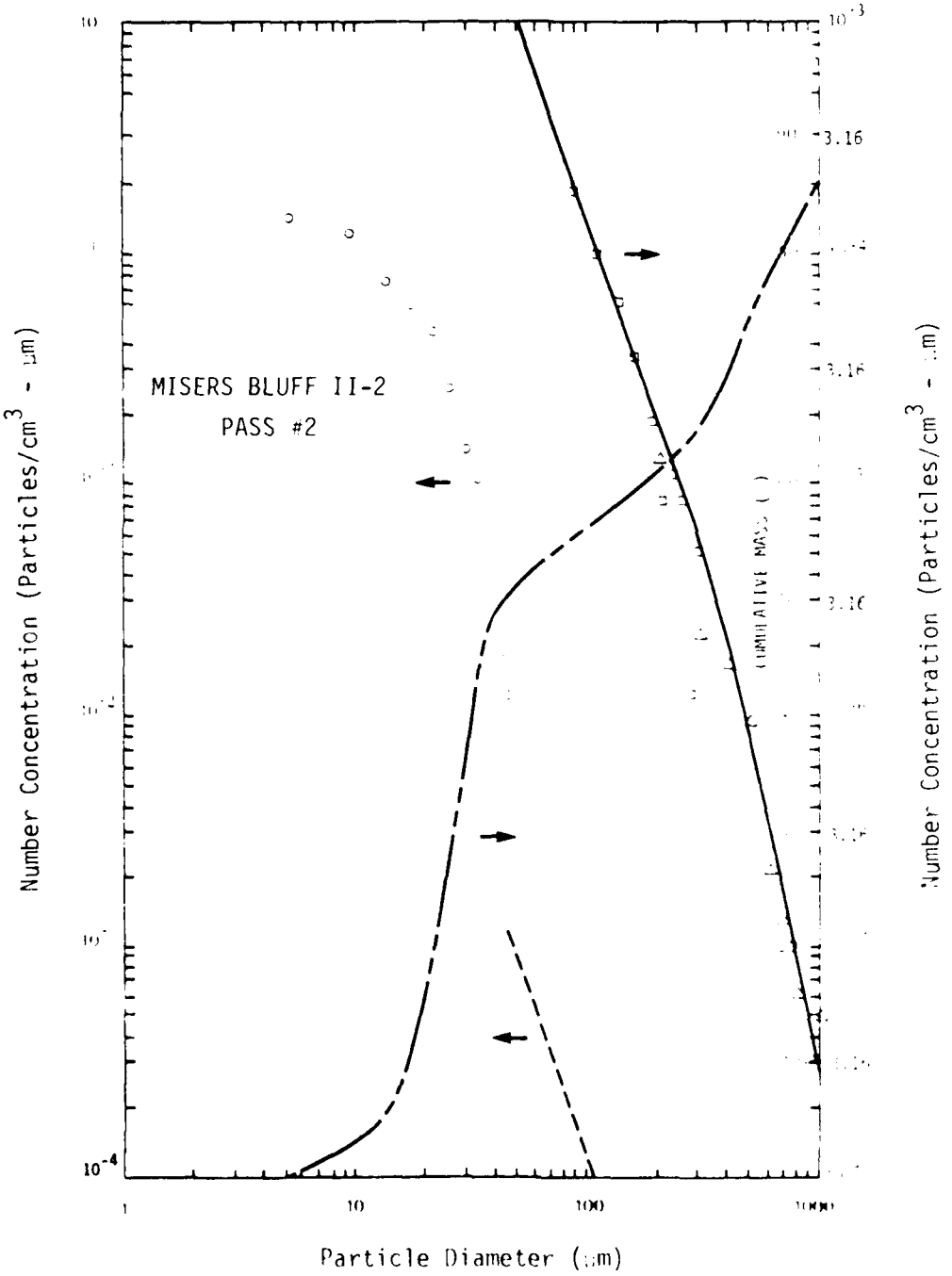

Figure 3.2(a). MISERS BLUFF II-2, Pass 2, Particle Size and Cumulative Mass Distributions

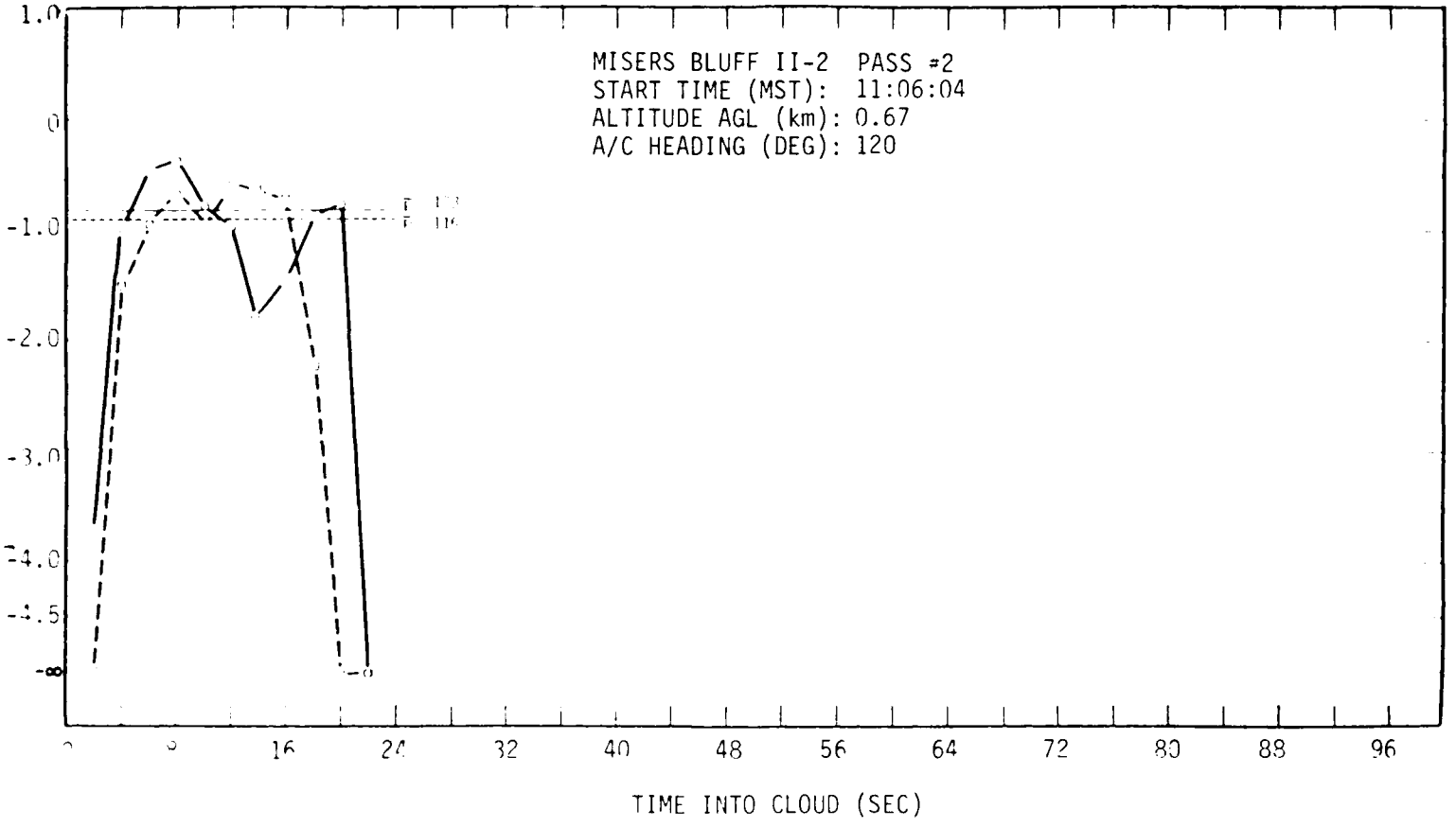

Figure 3.2(b). MISERS BLUFF II-2, Pass 2, Mass Concentration Time History

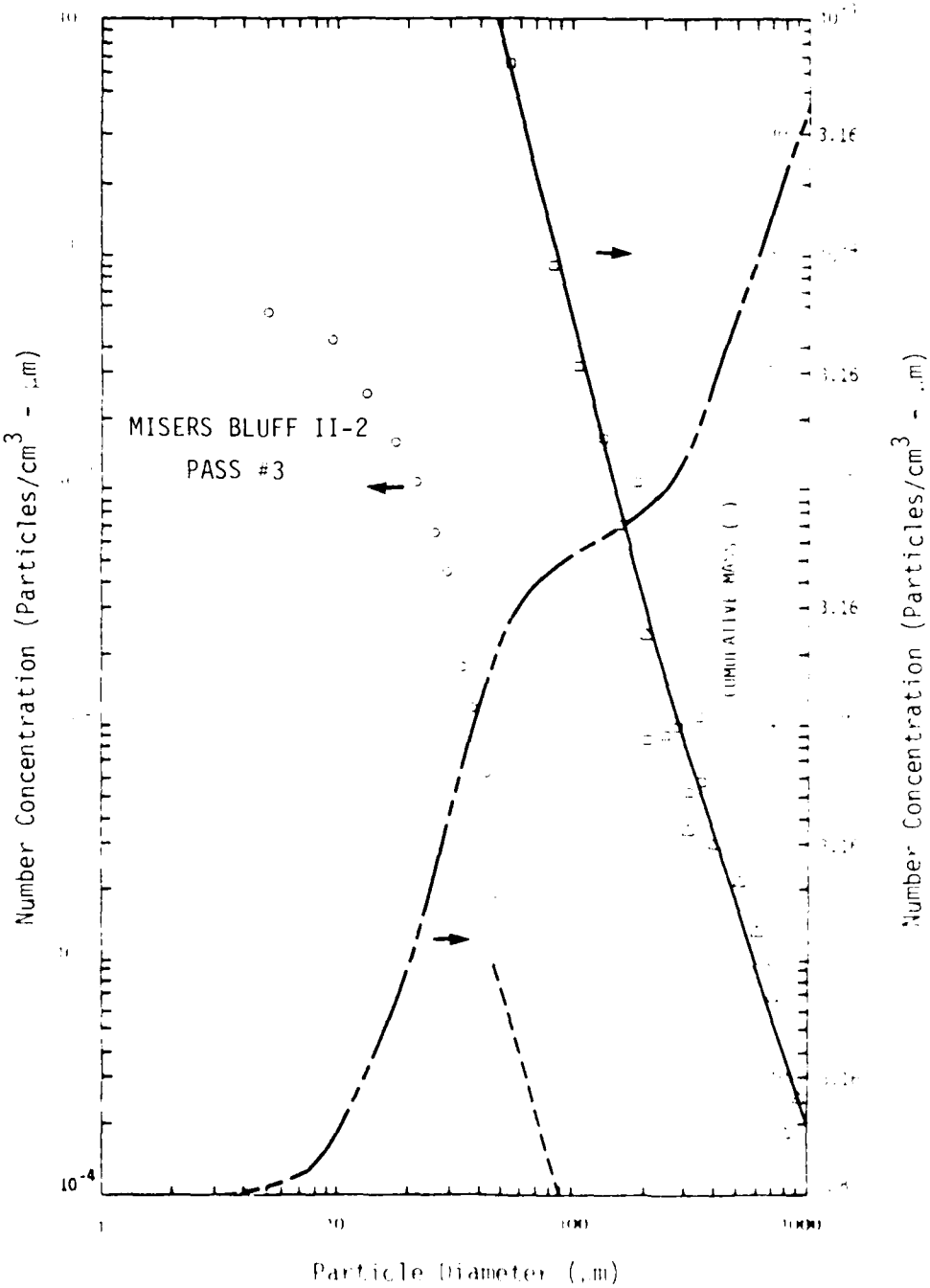

Figure 3.3(a). MISERS BLUFF II-2, Pass 3, Particle Size and Cumulative Mass Distributions

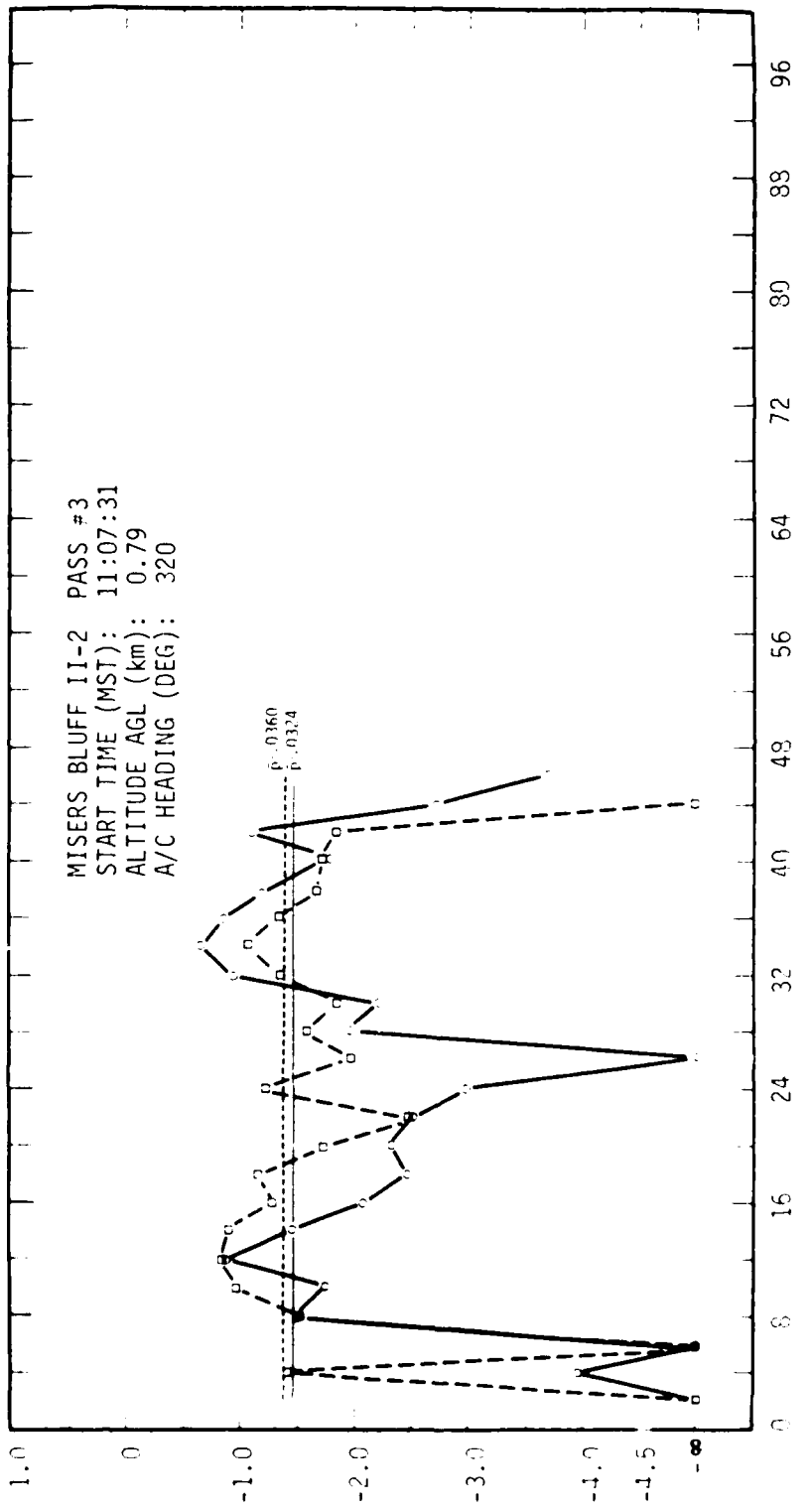

Figure 3.3(b). MISERS BLUFF II-2, Pass 3, Mass Concentration Time History

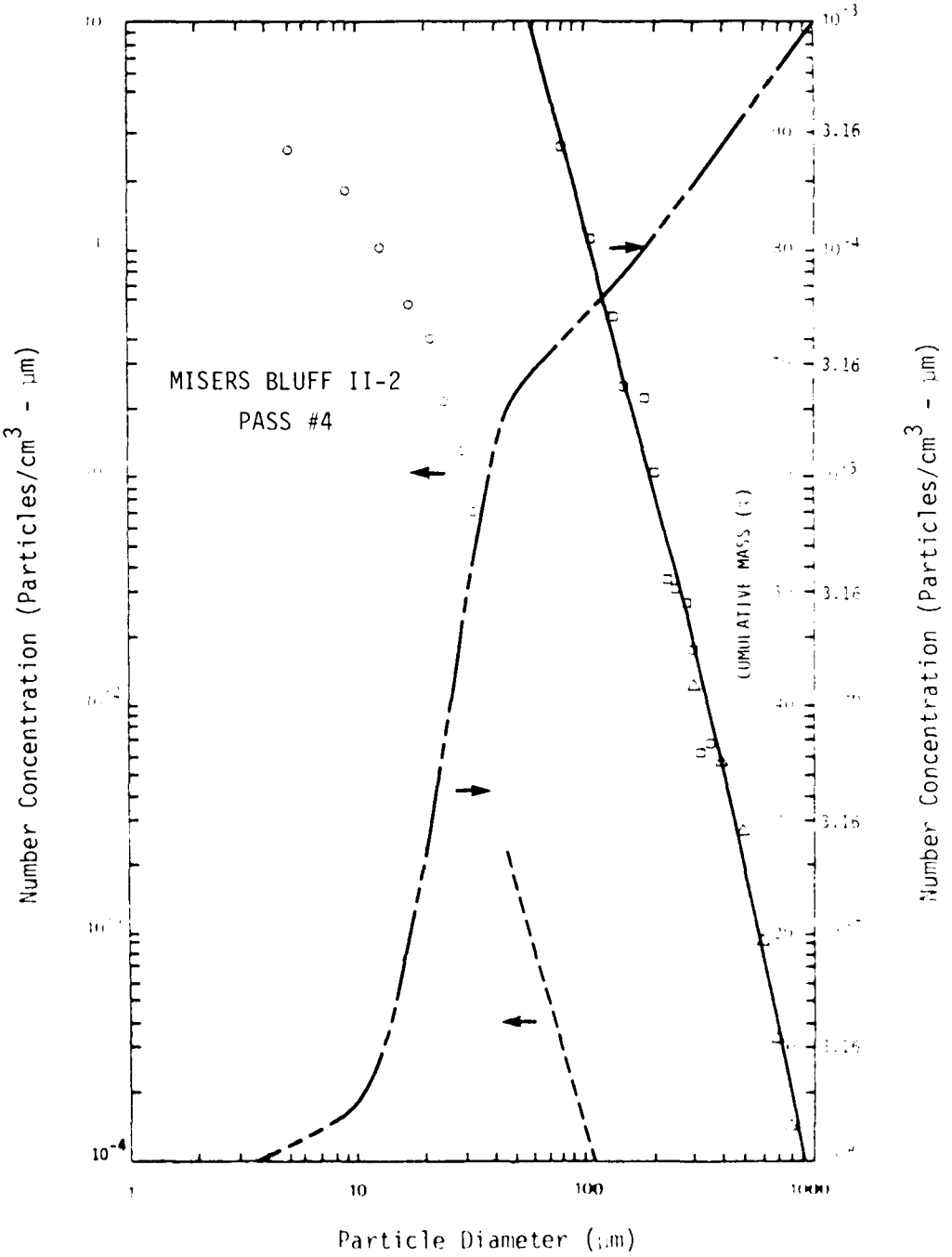

Figure 3.4(a). MISERS BLUFF II-2, Pass 4, Particle Size and Cumulative Mass Distributions

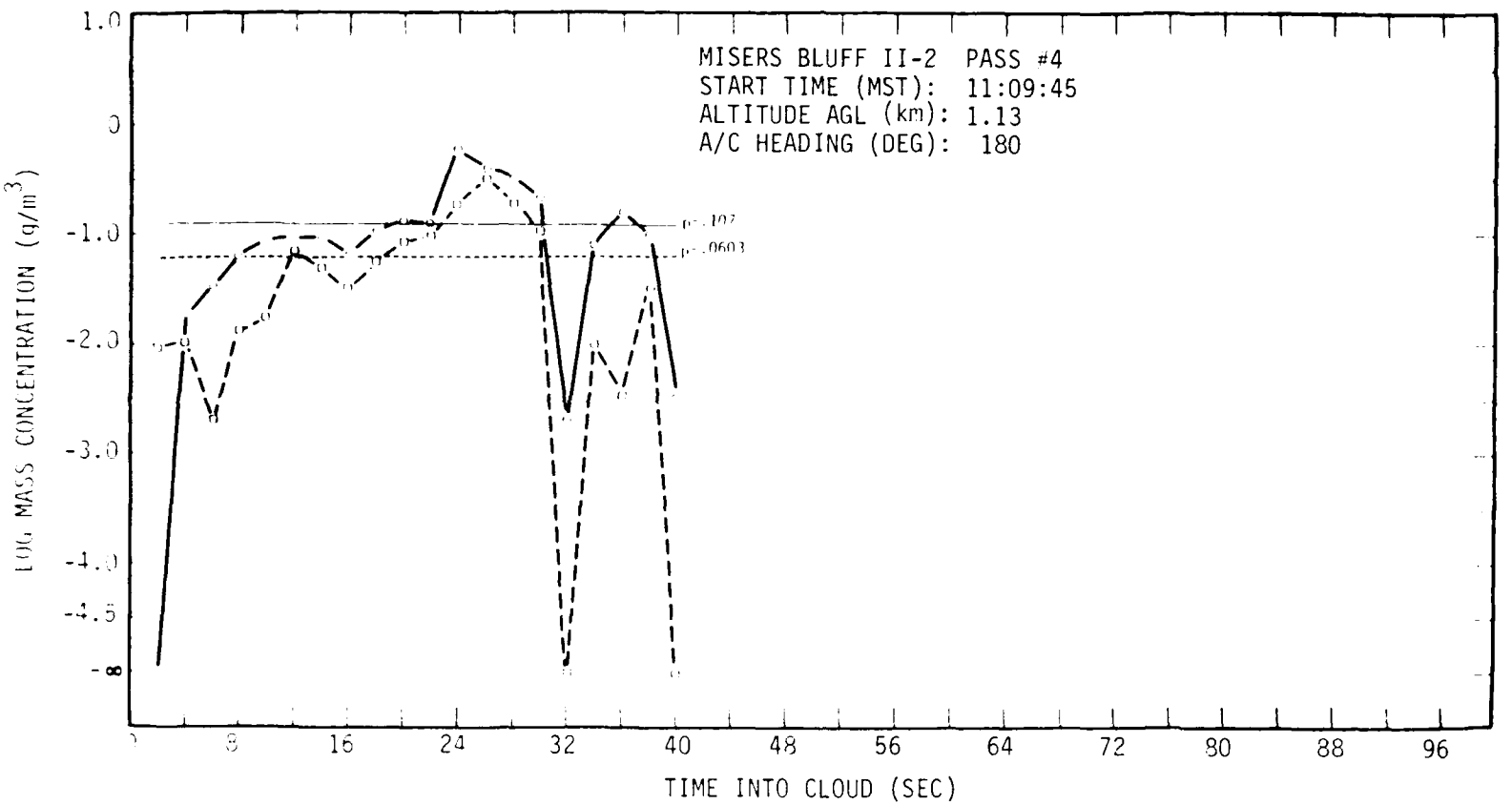

Figure 3.4(b). MISERS BLUFF II-2, Pass 4, Mass Concentration Time History

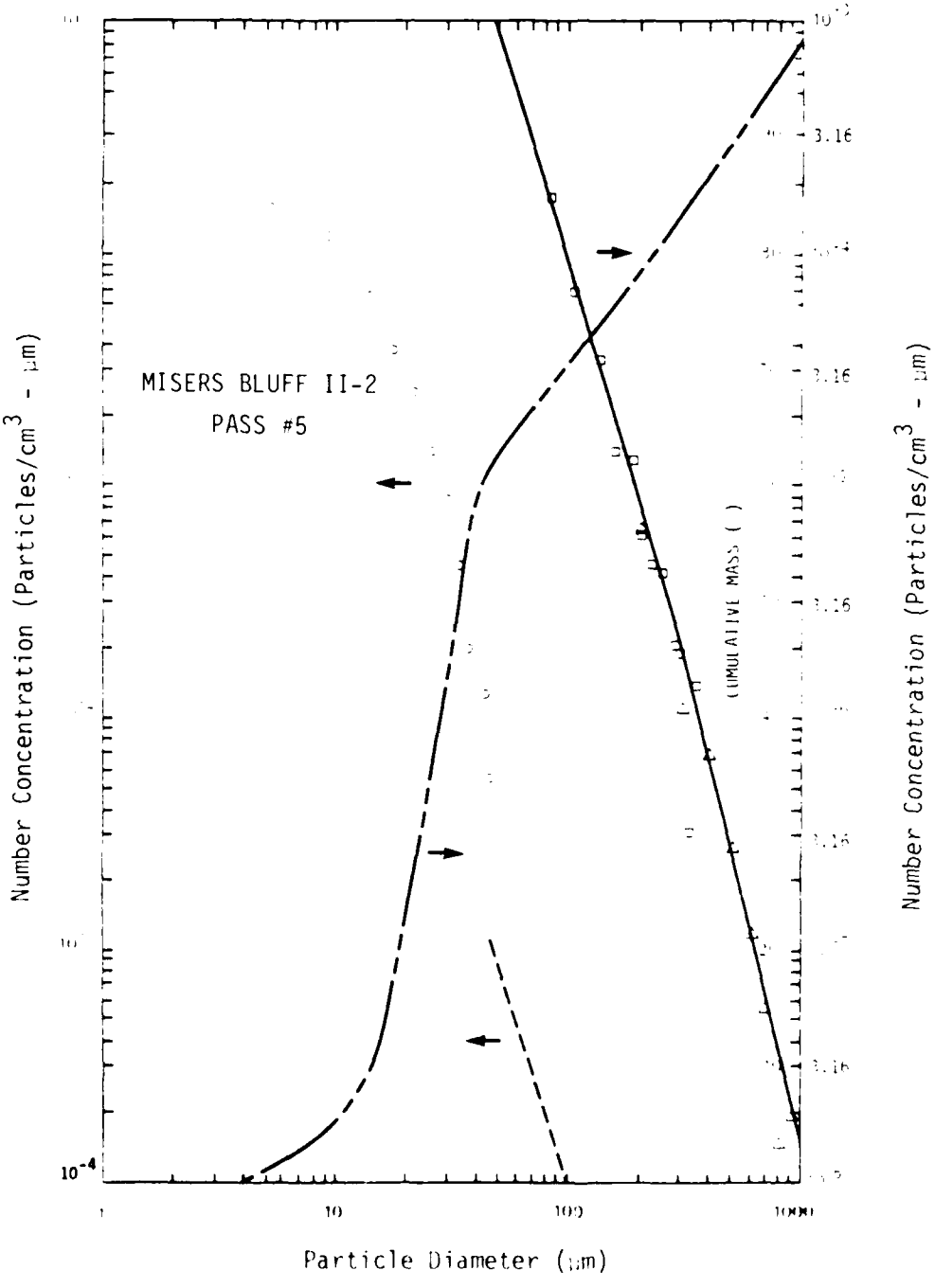

Figure 3.5(a). MISERS BLUFF II-2, Pass 5, Particle Size and Cumulative Mass Distributions

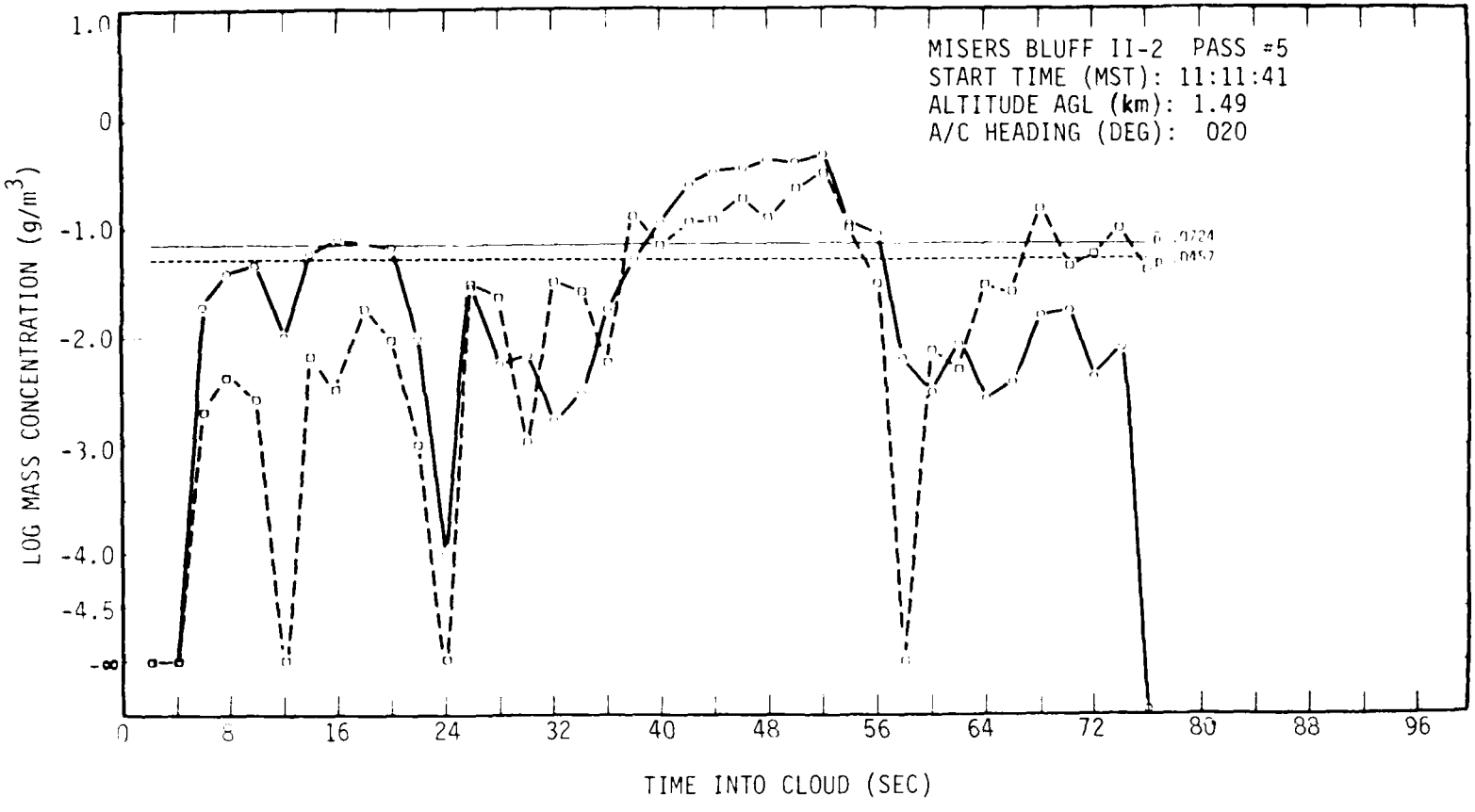

Figure 3.5(b). MISERS BLUFF II-2, Pass 5, Mass Concentration Time History

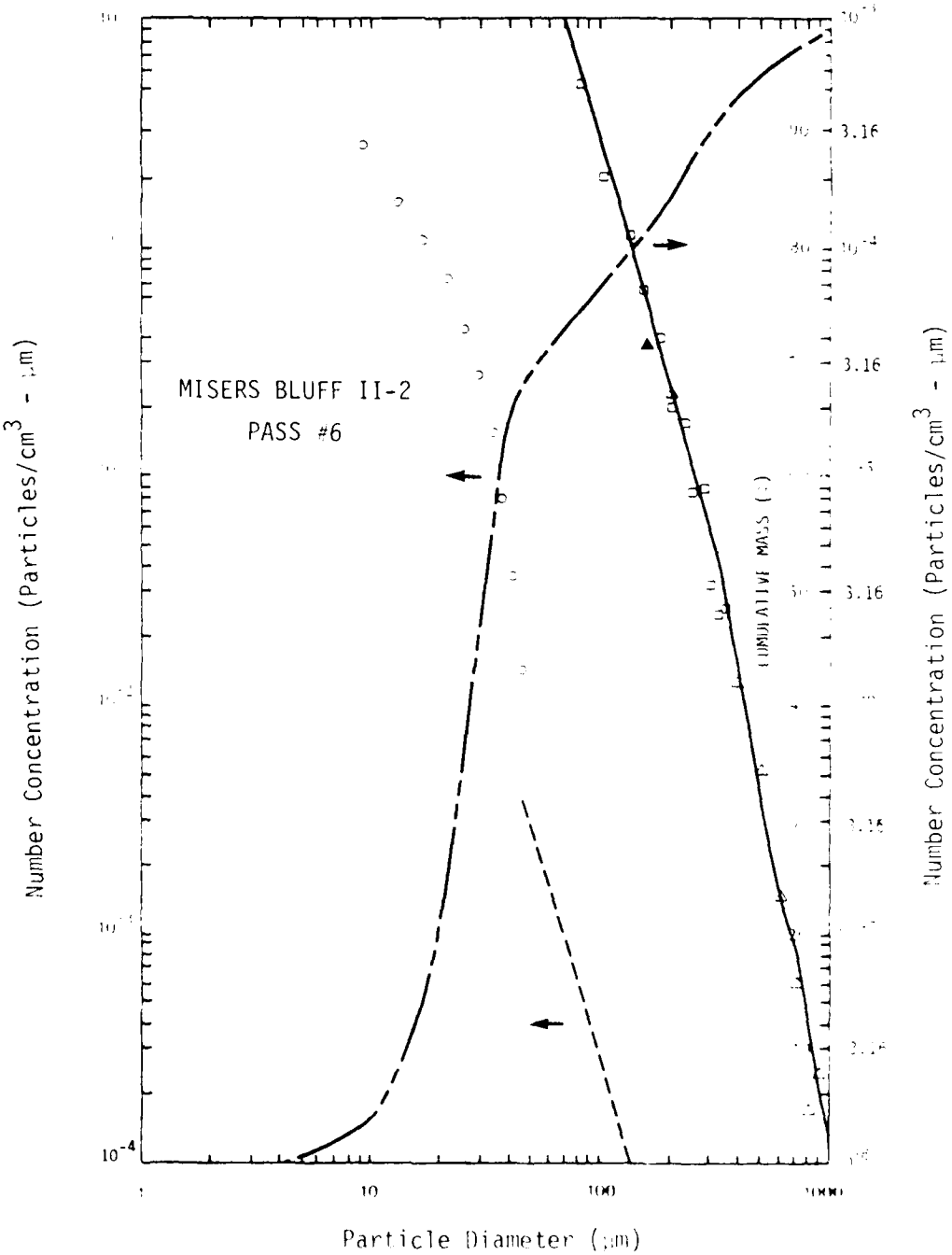

Figure 3.6(a). MISERS BLUFF II-2, Pass 6, Particle Size and Cumulative Mass Distributions

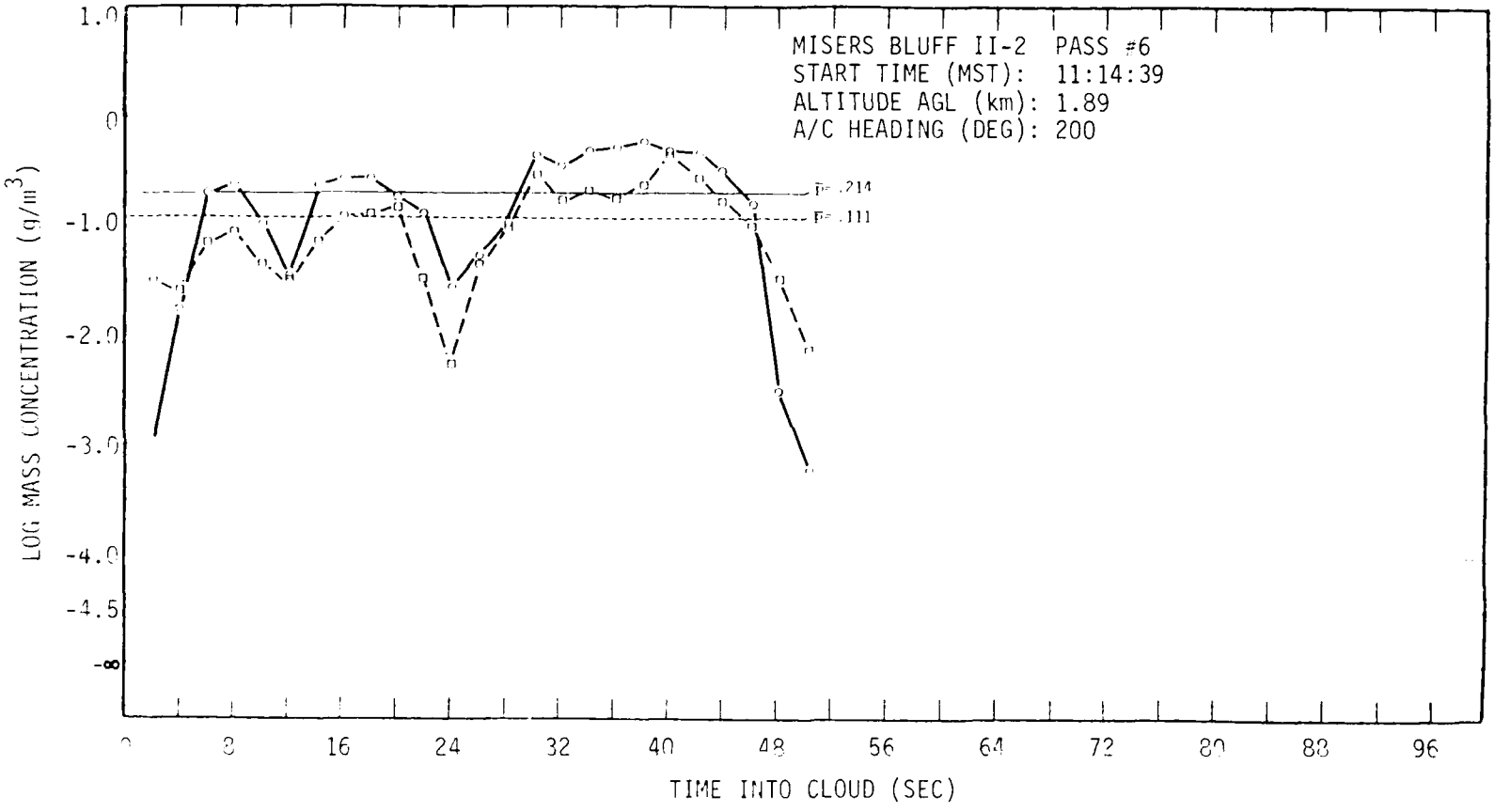

Figure 3.6(b). MISERS BLUFF II-2, Pass 6, Mass Concentration Time History

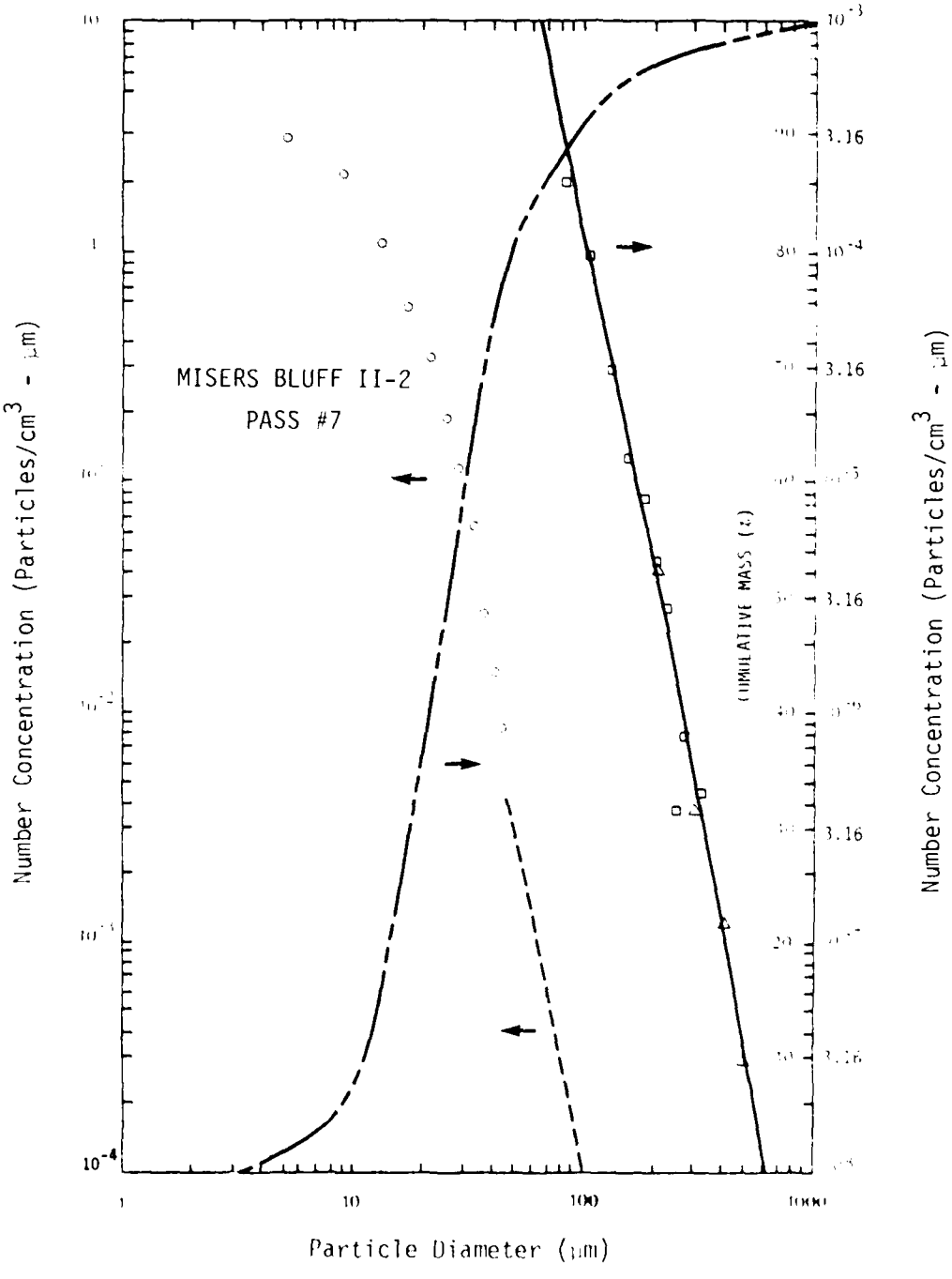

Figure 3.7(a). MISERS BLUFF II-2, Pass 7, Particle Size and Cumulative Mass Distributions

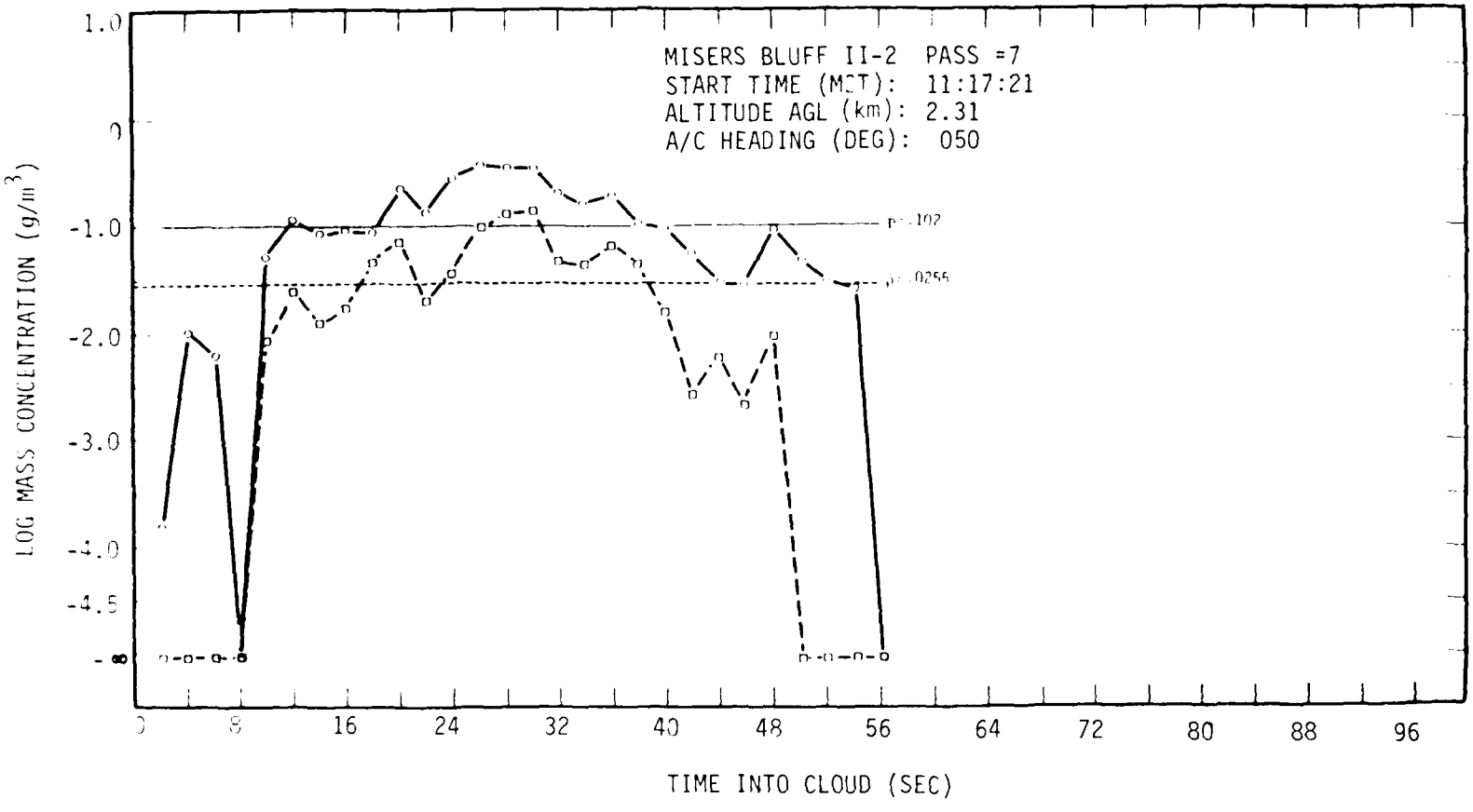

Figure 3.7(b). MISERS BLUFF II-2, Pass 7, Mass Concentration Time History

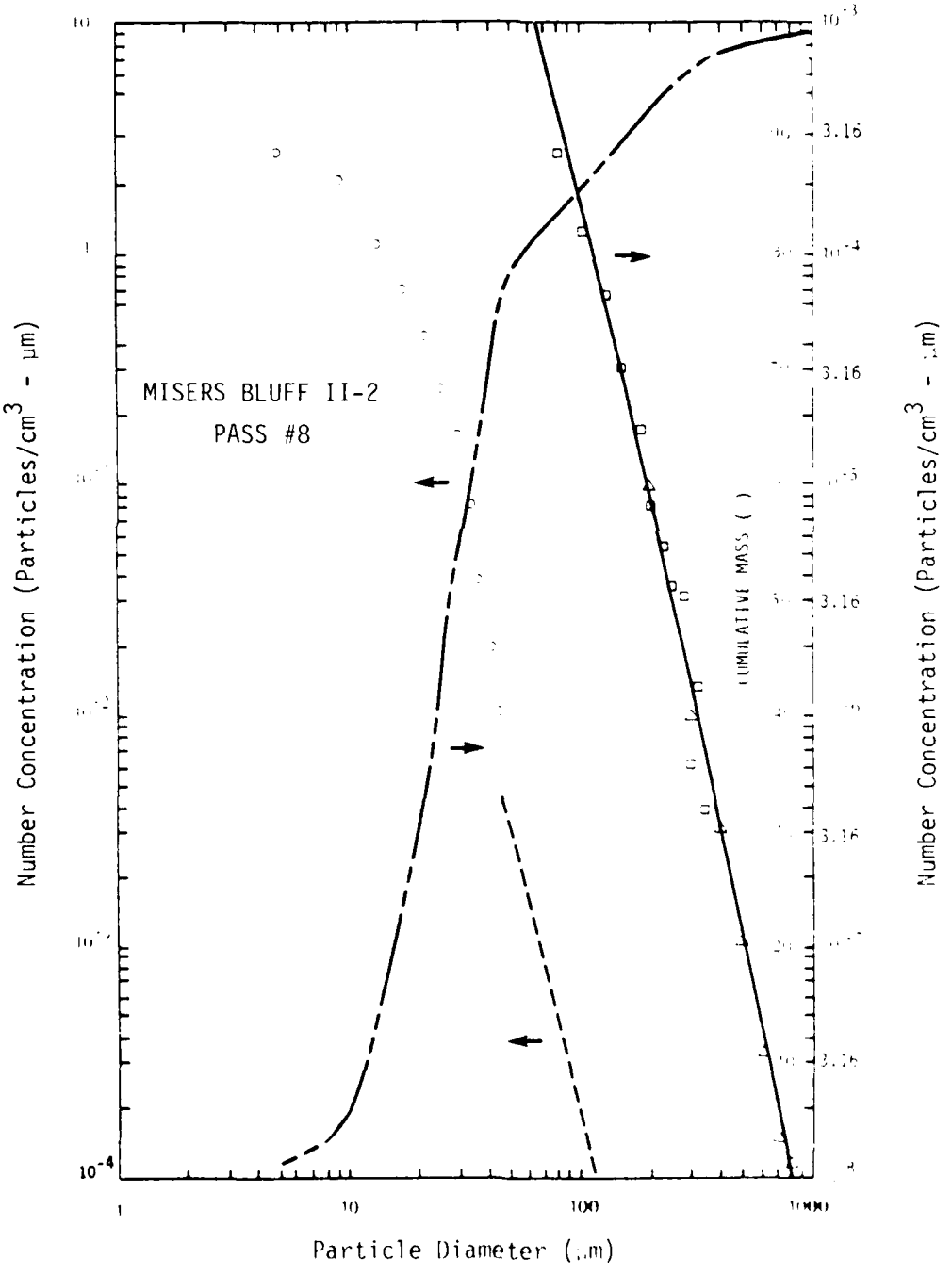

Figure 3.8(a). MISERS BLUFF II-2, Pass 8, Particle Size and Cumulative Mass Distributions

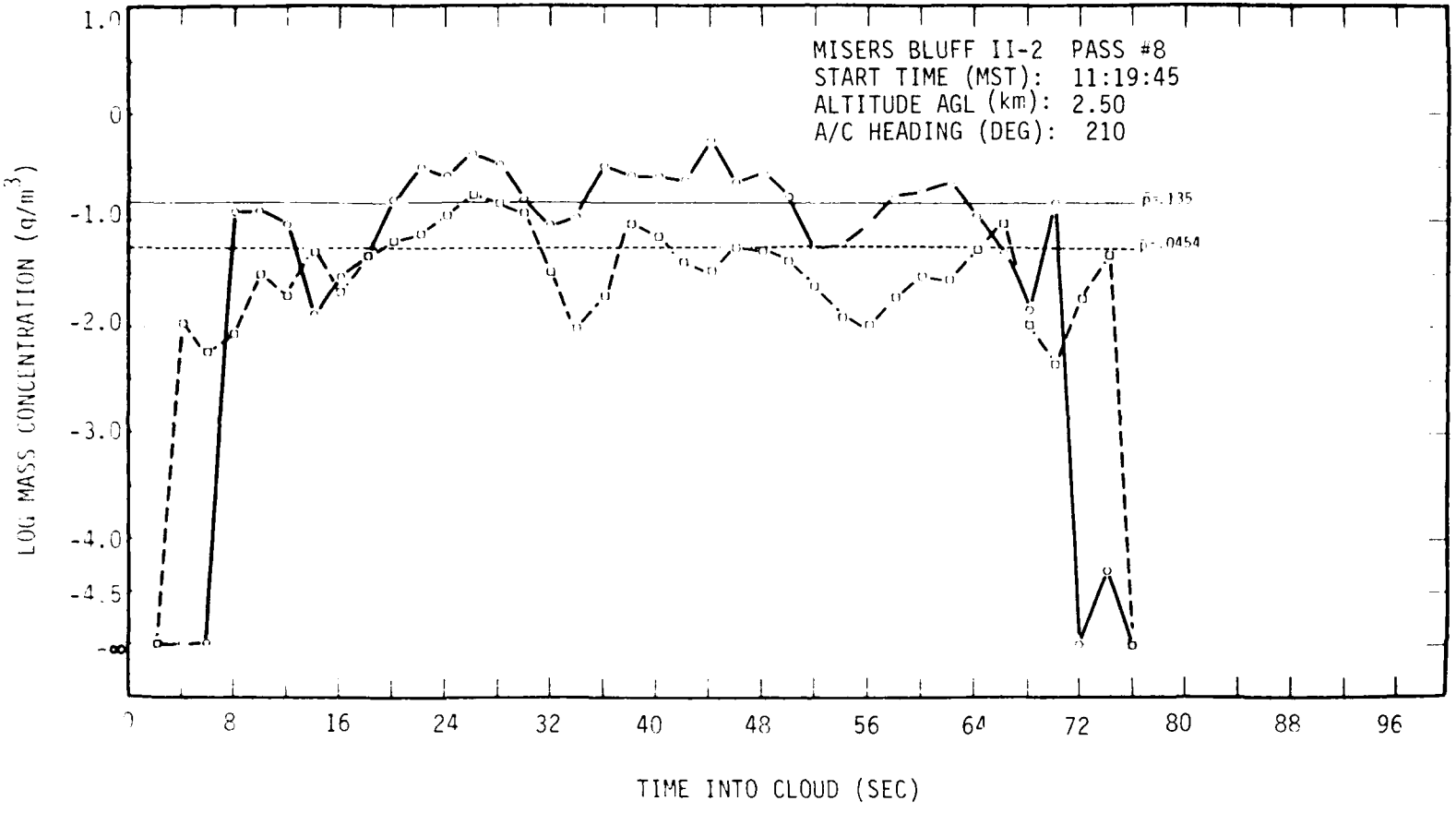

Figure 3.8(b). MISERS BLUFF II-2, Pass 8, Mass Concentration Time History

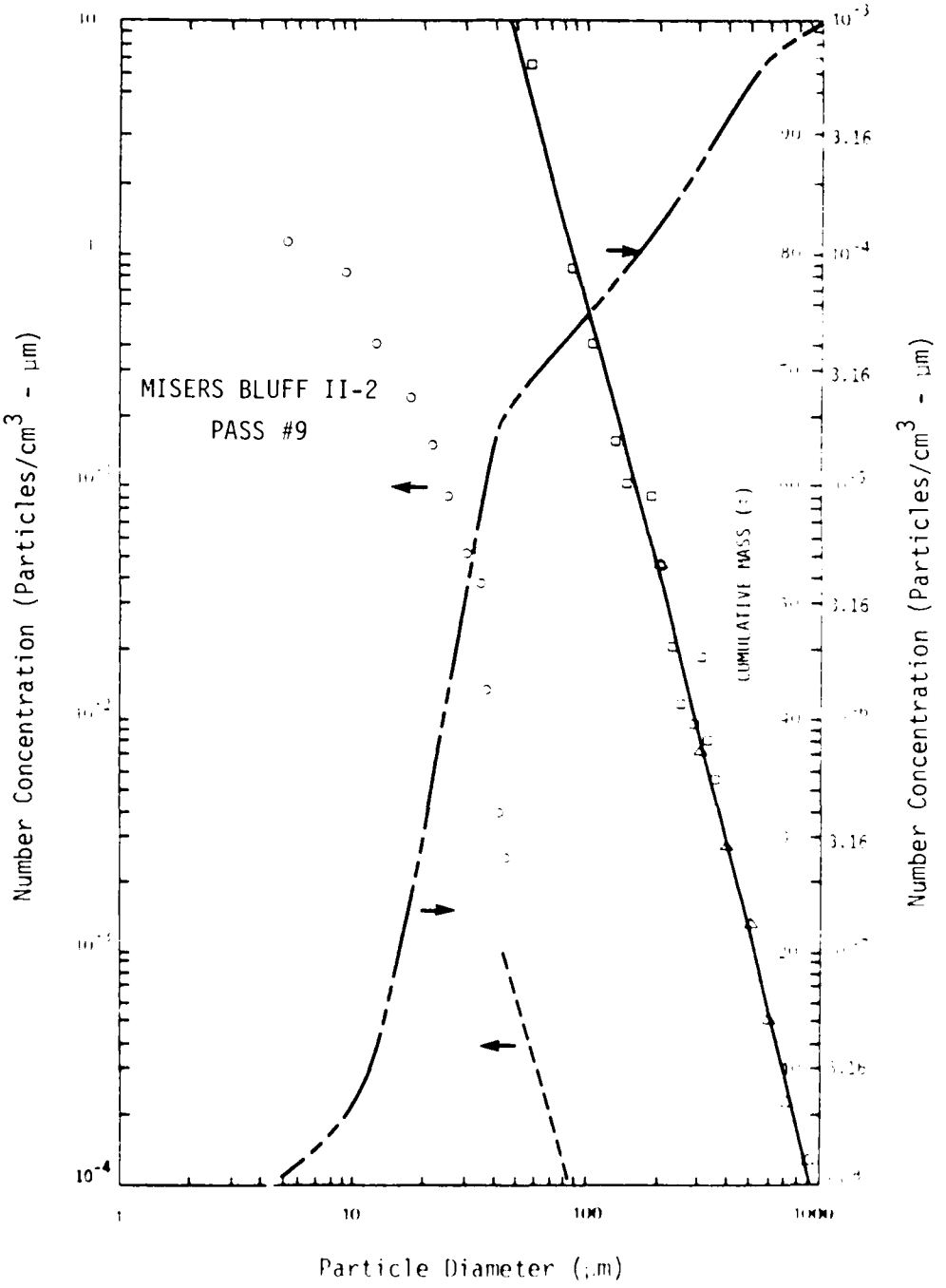

Figure 3.9(a). MISERS BLUFF II-2, Pass 9, Particle Size and Cumulative Mass Distributions

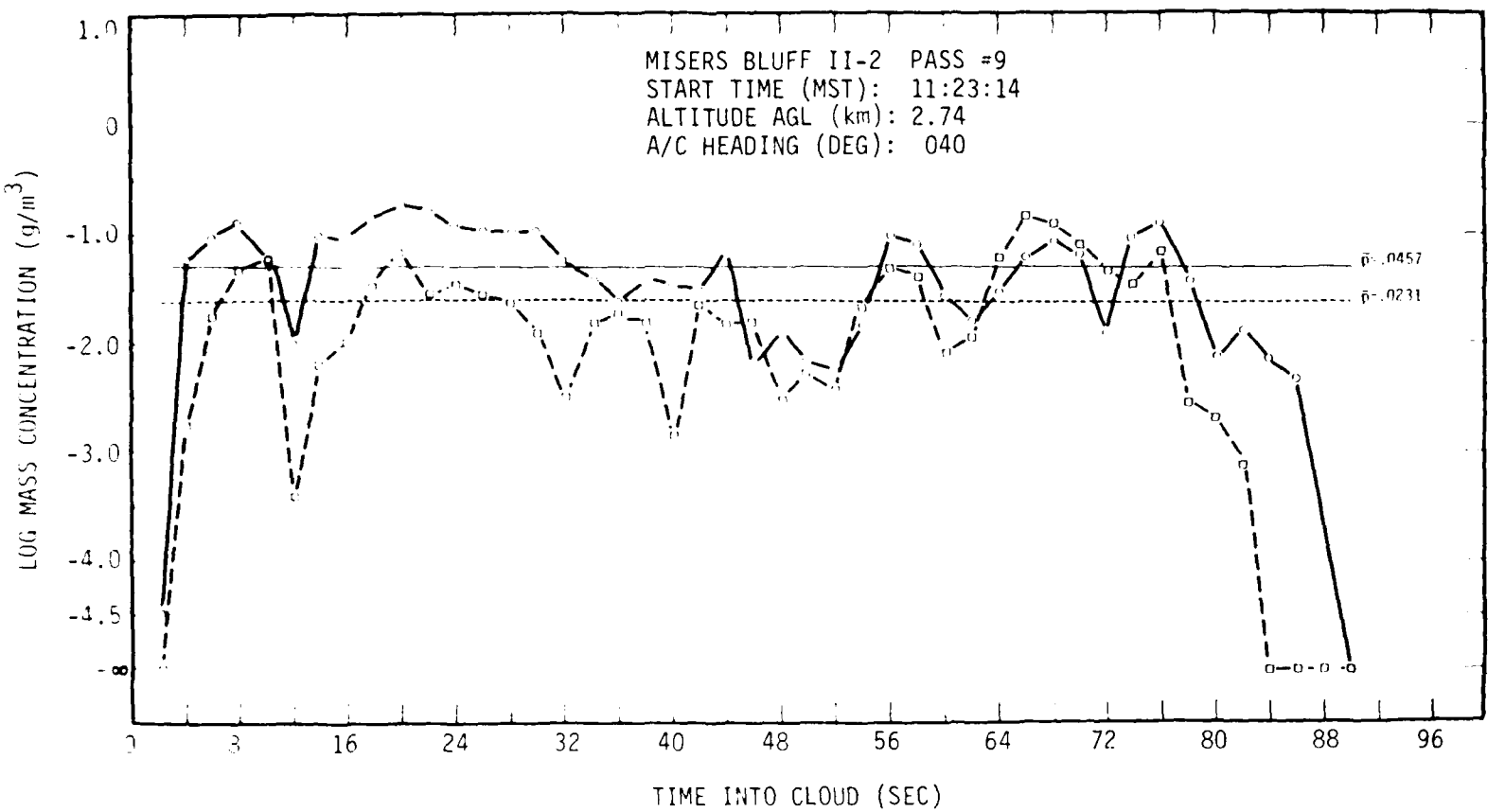

Figure 3.9(b). MISERS BLUFF II-2, Pass 9, Mass Concentration Time History

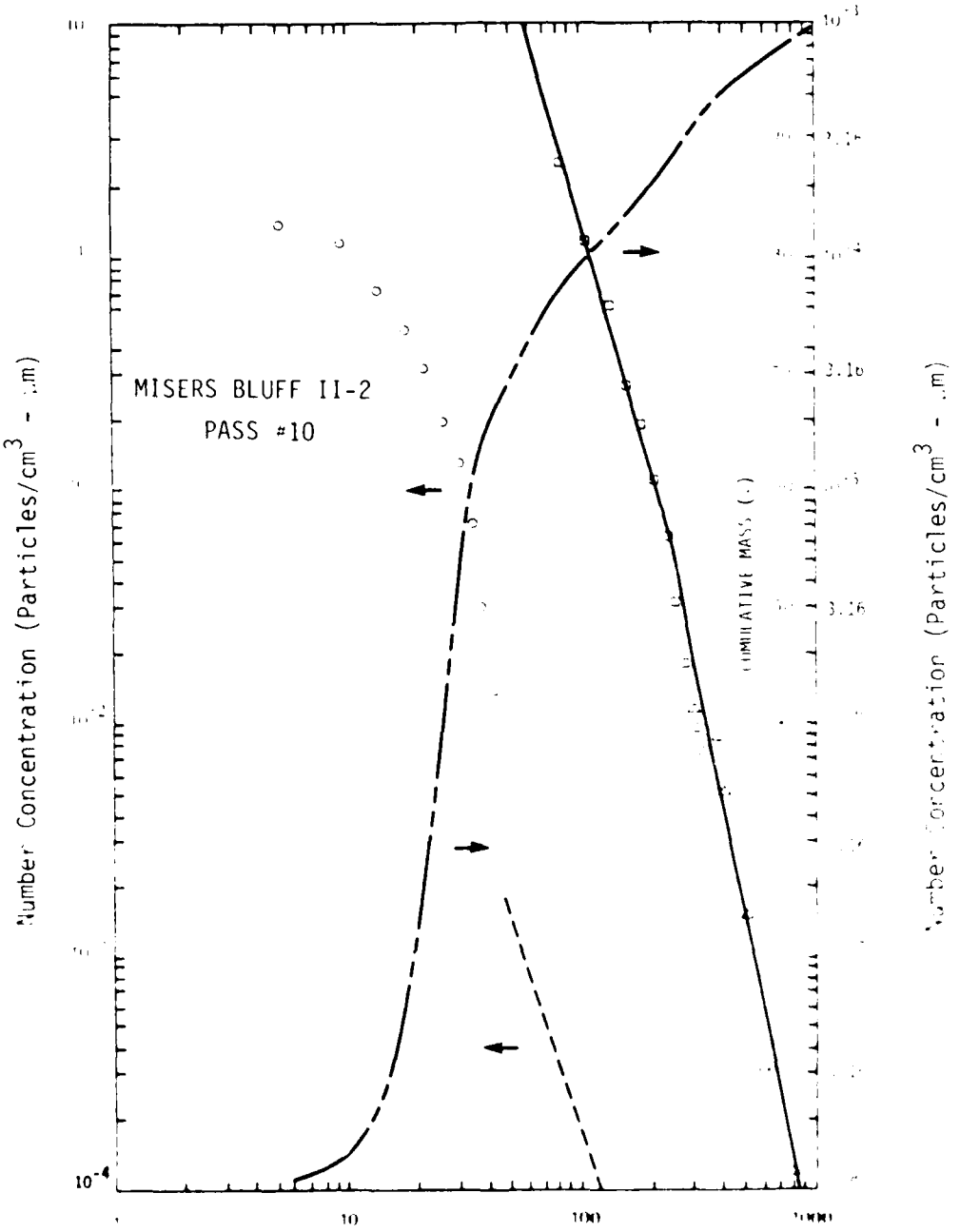

Figure 3.10(a). MISERS BLUFF II-2, Pass 10, Particle Size and Cumulative Mass Distributions

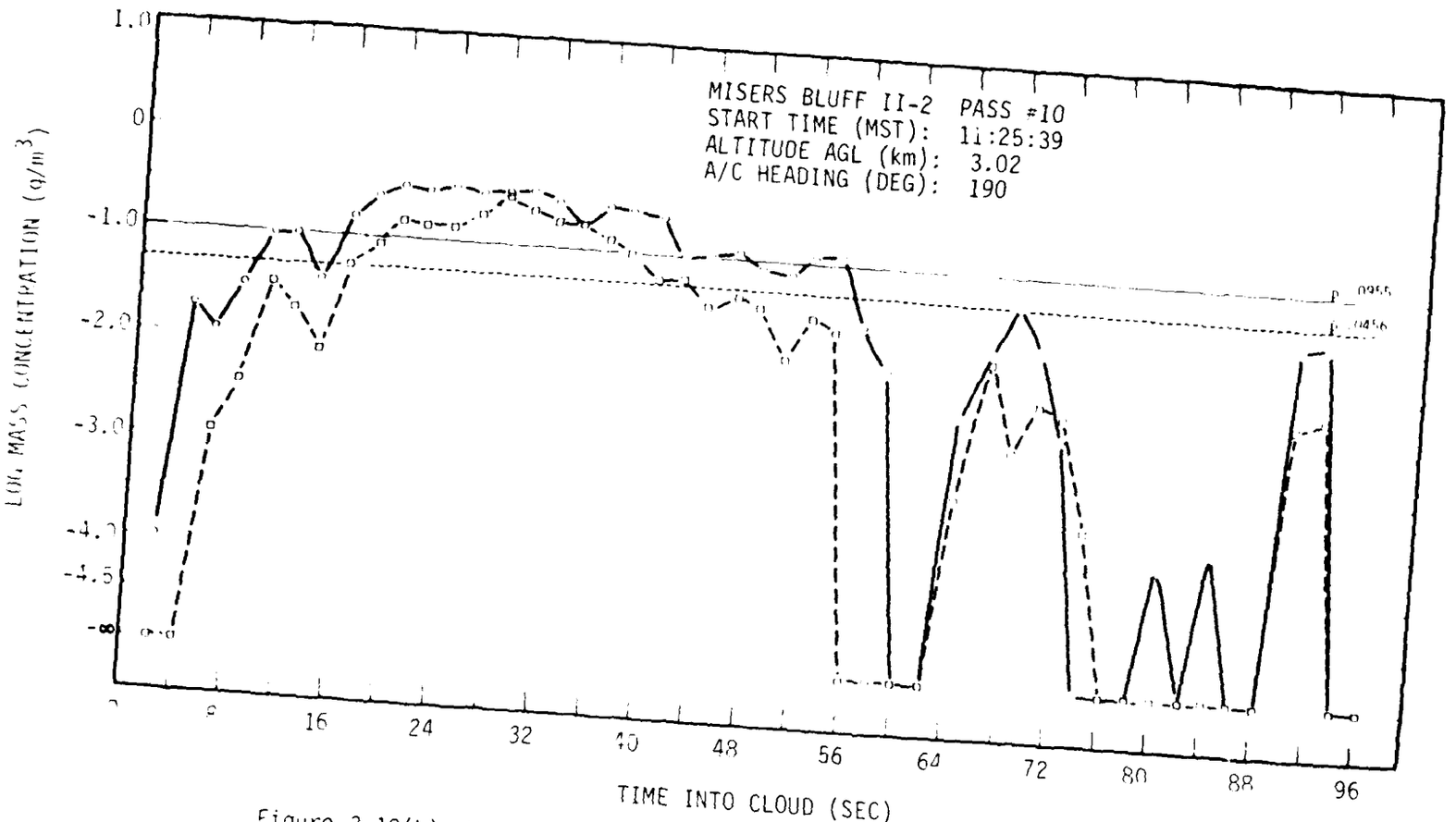

Figure 3.10(b). MISERS BLUFF II-2, Pass 10, Mass Concentration Time History

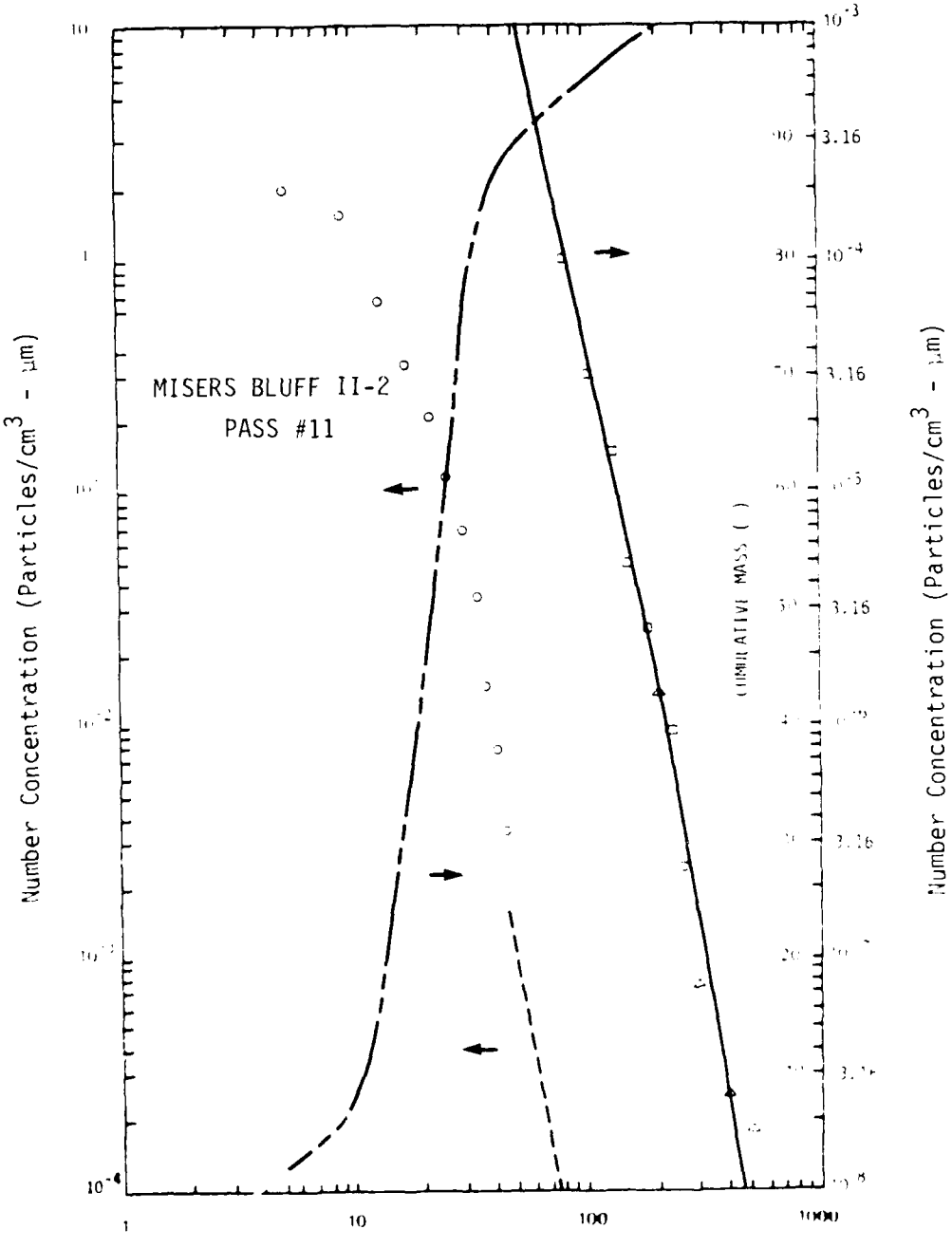

Figure 3.11(a). MISERS BLUFF II-2, Pass 11, Particle Size and Cumulative Mass Distributions

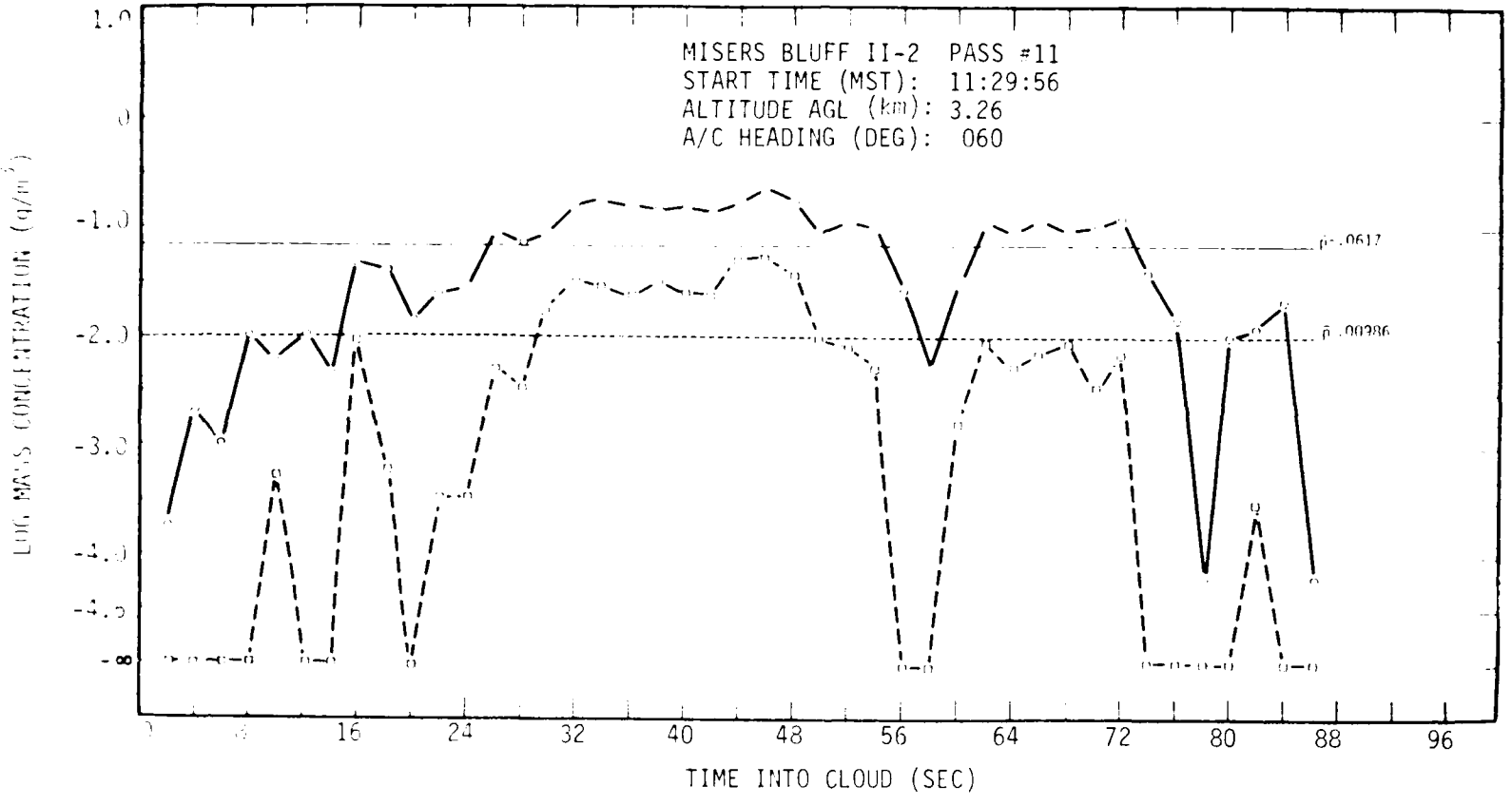

Figure 3.11(b). MISERS BLUFF II-2, Pass 11, Mass Concentration Time History

3-4 RECONSTRUCTING THE MISERS BLUFF II-2 DUST CLOUD

In a manner identical to that used in the MBII-1 dust cloud reconstructions (see Section 2-4 for methodology and assumptions), the multiple burst dust cloud was reconstructed at ten and twenty minutes after detonation to obtain "snapshots" of the entire cloud at several times for comparison purposes.

3-4.1 The MBII-2 Dust Cloud at Ten Minutes After Detonation

Table 3.2 is the summary of calculated mass values within the T+10 minute dust cloud as a function of altitude. Average mass concentrations have been calculated by summing mass contributions from all sized particles at a given altitude and then dividing by the estimated cloud volume at that altitude. Values of cumulative mass have been tabulated to insure that all cloud mass has been conserved in the reconstruction process.

As in the single burst dust cloud at T+10 minutes, some of the clouds mass (~7 percent) appears above the top of the visible cloud (see Section 2-4.1 for a discussion on the possible explanation for this contradiction between the inferred T+10 minute cloud and the visible cloud). Since this "phenomenon" is common to both dust clouds at T+10 minutes, it is not felt that the mass loading ratios would be significantly affected by it.

In order to smooth out some of the fluctuation in average mass concentrations in the cloud cap, passes 7 and 8 and passes 9 and 10 have been averaged. The calculated averages appear on the right-hand side of Table 3.2. Similarly, pass data from passes 2, 3, and 4 have been averaged in calculating an average mass concentration in the cloud stem.

3-4.2. The MBII-2 Dust Cloud at Twenty Minutes After Detonation

Table 3.3 summarizes the gross features of the multiple burst dust cloud at T+20 minutes. By this time, only 2.5 percent of the mass lofted appears above the visible cloud top. Further, "late time" fallout, i.e., the mass that is on the ground in Table 3.3,

Table 3.2 MISERS BLUFF II-2 Dust Cloud Reconstructed at Ten Minutes After Detonation

Pass #	2	3	4	5	6	7	8	9	10	11					
TAB (Min)	6.31	8.0	10.08	12.31	15.06	17.84	20.44	23.96	26.48	30.64					
Altitude (m)	620	790	1130	1490	1890	2310	2500	2740	3020	3260					
	Distribution of Mass (g) With Altitude at 10 Minutes After Detonation														
	Particle Size (Spherical Particles)														
	<47 μm				≥47 μm										
3200					3.00+7	8.30+6	1.00+7	9.11+7	1.70+8	3.16+7		3.71+8	3.71+8	Above Cloud	
3190					1.00+7	1.20+6	7.00+6	6.40+6	5.31+7	1.05+7		8.82+7	4.59+8	1.39+9	6.34-2
(11)	1.00+8				3.60+7	4.60+6	1.26+7	5.90+6	7.89+7	2.83+7		6.10+8	1.07+9	2.15+9	2.84-1
3140															
(10)	6.10+8				9.00+6	6.70+6	2.69+7	1.57+7				7.04+8	1.77+9	1.65+9	4.27-1
2890															
(9)	2.72+9				5.20+7	9.00+6	2.89+7	1.89+7				3.56+8	2.13+9	1.65+9	2.16-1
2620															
(8)	1.71+9			1.60+7	1.50+7	1.63+7	3.76+7					5.89+8	2.72+9	1.36+9	4.33-1
2310															
(7)	3.56+8			5.20+7	2.17+7	2.20+7						4.24+8	3.14+9	1.93+9	2.20-1
2100															
(6)	5.22+8			1.02+8	9.83+7							8.22+8	3.96+9	2.59+9	3.17-1
1690															
(5)	5.54+8			1.05+8								5.54+8	4.52+9	2.41+9	2.30-1
1310															
(4)	2.64+8		3.00+7									2.64+8	4.78+9	2.22+9	1.19-1
960															
(3)	5.26+7	2.00+6										5.26+7	4.83+9	1.46+9	3.60-2
780															
(2)	2.02+8	3.00+7	3.00+7									2.02+8	5.04+9	1.62+9	4.37-2
0															
	2.92+7	1.00+7	2.00+6									2.92+7	5.11+9	On Ground	

321

308

SIEM AVG 6.25-2

Table 3.3 MISERS BLUFF II-2 Dust Cloud Reconstructed at Twenty Minutes After Detonation

Pass #	2	3	4	5	6	7	8	9	10	11						
TAR (Min)	6.21	8.0	10.08	12.31	15.06	17.84	20.44	23.96	26.48	30.64						
Altitude (m)	670	790	1130	1490	1890	2310	2500	2740	3020	3260						
	Distribution of Mass (g) With Altitude at 20 Minutes After Detonation										Total Mass at Altitude g	Cumulative Mass g	Volume in Cloud Layer at T+20 Minutes m^3	Average Mass Concentration at T+20 Minutes g/m^3		
Altitude of Top and Bottom of Cloud Layer and Layer Number	Particle Size (Spherical Particles)															
	<45 μm						>45 μm									
3700								3.00+7	9.60+7	1.69+7	1.43+8	1.43+8	Above Cloud			
								1.57+7	5.40+7	1.43+7	8.40+7	2.27+8	3.59+9	2.34-2		
3390																
(11)	1.30+8							2.97+7	7.31+7	3.88+7	5.81+8	8.08+8	5.55+9	1.05-1		
3130																
(10)	6.10+8							2.80+7	7.89+7		7.53+8	1.56+9	4.25+9	1.77-1		
2880																.126
(9)	7.2+8						1.20+7	3.46+7			3.19+8	1.88+9	4.25+9	7.51-2		
2620																
(8)	1.31+8						1.46+8				6.20+8	2.50+9	3.51+9	1.77-1		.112
2405																
(7)	2.35+8					5.40+7					3.29+8	2.83+9	4.98+9	6.61-2		
2190																
(6)	6.20+8				9.53+7	7.20+6					7.23+8	3.55+9	6.70+9	1.08-1		
1690																
(5)	1.13+8			5.43+7	9.17+7	6.30+6					6.02+8	4.15+9	6.21+9	9.70-2		
1310																
(4)	1.69+8		1.73+7	3.73+7	5.30+7						2.77+8	4.43+9	5.22+9	4.85-2		
960																SIEM AVG 3.05-2
(3)	1.16+8		1.34+7	3.24+7	1.10+7						9.04+7	4.52+9	3.76+9	2.41-2		
530																
(2)	1.31+8	1.61+7	1.85+7	2.20+7	6.00+7	5.20+7					2.84+8	4.81+9	1.19+10	2.39-2		
0																
		3.20+7	3.30+7	1.33+7	1.00+7	1.30+7					3.09+8	5.11+9	On Ground			

accounts for ∿6 percent of the mass lofted. Recalling that at T+20 minutes, the "late time" fallout from the MBII-1 cloud amounted to only ∿2.2 percent of the lofted mass, the 6 percent value for MBII-2 supports the observation that a much greater percentage of the cloud's mass was in the form of particles that could "fall out" of the cloud, i.e., particles $\geq$ 47 μm.

3.4.3 Comparisons of the MBII-2 Dust Cloud at T+10 and T+20 Minutes

Figure 3.12(a) shows how particles $\geq$ 47 μm are being redistributed in the MBII-2 dust cloud as a function of altitude and time-after-burst. As in the MBII-1 cloud, the upper cloud layers are being depleted with time with a corresponding mass enhancement in the lower regions of the cloud.

Average mass concentrations within the MBII-2 dust cloud at T+10 and T+20 minutes have been plotted in Figure 3.12(b) as a function of altitude. Total mass aloft at T+20 minutes is nearly the same as that aloft at T+10 minutes (see Tables 3.2 and 3.3), while Figure 3.12(b) shows a factor of 2-3 decrease in average mass concentration with time. (Ten minutes of cloud diffusion resulted in a factor of 1.6 increase in the cloud radius at T+20 minutes; compare this with the 2.6 increase in cloud radius for the highly sheared MBII-1 dust cloud.) Within the same time frame, there was a factor of 7 decrease in the average mass concentration in the MBII-1 dust cloud (Section 2-4.3). This further supports the observation that the single burst dust cloud was strongly affected by significant variations in wind speed and direction aloft (shear) that were not evident in the wind profile obtained during the multiple burst event.

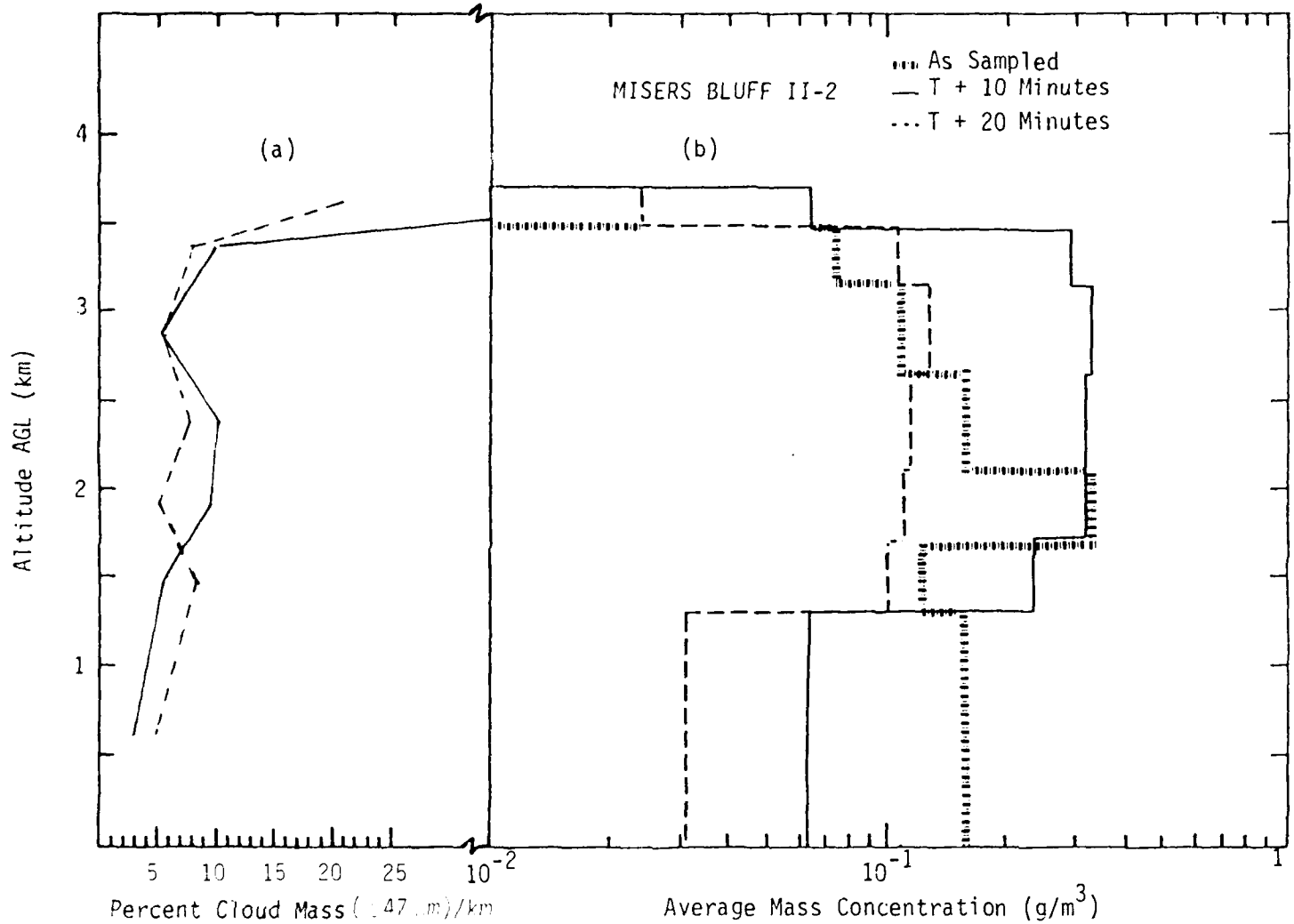

Figure 3.12. MISERS BLUFF II-2: Percent of Cloud Mass $\geq$ 47 μm and Average Mass Concentration As a Function of Altitude and Time After Detonation.

SECTION 4
SINGLE AND MULTIPLE BURST DUST CLOUD COMPARISONS

4-1 INTRODUCTION

In current multiple-burst dust cloud modeling, the total mass aloft at a given time after stabilization is assumed to be a simple addition of the masses calculated for the corresponding single-burst dust clouds. Therefore, if a dust cloud resulting from a single detonation contains X mass, the stabilized dust cloud from N identical detonations will contain NX mass at the same time after detonation.

The stabilized (T+10 minute) clouds for MISERS BLUFF II were loaded almost exclusively by very small particles. These high drag particles will tend to be contained in the visible cloud whose volume is dominated by the cloud cap. To take advantage of this result, only the MBII cloud caps will be compared at similar times after detonation.

4-2 MBII MASS LOADING RATIOS

Because most of the assumptions that were made in calculating total lofted mass (e.g., dust specific gravity, spherical particles, and circular cloud geometry) were the same for both the single and multiple burst dust clouds, multiplicative uncertainties attributable to these assumptions should cancel out, or tend to become less important, when mass loading ratios are calculated. These and other uncertainties are discussed in more detail in Section 5.

From Tables 2.2 and 3.2 (MBII dust clouds at T+10 minutes), calculated values of cumulative mass above the cloud stem show that 0.64×10^6 kg and 4.5×10^6 kg of dust remains aloft in the single and multiple burst cloud caps, respectively, at cloud stabilization. The mass loading ratio between the two dust clouds at this time is approximately 7.1. By twenty minutes after detonation, the single and multiple burst dust clouds contain 0.63×10^6 kg and 4.15×10^6 kg of dust, respectively, yielding a mass loading ratio of 6.6. The downward

trend of the mass loading ratio with time is due to the fact that the mass of the multiple burst cloud is comprised of a greater percentage of particles $\cdot 47$ μm which are "falling out" of the cloud cap. If a similar analysis were to be extended out to times greater than twenty minutes, it would be apparent that the mass loading ratio between the cloud caps asymtotically approaches a value of 6.0, i.e., the ratio of masses in the cloud caps being determined only by particles $\cdot 47$ μm. Within the range of measurement uncertainties, these calculated values of mass loading ratio appear to approximate what would be predicted by linear superposition, i.e., six.

Recalling that the T+10 minute dust cloud's mass loading ratio was calculated to be $\sim$7.1, measurement uncertainties aside, there is some evidence that the 18 percent "enhancement" (7.1/6) in mass loading could be real. First, the calculated enhancement in the mass loading ratio is governed by a factor of $\cdot 12$ increase in mass aloft of particles $\geq$ 47 μm in the MBII-2 dust cloud; a factor of six would have implied linear superposition. While differences in site geology (charges 3 and 4 were detonated over a silty/sandy surface layer approximately 0.5m thick; see Ref. 6) could account for this phenomenon, photographic records of the multiple burst event (Ref. 5) strongly suggest that an enhanced flow field did exist that could be responsible for lofting the large particles in the multiple burst cloud. Hence there was not only a source of large particles present for the MBII-2 dust cloud, but there also appears to be a mechanism present to loft these larger particles not evident in the MBII-1 cloud photography - enhanced flow fields.

Reiterating, the 18 percent increase in mass loading ratio could be attributable to measurement uncertainties, however, there is strong evidence that enhanced flow fields generated by interacting shockwaves may also be a factor.

4-3 MBII CLOUD VOLUME RATIO

In addition to predicting a six-fold increase in mass aloft at cloud stabilization, linear superposition implies that dust mass concentrations (g/m^3) are additive in regions where the dust clouds overlap. For instance, if six detonations occurred simultaneously at the same location, linear superposition would predict a multiple burst dust cloud that had the same dimensions as a single burst dust cloud but would contain six times the mass. This would imply that the average mass concentration within the stabilized multiple burst dust cloud would be six times that found in the single burst cloud at the same time-after-burst.

Figure 4.1 shows how some measured dimensions of the MBII multiple burst dust cloud (dashed lines) compare with those cloud dimensions that would be predicted by linearly superimposing six of the MBII single burst clouds (solid lines) at ten minutes after detonation. Figure 4.1(a) depicts the vertical cross-section of the measured and predicted multiple burst dust clouds while Figure 4.1(b) is an overhead (planar) view of the two dust clouds. The hexagonal array of dots in Figure 4.1(b) is the multiple burst charge configuration and has been drawn to scale (200 meter centerline diameter).

One immediate observation is that the measured volume of the multiple burst cloud is significantly greater than would be predicted by linear superposition. Calculations based on cloud diameter and thicknesses at T+10 minutes (Tables 2.2 and 3.2) reveal that the measured multiple burst cloud volume is 2.7 times that predicted by superimposing six of the single burst clouds. Assuming that the predicted multiple burst cloud contains 3.3×10^6 kg of dust (six times the mass in the single burst cloud), linear superposition would predict an average mass concentration in the multiple burst dust cloud of $0.67\ g/m^3$. The average mass concentration in the multiple burst dust cloud was measured as only $0.3\ g/m^3$ (see Table 3.2).

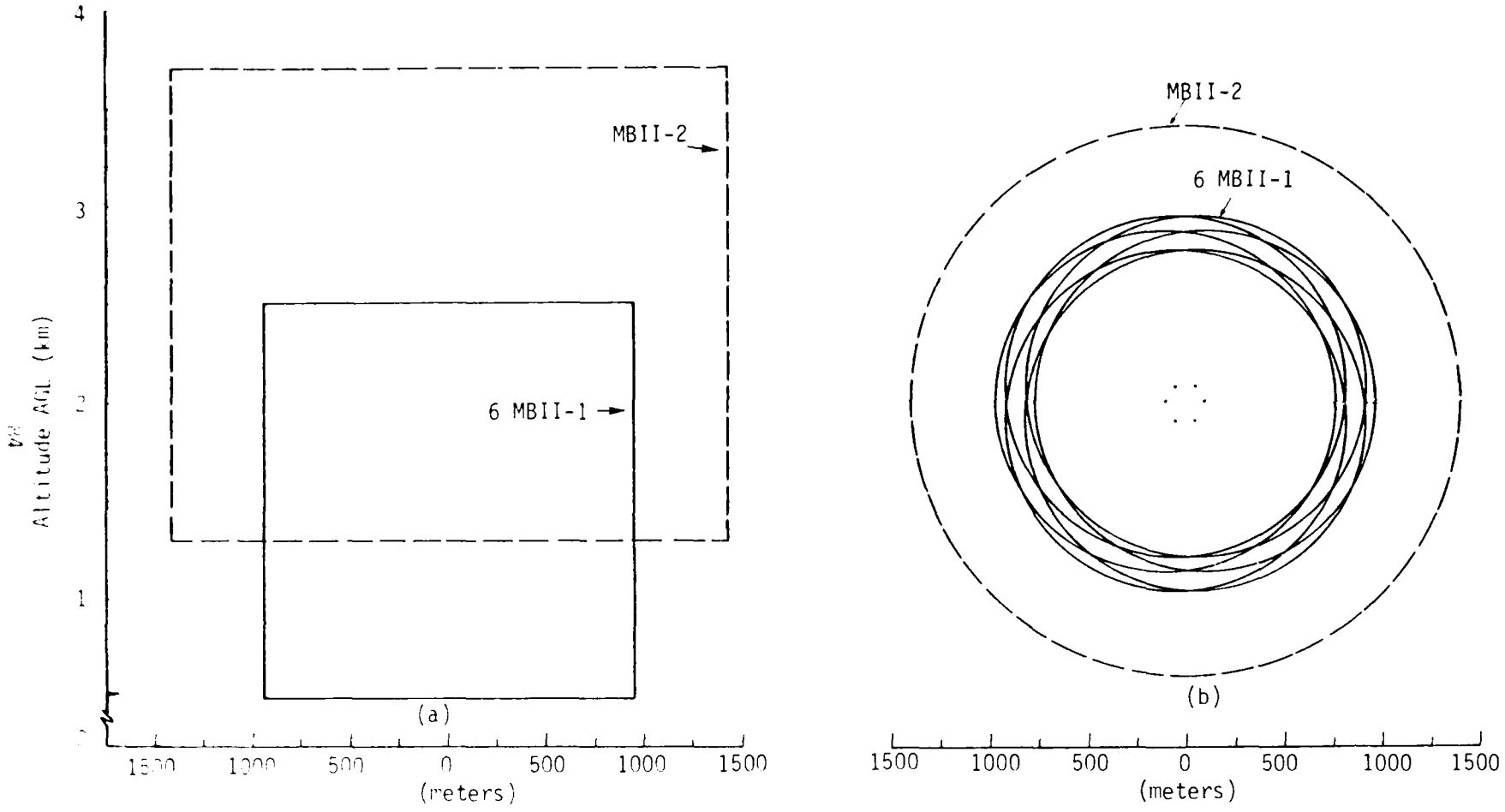

Figure 4.1. Vertical Cross Sections (a) and Overhead Planar Views (b) of the Measured and Predicted MBII Multiple Burst Dust Cloud at Ten Minutes After Detonation

Another interesting parameter to calculate is the total mass that would probably be encountered by a missle ascending (or descending) vertically through the stabilized dust clouds, i.e., $\int \rho dh$. Assuming that a cross sectional area of 1 m^2 is being swept by the "missile", calculations show that linear superposition would predict a value of integrated mass in the six MBII single burst clouds to be approximately twice that calculated for the MBII multiple burst dust cloud (1340 g versus ~720 g). It appears then that linear superposition of dust clouds, formed from closely spaced multiple detonations, tends to overestimate the dust environment (g/m^3). Further, this overestimate in mass concentration is due mainly to a corresponding underestimate in the multi-burst cloud volume predicted by linear superposition. However, if the number of burst in a given attack scenario is very large and closely spaced, and they encompass a relatively large area (unlike MBII-2), the central clouds will be radially confined and mass concentrations within this area would not drop off as sharply as indicated by MBII-2 (approximately a factor of 2). This would represent a "worst case" situation and linear superposition would probably yield very good results.

In addition to the apparent weaknesses of linear superposition in describing the multiple burst environments that have already been mentioned in this section, Figure 7.1(a) reveals another potential problem area -- that of inadequately describing the altitude and thickness of the multiple burst dust cloud. This aspect has also been raised by unpublished hydrocode (HULL) calculations. The primary cause is an energy superposition, i.e., six times the energy went into only 3 times the volume; the excess energy density was probably used primarily in raising the multiple burst cloud to a higher altitude. It is not felt that the slight differences in atmospheric temperature lapse rates existing at the time of each detonation contributed to this difference in cloud altitudes -- in fact, the air was more stable during the multiple burst test.

SECTION 5
UNCERTAINTIES IN THE MBII DUST CLOUD MASS CALCULATIONS

5-1 INTRODUCTION

The need to discuss uncertainties became particularly obvious when it is realized that the calculated values of total lofted mass during each of the two events in the MISERS BLUFF II program, exceeded a nuclear cloud "hydrodynamic limit" prediction. This "limit" is based on hydrocode flow field calculations (SHELL) which, for parametric nuclear dust cloud simulations, limits the total lofted mass to approximately one ton of dust per ton of nuclear yield. Due to the way net energy output is partitioned in nuclear devices (i.e., much of the energy being expended in the form of radiant energy), it is common practice to equate 1 ton of TNT yield to 2 tons of nuclear yield for blast simulations. The hydrodynamic limit for high explosive (HE) detonations is, therefore (for an exactly analogous flow field), two tons of dust per ton of TNT yield.

In the MBII single burst detonation (100 tons TNT equivalent), the total lofted mass was calculated to be 7.9×10^5 kg (Section 2-1) or 8.8 tons of dust per ton of yield. Similarly, total lofted mass in the multiple burst event (600 tons TNT equivalent) was calculated to be 5.1×10^6 kg (Section 3-1) or 9.4 tons of dust per ton of yield -- clearly much more than "allowed" by the HE hydrodynamic limit. The purpose of this section is to discuss some of the assumptions that were made in calculating these values of MBII lofted mass and assess their effect on the calculations. Further, the validity of using the nuclear hydrodynamic limit for limiting dust lofted in HE detonations is discussed in Section 5-3.

5-2 SOURCES FOR UNCERTAINTIES

5-2.1 In-Situ Sampling Profiles

The airborne dust cloud sampling missions were flight planned to sample both clouds from below the base to cloud top with over-pressure sampling pass altitudes. When possible, sampling passes were made in

generally up-wind/down-wind directions so that the aircraft traversed regions of subvisible fallout from higher altitudes for sheared clouds. The main purpose for having identical flight plans for both sampling missions was to insure a common data base for subsequent dust cloud reconstruction efforts and mass loading comparisons. The major drawback in the flight plans was that by sampling upwind/downwind, the largest "dimension" of the dust clouds was sampled at each pass altitude.

One of the assumptions made in the mass calculations was that the dust cloud was circular at each sampling altitude and the sampling pass length was the diameter of this circle. Clearly this assumption could lead to overestimating the mass at altitude, especially if the clouds had become elliptical due to wind induced shear and diffusion. Since all of the sampling passes were not made upwind/downwind (Ref. 2), a significant effort was expended in analyzing the sampling path length data and recomputing the cloud volume at each altitude assuming the cloud cross section was elliptical rather than circular. This effort resulted in decreasing the total mass lofted in the single and multiple burst clouds by 21 percent and 17 percent, respectively. To be conservative, let 25 percent be an upper limit for the mass overestimate due to assumptions concerning cloud geometry.

Another aspect of the in-situ sampling profiles, which could lead to significant errors in estimating the total mass lofted, is the time after detonation that initial penetrations of the clouds were made. For reasons pertaining to crew safety [illegible] flight operations on [illegible], in-situ sampling began much earlier in the single burst cloud, when mass concentrations were very high, than was possible in the multiple burst cloud. Hence, by the approach taken in sections 2-1 and 3-1, mass lofted in the multiple burst cloud would be underestimated due to early [illegible] fallout.

5-2.2 Dust Particle Shape and Specific Gravity

Throughout the entire comparative analysis, the dust particles have been assumed to be spherical in shape and have a specific density of 2.3 g/cm^3. Significant overestimates in calculated values of lofted mass could be incurred if the dust particles were, in fact, a totally different shape. Since most of the mass lofted is attributable to particles .47 μm in diameter (see Figure 4.1), this discussion will focus on particles in that range of the size spectrum.

At DNA's request for a secondary mission, the Air Force Technical Applications Center (AFTAC) flew three sampling passes through the top of the MBII multiple burst dust cloud between fifteen and twenty minutes after detonation. During each sampling pass, AFTAC obtained filter paper samples containing dust from the cloud and one-half of each filter was subsequently forwarded to SAI for analysis. The particular analysis performed on the samples was called a Suspended Particulate Evaluation and Classification (SPEC) (it was accomplished by Materials Consultants & Laboratories, Inc. of Monroeville, PA). The output from the SPEC analysis is a detailed description of particle size, shape, and chemistry (elements) for the approximately 1000 particles in each sample analyzed. With respect to the particle shape of dust particles .47 μ, the analysis revealed a most probable width-to-length ratio of 0.58, i.e., a length-to-width ratio (r) of 1.7. (Mean 0.56 and standard deviation 0.17.) Assuming the "real" shape of the particles were circular discs (see Appendix D) with an aspect ratio (r) of 1.7, mass calculations that were made assuming particle sphericity would overestimate the mass lofted by 15 percent (4r/6).

The AFTAC filter samples also provided SAI with a totally independent mass measurement from the MBII-2 dust cloud. By knowing the average weight of the filter papers prior to cloud penetration, the actual weight of dust acquired during each sampling pass could be extracted; dividing this value by the volume of air sampled during each pass (approximately 30-seconds of flight) yield

the pass averaged mass concentration. AFTAC furnished SAI with their best estimate of the filter paper tare weights and individual pass sample volumes. The "dirty" filter papers were weighed by SAI and mass concentrations were calculated for each sampling pass. Table 5.1 is a tabulation of this data.

Table 5.1 MBII-2 Dust Cloud Mass Concentrations Inferred From AFTAC Filter Paper Samples

Pass No.	Start Time (MST)	Altitude MSL (m)	Mass Concentration (g/m^3)
1	13:14:57	3540	.094 ± .02
2	13:17:16	3410	*
3	13:20:10	3350	.11 ± .04

*The dust contribution to the filter paper weight was not discernable using the best estimated tare weight. Filter paper appeared much "cleaner" than the others; probably penetrated patchy portions of the cloud cap.

With the exception of sampling pass 2, the AFTAC data indicates an average dust concentration within the top of the MBII-2 dust cloud of approximately 0.1 g/m^3 at 15-20 minutes after detonation. Comparing this number with that calculated for the same altitude layer (3140-3480m) in the reconstructed MBII-2 dust cloud (Table 3.3 or Figure 3.12), we see excellent agreement.

The SPEC analysis of particle sizes < 47 μm from the AFTAC filters also revealed that 30 percent of the total sample mass was contributed by particles < 15 μm. This is in very good agreement with the spectral data obtained by PMS.

Again it is encouraging to find such good agreement in the results obtained from two totally independent data bases. Based on the SPEC mass analysis and the calculated values of mass concentration from the AFTAC filter papers, it is felt that the assumptions made concerning the dust particles specific gravity being 2.3 was a reasonable one and did not lead to overestimating the total mass lofted.

5.3 VALIDITY OF THE NUCLEAR HYDRODYNAMIC LIMIT FOR HE TESTS

Based on the aforegoing discussion concerning possible sources of uncertainties in the MBII dust cloud mass calculations, it seems one could justify an approximate* 40 percent reduction in the calculated values of lofted mass for each event. This reduction would result in a lofting ability of 5.3 and 5.6 tons of dust per ton of TNT yield for the single and multiple burst event, respectively - still much greater than the 2 tons "permitted" by the HE hydrodynamic limit.

Exceeding the hydrodynamic limit is not unique to the MBII tests. For HE/ANFO event DICE THROW (500 tons TNT equivalent), it has been estimated that 6.8 tons of dust were lofted (above the initial fireball top) per ton of TNT yield (Ref 4), hence, the nuclear hydrodynamic limit may not be applicable to HE/ANFO dust clouds. One possible reason for this is that the dust loading mechanisms for nuclear and HE fireballs are very different. Nuclear fireballs are loaded with dust preferentially near the center line of the fireball flow field - in fact the parametric SHELL calculations commenced with all mass being initially placed in the inner one-eighth+ of the hemispherical fireball volume (surface burst). At this location initially, much of the mass would be lost immediately due to the base surge tendency along the centerline and would not be "available" for subsequent lofting. An HE fireball (ANFO-capped cylinder charge), however, is loaded by ejecta preferentially outside the center of the fireball. Being loaded in this region, the loss of mass along the stagnant center axis, as predicted by the parametric SHELL calculations, does not occur and more mass is "available" to be lofted. (Recall that for surface bursts, buoyant flow is initiated at the outside of the fireball.)

In summary, it is not felt that exceeding the hydrodynamic limit in MB dust clouds is contradictory to any limiting value

*[illegible]

+[illegible] of the fireball radius

predicted by SHELL calculations for a nuclear dust cloud. While the buoyant energy is comparable, the hydrodynamic flow fields of both the ejecta and the fireball are very different for nuclear and HE/ANFO bursts.

SECTION 6
CONCLUSIONS AND RECOMMENDATIONS

An indepth analysis of the data obtained during Phase 1 of the MISERS BLUFF II Cloud Sampling Program indicates that the MBII multiple burst dust cloud could not be completely modeled by linearly superimposing six of the MBII single burst clouds. As might be expected, the major weakness in the linear superposition modeling approach is its inability to treat the effects of the hydrodynamic and thermodynamic interactions occurring between the shock fronts/fireballs of a limited number of closely spaced, simultaneous detonations.

As a result of this weakness, several conclusions can be made based on the analysis performed in this report for the MBII dust clouds:

- Linearly superimposing six of the MBII single burst dust clouds at T+10 minutes resulted in overestimating the vertically integrated dust mass aloft (γ_{dh}) by a factor of ~2 over the measured, multiburst dust environment. This result is due mainly to the inability of linear superposition to accurately predict the volume of the dust cloud formed from a few closely spaced, interacting detonations.
- While overestimating the magnitude of the multiburst dust environment (mass concentrations), linear superposition appears to underestimate the areal extent of the actual environment that is produced in a closely spaced, multiburst situation. Again, this conclusion is a result of linear superposition not treating thermal energy dissipation and, hence, incorrectly predicting multiburst cloud volumes.
- Within the range of measurement uncertainties, linear superposition may predict reasonable values of mass aloft, i.e., γ_d, from N identical simultaneous detonations that each loft γ_d mass. However, the fact that a "seventh" burst [illegible]

AD-A087 856 SCIENCE APPLICATIONS INC MCLEAN VA F/G 19/4
MISERS BLUFF II CLOUD SAMPLING PROGRAM, DATA SUMMARY AND DUST C--ETC(U)
DEC 79 C R THOMAS, J E COCKAYNE DNA001-78-C-0217
UNCLASSIFIED SAI-80-118-WA DNA-5189F NL

2 OF 2
AD A087856

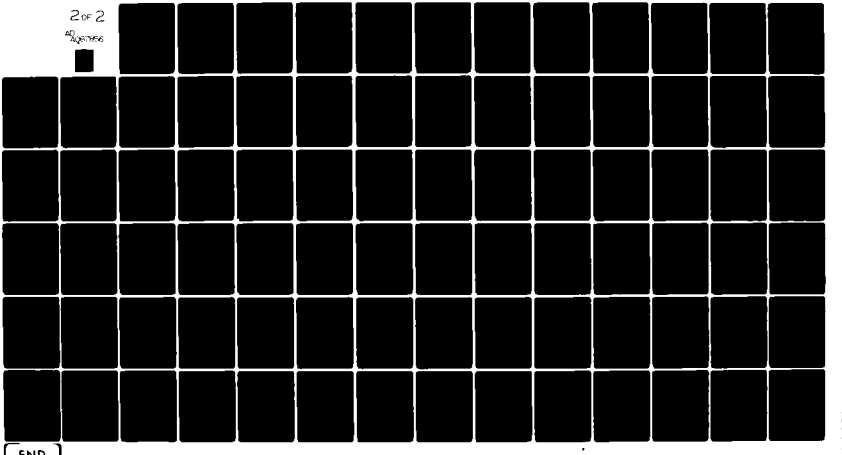

END
DATE FILMED
9-80
DTIC

central plume of dust was evident in the MBII-2 cloud photography, first visible approximately 20 seconds after detonation, provides strong evidence that the measured ∿7X increase in mass aloft in the multiple burst cloud may be very real.

Based on the above conclusions concerning the validity of utilizing linear superposition in defining dust clouds from a few closely spaced, multiple burst detonations, the following recommendations are made:

- Cloud volume calculations were, for the most part, derived from aircraft sampling pass lengths at or very near the times of dust cloud reconstructions (T+10 and T+20 minutes). More accurate values could be obtained by a detailed analysis of <u>all</u> the MBII dust cloud photography as taken from several azimuths. Because cloud volume calculations were instrumental in arriving at several of the conclusions, it is recommended that <u>all</u> photographic documentation (TIC and SRI) of the MBII dust clouds at T+10 minutes be analyzed to derive more accurate values of cloud volume.
- Some future analytical effort should be expended to understand how interacting fireballs dissipate their buoyant energy as they rise in the atmosphere. This information is needed to accurately predict dust cloud volumes and, hence, mass concentrations within <u>any</u> dust cloud generated by closely spaced, simultaneous detonations where linear superposition of cloud volume is not valid. The buoyant energy partitioning (for a suddenly released volume of buoyant fluid) is very important because only 5/14 "of the work done by buoyancy appears as kinetic energy of mean motion, ...; the balance (9/14) must go into turbulence and is eventually dissipated" (Ref. 7). Flow field interference could significantly decrease the kinetic part of

the buoyant energy and allow the turbulent portion to dominate; this perturbation in energy partitioning could cause the strongest flows to take the form of large eddies as evidenced in the MBII-2 dust cloud movies. This would suggest that multiple burst cloud volumes may be determined by turbulent flow as opposed to the strong vortical flow in single burst dust clouds.

- The possible ∿18 percent enhancement in the MBII dust cloud mass loading ratio may be due entirely to the uniqueness of the hexagonal charge configuration and the simultaneity of the detonations; i.e., this particular configuration may represent the "ideal" one for enhanced flow fields and mass lofting ability. For these reasons, any inferred mass loading enhancement would not have broad applicability in "real life" attack scenarios.

SECTION 7
REFERENCES

1. Thomas, C.R. and Cockayne, J.E., "MISERS BLUFF II Cloud Sampling Program: Procedures and Preliminary Results," Science Applications, Inc., Unpublished.

2. Knollenberg, R.G., "Results of the MISERS BLUFF II Aircraft Dust Particle Sampling Experiments," DNA 4951F, Particle Measuring Systems, Inc., April 1979 (U)

3. Hobbs, P.V., "Ice Physics," p. 679-687, Clarendon Press, Oxford, 1974.

4. Burns, A., and Crawley, P., "DICE THROW UHF/SHF Transmission Experiment (Vol. III)" DNA 4216T-3, SRI Project 3972, SRI International, August 1979.

5. Boquist, W.P. and Deuel, R.W., "Optical Measurements of MISERS BLUFF Multiburst Cloud Phenomenology," DNA 4896T, TIC 804, Technology International Corporation, September 1979 (U).

6. Roddy, D.J., "Geologic, Structural, and Aerial Stereophographic Studies of MISERS BLUFF Phase II Cratering: A Preliminary Report," U.S. Geological Survey, Flagstaff, Arizona, April 1979 (U).

7. Turner, J.S., "Buoyancy Effects in Fluids," Cambridge University Press, London 1973.

APPENDIX A
FALLOUT DATA ANALYSIS

A-1 INTRODUCTION

The procedures and preliminary results of the MBII fallout experiments fielded by SAI have been described in reference 1. Because of anomalously high wind, the fallout experiments were not totally successful in that fallout data was not obtained from the single burst cloud, hence, early time mass deposition and particle size distribution comparisons of single and multiple burst fallout data could not be accomplished. Analysis of the fallout from the multiple burst cloud has yielded meaningful results concerning the source of the early time fallout. Further, since some fallout samples were obtained from regions of the cloud where airborne sampling was accomplished, a more meaningful qualitative interpretation of the in-situ spectral data was possible (since fallout data is a time integrated sample, direct quantitative comparisons could not be made with the in-situ sampling data).

A-2 EXPERIMENT RESULTS

Fallout experiments were fielded for both events in the MISERS BLUFF II test series. Due to unfavorable and anomalous wind conditions existing in the vicinity of the test bed for the single burst detonation (23 June 1978), no fallout samples were acquired in the 56 fallout trays fielded for that particular test. During late August 1978, approximately 70 fallout trays were set out for the fallout experiment fielded for the multiple burst test. Figure A.1 is a topographical map of the immediate area surrounding ground zero and depicts the locations of the fallout trays fielded for this event. Favorable wind conditions on test day made it possible to obtain 18 dust particle samples from the multiple burst dust cloud; mostly to the north and north-northwest of GZ. The locations of the samples are shown in Figure A.2. Each unit on the grid equals 500 feet and the grid center (0, 0) is the single burst GZ. The solid squares (13) identify those fallout trays which contained measurable fallout while the empty squares depict areas of no recorded fallout. The squares

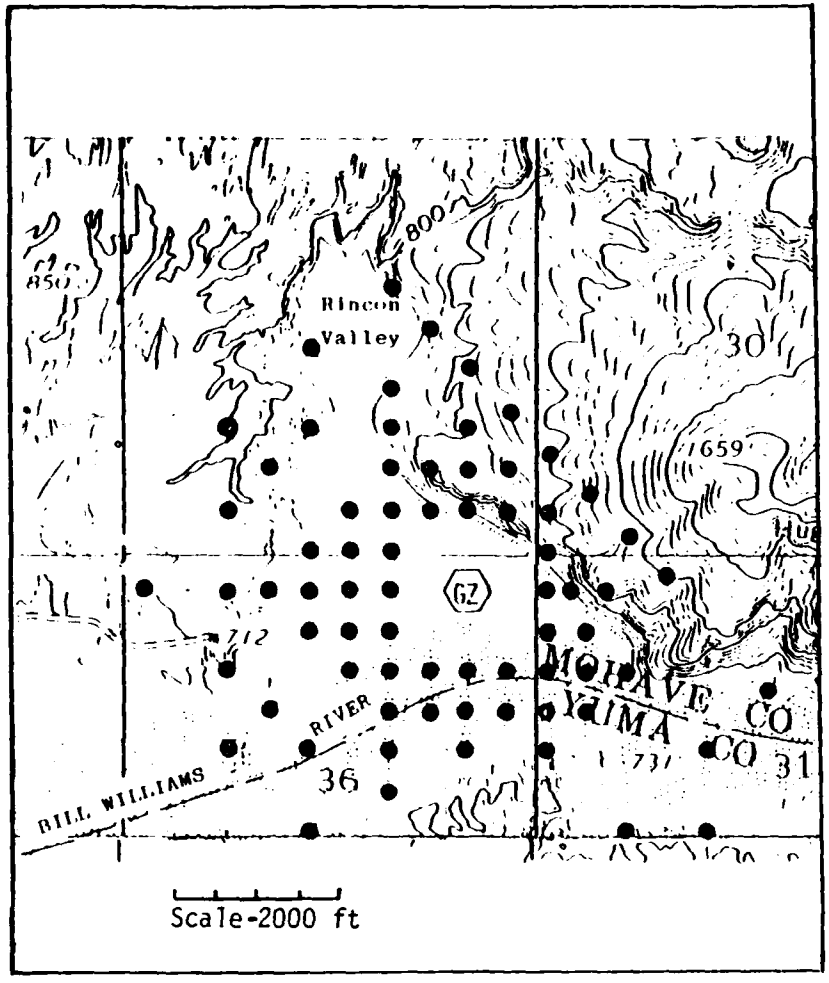

Figure A.1. Fallout Tray Locations for MISERS BLUFF II-2 Multiple Burst Event

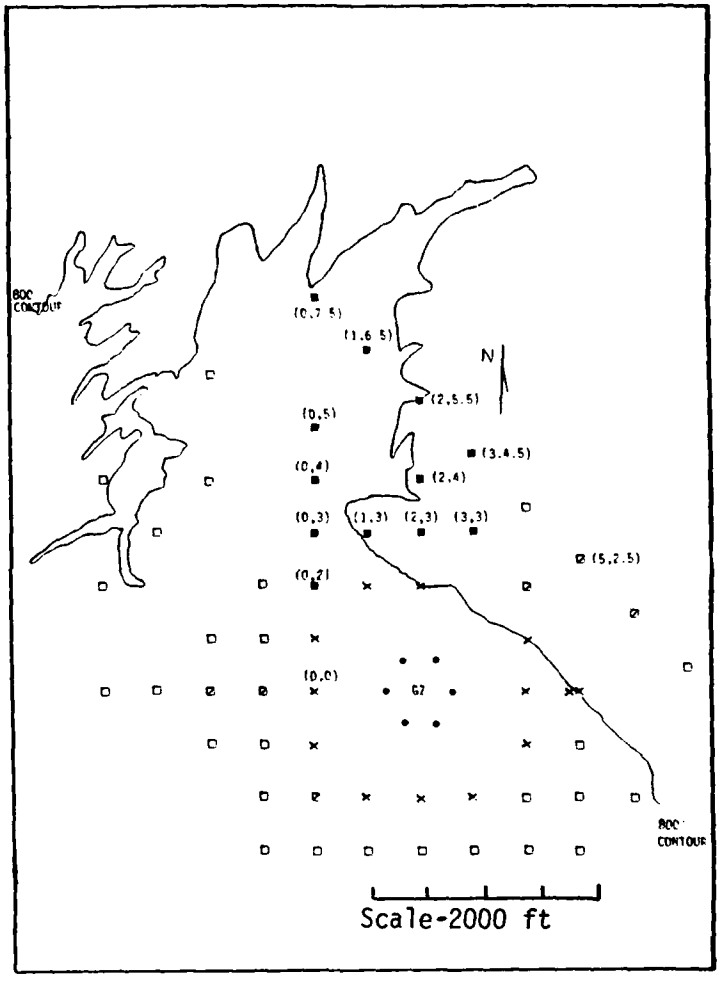

Figure A.2. Fallout Sample Locations For The MISERS BLUFF II-2 Dust Cloud

with diagonals (6) mark the location of dust samples that consisted of small quantities of very fine particles (< 90 μm) probably lofted by the blast wave passing over the loose surface soil. These samples were not attributed to dust cloud fallout. The X's show locations of the fallout trays that did not survive the high dynamic pressures within 1000 feet of the "GZ" for the array of bursts.

A-3 FALLOUT DATA ANALYSIS

A-3.1 Sample Sieving

In order to facilitate correlating the fallout data with the early time PSD* data obtained by aircraft sampling the cloud stem and cap, particle size distributions were obtained for the fallout samples. This was accomplished by dry sieving the fallout samples using standard sieving meshes and plotting soil gradation curves. These curves, which yield a percentage of the sample that is finer (or coarser) by weight than the total sample weight, were then used to construct mass distributions for each of the fallout samples. The ten standard sieve openings used in the fallout analysis were 2000, 1400, 1000, 710, 500, 250, 90, 63, 45, and 38 microns, although not all of the samples contained particles whose sizes spanned this large range of mesh sizes.

Of the 13 dust cloud fallout samples obtained from the multiple burst test, only 6 contained sufficient dust (> 0.3g) to obtain the accurate (0.01g resolution) weight measurements required to generate soil gradation curves. The remaining 7 fallout samples were sieved, but only to determine the maximum particle sizes (for both solid particles and aggregates) and to qualitatively estimate the range of particle diameters that constituted the majority of the particles in the sample. Table A.1 summarizes the results obtained from dry sieving the 13 fallout samples from the MINERS BLUFF II-2 dust cloud.

---

*Particle Size Distribution

Table A.1

Cumulative Mass Distributions for MISERS BLUFF II-2 Fallout Samples

Sample No.	Location	Percent By Weight Larger Than Indicated Mesh Opening (μm)										Largest Particle (mm)	
		2000	1400	1000	710	500	250	90	63	45	38	Solid	Aggregate
1	(3,3)	0	0	2	12	45	90	97	99	100		1.5	2.2
2	(2,4)	1	14	45	77	90	95	98	-	99	100	1.5	2.5
3	(1,3)	0.5	13	29	50	71	93	99.5	100			1.0	2.5
4	(1,6.5)	3	5	25	62	88	99	100				1.5	2.2
5	(0,5)	5	15	25	50	80	95	99.5	100			1.5	2.5
6	(0,7.5)	7	13	31	50	76	98	99	-	99.5	100	1.5	5.5x4x2
		Estimated Data for Small (< 0.3 g) Samples											
7	(5,2.5)						0	10		90		.10	-
8	(3,4.5)			0	10	90						.75	.75
9	(2,3)		0			10		90				1.0	-
10	(2,5.5)		0	10		90						1.3	1.3
11	(0,2)		0	10		90						1.0	1.2
12	(0,3)		10		90							1.1	2.4
13	(0,4)	0		10		90						1.2	2.2

The data contained in Table A.1 for fallout samples 1-6 have been plotted on standard soil gradation curve forms and are presented in Figures A.3 through A.5. (It should be noted here that our procedures used in sizing the fallout samples were not the same as those used in standard soil mechanics. There, the aggregates are broken down into their smallest component grain sizes prior to sieving and, hence, much of the medium and coarse "sand" evident on the fallout gradation curves would not be found if standard procedures were used.) Visual analysis of the large particle fallout revealed that the vast majority of the particles $\gtrsim$ 250 μm were actually aggregates that consisted of very fine sand or silt cemented together. This is mentioned to point out that caution should be exercised if comparisons are made between the fallout soil gradation curves and the in-situ soil characterization performed by the U.S. Army Waterways Experiment Station (WES) for the MISERS BLUFF II test bed soil.

A-3.2 Mass and Size Distributions of Fallout Samples

With the soil gradation data obtained from dry sieving the fallout samples, differential curves approximating the mass distributions of each sample were derived. Since the fallout experiment was designed to obtain information on the early time, large particle environment within the cloud, emphasis was placed on particle sizes $\gtrsim$ 250 μm.

Considering the mesh sizes used in the fallout analysis, the majority ($\geq$ 97 percent by weight) of the larger particles in each sample could be lumped by mass ($\Delta M(i)$), into six distinct size classes or bins. The range of particle diameters in each bin was limited by the mesh opening of the sieve in which the particles were contained (a_i) and the next, successively larger mesh size (a_{i+1}). The median particle size ($\bar{a}_i$) in each bin was represented by:

$$\bar{a}_i = a_i + \left(\frac{a_{i+1} - a_i}{2} \right)$$

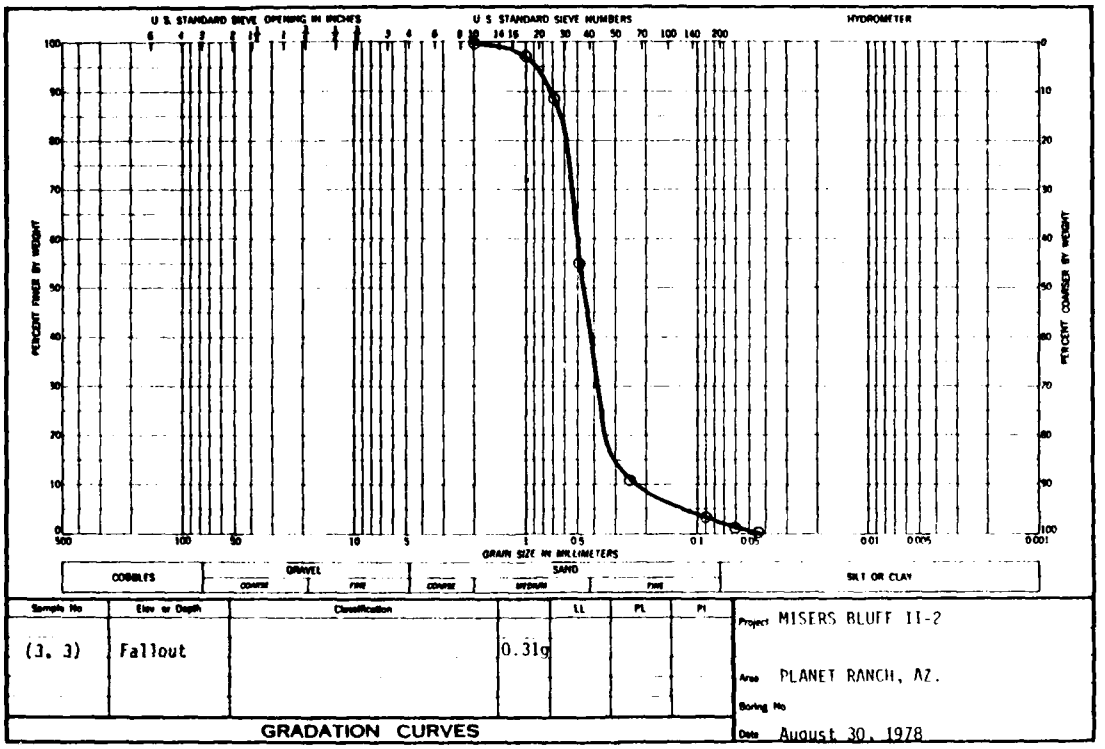

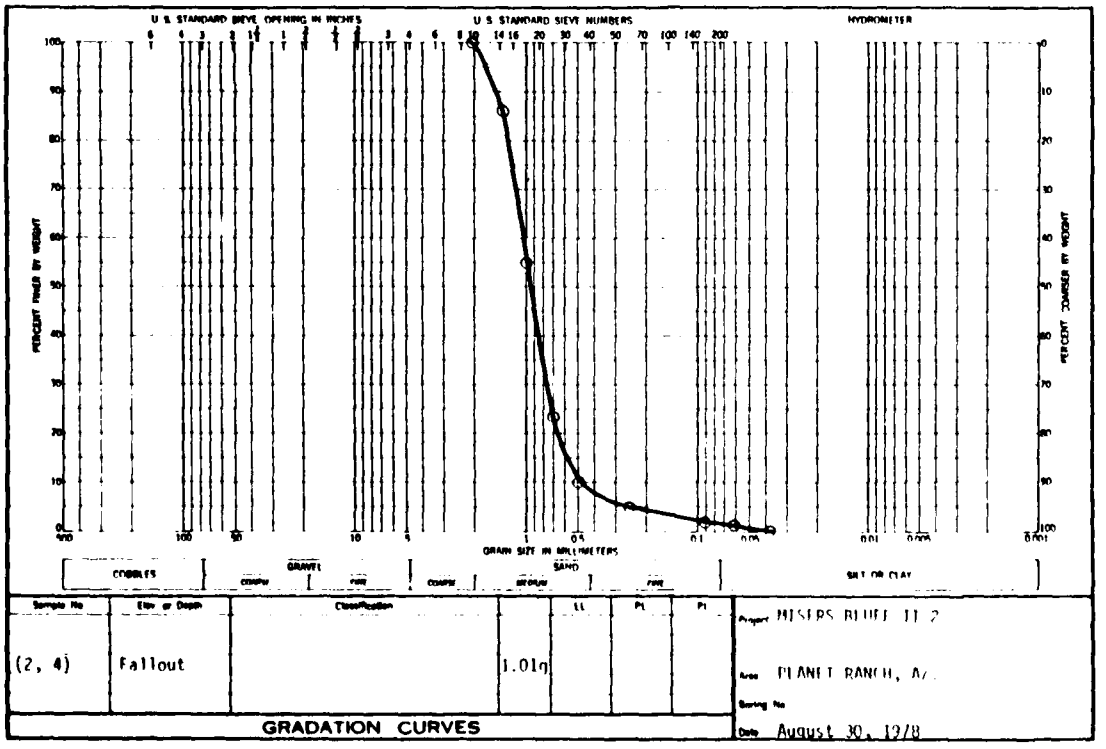

Figure A.3. MISERS BLUFF II-2 Fallout Sample Soil Gradation Curves

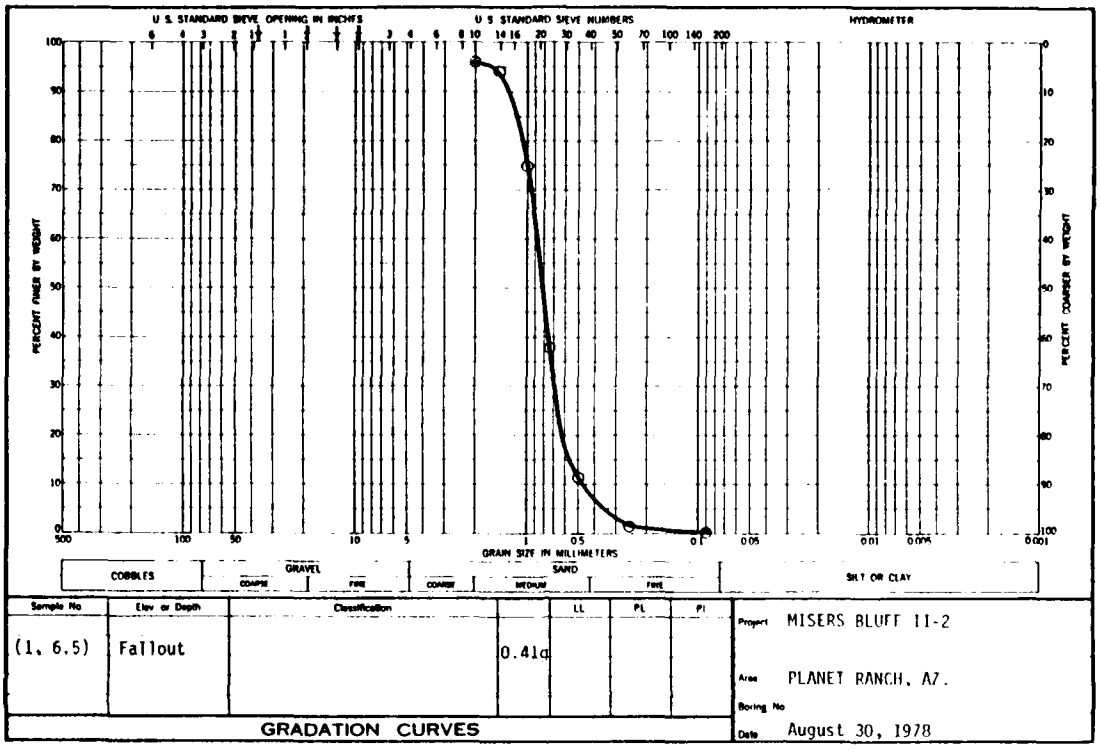

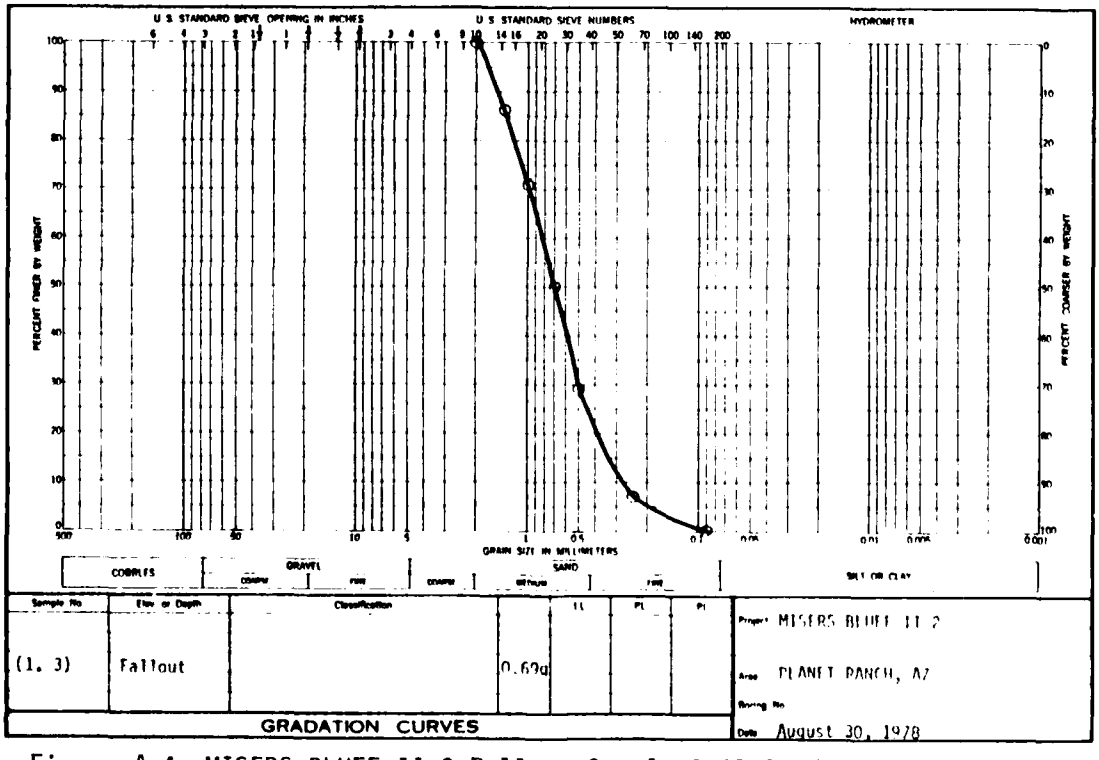

Figure A.4. MISERS BLUFF II-2 Fallout Sample Soil Gradation Curves

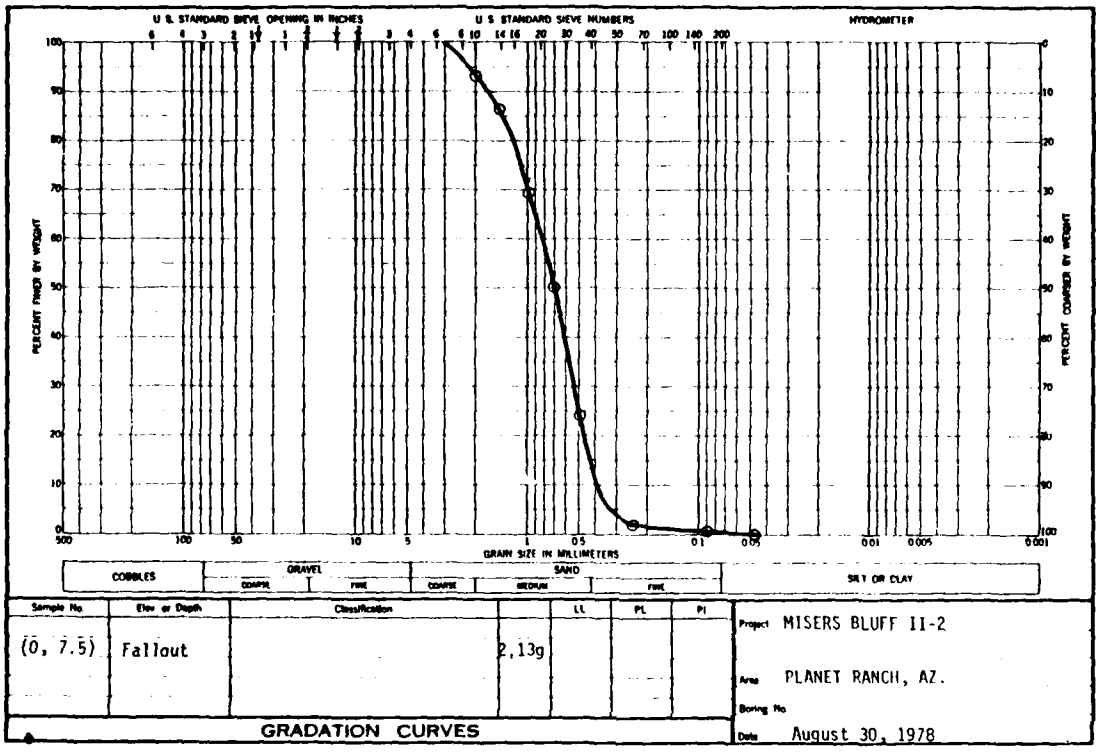

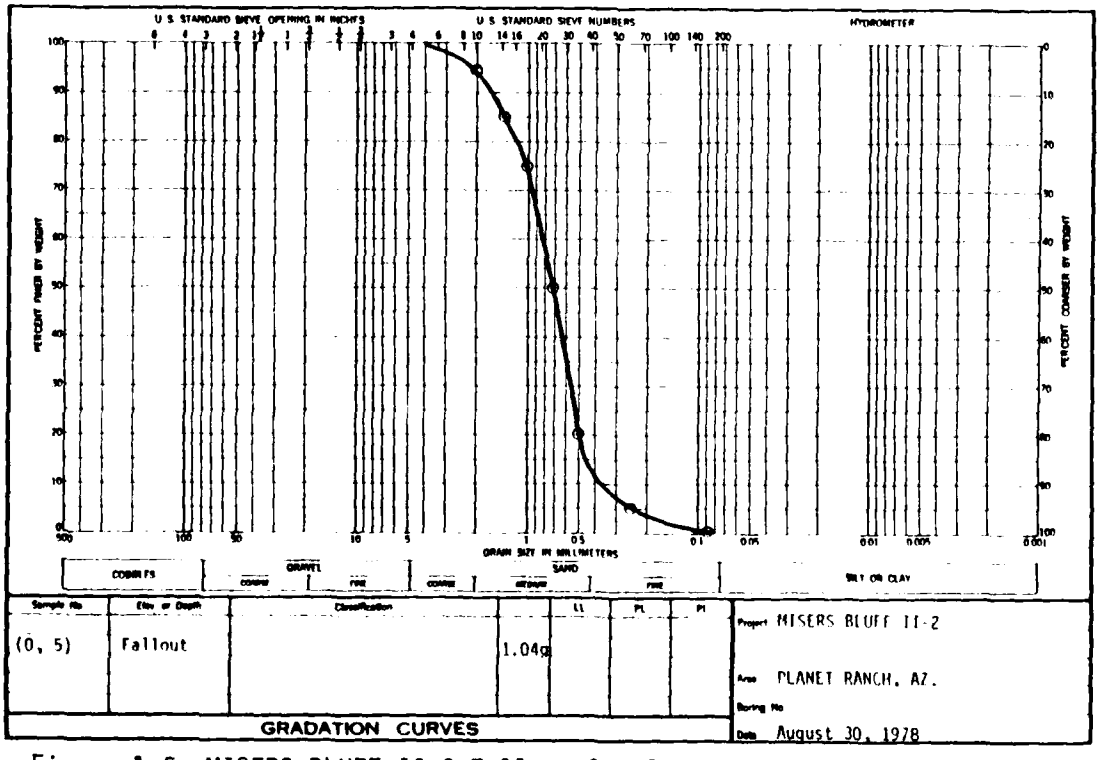

Figure A.5. MISERS BLUFF II-2 Fallout Sample Soil Gradation Curves

Table A.2 summarizes the range of each size bin (i), the bin widths (Δa_i), and the median bin diameters ($\bar{a}_i$) used in the MISERS BLUFF II-2 fallout analysis.

Table A.2
Size Bins for MBII-2 Fallout Particles

Bin (i)	a_i-a_{i+1} (μm)	Δa_i (μm)	$\bar{a}_i$ (μm)
1	90-250	160	170
2	250-500	250	375
3	500-710	210	605
4	710-1000	290	855
5	1000-1400	400	1200
6	1400-2000	600	1700

Values of $\Delta M(i)$ for each size bin can be obtained directly from Table A.1. These values were obtained for the six samples that contained a sufficient amount of dust for accurate weight determinations (Samples No. 1-6). Finally, with the values of $\Delta M(i)$ known for each bin (i), differential mass distributions were generated for each fallout sample using the functional form of:

$$\frac{\Delta M(i)}{\Delta a_i} \quad \text{vs.} \quad \bar{a}_i \ ,$$

which is an approximation to the continuous function

$$\frac{dM}{da} \quad \text{vs.} \quad a \ .$$

From the relationship:

$$\frac{dM}{da} = m(a) \frac{dN}{da} \ , \tag{1}$$

where $m(a) = Ka^3$
and dN is the number of particles in da, we can obtain

$$\frac{dN}{da} = K^{-1}\left(\frac{dM}{da}\right)\left(\frac{1}{a}\right)^3 \tag{2}$$

This continuous function can then be approximated by the expression:

$$\frac{\Delta N(i)}{\Delta a_i} = K^{-1} \left(\frac{\Delta M(i)}{\Delta a_i}\right)\left(\frac{1}{\bar{a}_i}\right)^3 , \qquad (3)$$

where $K^{-1} \propto \frac{6}{\pi\rho}$.

From Equation (3) it can be seen that curves proportional to the fallout sample size distributions (dN/da) can be approximated by plotting values of:

$$K^{-1} \left(\frac{\Delta M(i)}{\Delta a_i}\right)\left(\frac{1}{\bar{a}_i}\right)^3 \quad \text{vs.} \quad \bar{a}_i \quad .$$

Figures A.6 through A.8 contain plots of both $\Delta M(i)/\Delta a_i$ and $\Delta N(i)/\Delta a_i$ vs. $\bar{a}_i$ for fallout sample numbers 1-6; the smooth curves drawn through these points represent dM/da and dN/da vs. a. Again, a certain amount of caution should be exercised in interpreting the size distributions depicted in these figures. For example, $K^{-1} = 10^8$ was chosen only to allow both distributions to be plotted on the same scale, therefore, the number of particles obtained by integrating the size distribution between two particle diameters would be a gross overestimate. The curves do, however, approximate the shape (slope) of the particle size distributions over the size range of interest assuming the particle density (ρ) is not a function of particle size.

In interpreting the mass distributions, it should also be remembered that the plotted maximum values in the distributions correspond to a range of particle diameters that is represented by a median value (see Table A.1.). Fortunately, the mesh sizes selected for dry sieving the samples limit the actual particle diameter corresponding to the maximum value to be off, at most, 145 μm from the plotted median diameter.

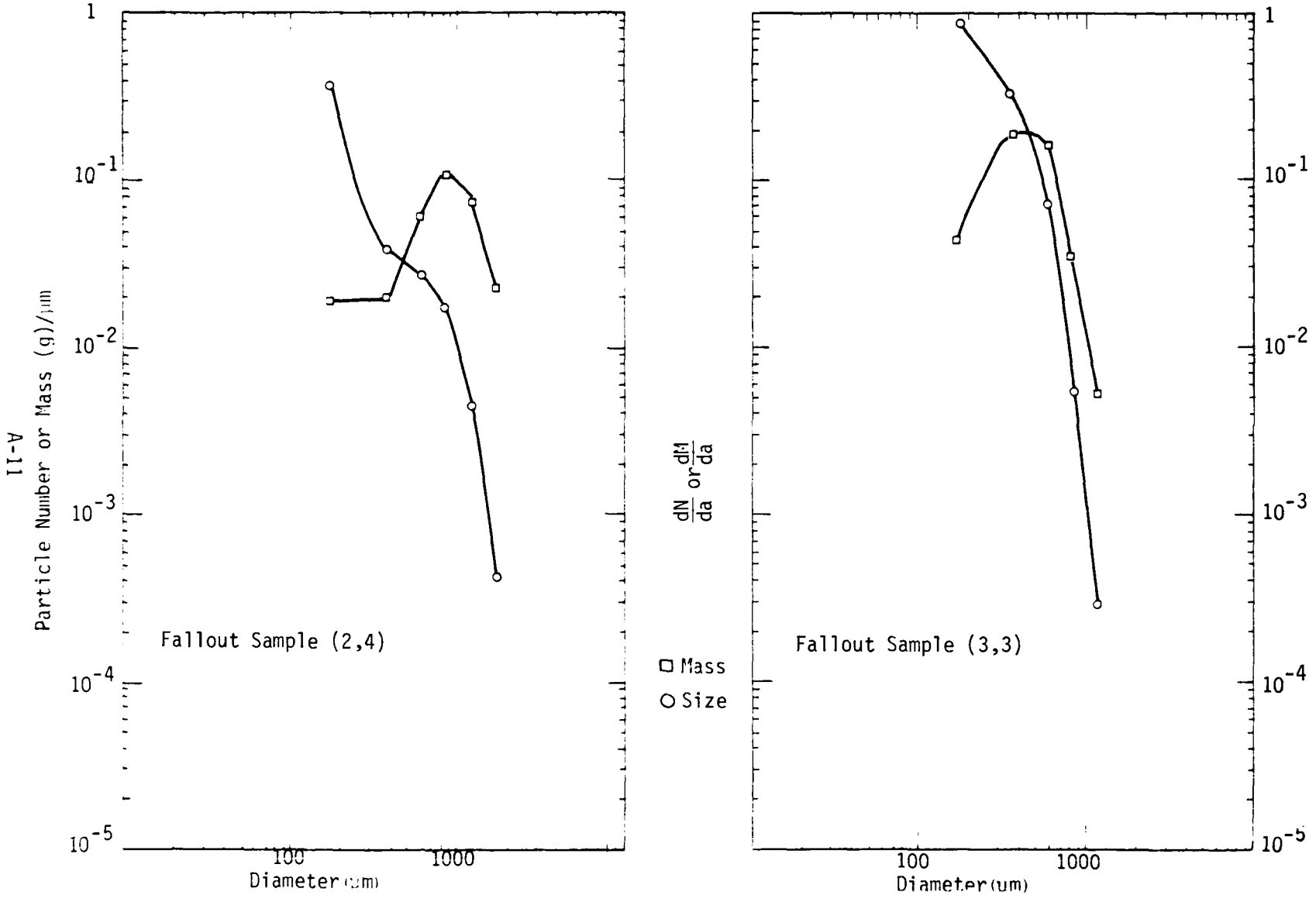

Figure A.6. MISERS BLUFF II-2 Fallout Sample Size and Mass Distributions

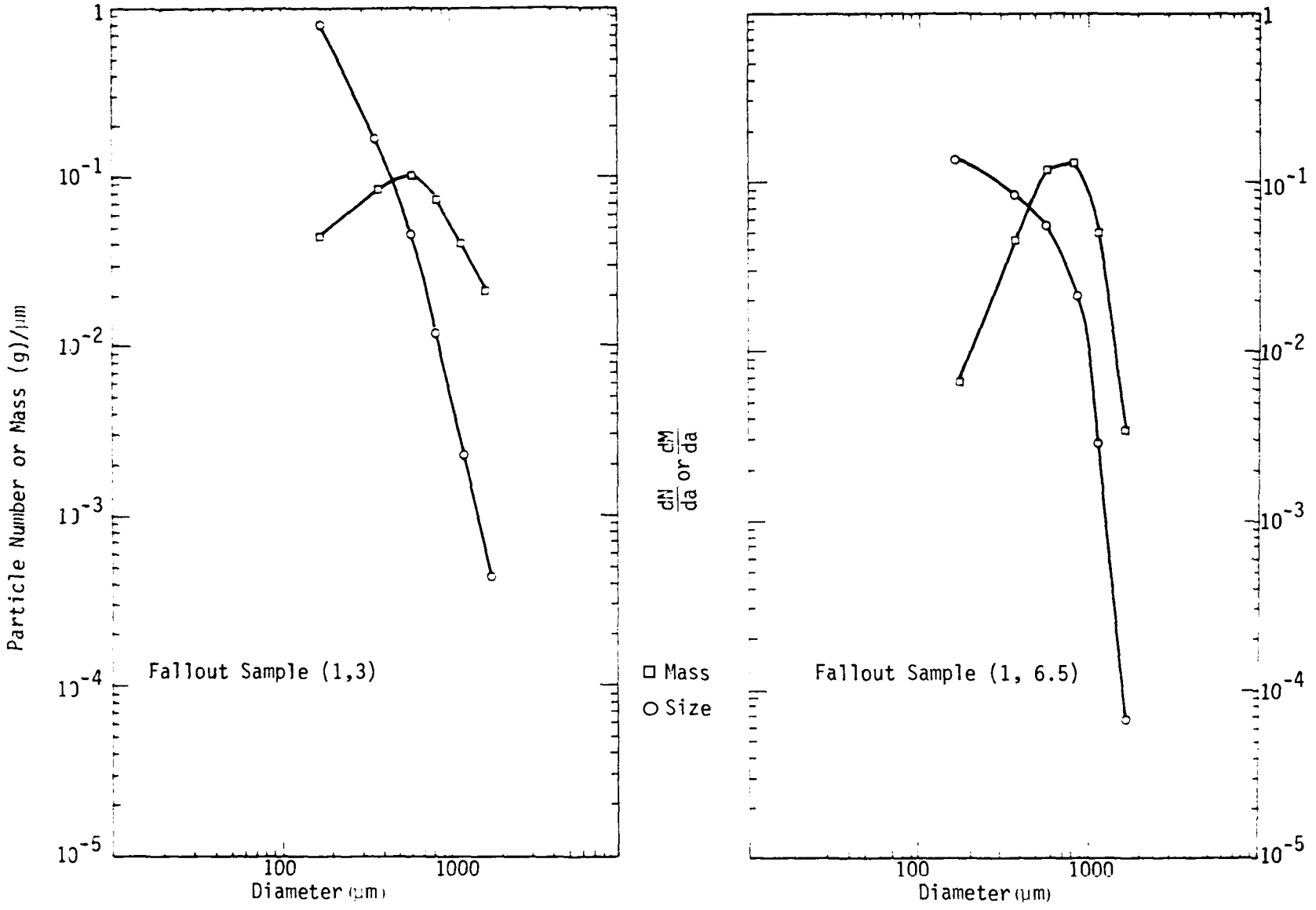

Figure A.7. MISERS BLUFF II-2 Fallout Sample Size and Mass Distributions

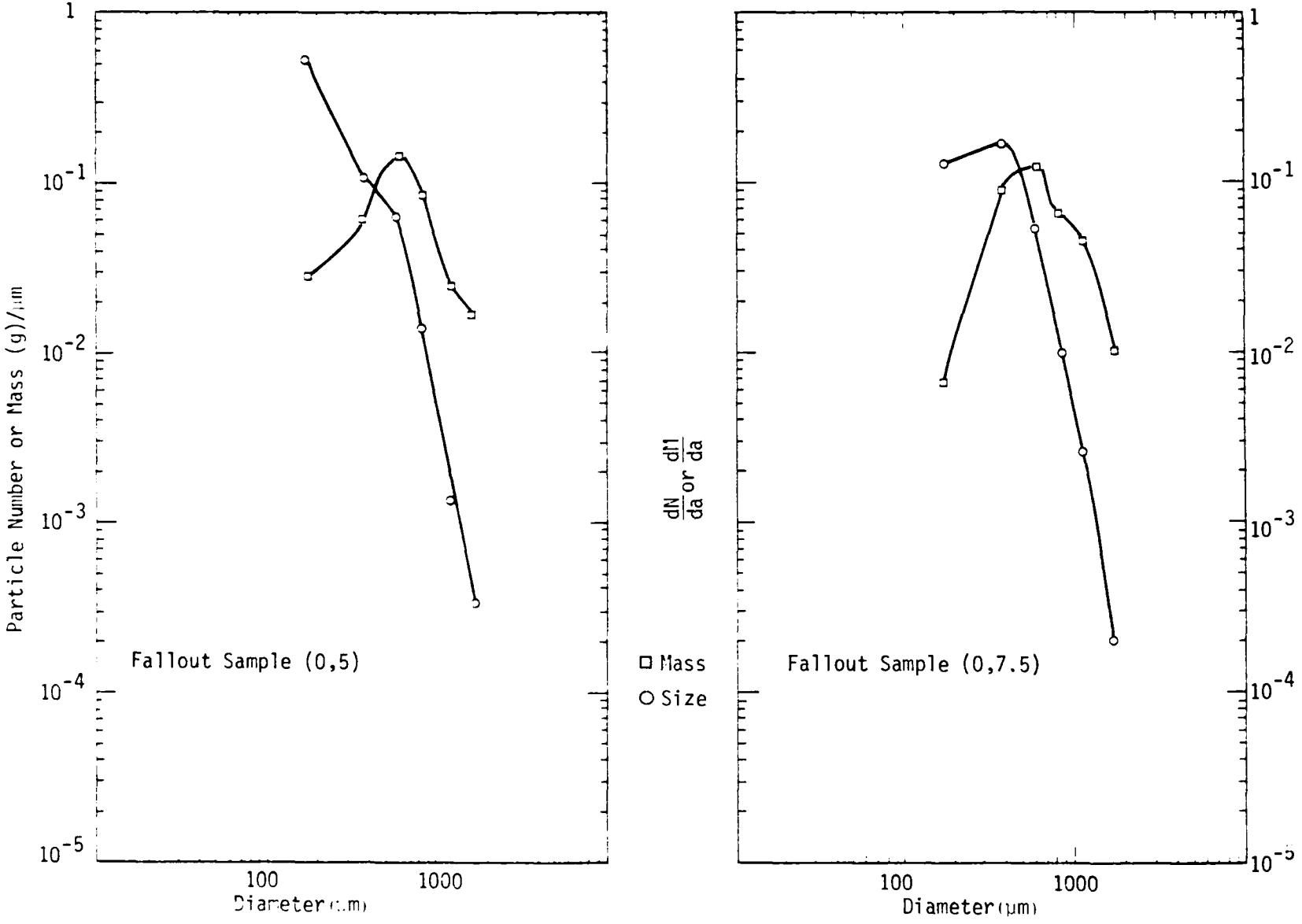

Figure A.8. MISERS BLUFF II-2 Fallout Sample Size and Mass Distributions

A-3.3 Source of MISERS BLUFF II-2 Close-In Fallout

In order to determine the source of the close-in fallout from the MISERS BLUFF II-2 dust cloud, it was necessary to develop a fallout model that would adequately describe the gross features of the fallout deposition. By calculating dust particle trajectories based on local wind conditions and particle fall velocities, and then tracing these trajectories backwards in time to possible source regions within the cloud, it soon became apparent that the cloud stem was the only viable source for the close-in fallout.

A-3.3.1 Fallout Modeling

The first step in attempting to model the close-in fallout was to see how, as a function of time, the cloud stem and cap traversed the array of fallout trays. The dust cloud cap and stem track data used in the analysis are depicted in Figure A.9. These data were obtained by Technology International Corporation (TIC) from photographic analysis of the MISERS BLUFF II-2 dust cloud. An obvious, and important feature to note is that the cloud cap moves to the north much faster than the cloud stem from T=0 to T+5 minutes; the reason for this being that, due to height differences, the horizontal motion of each portion of the cloud is being controlled by different wind conditions.

The cloud stem track data also revealed that the low level winds (surface to approximately 2000 feet AGL) measured at the Planet Ranch headquarters at detonation time could not be used in a definitive fallout analysis. The low level, orographic effects of the terrain in the vicinity of GZ (see Figure A.1) made it necessary to slightly revise the measured winds to account for the early time stem motion. The wind profile used in the fallout model is given in Table A.3 and was derived from photographed stem motion and upper level winds measured at detonation time.

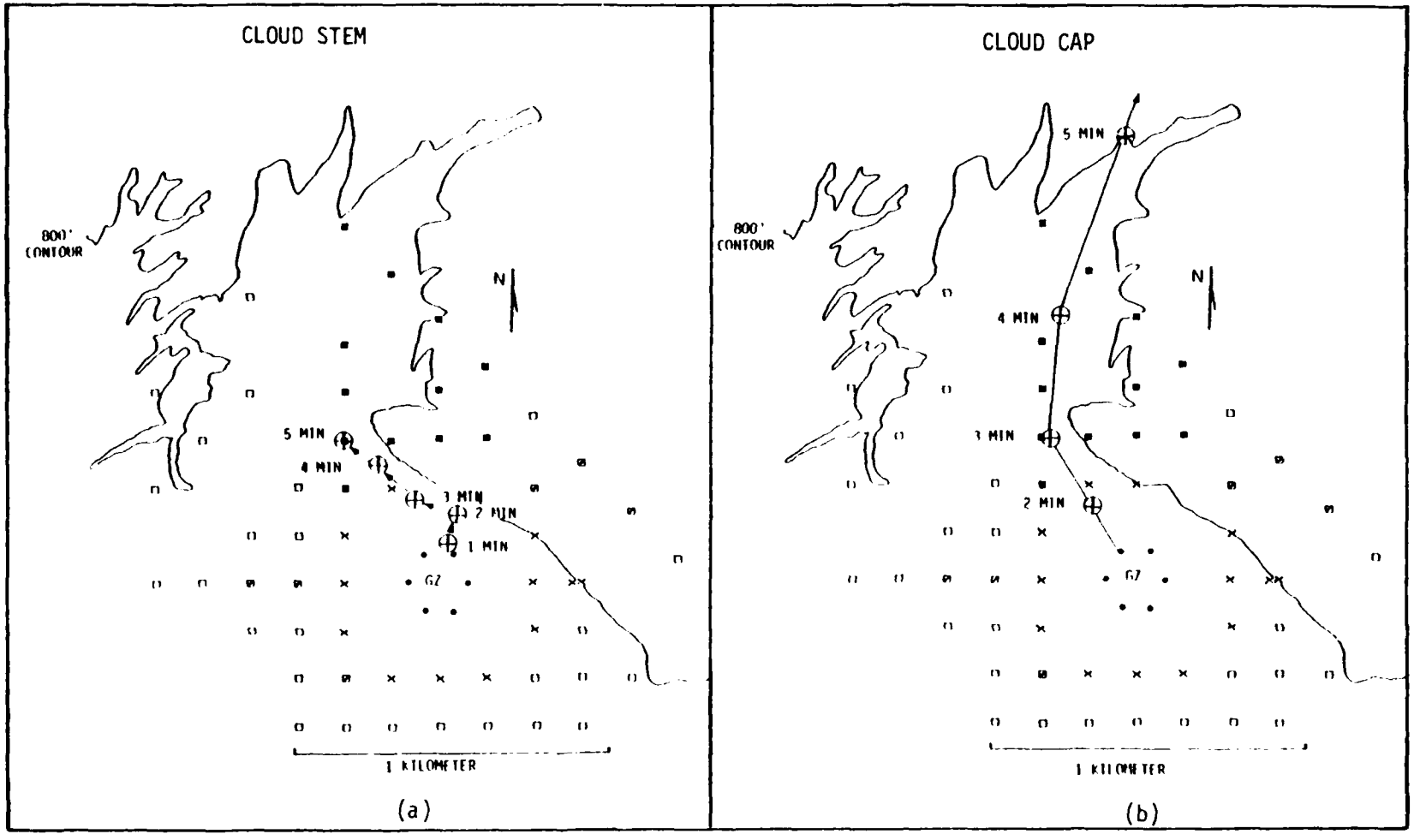

Figure A.9. MISERS BLUFF II-2 Dust Cloud Stem (a) and Cap (b) Movement From T+1 to T+5 Minutes After Detonation

Table A.3.

MISERS BLUFF II-2 200 Foot Layer Averaged Winds

Altitude (KFT AGL)	Winds (Deg/Knots)	Altitude (KFT AGL)	Winds (Deg/Knots)
sfc - 200[a]	200/04	1600 - 1800[a]	170/08
200 - 400[a]	200/04	1800 - 2000[b]	194/11
400 - 600[a]	200/04	2000 - 2200[b]	190/12
600 - 800[a]	180/04	2200 - 2400[b]	186/13
800 - 1000[a]	150/05	2400 - 2600[b]	182/14
1000 - 1200[a]	120/05	2600 - 2800[b]	178/14
1200 - 1400[a]	120/05	2800 - 3000[b]	713/15
1400 - 1600[a]	150/05	3000 - 3200[b]	162/12

[a]derived from stem track

[b]measured at time of detonation

In addition to the wind data available, particle fall velocities had to be estimated and used in conjunction with wind data in order to calculate fallout particle trajectories. Unfortunately, particle fall velocities will vary not only with particle area and mass, but also from region to region within the cloud, depending on the flow field being experienced. To keep the fallout model as simple as possible, it was assumed that, at any given time, some particles of all sizes within the dust cloud will be falling at their terminal fall velocities and that their trajectories will be determined by the velocities and the local wind conditions. With the trajectories calculated for various sized particles (see Appendix D for terminal fall velocity calculations) it was possible to begin at a fallout tray location and trace the trajectory backward in time to source regions within the dust cloud.

Figure A.10(a) shows the fallout sample locations and depicts the trajectories that various sized particles would have to follow from the dust cloud to be collected in several of the fallout trays. The numbers at intervals along the trajectories indicate the altitude of the particle at that (x, y) location on the grid. The envelope of all particle trajectories terminating at the sample locations should define the region of the dust cloud that was the source of the fallout. Figure A.10(b) shows this envelope and also the outlines of the cloud stem and cloud cap widths from T+1 to T+6 minutes. It is quite evident from this figure that the cloud cap, at least that portion of the cap lying outside the outline of the stem, contributed virtually nothing to the close-in fallout deposition.

To test the hypothesis that the MISERS BLUFF II-2 cloud stem was the source of the large particle fallout from the dust cloud, the simple fallout model was applied to dust particles within the stem region of the cloud. Stem width and height data, as a function of time-after-burst (TAB), was provided by TIC analysis of photographic data.

In the fallout model, the cloud stem at any time is represented by a vertically oriented cylinder of dust, hence, projecting a circular area in the x-y plane. In actuality, at times after T+2 minutes, the cloud stem began to slant as the top of the stem experienced higher wind velocities, and its projection in the x-y plane was an ellipse. The elliptical shape of the stem projection would tend to lengthen, but not broaden, the shape of the resulting fallout pattern.

The vertical cylinder of dust was divided into 200 foot layers so that dust particles in each layer could be subjected to the wind profile existing at detonation time (Table A.3). Again it was assumed that at least some of the particles in each layer would be falling at their terminal fall velocities. Dust particle trajectories were then calculated for 300, 500, and 1000 μm particles based on upper level winds and their respective fall velocities (see Figure A.10(a)). Based

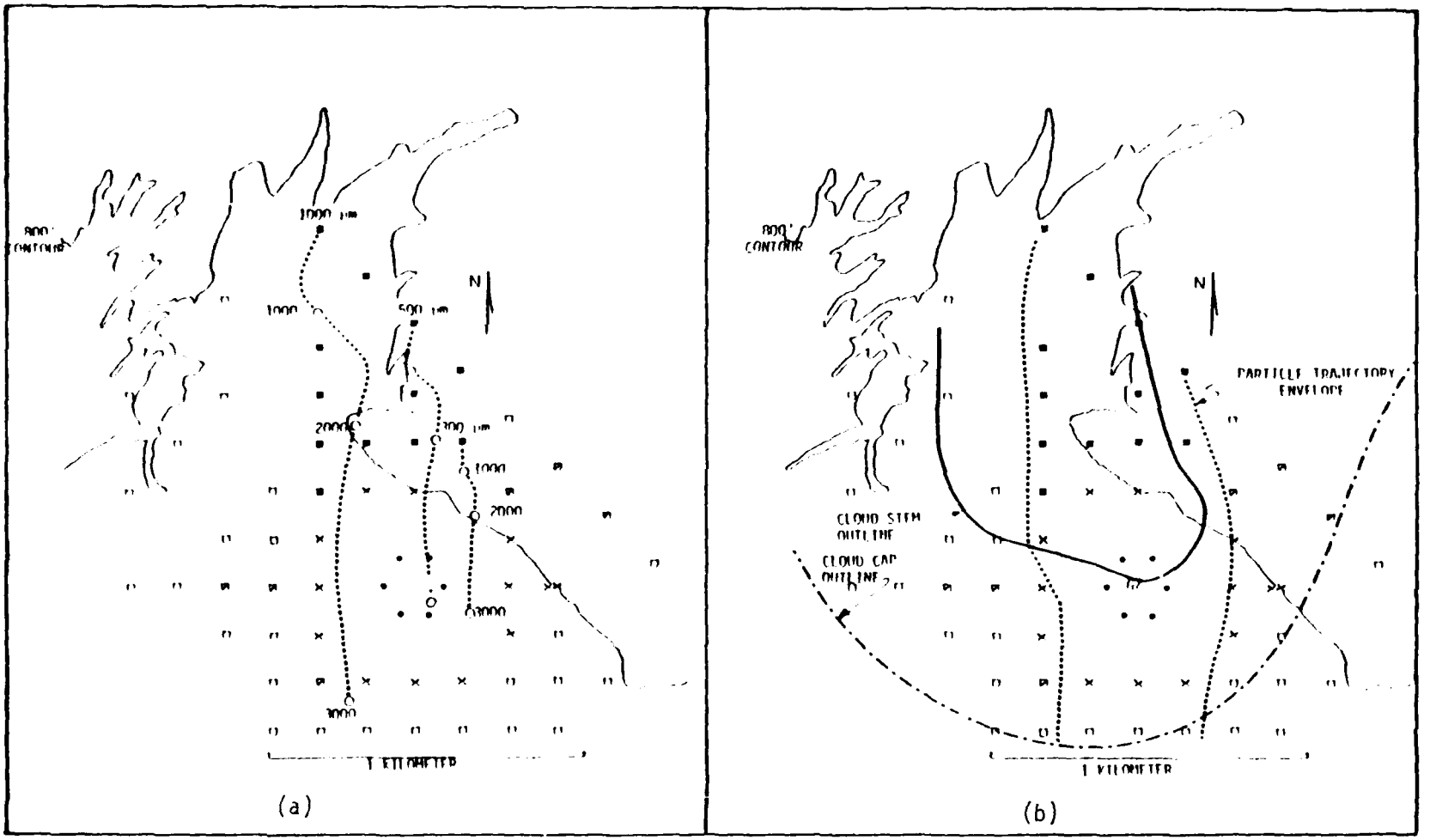

Figure A.10. MISERS BLUFF II-2 Fallout Particle Trajectories (a) and Trajectory Envelopes (b) For Fallout Particles $\geq$ 300 µm

on the calculated trajectories, particles of varying sizes in each dust layer were transported to the ground and contours (envelopes) were drawn on the surface depicting the area in which the single size particles from each layer would land.

Figures A.11(a)-(d) reveal the expected fallout deposition patterns from the cloud stem assuming particle fall begain at 2, 3, 4, and 5 minutes after burst. R_s and H_s refer to the stem radii and heights, respectively at each time-after-burst. The outline of the cloud cap is also shown on each one of the figures to show that early time fallout from this region of the cloud was not detected in the fallout trays. Except for predicting fallout in three trays where no fallout was collected, and no dust in one tray where fallout was sampled, it appears that the simple fallout model, which uses the cloud stem as the only source of fallout particles, adequately describes the gross features of the MISERS BLUFF II-2 dust cloud fallout.

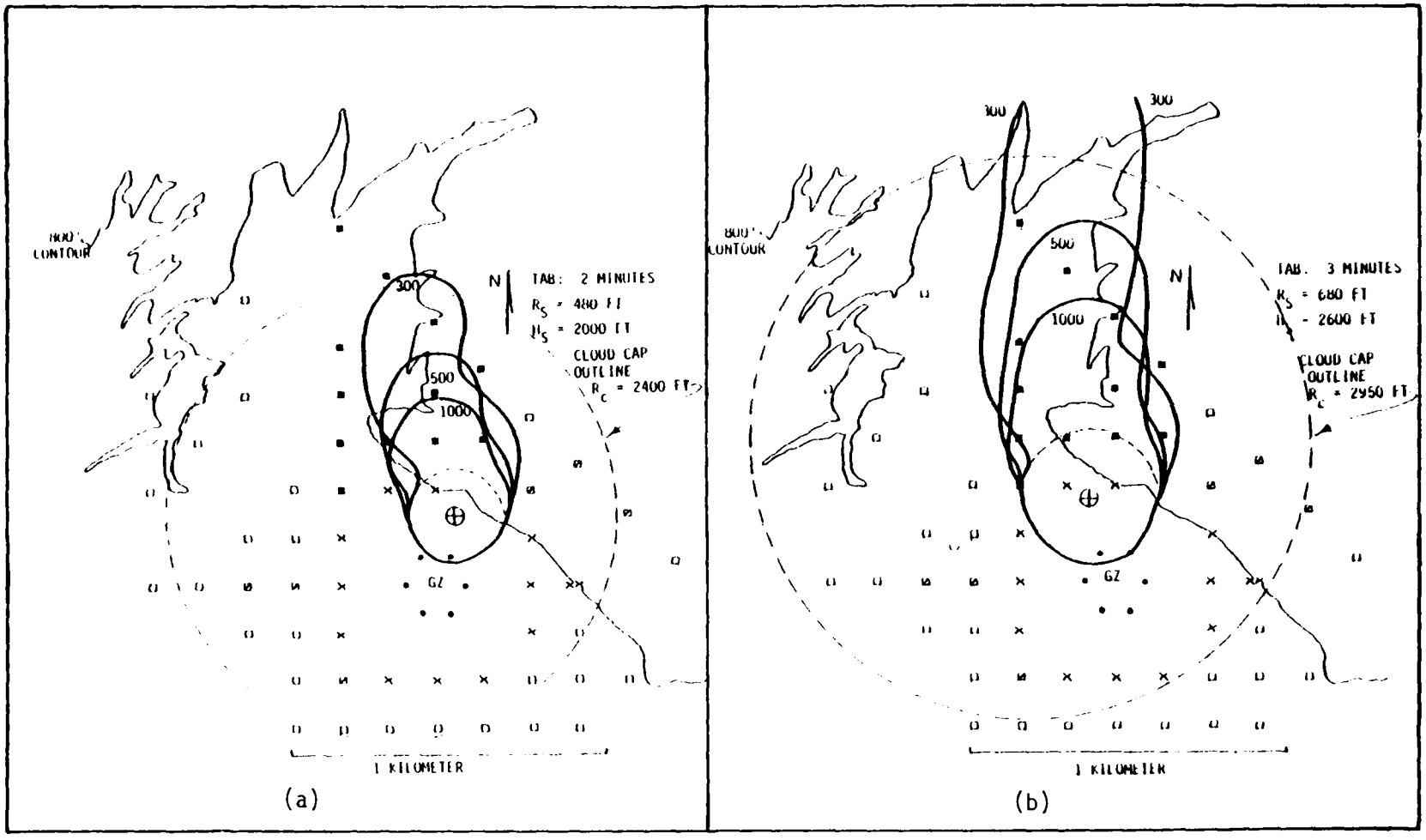

Figure A.11. Expected Fallout Deposition Pattern for Particle Sizes 1000, 500, and 300 μm From MISERS BLUFF II-2 Dust Cloud Stem at Two Minutes (a) and Three Minutes (b) After Detonation

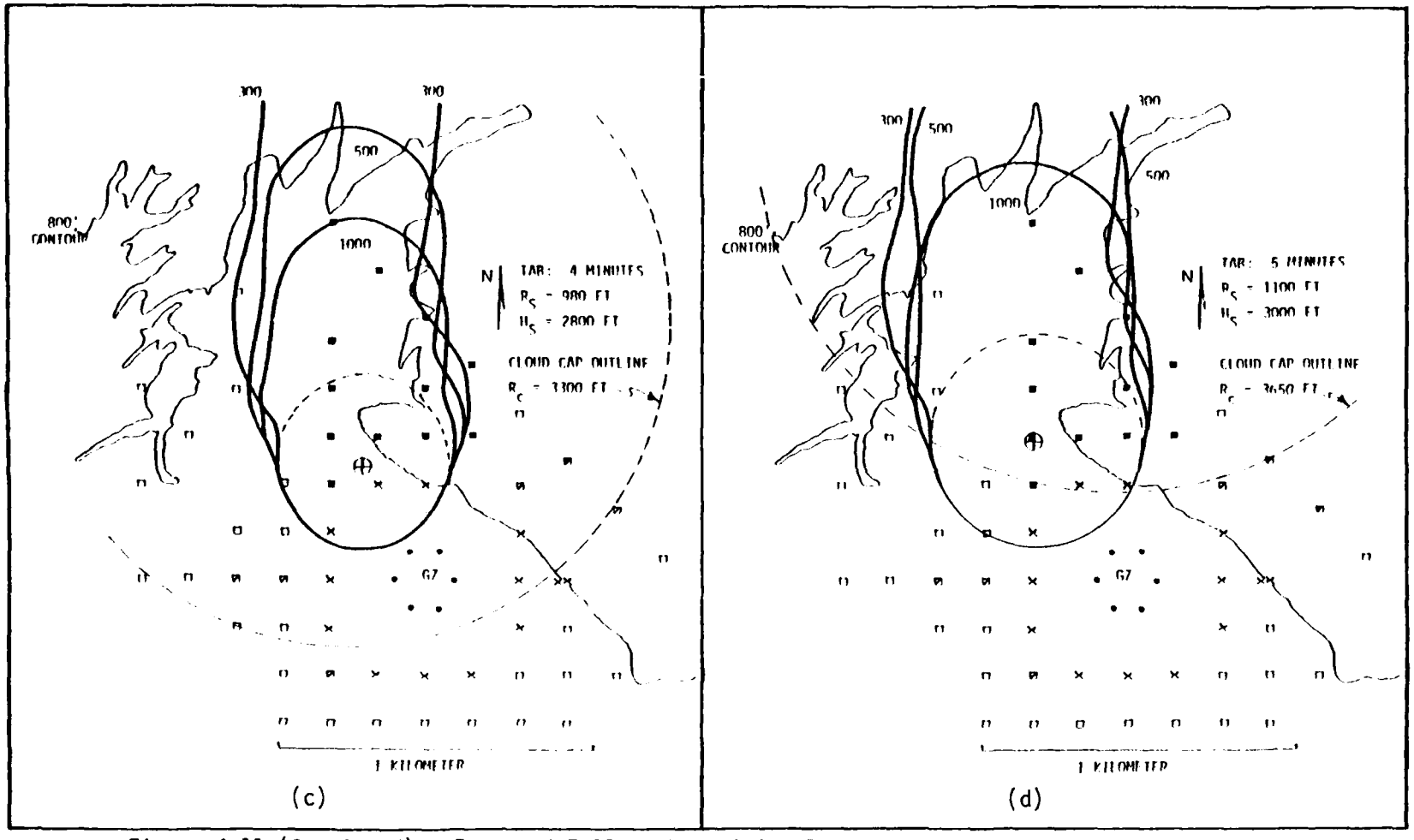

Figure A.11 (Continued). Expected Fallout Deposition Pattern for Particle Sizes 1000, 500, and 300 μm From MISERS BLUFF II-2 Dust Cloud Stem at Four Minutes (c) and Five Minutes (d) After Detonation

APPENDIX B

DETAILED DUST PARTICLE SPECTRAL DATA DERIVED FROM IN SITU SAMPLING OF THE MISERS BLUFF II DUST CLOUDS

B-1. INTRODUCTION

The basic format of the dust particle spectral data requested from Particle Measuring Systems, Inc. (PMS) was a two-second resolution time history of particle number concentrations (#/cc), by particle size, over the size range of particles anticipated for the MISERS BLUFF II dust clouds.

For three of the instruments employed in the sampling operation (FSSP, LAS-X, and OAP-200X), obtaining the two-second (~400 ft, ~120m) resolution within the dust clouds was possible via the instrument's interfacing with the on-board Data Acquisition System (DAS). (For a more detailed discussion on the instrumentation employed in the in-situ sampling operation, refer to Reference 2). Figure B.1 is an example of the spectral data derived from the FSSP probe output. Bin numbers 106-120 correlate with median particle diameters of 3-45 μm in 3 μm increments, i.e., 1.5-4.5 μm, 4.5-7.5, ..., 43.5-46.5 μm. Time of day (in seconds) is given in ten-second increments along the bottom of the figure; cloud entry and exit times are depicted by arrows. Each vertical column of numbers represents the particle number concentration (log ($\#/cm^3$)) in each size class of particles every two seconds. Two-second totals (log values) appear just above the time of day.

Figure B.2 is similar spectral data derived from the Two Dimensional Optical Array Imaging Probe (OAP-2D-C). Bin numbers 1-20 correlate with median particle diameters of 30-500 μm in 25 μm increments. Spectral data from the OAP-2D probes are recorded only when particles are present and, unlike the three probes mentioned above, this digital image data is stored in a buffer prior to being recorded. Since a buffer is "dumped" on tape only when it becomes full, it is

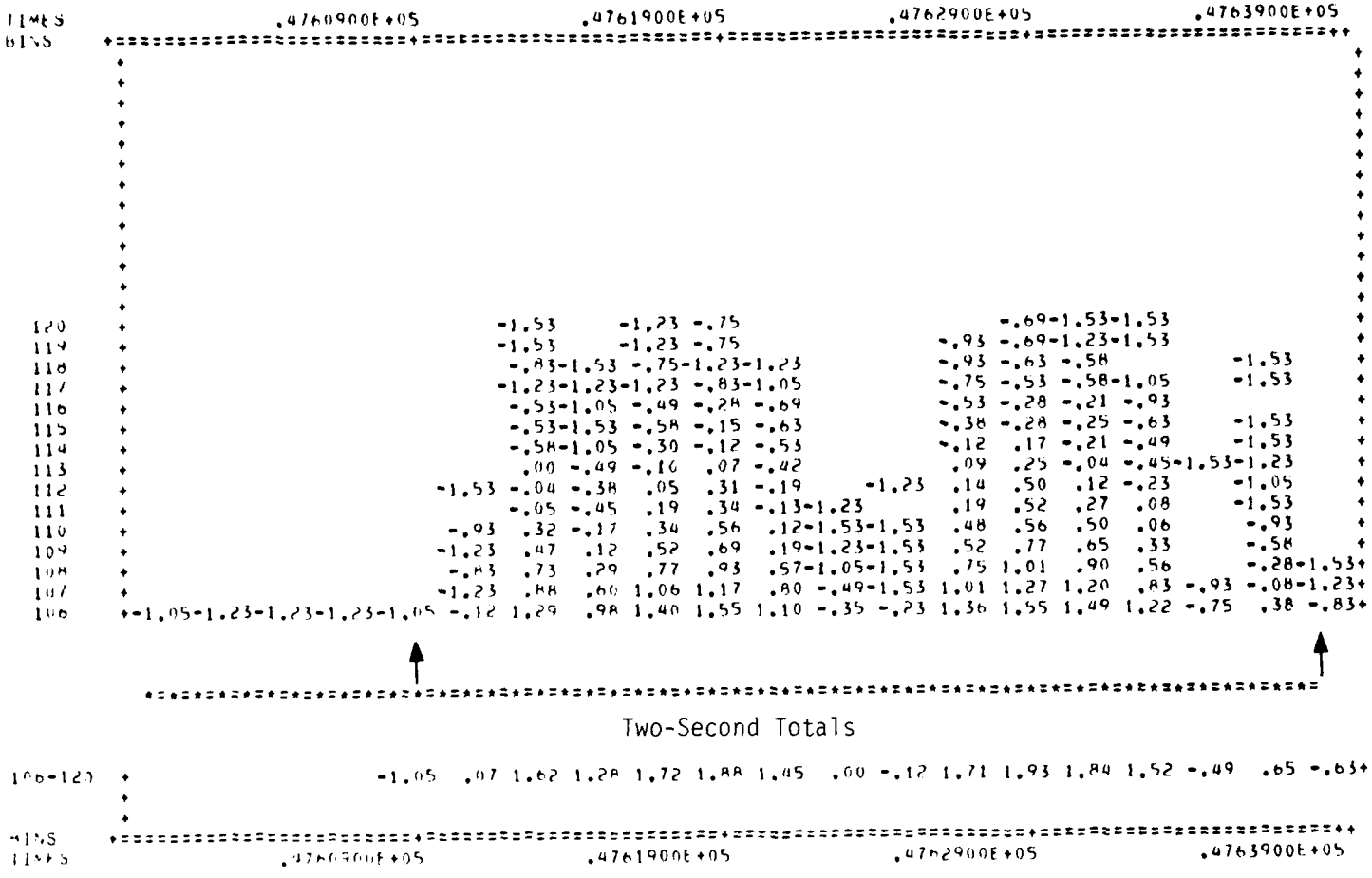

Figure B.1. Dust Particle Number Concentrations Versus Particle Size (3-47 μm) and Time For Pass #7, MISERS BLUFF II-I

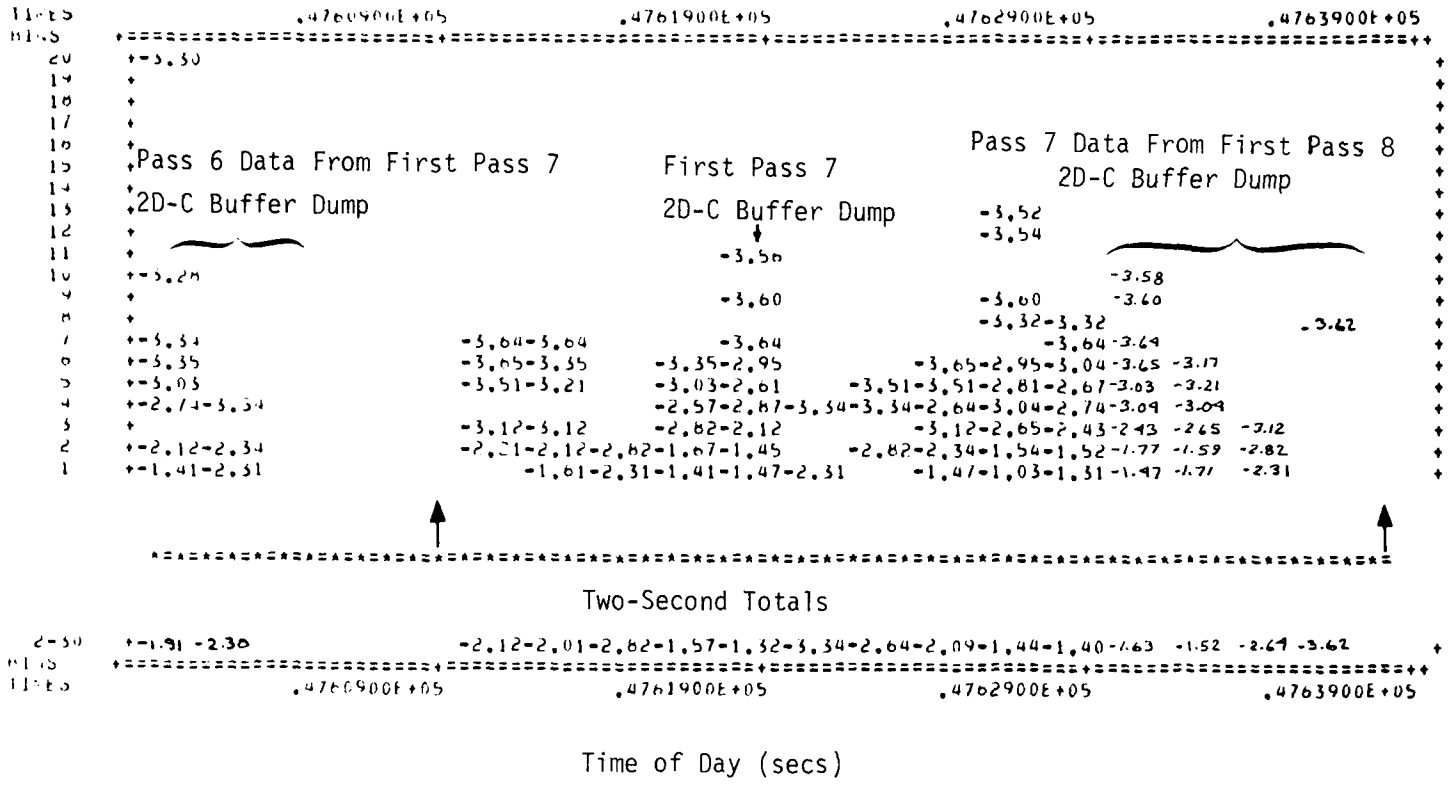

Figure B.2. Dust Particle Number Concentrations Versus Particle Size (>47 μm) and Time For Pass #7, MISERS BLUFF II-1

possible to acquire spectral data at the end of one sampling pass and have this data dumped during the next pass when the buffer fills. This delay is also true within regions of the cloud where large particle concentrations are low.

For this reason, obtaining the required two-second data resolution within the MBII dust clouds required a significant software development effort by PMS. Along with each image, the elapsed time since the last particle encounter is also stored in the buffer, and these times, along with the buffer dump times, are recorded. Hence, it was possible to "back out" the "location" (time of acquisition) of each particle encounter and place this data in its correct two-second interval. One remaining problem was that if more than approximately 7 seconds (OAP-2D-C) elapsed between particle encounters, the instrument's internal "clock" may have recycled several times and the "location" of these particles would be ambiguous by some multiple of 7 seconds. Fortunately, by comparing these "questionable" data points with the FSSP spectral data, it was possible to determine (judgementally) the most probable time of 2D data acquisition. (The OAP-2D-P instrument's internal "clock" recycled every ~28 seconds). Figure B.2 is a graphic example of how data was acquired during Pass 6 in the MBII-1 dust cloud and was not recorded until the buffer was filled and dumped during Pass 7. (The actual time between images in this example is 98 seconds, i.e., 14 clock cycles). This effort was successfully completed and we feel confident that the MISERS BLUFF II dust cloud spectral data represents the most detailed set of data made to date within any cloud - dust or water - with the 2D instruments.

B-2. DETAILED DUST PARTICLE SPECTRAL DATA PRESENTATION

Tables B.1 and B.2 are computer listings of all the MISERS BLUFF II two-second spectral data that were used in the analyses contained in this report. Table B.1 contains the spectral data

acquired during sampling passes 1-15 in the MISERS BLUFF II single burst dust cloud (MBII-1) while Table B.2 contains similar data from passes 1-11 in the multiple burst dust cloud (MBII-2). The format for both tables is basically the same; the only difference being Table B.2 contains spectral data for two more particle size ranges than does Table B.1. This is due to the OAP-2D-P instrument malfunctioning during the MBII-1 sampling mission and the addition of the LAS-X to the instrumentation suite fielded for the MBII-2 sampling mission (see Reference 1).

In both tables, the time in seconds after detonation, is given in the extreme left and right hand columns of each page. The asterisks refer to data intervals where the 2D spectral data has been added to a sampling pass as explained in section B-1. Extinction coefficients and radar reflectivity factors corresponding to the asterisked data intervals have not been corrected and are lined out.

Four particle parameters: (1) particle number concentration, (2) mass concentration, (3) extinction coefficient, and (4) radar reflectivity factor are listed for each two-second data acquisition interval. Of the four parameters, only the particle number concentration was measured; all other parameters have been calculated from these measured values assuming spherical particles.

B-2.1 Calculation of Mass Concentrations (g/m^3)

As previously mentioned, the only measured quantity available from the PMS data tapes was the particle number concentration (PNC) for each size class of particles during each two second data acquisition period. For each size class, the mass concentration (MC) is given by

$$MC(g/m^3) = PNC(\#/cm^3)10^6(cm^3/m^3)\ \text{Particle Mass}\ (g)$$

or

$$MC(g/m^3) = (PNC)\left(\frac{d^3}{6}\right)\rho \times 10^6$$

where d is the particle diameter in cm and ρ is the particle density in g/cm^3.

For each two-second interval, these values are summed over all size classes (44 for MBII-1 data and 64 for MBII-2 data) to yield the total mass concentration, whose logrithmic value is tabulated in Tables B.1 and B.2. The percent contribution to the total mass concentration from several particle size ranges has also been calculated for tabulation.

B-2.2 Calculation of Extinction Coefficients (1/km)

The extinction coefficient (EC) for each particle size class in a two-second data interval has been approximated by the Mie formula:

$$EC(1/km) = 2[PNC(\#/cm^3)10^5(cm/km)\ \text{Particle Area}\ (cm^2)]$$

or

$$EC(1/km) = (PNC)(\frac{\pi d^2}{2}) \times 10^5$$

where d is the particle diameter in cm (this significantly overestimates for $5d < \text{optical wavelength}$).

These values are also summed over all particle size classes present in each two-second data interval to obtain the total value whose logrithmic values have been tabulated. As with the mass concentrations, the percent contribution from several particle size ranges has also been tabulated.

B-2.3 Calculation of Radar Reflectivity Factors (mm^6/m^3)

Radar Reflectivity Factors (RRF) have also been calculated and tabulated for each two-second data acquisition interval. For each particle size class in a data acquisition interval, the RRF has been approximated by the Rayleigh formula:

$$RRF(mm^6/m^3) = PNC(\#/cm^3)10^6(cm^3/m^3)10^6(mm^6/cm^6)(\text{Particle Diameter})^6$$

or

$$RRF(mm^6/m^3) = PNC(d^6)\times 10^{12}$$

where d is again the particle diameter in cm (this significantly overestimates for 5d > radar wavelength).

The total radar reflectivity factor in each two-second data interval is obtained by summing over all particle size classes present in that interval. Logrithmic values of total radar reflectivity factor, plus the contribution to this total by several particle size ranges, are tabulated in Tables B.1 and B.2.

Table B-1. MISERS BLUFF II-1 Detailed Dust Particle Spectral Data

MISERS BLUFF II-1

TIME (SEC)	NUMBER CONCENTRATION (#/CC) PARTICLE DIAM(MICRON)			MASS CONCENTRATION (G/M**3) PARTICLE DIAM(MICRON)			EXTINCTION COEFFICIENT (1/KM) PARTICLE DIAM(MICRON)			RADAR REFLECTIVITY FACTOR ((MM**6)/(M**3)) PARTICLE DIAM(MICRON)			TIME (SEC)
	.3 -.47	>.47	TOTAL	.3 -.47	>.47	TOTAL	.3 -.47	>.47	TOTAL	.3 -.47	>.47	TOTAL	
	(LOGARITHM)			(PERCENT OF TOTAL)		(LOG)	(PERCENT OF TOTAL)		(LOG)	(PERCENT OF TOTAL)		(LOG)	
29	-1.05		-1.05	100.		-5.54	100.		-2.90	100.		-10.19	29
31	-1.23		-1.23	100.		-5.72	100.		-3.08	100.		-10.37	31
33	-.93		-.93	100.		-5.42	100.		-2.78	100.		-10.07	33
35	-.69		-.69	100.		-3.86	100.		-1.81	100.		-6.47	35
37	-.69		-.69	100.		-4.40	100.		-2.04	100.		-8.16	37
39	-.83		-.83	100.		-5.32	100.		-2.68	100.		-9.97	39
41	-1.05		-1.05	100.		-5.02	100.		-2.60	100.		-8.85	41
43	-1.05		-1.05	100.		-4.46	100.		-2.23	100.		-7.77	43
45	-.75		-.75	100.		-4.18	100.		-2.06	100.		-7.06	45
47	-1.23		-1.23	100.		-4.57	100.		-2.38	100.		-7.80	47
49	-.83		-.83	100.		-4.44	100.		-2.18	100.		-7.77	49
51	-.69		-.69	100.		-4.42	100.		-2.13	100.		-7.77	51
53	-.53		-.53	100.		-4.26	100.		-1.95	100.		-7.70	53
55	-.93		-.93	100.		-4.11	100.		-1.93	100.		-7.33	55
57	-.58		-.58	100.		-4.54	100.		-2.13	100.		-8.37	57
59	-.93		-.93	100.		-4.98	100.		-2.54	100.		-8.84	59
61	-.83		-.83	100.		-4.74	100.		-2.34	100.		-8.55	61
63	-.93		-.93	100.		-3.99	100.		-1.86	100.		-6.97	63
65	-.75		-.75	100.		-4.90	100.		-2.43	100.		-8.83	65
67	-1.23		-1.23	100.		-5.72	100.		-3.08	100.		-10.37	67
69	-1.53		-1.53	100.		-6.02	100.		-3.38	100.		-10.67	69
71	-.75		-.75	100.		-5.24	100.		-2.60	100.		-9.89	71
73	-1.53		-1.53	100.		-6.02	100.		-3.38	100.		-10.67	73
75	-.93		-.93	100.		-5.42	100.		-2.78	100.		-10.07	75
77	-1.53		-1.53	100.		-6.02	100.		-3.38	100.		-10.67	77
79	-1.23		-1.23	100.		-5.72	100.		-3.08	100.		-10.37	79
81	-.83		-.83	100.		-4.53	100.		-2.27	100.		-7.80	81
83	-.58		-.58	100.		-4.81	100.		-2.30	100.		-8.81	83
85	-.93		-.93	100.		-5.42	100.		-2.78	100.		-10.07	85
87	-.63		-.63	100.		-4.84	100.		-2.34	100.		-8.82	87
89	-1.23		-1.23	100.		-5.06	100.		-2.68	100.		-8.86	89
91	-.83		-.83	100.		-3.60	100.		-1.65	100.		-5.99	91
93	-1.23		-1.23	100.		-5.72	100.		-3.08	100.		-10.37	93
95	-1.53		-1.53	100.		-6.02	100.		-3.38	100.		-10.67	95
97													97
99	-1.53		-1.53	100.		-5.12	100.		-2.78	100.		-8.86	99
101	-.83		-.83	100.		-5.32	100.		-2.68	100.		-9.97	101
103	-.63		-.63	100.		-4.68	100.		-2.23	100.		-8.54	103
105	-.83		-.83	100.		-4.44	100.		-2.18	100.		-7.77	105
107	-1.53		-1.53	100.		-6.02	100.		-3.38	100.		-10.67	107
109	-.63		-.63	100.		-4.34	100.		-2.04	100.		-7.73	109
111	-.63		-.63	100.		-4.03	100.		-1.89	100.		-6.98	111
113	-.38		-.38	100.		-3.82	100.		-1.71	100.		-6.47	113
115	-.93		-.93	100.		-4.38	100.		-2.13	100.		-7.73	115
117													117
119	-1.23		-1.23	100.		-5.72	100.		-3.08	100.		-10.37	119
121	-.75	-3.47	-.75		100.	-1.66	3.2	96.8	-1.11		100.	-.02	121
123	-.83	-2.82	-.83	24.1	75.9	-3.40	64.1	35.9	-1.70	.5	99.7	-4.38	123
125	-.69		-.69	100.		-3.01	100.		-1.32	100.		-4.67	125
127	-.10		-.10	100.		-4.02	100.		-1.66	100.		-7.45	127

Table B-1. (Continued)

MISERS MODEL II-1

TIME (SEC)	NUMBER CONCENTRATION (#/CC) PARTICLE DIAM(MICRON) 3 -47 (LOGARITHM)	>47	TOTAL (LOG)	MASS CONCENTRATION (G/M**3) PARTICLE DIAM(MICRON) 3 -47 (PERCENT OF TOTAL)	>47	TOTAL (LOG)	EXTINCTION COEFFICIENT (1/KM) PARTICLE DIAM(MICRON) 3 -47 (PERCENT OF TOTAL)	>47	TOTAL (LOG)	RADAR REFLECTIVITY FACTOR ((MM**6)/(M**3)) PARTICLE DIAM(MICRON) 3 -47 (PERCENT OF TOTAL)	>47	TOTAL (LOG)	TIME (SEC)
129	-.83		-.83	100.		-5.32	100.		-2.68	100.		-9.97	129
131	-.69		-.69	100.		-4.35	100.		-2.06	100.		-7.73	131
133	-.63	-2.82	-.63	18.9	81.1	-3.43	63.4	36.6	-1.71	.1	99.9	-4.38	133
135	-.93	-2.82	-.92	3.4	96.6	-3.50	28.7	71.3	-1.99		100.	-4.38	135
137	-1.05		-1.05	100.		-5.54	100.		-2.90	100.		-10.19	137
139	-.75	-2.64	-.75	.7	99.3	-3.12	14.5	85.5	-1.76		100.	-3.63	139
→141	-.69		-.69	100.		-4.29	100.		-2.00	100.		-7.70	141
143	1.97	-1.64	1.97	93.7	6.3	-.54	98.9	1.1	1.26	4.7	95.3	-.97	143
145	1.77		1.77	100.		-.77	100.		1.04	100.		-2.48	145
147	-.49		-.49	100.		-3.22	100.		-1.29	100.		-5.52	147
1 149	-.49		-.49	100.		-3.84	100.		-1.71	100.		-6.75	149
151	-.28		-.28	100.		-3.84	100.		-1.59	100.		-7.17	151
153	1.08		1.08	100.		-1.62	100.		.26	100.		-3.49	153
155 *	.92	-1.53	.92	57.4	42.6	-1.57	100.		.09	100.		-3.85	155
157 *	.65	-3.12	.65	94.1	5.9	-2.11	100.		-.22	100.		-4.15	157
→159	-.53		-.53	100.		-3.66	100.		-1.60	100.		-6.36	159
161	-.42		-.42	100.		-3.75	100.		-1.65	100.		-6.45	161
163	-.38		-.38	100.		-3.86	100.		-1.67	100.		-6.91	163
165	-1.05		-1.05	100.		-4.20	100.		-2.13	100.		-7.06	165
167	-.49		-.49	100.		-4.98	100.		-2.34	100.		-9.63	167
169	-.53		-.53	100.		-3.82	100.		-1.69	100.		-6.74	169
171	-.83		-.83	100.		-4.94	100.		-2.48	100.		-8.84	171
173	-.58		-.58	100.		-3.75	100.		-1.64	100.		-6.68	173
175	-.75		-.75	100.		-3.66	100.		-1.74	100.		-6.00	175
177	-.69		-.69	100.		-4.57	100.		-2.18	100.		-8.38	177
179	-.42		-.42	100.		-3.78	100.		-1.60	100.		-6.86	179
181	-.49		-.49	100.		-3.93	100.		-1.72	100.		-7.19	181
183	-.93		-.93	100.		-4.76	100.		-2.38	100.		-8.55	183
185	-.53		-.53	100.		-4.02	100.		-1.86	100.		-6.98	185
187	-.49		-.49	100.		-3.93	100.		-1.68	100.		-7.27	187
189	-.53		-.53	100.		-3.39	100.		-1.39	100.		-5.86	189
191	-.42		-.42	100.		-3.52	100.		-1.46	100.		-6.27	191
193	-.69		-.69	100.		-4.70	100.		-2.27	100.		-8.54	193
→195	-.45		-.45	100.		-4.94	100.		-2.30	100.		-9.59	195
197	.83		.83	100.		-1.86	100.		-.04	100.		-3.56	197
199	1.76		1.76	100.		-.81	100.		1.00	100.		-2.52	199
201	1.71		1.71	100.		-.97	100.		.85	100.		-2.64	201
203	-.21		-.21	100.		-3.94	100.		-1.65	100.		-7.29	203
2 205	-.83		-.83	100.		-4.74	100.		-2.34	100.		-8.55	205
207	-.58		-.58	100.		-5.06	100.		-2.43	100.		-9.71	207
209	1.20		1.20	100.		-1.49	100.		.36	100.		-3.26	209
211	.22		.22	100.		-2.59	100.		-.67	100.		-4.57	211
213	.06		.06	100.		-2.60	100.		-.80	100.		-4.30	213
215	-.19		-.19	100.		-2.82	100.		-.94	100.		-4.91	215
→217	-.69		-.69	100.		-3.84	100.		-1.78	100.		-6.47	217
219	-.69		-.69	100.		-3.46	100.		-1.52	100.		-5.87	219
221	-.93		-.93	100.		-3.06	100.		-1.25	100.		-5.22	221
223	-1.05		-1.05	100.		-4.56	100.		-2.34	100.		-7.80	223
225	-.43	-1.53	-.43	1.7	98.3	-1.93	9.9	90.1	-.66		100.	-1.90	225
227	-.58	-3.12	-.58	16.3	83.7	-3.26	64.7	35.3	-1.67		100.	-3.72	227

Table B-1. (Continued)

MISERS RUDE II-1

TIME (SEC)	NUMBER CONCENTRATION (#/CC) PARTICLE DIAM(MICRON) 3 -47 (LOGARITHM)	>47	TOTAL	MASS CONCENTRATION (G/M**3) PARTICLE DIAM(MICRON) 3 -47 (PERCENT OF TOTAL)	>47	TOTAL (LOG)	EXTINCTION COEFFICIENT (1/KM) PARTICLE DIAM(MICRON) 3 -47 (PERCENT OF TOTAL)	>47	TOTAL (LOG)	RADAR REFLECTIVITY FACTOR ((MM**6)/(M**3)) PARTICLE DIAM(MICRON) 3 -47 (PERCENT OF TOTAL)	>47	TOTAL (LOG)	TIME (SEC)
→229	-.93		-.93	100.		-5.42	100.		-2.78	100.		-10.07	229
231	-.69	-1.74	-.65	.4	99.6	-2.12	4.8	95.2	-.88		100.	-2.11	231
233	2.11	-2.55	2.11	99.9	.1	-.34	100.		1.44	99.2	.8	-2.00	233
235	2.49		2.49	100.		-.12	100.		1.88	100.		-1.52	235
237 *	2.36	-1.69	2.36	97.7	2.3	-.03	99.7	.3	1.73	12.3	87.7	-.81	237
3 239 *	1.60	-1.33	1.60	79.2	20.8	-.65	100.		.97	100.		-2.78	239
241 *	.62	-1.96	.62	52.3	47.7	-1.49	100.		-.44	100.		-3.21	241
243 *	.23	-3.60	.23	46.6	53.4	-2.18	100.		-.63	100.		-4.34	243
→245	-.25		-.25	100.		-3.25	100.		-1.22	100.		-5.91	245
247	-.49		-.49	100.		-3.52	100.		-1.54	100.		-5.96	247
249	-.42		-.42	100.		-4.72	100.		-2.18	100.		-8.79	249
251	-.69		-.69	100.		-4.70	100.		-2.27	100.		-8.54	251
253	-.58		-.58	100.		-4.11	100.		-1.85	100.		-7.45	253
255	-1.23	-3.33	-1.23		100.	-2.48	3.0	97.0	-1.56		100.	-1.62	255
257	-.83	-1.33	-.55	.5	99.5	-1.33	4.9	95.1	-.31		100.	-.31	257
259	-.53	-1.96	-.52	1.0	98.0	-1.00	17.2	82.8	-.79		100.	-.83	259
261	-.53	-3.60	-.53	3.0	96.4	-2.43	49.0	51.0	-1.40		100.	-1.45	261
263	-.49		-.49	100.		-4.43	100.		-2.02	100.		-8.25	263
→265	-.63	-2.61	-.62	2.8	97.2	-2.23	29.5	70.5	-1.19		100.	-1.47	265
267	1.09	-1.46	1.10	55.0	45.0	-1.07	87.7	12.3	.49	.5	99.5	-.64	267
269	1.63	-1.30	1.63	67.5	32.5	-.76	94.1	5.9	.93	.2	99.8	-.04	269
271	1.54	-1.67	1.54	88.5	11.5	-.79	97.3	2.7	.92	5.6	94.4	-1.19	271
273	1.63	-1.46	1.63	88.1	11.9	-.81	97.0	3.0	.93	5.1	94.9	-1.21	273
275	1.96	-1.04	1.96	78.8	21.2	-.41	95.1	4.9	1.29	1.6	98.4	-.35	275
4 277	1.93	-1.04	1.93	80.0	20.0	-.37	95.8	4.2	1.31	.8	99.2	.03	277
279	2.18	-.82	2.18	83.0	17.0	-.13	96.3	3.7	1.56	1.0	99.0	.17	279
281	2.27	-.91	2.27	88.3	11.7	-.10	97.5	2.5	1.62	2.4	97.6	-.17	281
283 *	2.09	-1.49	2.09	95.2	4.8	-.40	100.		1.37	100.		-2.06	283
→285	-.63		-.63	100.		-3.78	100.		-1.72	100.		-6.45	285
287	-.30		-.30	100.		-3.11	100.		-1.12	100.		-5.73	287
289	-.17		-.17	100.		-2.80	100.		-.93	100.		-4.94	289
291	-1.05		-1.05	100.		-4.56	100.		-2.34	100.		-7.80	291
293	-.69		-.69	100.		-5.17	100.		-2.54	100.		-9.82	293
295	-.83		-.83	100.		-4.14	100.		-2.02	100.		-7.05	295
297	-.58		-.58	100.		-4.33	100.		-2.02	100.		-7.73	297
299	-.53		-.53	100.		-4.03	100.		-1.77	100.		-7.42	299
301	-.75		-.75	100.		-3.25	100.		-1.44	100.		-5.24	301
303	-.69		-.69	100.		-3.66	100.		-1.73	100.		-6.00	303
305	-.63		-.63	100.		-4.23	100.		-1.93	100.		-7.67	305
307	-.63		-.63	100.		-4.84	100.		-2.34	100.		-8.82	307
309													309
319	-.83		-.83	100.		-3.41	100.		-1.52	100.		-5.59	319
321	-.83		-.83	100.		-4.94	100.		-2.48	100.		-8.84	321
323	-1.15	-1.49	-.68	.2	99.8	-1.72	2.7	97.3	-.58		100.	-1.10	323
325	-.38		-.38	100.		-3.78	100.		-1.61	100.		-6.74	325
327	-.69		-.69	100.		-4.04	100.		-1.90	100.		-6.98	327
329	-.69	-1.87	-.66	.7	99.3	-2.23	7.5	92.5	-1.00		100.	-2.02	329
331	-.83		-.83	100.		-3.91	100.		-1.92	100.		-6.47	331
333	-.75		-.75	100.		-4.26	100.		-2.04	100.		-7.50	333
→335	-.63		-.63	100.		-3.28	100.		-1.39	100.		-5.53	335

5

Table B-1. (Continued)

USERS GUIDE II-1

TIME (SEC)	NUMBER CONCENTRATION (#/CC) PARTICLE DIAM(MICRON)			MASS CONCENTRATION (G/M**3) PARTICLE DIAM(MICRON)			EXTINCTION COEFFICIENT (1/KM) PARTICLE DIAM(MICRON)			RADAR REFLECTIVITY FACTOR ((MM**6)/(M**3)) PARTICLE DIAM(MICRON)			TIME (SEC)
	% -47	% >47	TOTAL	% -47	% >47	TOTAL	% -47	% >47	TOTAL	% -47	% >47	TOTAL	
	(LOGARITHM)			(PERCENT OF TOTAL)		(LOG)	(PERCENT OF TOTAL)		(LOG)	(PERCENT OF TOTAL)		(LOG)	
337	.43		.43	100.		-2.41	100.		-.55	100.		-4.28	337
339	1.60 -1.19		1.60	74.8	25.2	-.71	93.3	6.7	.94	1.8	98.2	-.69	339
341	1.97 -1.04		1.97	79.1	20.9	-.41	95.4	4.6	1.28	1.2	98.8	-.21	341
343	2.15 -1.50		2.15	96.4	3.6	-.31	99.1	.9	1.46	18.9	81.1	-1.28	343
345	1.46 -1.60		1.46	77.5	22.5	-.92	95.6	4.4	.76	.8	99.2	-.57	345
347	1.57 -2.11		1.57	92.5	7.5	-1.05	98.7	1.3	.77	5.9	94.1	-1.63	347
349 *	1.44 -2.16		1.44	97.6	2.4	-1.16	99.3	.7	.65	40.8	59.2	-2.78	349
351 *	1.57 -2.03		1.57	94.7	5.3	-.99	100.		.81	100.		-2.66	351
353	1.23		1.23	100.		-1.25	100.		.54	100.		-2.98	353
5 355	.39		.39	100.		-2.31	100.		-.43	100.		-4.37	355
357 *	.71 -2.06		.71	63.5	36.5	-1.68	100.		-.48	100.		-3.58	357
359 *	.87 -2.58		.87	92.0	8.0	-1.82	100.		.41	100.		-3.69	359
361 *	.86 -3.34		.86	95.1	4.9	-1.89	100.		-.03	100.		-3.77	361
363 *	.63 -2.59		.63	93.4	6.6	-1.94	100.		-.13	100.		-3.86	363
365	.62		.62	100.		-2.19	100.		-.28	100.		-4.21	365
367	.78		.78	100.		-2.23	100.		-.23	100.		-4.65	367
→ 369	-.75		-.75	100.		-4.43	100.		-2.15	100.		-7.77	369
371	-.69		-.69	100.		-3.90	100.		-1.81	100.		-6.75	371
373	-.69		-.69	100.		-4.70	100.		-2.27	100.		-8.54	373
375	-.53 -2.42		-.53	38.3	61.7	-3.31	73.9	26.1	-1.56	1.0	99.0	-4.38	375
377	-.58 -2.03		-.56	1.5	98.5	-2.24	16.7	83.3	-1.68		100.	-1.97	377
379													379
379	-.69 -2.86		-.67	.2	99.8	-2.12	4.4	95.6	-1.62		100.	-1.65	379
381	-1.05 -2.52		-1.04	2.2	97.8	-2.90	17.1	82.9	-1.57		100.	-3.37	381
383	-.69 -3.54		-.68	9.7	90.3	-3.16	54.1	45.9	-1.77		100.	-3.23	383
385	-1.23 -2.59		-1.21		100.	-1.76	2.6	97.4	-1.16		100.	-.22	385
387	-.49		-.49	100.		-3.39	100.		-1.39	100.		-5.99	387
389	-.63		-.63	100.		-3.41	100.		-1.51	100.		-5.59	389
→ 391	-.63		-.63	100.		-3.53	100.		-1.49	100.		-6.27	391
393	.25 -2.34		.25	59.0	41.0	-2.65	86.9	13.1	-.78	3.5	96.5	-3.89	393
395	.59 -1.87		.59	34.0	66.0	-1.68	78.4	21.6	-.20	.1	99.9	-.97	395
397	1.25 -1.38		1.25	76.3	23.7	-1.07	92.6	7.4	.60	2.6	97.4	-1.19	397
399	2.03 -1.15		2.03	73.5	26.5	-.32	96.0	4.0	1.33	.2	99.8	.58	399
6 401 *	1.86 -1.27		1.86	83.9	16.1	-.52	96.7	3.3	1.19	1.9	98.1	-.49	401
403 *	1.69 -1.91		1.69	87.6		-.25	100.		.98	100.		-2.49	403
405 *	1.70 -2.30		1.70	98.7		-.93	100.		.87	100.		-2.59	405
407	.17		.17	100.		-2.62	100.		-.69	100.		-4.74	407
→ 409	-.58		-.58	100.		-3.94	100.		-1.74	100.		-7.19	409
411	-.63		-.63	100.		-3.45	100.		-1.57	100.		-5.60	411
413	-.53		-.53	100.		-4.21	100.		-1.90	100.		-7.67	413
415	-.69		-.69	100.		-3.98	100.		-1.82	100.		-6.97	415
417	-.58		-.58	100.		-3.24	100.		-1.40	100.		-5.24	417
419	-.83		-.83	100.		-3.89	100.		-1.88	100.		-6.47	419
421	-.53		-.53	100.		-4.32	100.		-2.00	100.		-7.73	421
423	-.53		-.53	100.		-4.10	100.		-1.84	100.		-7.45	423
425	-.75		-.75	100.		-4.51	100.		-2.23	100.		-7.80	425
427	-.63		-.63	100.		-3.80	100.		-1.69	100.		-6.71	427
429	-.75		-.75	100.		-3.56	100.		-1.53	100.		-6.28	429
431	-.93		-.93	100.		-3.48	100.		-1.66	100.		-5.60	431
433	-.58		-.58	100.		-4.12	100.		-1.95	100.		-7.05	433

Table B-1. (Continued)

DISDRS MODE II-1

TIME (SEC)	NUMBER CONCENTRATION (#/CC) PARTICLE DIAM(MICRO) 3	>47	TOTAL (LOGARITHM)	MASS CONCENTRATION (G/M**3) PARTICLE DIAM(MICRO) 3	>47	TOTAL (LOG)	EXTINCTION COEFFICIENT (1/KM) PARTICLE DIAM(MICRON) 3	>47	TOTAL (LOG)	RADAR REFLECTIVITY FACTOR ((MM**6)/(M**3)) PARTICLE DIAM(MICRON) 3	>47	TOTAL (LOG)	TIME (SEC)
	-47 (PERCENT OF TOTAL)			-47 (PERCENT OF TOTAL)			-47 (PERCENT OF TOTAL)			-47 (PERCENT OF TOTAL)			
435	-1.05		-1.05	100.		-5.54	100.		-2.90	100.		-10.19	435
437	-.75		-.75	100.		-5.24	100.		-2.60	100.		-9.89	437
439	-.69		-.69	100.		-4.87	100.		-2.34	100.		-8.82	439
441	-.93		-.93	100.		-4.45	100.		-2.20	100.		-7.77	441
443	-.63		-.63	100.		-3.55	100.		-1.60	100.		-5.96	443
445	-.63		-.63	100.		-5.12	100.		-2.48	100.		-9.77	445
447	-.83		-.83	100.		-3.47	100.		-1.55	100.		-5.87	447
449	-.75		-.75	100.		-3.88	100.		-1.79	100.		-6.75	449
451	-.49		-.49	100.		-3.78	100.		-1.69	100.		-6.45	451
453	-.75		-.75	100.		-4.51	100.		-2.23	100.		-7.80	453
455	-1.05		-1.05	100.		-4.56	100.		-2.34	100.		-7.80	455
457	-.63		-.63	100.		-4.02	100.		-1.80	100.		-7.30	457
459	-.53		-.53	100.		-3.81	100.		-1.72	100.		-6.47	459
461	-.93		-.93	100.		-4.22	100.		-2.02	100.		-7.49	461
463	-.75		-.75	100.		-4.06	100.		-1.86	100.		-7.32	463
465	-.53		-.53	100.		-4.79	100.		-2.27	100.		-8.80	465
467	-.75		-.75	100.		-4.04	100.		-1.92	100.		-6.98	467
469	-.58		-.58	100.		-4.14	100.		-1.89	100.		-7.47	469
471	-.69		-.69	100.		-3.72	100.		-1.69	100.		-6.37	471
473	-.75		-.75	100.		-4.04	100.		-1.92	100.		-6.98	473
475	-.83		-.83	100.		-3.91	100.		-1.92	100.		-6.47	475
477	-.93		-.93	100.		-3.87	100.		-1.85	100.		-6.47	477
479													479
489	-.69		-.69	100.		-3.90	100.		-1.89	100.		-6.47	489
491	-.75		-.75	100.		-5.24	100.		-2.60	100.		-9.89	491
493	-1.05		-1.05	100.		-4.79	100.		-2.43	100.		-8.56	493
495	-.63		-.63	100.		-3.34	100.		-1.41	100.		-5.58	495
497	-1.05		-1.05	100.		-5.54	100.		-2.90	100.		-10.19	497
499	-.93	-2.31	-.91	.2	99.8	-2.77	5.3	94.7	-1.50		100.	-2.01	499
501	-1.05	-1.91	-1.00	100.		-1.02	.3	99.7	-.42		100.	.40	501
503	-1.23	-2.30	-1.19	.1	99.9	-2.01	2.8	97.2	-1.52		100.	-3.15	503
505	-1.24		-1.23	100.		-5.72	100.		-3.08	100.		-10.37	505
507	-1.23		-1.23	100.		-5.72	100.		-3.08	100.		-10.37	507
509	-1.05		-1.05	100.		-5.54	100.		-2.90	100.		-10.19	509
511	.07	-2.12	.07	18.0	82.0	-2.21	62.8	37.2	-.76		100.	-1.92	511
513	1.62	-2.01	1.62	93.6	6.4	-.96	98.7	1.3	.83	11.2	88.8	-1.73	513
515	1.28	-2.82	1.28	99.1	.9	-1.47	99.7	.3	.38	92.6	7.4	-3.25	515
517	1.72	-1.57	1.72	90.3	9.7	-.86	97.5	2.5	.91	15.5	84.5	-1.76	517
519	1.88	-1.52	1.88	84.9	15.1	-.61	96.7	3.3	1.12	2.5	97.5	-.70	519
521	1.45	-3.34	1.45	99.1	.9	-1.18	99.8	.2	.64	65.8	34.2	-2.77	521
523	.00	-2.64	.00	32.6	67.4	-2.59	79.5	20.5	-.95	.1	99.9	-2.69	523
525	-.12	-2.09	-.11	12.5	87.5	-2.15	45.9	54.1	-.81	.1	99.9	-2.12	525
527	1.71	-1.48	1.71	75.5	24.5	-.71	95.8	4.2	.98	.4	99.6	-.17	527
529	1.93	-1.40	1.93	91.3	8.7	-.51	98.0	2.0	1.23	9.2	90.8	-1.14	529
531	1.84	-1.63	1.80	89.7	10.3	-.70	100.		1.05	100.		-2.41	531
533	1.52	-1.52	1.52	84.3	15.7	-1.11	100.		.66	100.		-2.91	533
535	-.49	-3.69	-.49	40.9	59.1	-2.89	100.		-1.45	100.		-5.25	535
537	.65	-3.62	.65	79.6	20.4	-1.93	100.		-.23	100.		-3.65	537
539	-.63		-.63	100.		-4.34	100.		-2.04	100.		-7.73	539
541	.75		.75	100.		-2.09	100.		-.14	100.		-4.37	541

Table B-1. (Continued)

MISENS RUDE 11-1

TIME (SEC)	NUMBER CONCENTRATION (#/CC) PARTICLE DIAM(MICRON) 3	>47	TOTAL	MASS CONCENTRATION (G/M**3) PARTICLE DIAM(MICRON) 3	>47	TOTAL	EXTINCTION COEFFICIENT (1/KM) PARTICLE DIAM(MICRON) 3	>47	TOTAL	RADAR REFLECTIVITY FACTOR ((MM**6)/(M**3)) PARTICLE DIAM(MICRON) 3	>47	TOTAL	TIME (SEC)
	-47 (LOGARITHM)			-47 (PERCENT OF TOTAL)		(LOG)	-47 (PERCENT OF TOTAL)		(LOG)	-47 (PERCENT OF TOTAL)		(LOG)	
543	.92		.92	100.		-1.88	100.		.02	100.		-3.76	543
545	-.75		-.75	100.		-4.06	100.		-1.90	100.		-7.04	545
547	-.05		-.05	100.		-3.08	100.		-1.05	100.		-5.66	547
549	-.83		-.83	100.		-4.26	100.		-2.06	100.		-7.50	549
551	-.49		-.49	100.		-4.04	100.		-1.84	100.		-7.04	551
553	-.58		-.58	100.		-3.79	100.		-1.68	100.		-6.71	553
555	-.58		-.58	100.		-4.16	100.		-2.00	100.		-7.06	555
557	-.69		-.69	100.		-2.56	100.		-1.01	100.		-3.79	557
559	-.45		-.45	100.		-3.57	100.		-1.49	100.		-6.33	559
561	-.49		-.49	100.		-3.51	100.		-1.48	100.		-5.98	561
563	-.42		-.42	100.		-3.85	100.		-1.66	100.		-6.91	563
565	-.83		-.83	100.		-4.14	100.		-2.02	100.		-7.05	565
567	-.23		-.23	100.		-3.57	100.		-1.52	100.		-5.99	567
569	-.69		-.69	100.		-4.87	100.		-2.38	100.		-8.82	569
571	-1.23		-1.23	100.		-5.06	100.		-2.68	100.		-8.86	571
573	-.63		-.63	100.		-4.06	100.		-1.88	100.		-7.04	573
575	-.63		-.63	100.		-3.77	100.		-1.69	100.		-6.45	575
577	-.63		-.63	100.		-3.97	100.		-1.81	100.		-6.97	577
589	-.93		-.93	100.		-4.19	100.		-2.10	100.		-7.06	589
591	-.93		-.93	100.		-5.42	100.		-2.78	100.		-10.07	591
593	-1.23		-1.23	100.		-5.72	100.		-3.08	100.		-10.37	593
595	-1.23		-1.23	100.		-5.72	100.		-3.08	100.		-10.37	595
597	-.75		-.75	100.		-5.24	100.		-2.60	100.		-9.89	597
599	-.93	-1.63	-.86	.1	99.9	-1.69	1.3	98.7	-.65		100.	-.92	599
601	-1.05	-1.52	-.93		100.	-1.91	.6	99.4	-.69		100.	-1.85	601
603	-1.53	-2.64	-1.50	1.0	99.0	-3.11	10.2	89.8	-1.79		100.	-3.63	603
605	-.93	-3.62	-.93	.2	99.8	-2.62	9.8	90.2	-1.77		100.	-1.78	605
607	-.69		-.69	100.		-4.25	100.		-2.02	100.		-7.50	607
609	-.83		-.83	100.		-4.94	100.		-2.48	100.		-8.84	609
611	-.75	-2.42	-.74	.5	99.5	-2.97	10.2	89.8	-1.61		100.	-3.56	611
613	-.93	-3.51	-.93	.5	99.5	-3.10	17.1	82.9	-2.01		100.	-2.85	613
▶ 615	-.75		-.75	100.		-5.24	100.		-2.60	100.		-9.89	615
617	1.26		1.26	100.		-1.29	97.0	3.0	.52	4.8	95.2	-1.61	617
619 *	1.88	-1.37	1.88	96.9	3.1	-.60	100.		1.17	100.		-2.30	619
621	1.52		1.52	100.		-1.12	100.		.70	100.		-2.87	621
623 *	1.65	-1.99	1.65	79.9	20.1	-.81	100.		.88	100.		-2.50	623
625 *	1.65	-1.02	1.65	46.6	53.4	-.69	95.4	4.6	.85	1.2	98.8	-.71	625
8 627 *	1.63	-1.75	1.63	88.8	11.2	-.93	86.6	13.4	.87	.4	99.6	-.10	627
629 *	1.40	-1.85	1.40	89.5	10.5	-1.12	100.		.63	100.		-2.89	629
631 *	1.28	-1.82	1.28	91.6	8.4	-1.63	100.		.24	100.		-3.51	631
633 *	1.50	-2.08	1.50	97.3	2.7	-1.19	100.		.61	100.		-2.86	633
635 *	1.49	-3.37	1.49	97.1	2.9	-1.08	100.		.69	100.		-2.73	635
▶ 637	-.53		-.53	100.		-4.44	100.		-2.04	100.		-8.25	637
639	-.93		-.93	100.		-4.38	100.		-2.13	100.		-7.73	639
641	-.58		-.58	100.		-3.43	100.		-1.53	100.		-5.59	641
643	-.93		-.93	100.		-4.98	100.		-2.54	100.		-8.84	643
645	-.75	-1.75	-.71		100.	-1.75	1.4	98.6	-.75		100.	-.90	645
647	-.58	-1.43	-.55	.4	99.6	-1.87	6.5	93.5	-.83		100.	-1.89	647
649	-.69	-1.82	-.66	9.2	90.8	-2.86	30.1	69.9	-.80	.1	99.9	-1.66	649
651	-.63	-2.08	-.61	32.9	67.1	-2.53	56.9	43.1	-1.00	3.0	97.0	-3.38	651

Table B-1. (Continued)

USERS GUIDE II-1

TIME (SEC)	NUMBER CONCENTRATION (#/CC) PARTICLE DIAM(MICRON) 3 -47 (LOGARITHM)	>47	TOTAL	MASS CONCENTRATION (G/M**3) PARTICLE DIAM(MICRON) 3 -47 (PERCENT OF TOTAL)	>47	TOTAL (LOG)	EXTINCTION COEFFICIENT (1/KM) PARTICLE DIAM(MICRON) 3 -47 (PERCENT OF TOTAL)	>47	TOTAL (LOG)	RADAR REFLECTIVITY FACTOR ((MM**6)/(M**3)) PARTICLE DIAM(MICRON) 3 -47 (PERCENT OF TOTAL)	>47	TOTAL (LOG)	TIME (SEC)
653	-.42	-3.27	-.42	4.3	95.7	-2.73	44.0	56.0	-1.53		100.	-2.36	653
655	-.93	-2.46	-.42	2.9	97.1	-2.61	22.9	77.1	-1.40		100.	-2.35	655
657	-.75		-.75	100.		-4.18	100.		-2.06	100.		-7.06	657
659													659
659	-.93		-.93	100.		-5.42	100.		-2.78	100.		-10.07	659
661	-.03	-3.51	-.03	56.4	43.6	-2.74	92.4	7.6	-.98	.3	99.7	-2.84	661
663	.42		.42	100.		-2.38	100.		-.49	100.		-4.49	663
665	.96	-2.47	.96	92.4	7.6	-1.74	97.8	2.2	.01	27.5	72.5	-2.68	665
667	1.29	-2.16	1.29	84.0	16.0	-1.55	97.1	2.9	.28	3.9	96.1	-1.91	667
669	1.54	-1.81	1.54	83.4	16.6	-1.01	97.1	2.9	.73	.8	99.2	-.65	669
671	1.30	-3.12	1.30	99.2	.8	-1.26	99.8	.2	.53	85.5	14.5	-2.88	671
673	.20	-2.65	.20	33.4	66.6	-2.17	83.6	16.4	-.67	.1	99.9	-1.44	673
675	.49	-2.69	.49	57.9	42.1	-1.95	92.5	7.5	-.32	.3	99.7	-1.43	675
677	1.37	-1.80	1.37	73.2	26.8	-1.22	94.2	5.8	.50	1.9	98.1	-1.35	677
679	1.15	-2.82	1.15	98.9	1.1	-1.54	99.6	.4	.30	92.6	7.4	-3.25	679
681	1.61	-1.40	1.61	64.7	35.3	-.67	93.4	6.6	.93	.2	99.8	.24	681
683	1.91		1.91	100.		-.59	100.		1.19	100.		-2.23	683
685	1.66		1.66	100.		-.86	100.		.92	100.		-2.49	685
687	1.38		1.38	100.		-1.33	100.		.52	100.		-3.13	687
689	.32		.32	100.		-2.33	100.		-.58	100.		-3.76	689
691	-.49		-.49	100.		-3.32	100.		-1.31	100.		-5.95	691
693	-.42		-.42	100.		-3.75	100.		-1.65	100.		-6.45	693
695	-.69		-.69	100.		-4.87	100.		-2.38	100.		-8.82	695
697	-.33		-.33	100.		-3.92	100.		-1.70	100.		-6.97	697
699	-.75		-.75	100.		-4.59	100.		-2.20	100.		-8.38	699
701	-.75		-.75	100.		-5.24	100.		-2.60	100.		-9.89	701
703	-.75		-.75	100.		-4.51	100.		-2.23	100.		-7.80	703
705	-.53		-.53	100.		-3.90	100.		-1.74	100.		-6.92	705
707	-.63		-.63	100.		-4.84	100.		-2.34	100.		-8.82	707
709	-.58		-.58	100.		-3.68	100.		-1.62	100.		-6.37	709
711	-.53		-.53	100.		-3.64	100.		-1.56	100.		-6.40	711
713	-.75		-.75	100.		-3.70	100.		-1.67	100.		-6.37	713
715	-.75		-.75	100.		-4.43	100.		-2.15	100.		-7.77	715
717	-.30		-.30	100.		-3.20	100.		-1.26	100.		-5.49	717
719	-.15		-.15	100.		-3.29	100.		-1.21	100.		-5.90	719
721	-.30		-.30	100.		-3.11	100.		-1.21	100.		-5.29	721
723	-.28		-.28	100.		-2.92	100.		-1.04	100.		-5.05	723
725	-.15		-.15	100.		-3.17	100.		-1.11	100.		-5.89	725
727	-.58		-.58	100.		-3.79	100.		-1.62	100.		-6.86	727
729	-.75		-.75	100.		-3.91	100.		-1.78	100.		-6.92	729
731	-.45		-.45	100.		-2.63	100.		-1.01	100.		-3.98	731
733	.13		.13	100.		-2.68	100.		-.71	100.		-5.09	733
735	-.38		-.38	100.		-3.32	100.		-1.38	100.		-5.57	735
737	-.07		-.07	100.		-2.49	100.		-.83	100.		-3.79	737
739													739
759	-.28	-2.82	-.27	30.6	69.4	-3.36	75.0	25.0	-1.54	.3	99.7	-4.38	759
761	-.63	-2.82	-.63	25.9	74.1	-3.39	68.1	31.9	-1.65	.3	99.7	-4.38	761
763	-1.05		-1.05	100.		-4.56	100.		-2.34	100.		-7.80	763
765	-.49		-.49	100.		-4.04	100.		-1.84	100.		-7.04	765
767	-.69		-.69	100.		-4.35	100.		-2.06	100.		-7.73	767

Table B-1. (Continued)

SIGMA MODEL II-1

TIME (SEC)	NUMBER CONCENTRATION (#/CC) PARTICLE DIAM(MICRON)			MASS CONCENTRATION (G/M**3) PARTICLE DIAM(MICRON)			EXTINCTION COEFFICIENT (1/KM) PARTICLE DIAM(MICRON)			RADAR REFLECTIVITY FACTOR ((MM**6)/(M**3)) PARTICLE DIAM(MICRON)			TIME (SEC)
	3 -47	>47	TOTAL	3 -47	>47	TOTAL	3 -47	>47	TOTAL	3 -47	>47	TOTAL	
	(LOGARITHM)			(PERCENT OF TOTAL)		(LOG)	(PERCENT OF TOTAL)		(LOG)	(PERCENT OF TOTAL)		(LOG)	
769	-.75		-.75	100.		-4.18	100.		-2.96	100.		-7.06	769
771	-1.05		-1.05	100.		-4.56	100.		-2.34	100.		-7.80	771
773	-.75		-.75	100.		-4.90	100.		-2.43	100.		-8.83	773
775	-.83		-.83	100.		-4.26	100.		-2.06	100.		-7.50	775
777	.18	-3.65	.18	53.8	46.2	-2.67	93.9	6.1	-.86	.1	99.9	-2.53	777
779	.83	-2.55	.83	81.1	18.9	-1.78	96.1	3.9	-.05	2.6	97.4	-2.04	779
781	1.08		1.08	100.		-1.37	100.		.37	100.		-2.93	781
783	.76		.76	100.		-1.87	100.		-.07	100.		-3.57	783
785	.64		.64	100.		-2.02	100.		-.18	100.		-3.88	785
787	.91		.91	100.		-1.68	100.		.10	100.		-3.25	787
789	.40		.40	100.		-2.09	100.		-.38	100.		-3.47	789
791	-.17		-.17	100.		-3.33	100.		-1.33	100.		-5.58	791
793	.01		.01	100.		-2.28	100.		-.56	100.		-3.85	793
795	.08		.08	100.		-3.09	100.		-1.05	100.		-5.62	795
797	-.28		-.28	100.		-3.65	100.		-1.47	100.		-6.77	797
799	-.69		-.69	100.		-4.16	100.		-1.92	100.		-7.47	799
801	.09		.09	100.		-2.86	100.		-.87	100.		-5.23	801
803	.39		.39	100.		-2.46	100.		-.60	100.		-4.28	803
805	-.33		-.33	100.		-2.94	100.		-1.10	100.		-4.89	805
807	-.30		-.30	100.		-3.01	100.		-1.10	100.		-5.25	807
809	-.25		-.25	100.		-2.65	100.		-1.02	100.		-3.98	809
811	-.38		-.38	100.		-3.77	100.		-1.59	100.		-6.86	811
813	-.93		-.93	100.		-5.42	100.		-2.78	100.		-10.07	813
815	-.63		-.63	100.		-4.84	100.		-2.34	100.		-8.82	815
817	-1.05		-1.05	100.		-4.16	100.		-2.06	100.		-7.05	817
819	-.69		-.69	100.		-4.17	100.		-2.04	100.		-7.06	819
821	-.53		-.53	100.		-4.39	100.		-2.06	100.		-7.76	821
823	-.58		-.58	100.		-4.54	100.		-2.13	100.		-8.37	823
825	-.75		-.75	100.		-4.04	100.		-1.92	100.		-6.98	825
827	-.53		-.53	100.		-3.43	100.		-1.46	100.		-5.87	827
829	-1.05		-1.05	100.		-4.16	100.		-2.06	100.		-7.05	829
831	-.93		-.93	100.		-4.22	100.		-2.02	100.		-7.49	831
833	-.58		-.58	100.		-3.23	100.		-1.40	100.		-5.24	833
835	-.83		-.83	100.		-4.74	100.		-2.34	100.		-8.55	835
837	-.49		-.49	100.		-3.78	100.		-1.69	100.		-6.45	837
839	-.63		-.63	100.		-3.95	100.		-1.78	100.		-6.97	839
841	-.69		-.69	100.		-3.44	100.		-1.55	100.		-5.60	841
843	-.83		-.83	100.		-5.32	100.		-2.68	100.		-9.97	843
845	-.75		-.75	100.		-4.49	100.		-2.13	100.		-8.26	845
847	-.69		-.69	100.		-4.00	100.		-1.81	100.		-7.02	847
849													849
849	-.83		-.83	100.		-5.32	100.		-2.68	100.		-9.97	849
851	-.63		-.63	100.		-5.12	100.		-2.48	100.		-9.77	851
853	-.83		-.83	100.		-5.32	100.		-2.68	100.		-9.97	853
855	-1.53		-1.53	100.		-6.02	100.		-3.38	100.		-10.67	855
857	-1.05		-1.05	100.		-5.54	100.		-2.90	100.		-10.19	857
859	-1.05		-1.05	100.		-5.54	100.		-2.90	100.		-10.19	859
861	-1.53		-1.53	100.		-6.02	100.		-3.38	100.		-10.67	861
863	-1.23		-1.23	100.		-5.72	100.		-3.08	100.		-10.37	863
865	-.83		-.83	100.		-5.21	100.		-1.34	100.		-5.52	865

Table B-1 (Continued)

PISERS RUN# 11-1

TIME (SEC)	NUMBER CONCENTRATION (#/CC) PARTICLE DIAM(MICRON) 3 -47 (LOGARITHM)	>47	TOTAL	MASS CONCENTRATION (G/M**3) PARTICLE DIAM(MICRON) 3 -47 (PERCENT OF TOTAL)	>47	TOTAL (LOG)	EXTINCTION COEFFICIENT (1/KM) PARTICLE DIAM(MICRON) 3 -47 (PERCENT OF TOTAL)	>47	TOTAL (LOG)	RADAR REFLECTIVITY FACTOR ((MM**6)/(M**3)) PARTICLE DIAM(MICRON) 3 -47 (PERCENT OF TOTAL)	>47	TOTAL (LOG)	TIME (SEC)
867	-1.23		-1.23	100.		-5.72	100.		-3.08	100.		-10.37	867
869	-1.05		-1.05	100.		-5.54	100.		-2.90	100.		-10.19	869
871	-1.23		-1.23	100.		-5.72	100.		-3.08	100.		-10.37	871
873	-1.05		-1.05	100.		-5.54	100.		-2.90	100.		-10.19	873
875	-.93		-.93	100.		-5.42	100.		-2.78	100.		-10.07	875
877	-.63		-.63	100.		-5.12	100.		-2.48	100.		-9.77	877
879	-1.53		-1.53	100.		-6.02	100.		-3.38	100.		-10.67	879
881	-1.05		-1.05	100.		-5.54	100.		-2.90	100.		-10.19	881
883	-1.53		-1.53	100.		-6.02	100.		-3.38	100.		-10.67	883
885	-1.05		-1.05	100.		-5.54	100.		-2.90	100.		-10.19	885
887	-1.05		-1.05	100.		-5.54	100.		-2.90	100.		-10.19	887
889	-1.23		-1.23	100.		-5.72	100.		-3.08	100.		-10.37	889
891	-1.23		-1.23	100.		-5.72	100.		-3.08	100.		-10.37	891
893	-1.23		-1.23	100.		-5.72	100.		-3.08	100.		-10.37	893
895	-.83		-.83	100.		-4.94	100.		-2.48	100.		-8.84	895
897	-1.53		-1.53	100.		-6.02	100.		-3.38	100.		-10.67	897
899	-.49		-.49	100.		-4.38	100.		-2.04	100.		-7.76	899
901	-.63		-.63	100.		-3.66	100.		-1.62	100.		-6.36	901
903	-1.05		-1.05	100.		-4.56	100.		-2.34	100.		-7.80	903
905	-.83		-.83	100.		-4.30	100.		-2.04	100.		-7.70	905
907	-.53		-.53	100.		-3.51	100.		-1.48	100.		-6.15	907
909	-.69		-.69	100.		-4.09	100.		-1.93	100.		-7.04	909
911	-.75		-.75	100.		-4.90	100.		-2.43	100.		-8.83	911
913	-.75		-.75	100.		-4.90	100.		-2.43	100.		-8.83	913
915	-.58		-.58	100.		-4.66	100.		-2.20	100.		-8.54	915
917	-.75		-.75	100.		-4.21	100.		-1.98	100.		-7.48	917
919													919
929	-.33	-2.66	-.32	42.2	57.8	-2.37	75.8	24.2	-.96	.8	99.2	-2.10	929
931	-.83	-2.86	-.83	1.4	98.6	-2.68	18.7	81.3	-1.54		100.	-2.52	931
933	-.75	-2.32	-.74	.5	99.5	-2.61	10.2	89.8	-1.43		100.	-2.13	933
935	-.58	-2.64	-.57	5.8	94.2	-3.09	39.4	60.6	-1.61		100.	-3.63	935
937	-.63		-.63	100.		-4.03	100.		-1.89	100.		-6.98	937
939	-.45		-.45	100.		-3.08	100.		-1.22	100.		-5.17	939
941	-.69	-3.12	-.68	78.9	21.1	-2.67	90.3	9.7	-1.11	25.1	74.9	-3.59	941
943	-.69	-2.82	-.68	84.6	15.4	-2.71	89.8	10.2	-1.15	60.6	39.4	-3.98	943
→ 945	-1.05		-1.05	100.		-4.20	100.		-2.13	100.		-7.06	945
947	-.04		-.04	100.		-2.79	100.		-.96	100.		-4.61	947
949	.49	-3.05	.49	47.1	52.9	-1.79	90.7	9.3	-.28	.1	99.9	-.90	949
951	.61	-2.76	.61	89.2	10.8	-1.92	97.5	2.5	-.20	8.3	91.7	-2.48	951
953	1.24	-1.50	1.24	83.0	17.0	-.95	95.0	5.0	.72	5.2	94.8	-1.34	953
955	1.00	-2.82	1.00	90.2	9.8	-1.28	98.4	1.6	.43	4.4	95.6	-1.57	955
957	.73	-2.48	.73	51.3	48.7	-1.31	93.0	7.0	.18	.1	99.9	-.02	957
959	.93	-2.27	.93	58.7	41.3	-1.57	94.0	6.0	.07	.1	99.9	-.66	959
12 961	.92	-3.65	.92	95.1	4.9	-1.69	99.3	.7	.10	11.1	88.9	-2.47	961
963	.19	-2.74	.19	80.8	19.2	-2.24	94.2	5.8	-.58	8.1	91.9	-2.80	963
965	.82	-1.95	.82	72.3	27.7	-1.39	92.9	7.1	.24	1.4	98.6	-1.29	965
967	1.27	-2.06	1.27	83.4	16.6	-1.14	96.9	3.1	.55	1.8	98.2	-1.05	967
969	1.35	-2.08	1.35	73.5	26.5	-1.10	95.6	4.4	.57	.7	99.3	-.67	969
971	1.37	-1.78	1.37	87.3	12.7	-1.21	96.6	3.4	.57	15.5	84.5	-2.17	971
973	1.36	-1.81	1.36	81.9	18.1	-1.31	95.8	4.2	.46	3.3	96.7	-1.60	973

Table B-1. (Continued)

MISERS RIDGE 11-1

TIME (SEC)		NUMBER CONCENTRATION (#/CC) PARTICLE DIAM(MICRON) 3 -47 (LOGARITHM)	>47	TOTAL	MASS CONCENTRATION (G/M**3) PARTICLE DIAM(MICRON) 3 -47 (PERCENT OF TOTAL)	>47	TOTAL (LOG)	EXTINCTION COEFFICIENT (1/KM) PARTICLE DIAM(MICRON) 3 -47 (PERCENT OF TOTAL)	>47	TOTAL (LOG)	RADAR REFLECTIVITY FACTOR ((MM**6)/(M**3)) PARTICLE DIAM(MICRON) 3 -47 (PERCENT OF TOTAL)	>47	TOTAL (LOG)	TIME (SEC)
975		1.37	-1.89	1.37	85.5	14.5	-1.07	96.8	3.2	.65	4.9	95.1	-1.48	975
977		1.29	-2.06	1.29	83.6	16.4	-1.21	96.3	3.7	.51	5.9	94.1	-1.72	977
979		1.29	-2.04	1.29	86.1	13.9	-1.22	96.9	3.1	.50	5.9	94.1	-1.66	979
981		1.28	-1.95	1.28	52.3	47.7	-1.01	93.1	6.9	.51		100.	.37	981
983		1.32	-1.89	1.32	94.8	5.2	-1.13	98.2	1.8	.62	38.8	61.2	-2.42	983
985		1.31	-1.94	1.31	81.7	18.3	-1.23	96.2	3.8	.49	2.2	97.8	-1.27	985
987		1.17	-2.92	1.17	93.8	6.2	-1.48	98.8	1.2	.30	21.6	78.4	-2.48	987
989	*	.98	-3.65	.98	96.3	3.7	-1.57	~~100.~~		~~.16~~	~~100.~~		~~-3.09~~	~~989~~
991	*	1.04	-2.02	1.04	76.4	23.6	-1.36	~~100.~~		~~.27~~	~~100.~~		~~-3.02~~	~~991~~
993	*	.94	-2.15	.94	69.1	30.9	-1.64	~~100.~~		~~.02~~	~~100.~~		~~-3.37~~	~~993~~
12 995	*	.57	-2.75	.57	58.5	41.5	-1.89	~~100.~~		~~-.29~~	~~100.~~		~~-3.85~~	~~995~~
997	*	.54	-2.94	.54	75.6	24.4	-1.81	~~100.~~		~~-.16~~	~~100.~~		~~-3.62~~	~~997~~
999	*	.33		.33	100.		-2.61	~~100.~~		~~-.68~~	~~100.~~		~~-4.70~~	~~999~~
1001	*	.49		.49	100.		-2.56	~~100.~~		~~-.57~~	~~100.~~		~~-4.88~~	~~1001~~
1003	*	.19	-3.12	.19	77.2	22.8	-2.70	~~100.~~		~~-.84~~	~~100.~~		~~-5.03~~	~~1003~~
1005	*	.18		.18	100.		-2.60	100.		-.74	100.		-4.51	1005
1007	*	.75	-2.92	.75	98.2	1.8	-1.78	~~100.~~		~~-.01~~	~~100.~~		~~-3.47~~	~~1007~~
1009	*	1.20	-2.23	1.20	78.0	22.0	-1.26	~~100.~~		~~.48~~	~~100.~~		~~-2.94~~	~~1009~~
1011	*	1.15	-1.80	1.15	83.9	16.6	-1.27	~~100.~~		~~.38~~	100.		-2.87	~~1011~~
1013		.15		.15	100.		-2.83	100.		-.92	100.		-4.84	1013
→ 1015		-.63		-.63	100.		-4.34	100.		-2.04	100.		-7.73	1015
1017		-.69		-.69	100.		-4.87	100.		-2.38	100.		-8.82	1017
1019		-.75		-.75	100.		-4.90	100.		-2.43	100.		-8.83	1019
1021		-.63		-.63	100.		-3.81	100.		-1.74	100.		-6.47	1021
1023		-.75		-.75	100.		-4.43	100.		-2.15	100.		-7.77	1023
1025		-.58		-.58	100.		-3.94	100.		-1.77	100.		-6.97	1025
1027		-.69		-.69	100.		-3.85	100.		-1.72	100.		-6.87	1027
1029		-.63		-.63	100.		-4.24	100.		-2.00	100.		-7.50	1029
1031		-.83		-.83	100.		-5.32	100.		-2.68	100.		-9.97	1031
1033		-.83		-.83	100.		-4.19	100.		-2.08	100.		-7.06	1033
1035		-.63		-.63	100.		-3.35	100.		-1.43	100.		-5.69	1035
1037		-.58		-.58	100.		-4.08	100.		-1.90	100.		-7.04	1037
1039		-.63		-.63	100.		-4.13	100.		-1.97	100.		-7.05	1039
1041		-.58		-.58	100.		-3.94	100.		-1.77	100.		-6.97	1041
1043		-.63		-.63	100.		-4.68	100.		-2.23	100.		-8.54	1043
1045		-.58		-.58	100.		-3.68	100.		-1.58	100.		-6.57	1045
1047		-.45		-.45	100.		-3.41	100.		-1.48	100.		-5.59	1047
1049		-.49		-.49	100.		-3.52	100.		-1.47	100.		-6.27	1049
1051		-1.05		-1.05	100.		-5.02	100.		-2.60	100.		-8.85	1051
1053		-.69		-.69	100.		-3.98	100.		-1.82	100.		-6.97	1053
1055		-.69		-.69	100.		-4.70	100.		-2.27	100.		-8.54	1055
1057		-.83		-.83	100.		-3.21	100.		-1.39	100.		-5.24	1057
1059		-.63		-.63	100.		-3.70	100.		-1.66	100.		-6.37	1059
1061		-.58		-.58	100.		-3.83	100.		-1.76	100.		-6.47	1061
1063		-.42		-.42	100.		-3.64	100.		-1.52	100.		-6.55	1063
1065		-.83		-.83	100.		-3.92	100.		-1.79	100.		-6.92	1065
1067		-.69		-.69	100.		-3.08	100.		-1.29	100.		-4.94	1067
1069		-.58		-.58	100.		-3.87	100.		-1.76	100.		-6.75	1069
1071		-.49		-.49	100.		-4.62	100.		-2.15	100.		-8.53	1071
1073		-.58		-.58	100.		-4.54	100.		-2.13	100.		-8.37	1073

Table B-1. (Continued)

USERS MODEL II-1

TIME (SEC)	NUMBER CONCENTRATION (#/CC) PARTICLE DIAM(MICRON) 3 -47	>47	TOTAL (LOGARITHM)	MASS CONCENTRATION (G/M**3) PARTICLE DIAM(MICRON) 3 -47	>47	TOTAL (LOG)	EXTINCTION COEFFICIENT (1/KM) PARTICLE DIAM(MICRON) 3 -47	>47	TOTAL (LOG)	RADAR REFLECTIVITY FACTOR ((MM**6)/(M**3)) PARTICLE DIAM(MICRON) 3 -47	>47	TOTAL (LOG)	TIME (SEC)
				(PERCENT OF TOTAL)			(PERCENT OF TOTAL)			(PERCENT OF TOTAL)			
1075	-.83		-.83	100.		-4.94	100.		-2.48	100.		-8.84	1075
1077	-.93		-.93	100.		-3.74	100.		-1.75	100.		-6.37	1077
1079													1079
1089	-.83		-.83	100.		-3.94	100.		-1.82	100.		-6.92	1089
1091	-.58	-3.65	-.58	42.3	57.7	-2.77	82.8	12.2	-1.16	.1	99.9	-2.53	1091
1093	-1.85	-2.92	-1.81	.2	99.8	-1.33	3.9	96.1	-.65		100.	.38	1093
1095	-.43	-2.15	-.42	1.7	98.3	-2.14	14.1	85.9	-1.02		100.	-1.78	1095
1097	-.58	-2.75	-.57	10.7	89.3	-2.22	61.1	38.9	-1.07		100.	-1.16	1097
1099	-1.23	-2.92	-1.22	.7	99.3	-2.41	11.8	88.2	-1.45		100.	-1.70	1099
1101	-.62		-.69	100.		-3.55	100.		-1.54	100.		-6.16	1101
1103	-.63		-.63	100.		-4.84	100.		-2.34	100.		-8.82	1103
1105	-.93	-3.12	-.93	2.3	97.7	-3.33	28.0	72.0	-1.98		100.	-3.72	1105
1107	-.63		-.63	100.		-4.49	100.		-2.18	100.		-7.80	1107
1109	-.83	-2.82	-.83	31.1	68.9	-3.36	66.9	33.1	-1.66	.8	99.2	-4.38	1109
1111	-.91	-2.23	-.91	.1	99.9	-1.93	3.6	96.4	-1.09		100.	-.66	1111
1113	-.43	-1.89	-.39	.1	99.9	-2.45	2.5	97.5	-.87		100.	-1.90	1113
1115	-.83	-2.34	-.82	11.5	88.5	-2.76	41.4	58.6	-1.30	.1	99.9	-3.33	1115
1117	.10	-2.49	.10	53.3	46.7	-2.33	86.0	14.0	-.66	.5	99.5	-2.47	1117
1119	.95	-2.70	.95	95.2	4.8	-1.71	98.8	1.2	.10	35.0	65.0	-3.02	1119
1121	1.03		1.03	100.		-1.66	100.		.15	100.		-3.40	1121
1123	.34	-3.62	.34	53.2	46.8	-2.29	93.7	6.3	-.61	.2	99.8	-1.78	1123
1125	.76	-2.23	.76	9.4	90.6	-.97	72.9	27.1	-.01		100.	1.06	1125
1127	1.19	-2.11	1.19	72.6	27.4	-1.33	95.9	4.1	.36	.3	99.7	-.66	1127
1129	.94	-2.27	.94	94.5	5.5	-1.60	98.0	2.0	.17	56.6	43.4	-3.14	1129
1131	.43		.43	100.		-2.28	100.		-.54	100.		-3.59	1131
1133	.61	-2.52	.61	23.9	76.1	-1.72	80.3	19.7	-.35		100.	-.63	1133
1135	.74		.74	100.		-1.95	100.		-.11	100.		-3.75	1135
1137	.80	-2.82	.80	98.0	2.0	-1.82	99.2	.8	-.05	91.4	8.6	-3.31	1137
1139	.60	-2.91	.60	49.2	50.8	-2.03	90.6	9.4	-.38	.3	99.7	-1.67	1139
1141	.99	-2.09	.99	78.6	21.4	-1.47	95.7	4.3	.21	1.0	99.0	-1.15	1141
1143	1.08	-2.44	1.08	80.6	19.4	-1.41	96.5	3.5	.29	1.7	98.3	-1.37	1143
1145	1.16	-1.92	1.16	81.8	18.2	-1.34	95.6	4.4	.38	4.6	95.4	-1.68	1145
1147	1.23	-2.07	1.23	84.1	15.9	-1.34	96.7	3.3	.39	2.1	97.9	-1.40	1147
1149	1.20	-2.13	1.20	88.0	12.0	-1.49	97.1	2.9	.31	10.5	89.5	-2.40	1149
1151	1.25	-2.19	1.25	83.0	17.0	-1.34	97.0	3.0	.40	2.4	97.6	-1.43	1151
1153	1.20	-2.06	1.20	86.2	13.8	-1.50	96.7	3.3	.32	9.4	90.6	-2.36	1153
1155	1.16	-2.17	1.16	81.7	18.3	-1.28	95.9	4.1	.43	5.1	94.9	-1.78	1155
1157	1.22	-1.73	1.22	86.9	13.1	-1.20	95.9	4.1	.50	10.1	89.9	-1.81	1157
1159	1.17	-2.32	1.17	91.3	8.7	-1.33	98.0	2.0	.43	13.5	86.5	-2.19	1159
1161	1.29	-1.73	1.29	80.0	20.0	-1.10	95.2	4.8	.57	1.8	98.2	-1.02	1161
1163	1.19	-1.91	1.19	61.4	38.6	-1.43	91.4	8.6	.23	.3	99.7	-.88	1163
1165	1.30	-2.46	1.30	88.7	11.3	-1.38	98.0	2.0	.40	5.6	94.4	-1.88	1165
1167	1.16	-2.21	1.16	95.8	4.2	-1.54	98.5	1.5	.28	74.1	25.9	-3.19	1167
1169	1.14	-2.48	1.14	95.6	4.4	-1.44	98.9	1.1	.32	19.9	80.1	-2.42	1169
1171	1.29	-1.92	1.29	87.2	12.8	-1.27	96.6	3.4	.46	13.7	86.3	-1.99	1171
1173	1.25	-1.95	1.25	61.9	38.1	-1.18	93.2	6.8	.47	.3	99.7	-.62	1173
1175	1.12	-1.83	1.12	79.6	20.4	-1.32	94.7	5.3	.38	3.7	96.3	-1.61	1175
1177	1.24	-2.46	1.24	92.7	7.3	-1.37	98.7	1.3	.42	6.0	94.0	-1.96	1177
1179	1.31		1.31	100.		-1.16	100.		.60	100.		-2.77	1179
1181	1.23		1.23	100.		-1.29	100.		.49	100.		-2.91	1181

Table B-1. (Continued)

MISERS (RUFF 11-1

TIME (SEC)	NUMBER CONCENTRATION (#/CC) PARTICLE DIAM(MICRON) 3 -47	>47	TOTAL	MASS CONCENTRATION (G/M**3) PARTICLE DIAM(MICRON) 3 -47	>47	TOTAL	EXTINCTION COEFFICIENT (1/KM) PARTICLE DIAM(MICRON) 3 -47	>47	TOTAL	RADAR REFLECTIVITY FACTOR ((MM**6)/(M**3)) PARTICLE DIAM(MICRON) 3 -47	>47	TOTAL	TIME (SEC)
	(LOGARITHM)			(PERCENT OF TOTAL)		(LOG)	(PERCENT OF TOTAL)		(LOG)	(PERCENT OF TOTAL)		(LOG)	
1183	1.05		1.05	100.		-1.45	100.		.33	100.		-3.15	1183
1185	.88		.88	100.		-1.54	100.		.18	100.		-3.16	1185
1187	.73		.73	100.		-1.95	100.		-.17	100.		-3.53	1187
1189	-.03		-.03	100.		-2.44	100.		-.68	100.		-4.11	1189
1191	-.30		-.30	100.		-3.62	100.		-1.41	100.		-6.88	1191
1193	-.83		-.83	100.		-4.21	100.		-2.00	100.		-7.49	1193
1195	-.75		-.75	100.		-4.29	100.		-2.02	100.		-7.70	1195
1197	-.49		-.49	100.		-4.62	100.		-2.15	100.		-8.53	1197
1199	-.83		-.83	100.		-4.53	100.		-2.27	100.		-7.80	1199
1201	-.75		-.75	100.		-4.90	100.		-2.43	100.		-8.83	1201
1203	-.63		-.63	100.		-4.03	100.		-1.89	100.		-6.98	1203
1205	-.75		-.75	100.		-4.72	100.		-2.30	100.		-8.55	1205
1207	-.69		-.69	100.		-4.01	100.		-1.86	100.		-6.98	1207
1209	-.58		-.58	100.		-4.40	100.		-2.08	100.		-7.77	1209
1211	-.93		-.93	100.		-5.42	100.		-2.78	100.		-10.07	1211
1213	-1.05		-1.05	100.		-5.02	100.		-2.60	100.		-8.85	1213
1215	-.58		-.58	100.		-4.45	100.		-2.06	100.		-8.25	1215
1217	-.69		-.69	100.		-2.99	100.		-1.21	100.		-4.95	1217
1219	-.83		-.83	100.		-4.44	100.		-2.18	100.		-7.77	1219
1221	-.42		-.42	100.		-3.23	100.		-1.37	100.		-5.24	1221
1223	-.69		-.69	100.		-4.13	100.		-1.98	100.		-7.05	1223
1225	-.75		-.75	100.		-3.23	100.		-1.40	100.		-5.24	1225
1227	-.53		-.53	100.		-3.69	100.		-1.64	100.		-6.37	1227
1229	-.63		-.63	100.		-4.84	100.		-2.34	100.		-8.82	1229
1231	-.75		-.75	100.		-4.36	100.		-2.08	100.		-7.73	1231
1233	-.49		-.49	100.		-2.87	100.		-1.18	100.		-4.42	1233
1235	-.53		-.53	100.		-3.90	100.		-1.74	100.		-6.92	1235
1237	-.58		-.58	100.		-3.21	100.		-1.29	100.		-5.61	1237
1239	-.53		-.53	100.		-3.88	100.		-1.71	100.		-6.91	1239
1241	-1.05		-1.05	100.		-4.56	100.		-2.34	100.		-7.80	1241
1243	-.75		-.75	100.		-3.73	100.		-1.66	100.		-6.43	1243
1245	-.75		-.75	100.		-3.79	100.		-1.74	100.		-6.45	1245
1247	-.75		-.75	100.		-4.26	100.		-2.04	100.		-7.50	1247
1249	-.75		-.75	100.		-4.51	100.		-2.23	100.		-7.80	1249
1251	-.83		-.83	100.		-4.37	100.		-2.10	100.		-7.73	1251
1253	-.58		-.58	100.		-4.54	100.		-2.15	100.		-8.37	1253
1255	-.83		-.83	100.		-4.74	100.		-2.34	100.		-8.55	1255
1257	-.63		-.63	100.		-4.41	100.		-2.10	100.		-7.77	1257
1259	-.69		-.69	100.		-3.82	100.		-1.79	100.		-6.45	1259
1261	-.75		-.75	100.		-4.72	100.		-2.30	100.		-8.55	1261
1263	-.83		-.83	100.		-3.62	100.		-1.67	100.		-5.99	1263
1265	-.75		-.75	100.		-3.48	100.		-1.65	100.		-5.60	1265
1267	-.83		-.83	100.		-3.61	100.		-1.57	100.		-6.45	1267
1269	-.42		-.42	100.		-3.77	100.		-1.62	100.		-6.71	1269
1271	-.83		-.83	100.		-4.44	100.		-2.18	100.		-7.77	1271
1273	-.45		-.45	100.		-4.42	100.		-2.00	100.		-8.25	1273
1275	-.69		-.69	100.		-3.46	100.		-1.52	100.		-5.87	1275
1277	-.93		-.93	100.		-3.65	100.		-1.73	100.		-6.00	1277
1279	-.49		-.49	100.		-3.65	100.		-1.69	100.		-6.00	1279
1281	-.75		-.75	100.		-3.52	100.		-1.55	100.		-5.96	1281

Table B-1. (Continued)

MYERS BLUFF 11-1

TIME (SEC)	NUMBER CONCENTRATION (#/CC) PARTICLE DIAM(MICRON)			MASS CONCENTRATION (G/M**3) PARTICLE DIAM(MICRON)			EXTINCTION COEFFICIENT (1/KM) PARTICLE DIAM(MICRON)			RADAR REFLECTIVITY FACTOR ((MM**6)/(M**3)) PARTICLE DIAM(MICRON)			TIME (SEC)
	.3 -.47	>.47	TOTAL	.3 -.47	>.47	TOTAL	.3 -.47	>.47	TOTAL	.3 -.47	>.47	TOTAL	
	(LOGARITHM)			(PERCENT OF TOTAL)		(LOG)	(PERCENT OF TOTAL)		(LOG)	(PERCENT OF TOTAL)		(LOG)	
1283	-.49		-.49	100.		-2.66	100.		-1.07	100.		-3.98	1283
1285	-.63		-.63	100.		-4.68	100.		-2.23	100.		-8.54	1285
1287	-.58		-.58	100.		-3.92	100.		-1.74	100.		-6.96	1287
1289	-.83		-.83	100.		-3.91	100.		-1.92	100.		-6.47	1289
1291	-.83		-.83	100.		-4.94	100.		-2.48	100.		-8.84	1291
1293	-1.05		-1.05	100.		-4.79	100.		-2.43	100.		-8.56	1293
1295	-1.05		-1.05	100.		-5.54	100.		-2.90	100.		-10.19	1295
1297	-.93		-.93	100.		-4.98	100.		-2.54	100.		-8.84	1297
1299	-1.23		-1.23	100.		-3.92	100.		-1.97	100.		-6.47	1299
1301	-1.05		-1.05	100.		-4.46	100.		-2.23	100.		-7.77	1301
1303	-1.23		-1.23	100.		-4.21	100.		-2.15	100.		-7.06	1303
1305	-1.23		-1.23	100.		-4.47	100.		-2.27	100.		-7.77	1305
1307	-1.05		-1.05	100.		-5.02	100.		-2.60	100.		-8.85	1307
1309	-1.05		-1.05	100.		-4.56	100.		-2.34	100.		-7.80	1309
1311	-1.05		-1.05	100.		-5.54	100.		-2.90	100.		-10.19	1311
1313	-.75		-.75	100.		-3.13	100.		-1.38	100.		-4.94	1313
1315	-1.05		-1.05	100.		-5.54	100.		-2.90	100.		-10.19	1315
1317	-.83		-.83	100.		-4.94	100.		-2.48	100.		-8.84	1317
1319	-.75		-.75	100.		-5.24	100.		-2.60	100.		-9.89	1319
1321	-1.05		-1.05	100.		-4.79	100.		-2.43	100.		-8.56	1321
1323	-.63		-.63	100.		-3.92	100.		-1.75	100.		-6.96	1323
1325	-.83		-.83	100.		-4.30	100.		-2.04	100.		-7.70	1325
1327	-.69		-.69	100.		-2.97	100.		-1.20	100.		-4.85	1327
1329													1329
1329	-.75		-.75	100.		-3.57	100.		-1.59	100.		-6.16	1329
1331	-1.23		-1.23	100.		-5.72	100.		-3.08	100.		-10.37	1331
1333	-1.05		-1.05	100.		-5.54	100.		-2.90	100.		-10.19	1333
1335	-1.53		-1.53	100.		-6.02	100.		-3.38	100.		-10.67	1335
1337	-1.23		-1.23	100.		-5.72	100.		-3.08	100.		-10.37	1337
1339	-1.05		-1.05	100.		-5.54	100.		-2.90	100.		-10.19	1339
1341	-1.05		-1.05	100.		-5.54	100.		-2.90	100.		-10.19	1341
1343	-1.23		-1.23	100.		-5.72	100.		-3.08	100.		-10.37	1343
1345	-.93		-.93	100.		-4.54	100.		-2.30	100.		-7.80	1345
1347	-.83		-.83	100.		-5.32	100.		-2.68	100.		-9.97	1347
1349	-1.53		-1.53	100.		-6.02	100.		-3.38	100.		-10.67	1349
1351	-1.05		-1.05	100.		-5.54	100.		-2.90	100.		-10.19	1351
1353	-.83		-.83	100.		-4.94	100.		-2.48	100.		-8.84	1353
1355	-1.23		-1.23	100.		-5.72	100.		-3.08	100.		-10.37	1355
1357	-.83		-.83	100.		-5.32	100.		-2.68	100.		-9.97	1357
1359	-.58		-.58	100.		-4.81	100.		-2.30	100.		-8.81	1359
1361	-.93		-.93	100.		-5.42	100.		-2.78	100.		-10.07	1361
1363	-.69		-.69	100.		-4.87	100.		-2.38	100.		-8.82	1363
1365	-.93		-.93	100.		-5.42	100.		-2.78	100.		-10.07	1365
1367	-.53		-.53	100.		-4.05	100.		-1.85	100.		-7.04	1367
1369	-.75		-.75	100.		-4.72	100.		-2.30	100.		-8.55	1369
1371	-.58		-.58	100.		-4.66	100.		-2.20	100.		-8.54	1371
1373	-.69		-.69	100.		-4.87	100.		-2.38	100.		-8.82	1373
1375	-.69		-.69	100.		-4.87	100.		-2.38	100.		-8.82	1375
1377	-1.05		-1.05	100.		-5.54	100.		-2.90	100.		-10.19	1377
1379	-.83		-.83	100.		-4.94	100.		-2.48	100.		-8.84	1379

Table B-1. (Continued)

KISERS RIVER II-1

TIME (SEC)	NUMBER CONCENTRATION (#/CC) PARTICLE DIAM(MICRON) 3 -47 (LOGARITHM)	>47	TOTAL	MASS CONCENTRATION (G/M**3) PARTICLE DIAM(MICRON) 3 -47 (PERCENT OF TOTAL)	>47	TOTAL (LOG)	EXTINCTION COEFFICIENT (1/KM) PARTICLE DIAM(MICRON) 3 -47 (PERCENT OF TOTAL)	>47	TOTAL (LOG)	RADAR REFLECTIVITY FACTOR ((MM**6)/(M**3)) PARTICLE DIAM(MICRON) 3 -47 (PERCENT OF TOTAL)	>47	TOTAL (LOG)	TIME (SEC)
1381	-.69		-.69	100.		-5.17	100.		-2.54	100.		-9.82	1381
1383	-1.23		-1.23	100.		-4.81	100.		-2.48	100.		-8.56	1383
1385	-.69		-.69	100.		-3.56	100.		-1.52	100.		-6.28	1385
1387	-.63		-.63	100.		-3.53	100.		-1.55	100.		-5.96	1387
1389	-.75		-.75	100.		-5.24	100.		-2.60	100.		-9.89	1389
1391	-.83		-.83	100.		-4.53	100.		-2.27	100.		-7.80	1391
1393	-.83		-.83	100.		-3.67	100.		-1.64	100.		-6.36	1393
1395	-.45		-.45	100.		-3.93	100.		-1.74	100.		-6.97	1395
1397	-.58		-.58	100.		-4.08	100.		-1.90	100.		-7.04	1397
1399	-.93		-.93	100.		-5.42	100.		-2.78	100.		-10.07	1399
1401	-.58		-.58	100.		-4.08	100.		-1.90	100.		-7.04	1401
1403	-.69		-.69	100.		-4.42	100.		-2.13	100.		-7.77	1403
1405	-.69		-.69	100.		-4.01	100.		-1.86	100.		-6.98	1405
1407	-.93		-.93	100.		-4.76	100.		-2.38	100.		-8.55	1407
1409	-.69		-.69	100.		-5.17	100.		-2.54	100.		-9.82	1409
1411													1411
1413	-.38	-2.52	-.38	72.7	27.3	-2.65	88.1	11.9	-.92	16.3	83.7	-4.00	1413
1415	.84	-2.18	.84	81.2	18.8	-1.89	94.5	5.5	-.09	10.3	89.7	-2.91	1415
1417	.98	-2.18	.98	91.5	8.5	-1.67	97.1	2.9	.09	34.9	65.1	-2.94	1417
1419	1.20	-2.01	1.20	91.1	8.9	-1.34	97.2	2.8	.38	27.6	72.4	-2.32	1419
1421	1.24	-1.86	1.24	85.7	14.3	-1.10	96.7	3.3	.57	3.6	96.4	-1.26	1421
1423	1.17	-1.85	1.17	65.4	34.6	-1.39	92.7	7.3	.33	.7	99.3	-1.25	1423
1425	1.27	-1.94	1.27	83.8	16.2	-1.12	96.4	3.6	.56	3.6	96.4	-1.26	1425
1427	1.19	-1.81	1.19	64.1	35.9	-1.11	93.4	6.6	.47	.2	99.8	-.19	1427
1429	1.07	-1.72	1.07	78.3	21.7	-1.33	93.3	6.7	.34	5.7	94.3	-1.74	1429
1431	1.18	-1.85	1.18	80.6	19.4	-1.22	95.7	4.3	.47	1.6	98.4	-1.09	1431
1433	1.20	-1.83	1.21	73.5	26.5	-1.23	94.3	5.7	.44	1.1	98.9	-1.00	1433
1435	1.20	-2.19	1.20	88.2	11.8	-1.26	97.3	2.7	.46	6.3	93.7	-1.67	1435
1437	.79	-2.46	.79	89.6	10.4	-1.93	97.3	2.7	-.08	12.5	87.5	-3.12	1437
1439	-.12	-2.52	-.11	37.1	62.9	-3.01	76.2	23.8	-1.22	.8	99.2	-4.08	1439
1441	-.30		-.30	100.		-3.29	100.		-1.31	100.		-5.57	1441
1443	.66		.66	100.		-2.05	100.		-.26	100.		-3.54	1443
1445	.49		.49	100.		-2.23	100.		-.43	100.		-3.85	1445
1447	.70		.70	100.		-2.38	100.		-.41	100.		-4.31	1447
1449	.78	-2.18	.78	88.0	12.0	-1.82	95.7	4.3	-.07	30.5	69.5	-2.97	1449
1451	1.10	-2.42	1.10	94.5	5.5	-1.71	98.4	1.6	.13	55.2	44.8	-3.21	1451
1453	1.02	-2.86	1.02	74.3	25.7	-1.63	96.2	3.8	.09	.8	99.2	-1.46	1453
1455	1.23	-1.98	1.23	79.8	20.2	-1.31	96.0	4.0	.41	1.5	98.5	-1.26	1455
1457	1.23	-1.85	1.23	88.9	11.1	-1.22	96.8	3.2	.52	14.3	85.7	-2.10	1457
1459	1.20	-1.97	1.20	82.1	17.9	-1.30	96.1	3.9	.42	2.3	97.7	-1.37	1459
1461	1.22	-1.85	1.22	82.6	17.4	-1.20	95.9	4.1	.48	1.7	98.3	-1.13	1461
1463	1.26	-2.07	1.26	74.4	25.6	-1.29	95.7	4.3	.44	.5	99.5	-.88	1463
1465	1.24	-2.07	1.24	81.2	18.8	-1.57	96.1	3.9	.27	2.5	97.5	-2.01	1465
1467	1.26	-2.39	1.26	92.9	7.1	-1.43	98.6	1.4	.36	8.8	91.2	-2.08	1467
1469	1.31	-1.71	1.31	84.0	16.0	-1.49	96.6	3.4	.38	7.8	92.2	-2.35	1469
1471	1.19	-2.09	1.19	87.6	12.4	-1.57	100.		.21	100.		-3.34	1471
1473	1.10	-2.32	1.10	73.8	26.2	-1.82	100.		-.00	100.		-4.00	1473
1475	1.00	-2.28	1.00	82.7	17.3	-1.58	100.		.17	100.		-3.37	1475
1477	1.08	-2.34	1.08	96.5	3.5	-1.36	100.		.36	100.		-2.95	1477
1479	.26	-2.82	.26	86.3	13.7	-2.46	100.		-.83	100.		-4.60	1479

Table B-1. (Continued)

MISERS MODEL II-1

TIME (SEC)	NUMBER CONCENTRATION (#/CC) PARTICLE DIAM(MICRON) 3 -47 (LOGARITHM)	>47	TOTAL	MASS CONCENTRATION (G/M**3) PARTICLE DIAM(MICRON) 3 -47 (PERCENT OF TOTAL)	>47	TOTAL (LOG)	EXTINCTION COEFFICIENT (1/KM) PARTICLE DIAM(MICRON) 3 -47 (PERCENT OF TOTAL)	>47	TOTAL (LOG)	RADAR REFLECTIVITY FACTOR ((MM**6)/(M**3)) PARTICLE DIAM(MICRON) 3 -47 (PERCENT OF TOTAL)	>47	TOTAL (LOG)	TIME (SEC)
14													
1481	-.45		-.45	100.		-4.50	100.		-2.06	100.		-8.37	1481
1483	-.83		-.83	100.		-4.53	100.		-2.27	100.		-7.80	1483
1485	-.63		-.63	100.		-3.85	100.		-1.80	100.		-6.47	1485
1487	-.75		-.75	100.		-4.59	100.		-2.20	100.		-8.38	1487
1489	-.83		-.83	100.		-2.47	100.		-.98	100.		-3.61	1489
1491	-.53		-.53	100.		-3.06	100.		-1.26	100.		-4.93	1491
1493	-.75		-.75	100.		-4.18	100.		-2.06	100.		-7.06	1493
1495	-1.05		-1.05	100.		-5.02	100.		-2.60	100.		-8.85	1495
1497	-.75		-.75	100.		-4.43	100.		-2.15	100.		-7.77	1497
1499	-1.05		-1.05	100.		-3.89	100.		-1.82	100.		-6.75	1499
1501	-.69		-.69	100.		-4.29	100.		-2.00	100.		-7.70	1501
1503	-1.53		-1.53	100.		-6.02	100.		-3.38	100.		-10.67	1503
1505	-.75		-.75	100.		-3.83	100.		-1.80	100.		-6.45	1505
1507	-1.23		-1.23	100.		-5.72	100.		-3.08	100.		-10.37	1507
1509	-.83		-.83	100.		-4.74	100.		-2.34	100.		-8.55	1509
1511	-.53	-2.21	-.52	7.7	92.3	-2.88	34.2	65.8	-1.36	.1	99.9	-3.78	1511
1513	-.75	-2.09	-.73	2.8	97.2	-2.46	18.3	81.7	-1.14		100.	-2.83	1513
1515	-1.05	-2.32	-1.03	26.9	73.1	-2.26	57.3	42.7	-.94	.4	99.6	-2.82	1515
1517	-.53	-2.28	-.52	4.7	95.3	-2.32	27.6	72.4	-1.14		100.	-1.75	1517
1519	-1.21	-2.34	-1.20	.6	99.4	-2.82	6.6	93.4	-1.58		100.	-3.33	1519
1521	-.93	-2.82	-.92	1.2	98.8	-3.51	18.7	81.3	-2.05		100.	-4.38	1521
1523	-.63		-.63	100.		-4.09	100.		-1.92	100.		-7.04	1523
1525	-.93		-.93	100.		-4.98	100.		-2.54	100.		-8.84	1525
1527	-.42		-.42	100.		-3.19	100.		-1.35	100.		-5.22	1527
1539	-.07	-2.07	-.06	70.7	29.3	-2.03	86.8	13.2	-.41	11.2	88.8	-2.81	1539
1541	.75	-2.20	.75	75.2	24.8	-1.65	93.6	6.4	.01	2.9	97.1	-1.87	1541
1543	1.10	-2.22	1.10	84.6	15.4	-1.23	97.0	3.0	.45	2.3	97.7	-1.31	1543
1545	.86	-1.89	.86	76.6	23.4	-1.50	93.1	6.9	.19	5.3	94.7	-1.99	1545
1547	.77	-1.92	.77	73.0	27.0	-1.48	92.8	7.2	.16	1.5	98.5	-1.44	1547
1549	1.21	-2.25	1.21	84.0	16.0	-1.30	96.7	3.3	.41	4.0	96.0	-1.57	1549
1551	1.11	-2.00	1.11	85.4	14.6	-1.37	96.3	3.7	.35	4.5	95.5	-1.71	1551
1553	1.22	-1.82	1.22	85.1	14.9	-1.32	95.8	4.2	.43	10.5	89.5	-2.13	1553
1555	1.37	-2.05	1.37	92.5	7.5	-1.22	98.1	1.9	.53	12.7	87.3	-1.91	1555
1557	1.37	-1.83	1.37	81.8	18.2	-1.21	95.8	4.2	.53	3.8	96.2	-1.63	1557
1559	1.24	-1.77	1.24	76.1	23.9	-1.36	94.1	5.9	.36	2.5	97.5	-1.57	1559
1561	1.41	-1.58	1.41	76.6	23.4	-1.07	94.5	5.5	.62	1.5	98.5	-.96	1561
15 1563	1.35	-2.64	1.35	99.0	1.0	-1.14	99.6	.4	.62	87.7	12.3	-2.72	1563
1565	1.31		1.31	100.		-1.26	100.		.54	100.		-2.98	1565
1567	1.45		1.45	100.		-1.20	100.		.60	100.		-2.80	1567
1569	1.37		1.37	100.		-1.49	100.		.36	100.		-3.16	1569
1571	1.17		1.17	100.		-1.53	100.		.25	100.		-3.04	1571
1573	1.08		1.08	100.		-1.79	100.		.09	100.		-3.45	1573
1575	.45		.45	100.		-2.22	100.		-.40	100.		-3.97	1575
1577	-.69		-.69	100.		-4.42	100.		-2.13	100.		-7.77	1577
1579	-.93		-.93	100.		-3.79	100.		-1.76	100.		-6.45	1579
1581	-1.05		-1.05	100.		-5.02	100.		-2.60	100.		-8.85	1581
1583	-.93	-2.34	-.91	.3	99.7	-1.58	7.0	93.0	-.89		100.	-.01	1583
1585	-.75	-1.61	-.70	.3	99.7	-1.84	4.6	95.4	-.68		100.	-1.35	1585
1587	-.83	-1.73	-.78	.2	99.8	-2.22	2.9	97.1	-.94		100.	-2.28	1587
1589	-.83	-2.12	-.81	.5	99.5	-2.67	7.1	92.9	-1.33		100.	-3.26	1589

Table B-1. (Continued)

MISERS BLUFF II-1

TIME (SEC)	NUMBER CONCENTRATION (#/CC) PARTICLE DIAM(MICRON) 3 -47 (LOGARITHMS)	>47	TOTAL	MASS CONCENTRATION (G/M**3) PARTICLE DIAM(MICRON) 3 -47 (PERCENT OF TOTAL)	>47	TOTAL (LOG)	EXTINCTION COEFFICIENT (1/KM) PARTICLE DIAM(MICRON) 3 -47 (PERCENT OF TOTAL)	>47	TOTAL (LOG)	RADAR REFLECTIVITY FACTOR ((MM**6)/(M**3)) PARTICLE DIAM(MICRON) 3 -47 (PERCENT OF TOTAL)	>47	TOTAL (LOG)	TIME (SEC)
1591	-1.05	-2.27	-1.03	2.0	98.0	-2.86	13.6	86.4	-1.47		100.	-3.50	1591
1593	-.63	-2.58	-.62	1.1	98.9	-2.59	18.5	81.5	-1.42		100.	-2.38	1593
1595	-.03	-2.70	-.02	21.0	79.0	-2.93	72.5	27.5	-1.26		100.	-3.20	1595
1597	1.01	-2.12	1.01	87.0	13.0	-1.79	95.9	4.1	.03	31.5	68.5	-3.10	1597
1599	1.17	-1.95	1.17	76.7	23.3	-1.43	95.1	4.9	.34	1.4	98.6	-1.59	1599
1601	1.22	-1.90	1.22	86.5	13.5	-1.16	96.6	3.4	.54	7.4	92.6	-1.70	1601
1603	1.11	-2.08	1.11	93.9	6.1	-1.37	97.8	2.2	.36	57.9	42.1	-2.75	1603
1605	1.24	-1.99	1.24	84.1	15.9	-1.17	96.5	3.5	.51	3.0	97.0	-1.31	1605
1607	1.28	-2.39	1.28	96.5	3.5	-1.27	99.0	1.0	.50	42.1	57.9	-2.53	1607
1609	1.14		1.14	100.		-1.49	100.		.32	100.		-3.22	1609
1611	1.03		1.03	100.		-1.54	100.		.23	100.		-3.15	1611
1613	-.12		-.12	100.		-3.35	100.		-1.24	100.		-6.11	1613
1615	-.53		-.53	100.		-3.97	100.		-1.79	100.		-6.97	1615
1617	-.30		-.30	100.		-3.31	100.		-1.29	100.		-5.87	1617
1619	-.53		-.53	100.		-4.21	100.		-1.90	100.		-7.67	1619
1621	-.45		-.45	100.		-2.82	100.		-1.09	100.		-4.60	1621
1623	-.58		-.58	100.		-4.33	100.		-2.02	100.		-7.73	1623
1625	-.19		-.19	100.		-3.57	100.		-1.43	100.		-6.39	1625
1627	-.28		-.28	100.		-2.91	100.		-1.11	100.		-4.66	1627
1629	-.30		-.30	100.		-3.62	100.		-1.52	100.		-6.35	1629
1631	-.58		-.58	100.		-3.28	100.		-1.46	100.		-5.25	1631
1633	-.38		-.38	100.		-2.77	100.		-1.01	100.		-4.41	1633
1635	-.30		-.30	100.		-2.41	100.		-.76	100.		-3.89	1635
1637	.27		.27	100.		-2.85	100.		-.85	100.		-5.14	1637
1639	.26		.26	100.		-2.74	100.		-.86	100.		-4.56	1639
1641	-.19		-.19	100.		-2.96	100.		-1.11	100.		-4.90	1641
1643	-.33		-.33	100.		-2.82	100.		-1.08	100.		-4.64	1643
1645	-.93		-.93	100.		-4.98	100.		-2.54	100.		-8.84	1645
1647	-.93		-.93	100.		-3.68	100.		-1.79	100.		-6.00	1647
1649	-.93		-.93	100.		-4.76	100.		-2.38	100.		-8.55	1649
1651	-.75		-.75	100.		-4.43	100.		-2.15	100.		-7.77	1651
1653	-.35		-.35	100.		-3.20	100.		-1.32	100.		-5.24	1653
1655	-.53		-.53	100.		-4.46	100.		-2.13	100.		-7.80	1655
1657	-.42		-.42	100.		-2.88	100.		-1.03	100.		-5.09	1657
1659													1659
1669	-.93		-.93	100.		-5.42	100.		-2.78	100.		-10.07	1669
1671	-.83		-.83	100.		-5.32	100.		-2.68	100.		-9.97	1671
1673	.06		.06	100.		-3.37	100.		-1.22	100.		-6.13	1673
1675	.63	-2.82	.63	98.1	1.9	-1.80	99.2	.8	-.05	88.7	11.3	-3.43	1675
1677	.19		.19	100.		-2.34	100.		-.55	100.		-4.05	1677
1679	-.63		-.63	100.		-4.84	100.		-2.34	100.		-8.82	1679
1681	-.58	-2.76	-.57	7.8	92.2	-2.69	47.1	52.9	-1.36		100.	-2.47	1681
1683	-.45	-2.70	-.45	67.1	32.9	-2.55	88.5	11.5	-.89	3.0	97.0	-3.19	1683
1685	-.13	-2.42	-.13	47.4	52.6	-2.69	80.3	19.7	-.95	1.4	98.6	-3.55	1685
1687	.20	-2.74	.20	92.2	7.8	-1.85	97.6	2.4	-.20	19.1	80.9	-2.74	1687
1689	-.13		-.13	100.		-3.27	100.		-1.24	100.		-5.81	1689
1691	.22	-3.12	.23	94.5	5.5	-2.08	98.3	1.7	-.36	48.1	51.9	-3.43	1691
1693	-.21	-3.65	-.21	53.3	46.7	-2.67	90.3	9.7	-1.06	.4	99.6	-2.52	1693
1695	-.63	-2.26	-.62	.9	99.1	-2.09	13.4	86.6	-1.09		100.	-1.31	1695
1697	1.05	-1.81	1.05	53.9	46.1	-1.38	90.4	9.6	.24	.2	99.8	-.86	1697

Table B-2. MISERS BLUFF II-2 Detailed Dust Particle Spectral Data

TIME (SEC)	MASS CONCENTRATION (G/M**3) PARTICLE DIAM(MICRON) <3	3 -46	47 -470	>470	TOTAL	EXTINCTION COEFFICIENT (1/KM) PARTICLE DIAM(MICRON) <3	3 -46	47 -470	>470	TOTAL	RADAR REFLECTIVITY FACTOR ((MM**6)/(M**3)) PARTICLE DIAM(MICRON) <3	3 -46	47 -470	>470	TOTAL	TIME (SEC)
	(LOG)					(PERCENT OF TOTAL)				(LOG)	(PERCENT OF TOTAL)				(LOG)	
230	2.14	-1.63			2.14	10.9	89.1			-0.83	69.5	30.5			-1.94		100.			-8.86	230
232	2.17	-1.53			2.17	3.0	96.9			-0.97	88.0	12.0			-2.02	.3	99.7			-9.34	232
234	2.21	-.93			2.21	12.4	87.6			-0.89	66.5	33.5			-1.86	.1	99.9			-8.73	234
236	2.19	-.69			2.19	1.3	98.7			-0.81	24.7	75.3			-1.41		100.			-6.48	236
238	2.19	-1.23			2.19	10.8	89.2			-0.97	78.0	22.0			-1.98	.1	99.9			-9.04	238
240	2.19	-1.35			2.19	10.8	89.2			-0.91	71.2	28.8			-1.92	.1	99.9			-8.86	240
242	2.19	-1.35			2.19	21.4	78.6			-0.77	74.4	25.6			-1.87	.3	99.7			-8.86	242
244	2.19	-1.23			2.19	2.8	97.2			-0.87	49.9	50.1			-1.75		100.			-6.85	244
246	2.20	-.93			2.20	7.9	92.1			-0.82	59.3	40.7			-1.85		100.			-8.64	246
248	2.16				2.16	100.				-5.76	100.				-2.10	100.				-12.58	248
250	2.19	-1.23			2.19	6.3	93.7			-0.89	63.6	36.4			-1.87		100.			-7.79	250
252	2.19	-1.23			2.19	3.2	96.8			-0.87	48.4	51.6			-1.76		100.			-6.85	252
254	2.17	-1.53			2.17	2.1	97.9			-0.10	50.2	49.8			-1.80		100.			-6.85	254
256	2.16	-1.53			2.16	9.4	90.6			-0.54	70.3	29.7			-1.90		100.			-7.81	256
258	2.19	-1.23			2.19	6.4	93.6			-0.89	63.0	37.0			-1.88		100.			-7.79	258
260	2.17	-1.53			2.17	49.9	50.1			-5.05	89.5	10.5			-1.96	6.5	93.5			-9.31	260
262	2.19	-1.53			2.19	47.8	52.2			-5.07	89.9	10.1			-1.94	1.6	98.4			-9.33	262
264	2.16	-.75			2.17	1.3	98.7			-3.91	32.5	67.5			-1.62		100.			-6.80	264
266	2.19	-1.23			2.19	18.5	81.5			-0.96	78.5	21.5			-1.97	.1	99.9			-9.04	266
268	2.21	-1.23			2.21	15.7	84.3			-0.98	78.1	21.9			-1.98		100.			-9.04	268
270	2.19	-1.53			2.19	3.3	96.7			-0.89	53.5	46.5			-1.77		100.			-6.85	270
272	2.19	-1.23			2.19	4.1	95.9			-0.27	52.9	47.1			-1.80		100.			-7.50	272
274	2.19	-1.35			2.19	5.5	94.5			-0.83	58.3	41.7			-1.84		100.			-7.78	274
276	2.30	.37		-4.91	2.39	.3	85.9		13.8	-1.83	6.1	93.2		.7	-.11		.1		99.9	-.63	276
278	2.32	-.63		-4.58	2.32	.1	18.6		81.3	-1.04	17.7	70.6		11.7	-.81				100.	.39	278
280	2.57	-.43		-3.93	2.57	.2	.3		99.4	-1.38	54.0	8.4		37.6	-.68				100.	1.07	280
282	2.72	.30		-4.28	2.72	.3	18.2		81.5	-1.45	20.6	73.1		6.3	-.14				100.	1.27	282
284	2.91	.43			2.91	2.4	97.6			-2.04	30.2	69.8			-.05		100.			-4.00	284
286	2.77	-.23			2.78	14.6	85.4			-3.20	71.9	28.1			-.75		100.			-5.76	286
288	2.74	-.75			2.74	31.7	68.3			-3.24	87.3	12.7			-.61		100.			-5.59	288
290	2.91	-1.23			2.91	98.1	1.9			-3.33	99.5	.5			-.32	71.7	28.3			-8.49	290
292	2.77	-1.23			2.77	75.5	24.5			-3.91	96.4	3.6			-.87	2.1	97.9			-7.78	292
294	2.46	-.75			2.46	8.9	91.1			-4.00	62.7	37.3			-1.40		100.			-7.32	294
296	2.28	-1.23			2.28	5.4	94.6			-4.25	60.9	39.1			-1.72		100.			-7.50	296
298	2.22	-1.53			2.22	10.4	89.6			-4.54	71.2	28.8			-1.89	.1	99.9			-7.81	298
300	2.16				2.16	100.				-5.75	100.				-2.10	100.				-12.34	300
301	2.17	-1.23			2.17	4.2	95.8			-4.27	52.9	47.1			-1.80		100.			-7.50	301
307	2.19	-1.23			2.19	17.9	82.1			-4.97	77.9	22.1			-1.98	.1	99.9			-9.04	307
309	2.18	-1.35			2.18	7.6	92.4			-4.83	58.8	41.2			-1.83	.1	99.9			-7.78	309
311	2.18	-1.23			2.18	4.1	95.9			-4.67	51.4	48.6			-1.73		100.			-6.85	311
313	2.19	-1.23			2.19	14.2	85.8			-4.99	75.9	24.1			-2.02		100.			-9.04	313
315	2.17	-1.23			2.17	10.4	89.6			-4.47	65.9	34.1			-1.84	.1	99.9			-7.79	315
317	2.15	-1.53			2.15	7.4	92.6			-4.65	68.0	32.0			-1.93		100.			-7.81	317
319	2.17				2.17	100.				-5.65	100.				-2.08	100.				-11.57	319
321	2.17				2.17	100.				-5.76	100.				-2.11	100.				-12.11	321
323	2.19	-1.23			2.19	16.0	83.4			-4.97	77.5	22.5			-1.99	.1	99.9			-9.04	323
325	2.19	-1.23			2.19	18.1	81.9			-4.97	77.7	22.3			-1.98	.1	99.9			-9.04	325
327	2.19	-.63			2.19	4.2	95.8			-4.39	51.7	48.3			-1.83		100.			-7.77	327
329	2.19	-1.53			2.19	2.1	97.9			-4.23	46.9	53.1			-1.77		100.			-6.85	329
331	2.19	-1.53			2.19	9.4	90.6			-4.56	71.1	28.9			-1.89		100.			-7.81	331

Table B-2. (Continued)

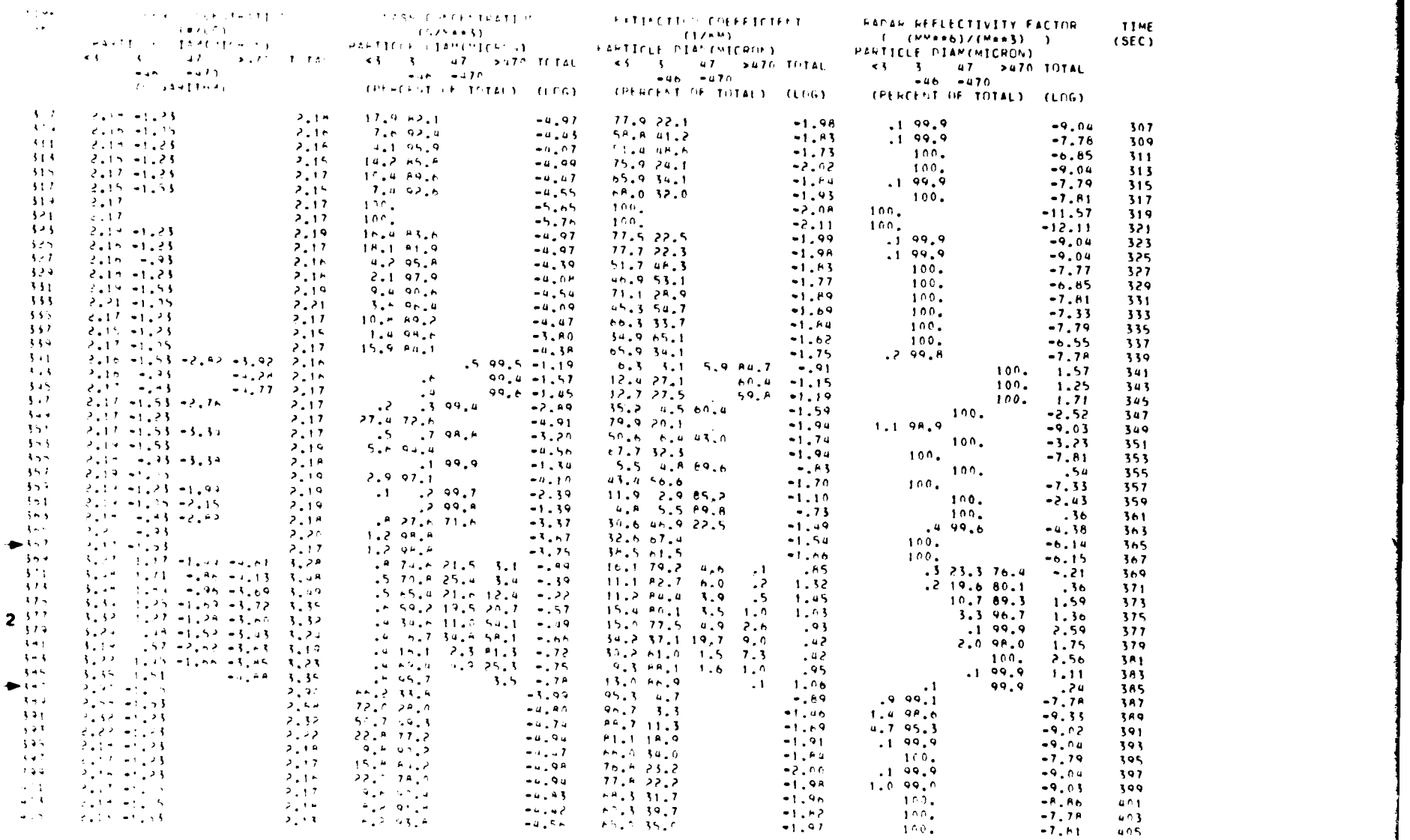

Table B-2. (Continued)

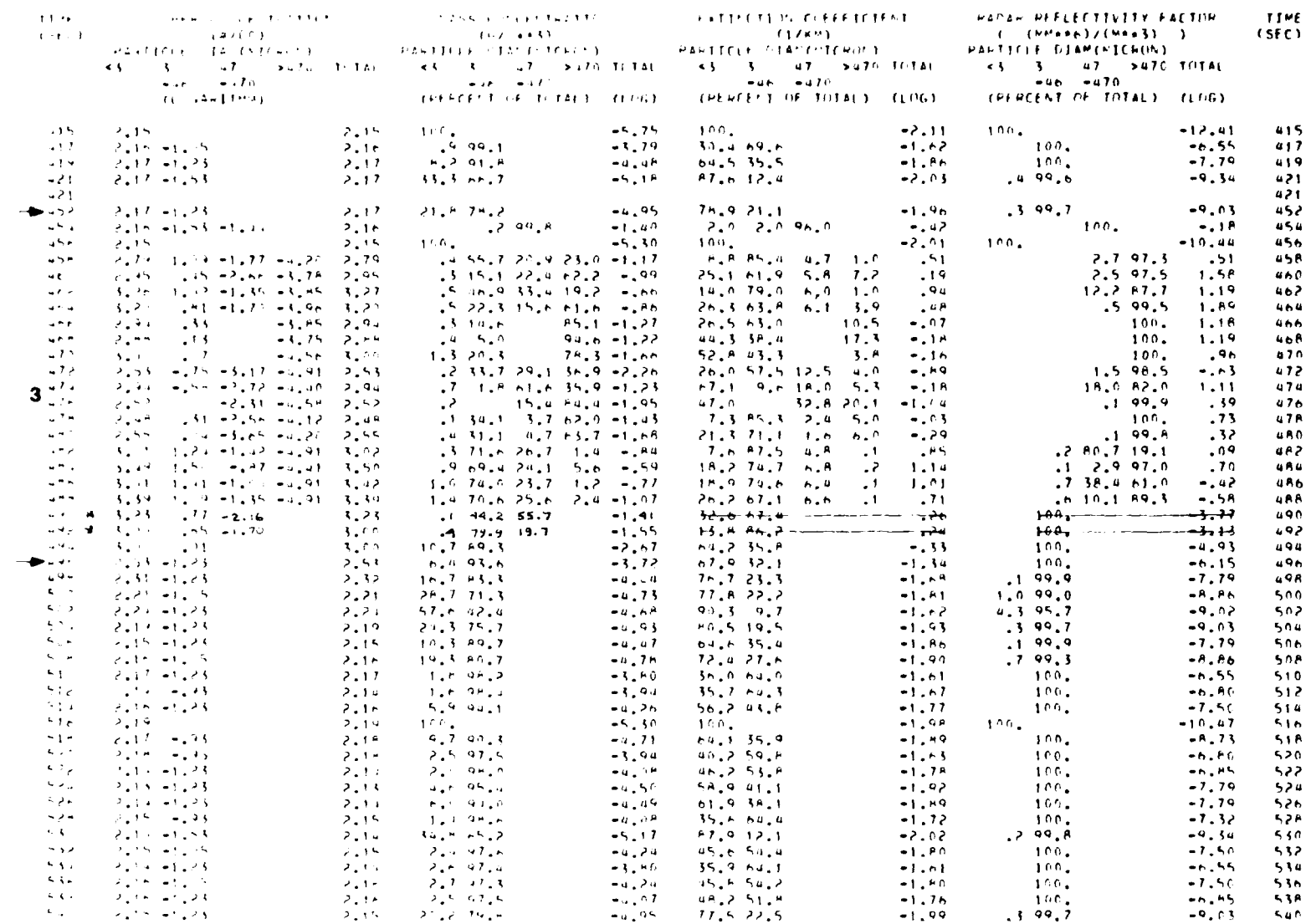

TIME (SEC)	WATER CONTENT (G/M**3) PARTICLE DIAMETER (MICRONS) <3	3 -47	47 -470	>470	TOTAL	MASS CONCENTRATION (G/M**3) PARTICLE DIAMETER (MICRONS) <3	3 -47	47 -470	>470	TOTAL	(LOG)	EXTINCTION COEFFICIENT (1/KM) PARTICLE DIAMETER (MICRON) <3	3 -46	47 -470	>470	TOTAL	(LOG)	RADAR REFLECTIVITY FACTOR ((MM**6)/(M**3)) PARTICLE DIAM(MICRON) <3	3 -46	47 -470	>470	TOTAL	(LOG)	TIME (SEC)
						(PERCENT OF TOTAL)						(PERCENT OF TOTAL)						(PERCENT OF TOTAL)						
415	2.15				2.15	100.					-5.75	100.					-2.11	100.					-12.41	415
417	2.16	-1.45			2.16	.9	99.1				-3.79	33.4	66.6				-1.62		100.				-6.55	417
419	2.17	-1.23			2.17	8.2	91.8				-4.48	64.5	35.5				-1.86		100.				-7.79	419
421	2.17	-1.53			2.17	33.3	66.7				-5.18	87.6	12.4				-2.03	.4	99.6				-9.34	421
421																								421
452	2.17	-1.23			2.17	21.8	78.2				-4.95	78.9	21.1				-1.96	.3	99.7				-9.03	452
454	2.16	-1.53	-1.11		2.16		.2	99.8			-1.60	2.0	2.0	96.0			-.42			100.			-.18	454
456	2.15				2.15	100.					-5.30	100.					-2.01	100.					-10.44	456
458	2.74	1.39	-1.77	-4.25	2.79	.4	55.7	20.9	23.0		-1.17	8.8	85.4	4.7	1.0		.51			2.7	97.3		.51	458
460	2.45	.45	-2.66	-3.78	2.96	.3	15.1	22.4	62.2		-.99	25.1	61.9	5.8	7.2		.19			2.5	97.5		1.58	460
462	3.26	1.13	-1.35	-3.45	3.27	.5	10.9	33.4	19.2		-.86	14.0	79.0	6.0	1.0		.94			12.2	87.7		1.19	462
464	3.23	.41	-1.73	-3.96	3.23	.5	22.3	15.6	61.6		-.86	26.3	63.8	6.1	3.9		.48			.5	99.5		1.89	464
466	2.94	.33		-3.85	2.94	.3	14.6		85.1		-1.27	26.5	63.0		10.5		-.07				100.		1.18	466
468	2.88	.13		-3.75	2.88	.4	5.0		94.6		-1.22	44.3	38.4		17.3		-.18				100.		1.19	468
470	3.01	.17		-4.56	3.00	1.3	20.3		78.3		-1.66	52.8	43.3		3.8		-.16				100.		.96	470
472	2.53	-.75	-5.17	-4.91	2.53	.2	33.7	29.1	36.9		-2.26	26.0	57.5	12.5	4.0		-.89			1.5	98.5		-.63	472
474	2.94	-.56	-3.72	-4.40	2.94	.7	1.8	61.6	35.9		-1.23	67.1	9.6	18.0	5.3		-.18			18.0	82.0		1.11	474
476	2.53		-2.31	-4.54	2.53	.2		15.4	84.4		-1.95	47.0		32.8	20.1		-1.74			.1	99.9		.39	476
478	2.68	.31	-3.56	-4.12	2.68	.1	30.1	3.7	62.0		-1.43	7.3	85.3	2.4	5.0		-.03				100.		.73	478
480	2.55	.14	-3.65	-4.26	2.55	.4	31.1	8.7	59.7		-1.68	21.3	71.1	1.6	6.0		-.29			.1	99.8		.32	480
482	3.01	1.24	-1.43	-4.91	3.02	.3	71.6	26.7	1.4		-.84	7.6	87.5	4.8	.1		.45		.2	80.7	19.1		.09	482
484	3.49	1.50	-.47	-4.41	3.50	.9	69.4	24.1	5.6		-.59	18.2	74.7	6.8	.2		1.14		.1	2.9	97.0		.70	484
486	3.41	1.41	-1.51	-4.91	3.42	1.6	74.6	23.7	1.2		-.77	18.9	74.6	6.4	.1		1.01		.7	38.4	61.0		-.42	486
488	3.34	1.30	-1.35	-4.91	3.34	1.4	70.6	25.6	2.4		-1.07	28.2	67.1	4.6	.1		.71		.6	10.1	89.3		-.58	488
490	3.23	.77	-2.16		3.23	.1	44.2	55.7			-1.41	52.6	47.4				-.26		100.				-3.77	490
492	3.60	.95	-1.70		3.60	.3	79.9	19.7			-1.55	53.8	46.2				.24		100.				-3.13	492
494	3.00	.31			3.00	10.7	89.3				-2.67	64.2	35.8				-.33		100.				-4.93	494
496	2.53	-1.23			2.53	6.4	93.6				-3.72	67.9	32.1				-1.34		100.				-6.15	496
498	2.32	-1.23			2.32	16.7	83.3				-4.14	76.7	23.3				-1.69	.1	99.9				-7.79	498
500	2.21	-1.5			2.21	28.7	71.3				-4.73	77.8	22.2				-1.81	1.0	99.0				-8.86	500
502	2.21	-1.23			2.21	57.6	42.4				-4.68	90.3	9.7				-1.62	4.3	95.7				-9.02	502
504	2.19	-1.23			2.19	24.3	75.7				-4.63	80.5	19.5				-1.93	.3	99.7				-9.03	504
506	2.15	-1.23			2.15	10.3	89.7				-4.07	64.6	35.4				-1.86	.1	99.9				-7.79	506
508	2.14	-1.5			2.14	19.3	80.7				-4.78	72.4	27.6				-1.90	.7	99.3				-8.86	508
510	2.17	-1.23			2.17	1.6	98.3				-3.80	34.0	66.0				-1.61		100.				-6.55	510
512	2.14	-.43			2.14	1.6	98.4				-3.84	35.7	64.3				-1.67		100.				-6.80	512
514	2.16	-1.23			2.16	5.9	94.1				-4.26	56.2	43.8				-1.77		100.				-7.50	514
516	2.19				2.19	100.					-5.50	100.					-1.98	100.					-10.47	516
518	2.17	-.93			2.18	6.7	93.3				-4.71	64.3	35.9				-1.89		100.				-8.73	518
520	2.14	-.43			2.14	2.5	97.5				-3.94	46.2	53.8				-1.63		100.				-6.80	520
522	2.11	-1.23			2.11	2.1	97.9				-4.38	46.2	53.8				-1.78		100.				-6.85	522
524	2.13	-1.23			2.13	4.1	95.9				-4.56	58.9	41.1				-1.92		100.				-7.79	524
526	2.14	-1.23			2.14	8.1	91.9				-4.49	61.9	38.1				-1.89		100.				-7.79	526
528	2.15	-.93			2.15	1.1	98.9				-4.08	35.6	64.4				-1.72		100.				-7.32	528
530	2.14	-1.53			2.14	34.8	65.2				-5.17	87.9	12.1				-2.02	.2	99.8				-9.34	530
532	2.15	-1.23			2.15	2.6	97.4				-4.24	45.6	54.4				-1.80		100.				-7.50	532
534	2.14	-1.23			2.14	2.9	97.1				-3.98	35.9	64.1				-1.61		100.				-6.55	534
536	2.14	-1.5			2.14	2.7	97.3				-4.24	45.8	54.2				-1.80		100.				-7.50	536
538	2.14	-1.23			2.14	2.5	97.5				-4.07	48.2	51.8				-1.76		100.				-6.85	538
540	2.15	-1.23			2.15	22.2	77.8				-4.95	77.5	22.5				-1.99	.3	99.7				-9.03	540

Table B-2. (Continued)

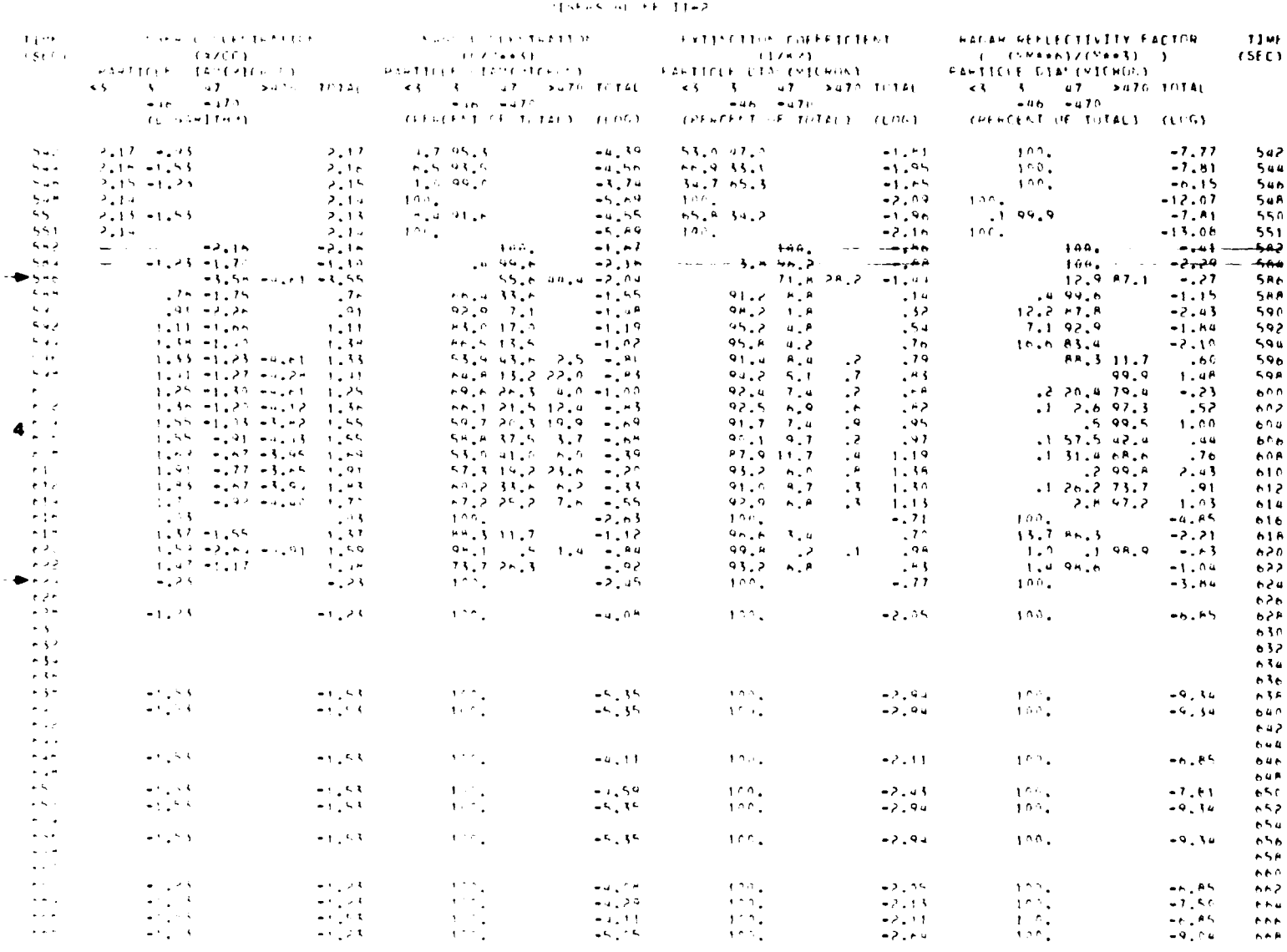

Table B-2. (Continued)

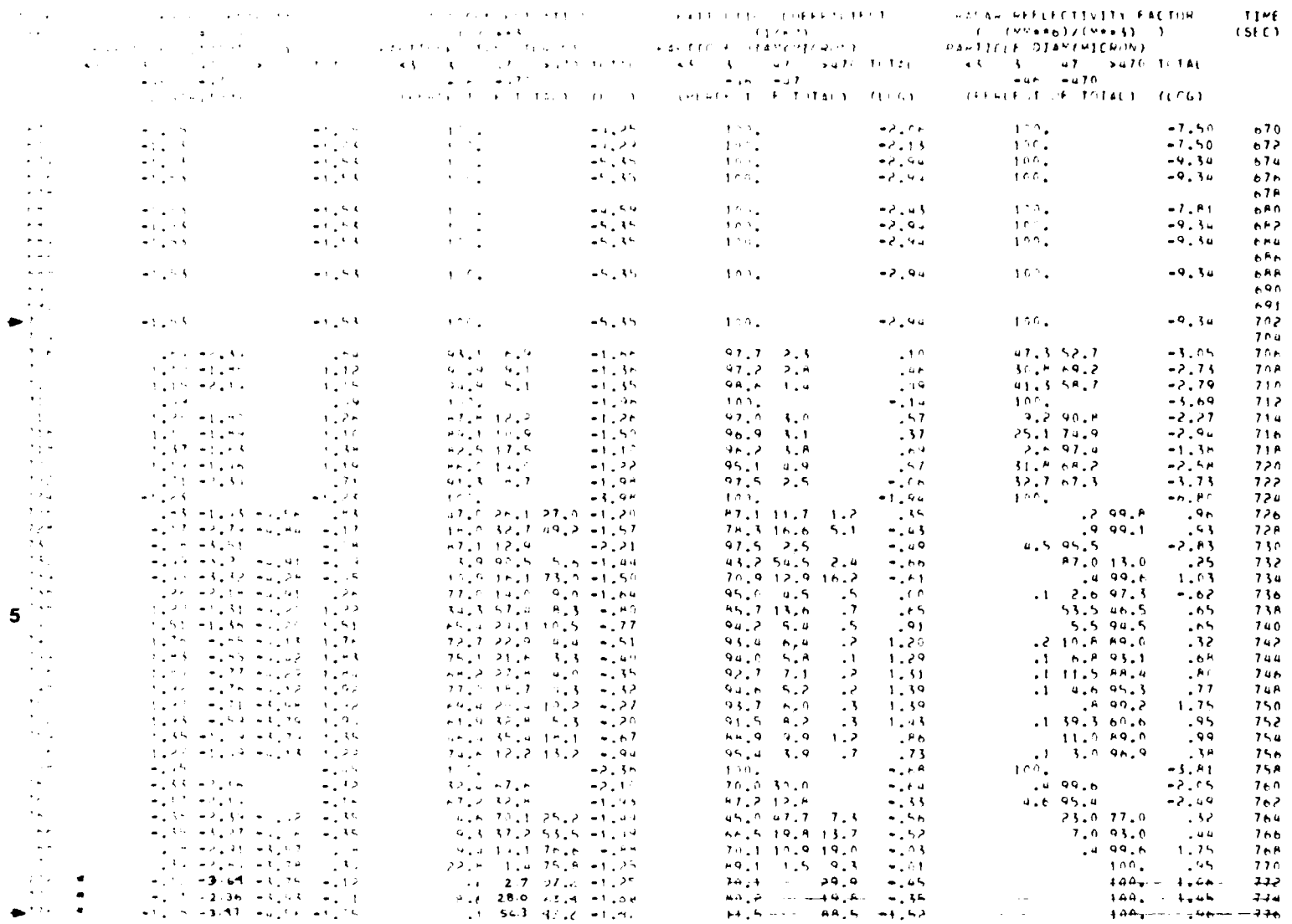

Table B-2. (Continued)

TIME (SEC)	MASS EXTINCTION COEFFICIENT (1/KM) (GM/M**3) PARTICLE DIAM(MICRON) <.6	.6 TO 3	3 TO 47	>47	TOTAL	MASS SCATTERING COEFFICIENT (1/KM) (GM/M**3) PARTICLE DIAM(MICRON) <.6	.6 TO 3	3 TO 47	>47	TOTAL (LOG)	PARTICLE EXTINCTION COEFFICIENT (1/KM) PARTICLE DIAM(MICRON) <.6	.6 TO 3	3 TO 47	>47	TOTAL (LOG)	RADAR REFLECTIVITY FACTOR Z (MM**6)/(M**3) PARTICLE DIAM(MICRON) <.6	.6 TO 3	3 TO 47	>47	TOTAL (LOG)	TIME (SEC)
778			-.93					100.			-3.38			100.			-1.38			100.		-5.13	778
780																							780
782																							782
784			-1.53					100.			-5.35			100.			-2.94			100.		-9.34	784
786																							786
788																							788
790			-1.53					100.			-4.59			100.			-2.43			100.		-7.81	790
792			-1.23					100.			-5.05			100.			-2.64			100.		-9.04	792
794			-.83					100.			-4.65			100.			-2.24			100.		-8.64	794
796																							796
798																							798
800																							800
802																							802
804																							804
806																							806
808			-1.53					100.			-5.35			100.			-2.94			100.		-9.34	808
810			-1.53					100.			-5.35			100.			-2.94			100.		-9.34	810
812																							812
814			-1.35					100.			-4.46			100.			-2.22			100.		-7.78	814
816			-1.23					100.			-4.52			100.			-2.31			100.		-7.79	816
818			-1.53					100.			-3.76			100.			-1.47			100.		-6.15	818
820			-1.53					100.			-5.35			100.			-2.94			100.		-9.34	820
822			-1.53					100.			-5.35			100.			-2.94			100.		-9.34	822
824			-1.53					100.			-5.35			100.			-2.94			100.		-9.34	824
826			-1.53					100.			-5.35			100.			-2.94			100.		-9.34	826
828			-.93					100.			-4.41			100.			-2.14			100.		-7.77	828
830			-1.23					100.			-3.75			100.			-1.44			100.		-6.15	830
832																							832
834																							834
836			-1.25					100.			-4.88			100.			-2.46			100.		-8.86	836
838			-1.53					100.			-5.35			100.			-2.94			100.		-9.34	838
840																							840
842																							842
844			-1.25					100.			-4.88			100.			-2.46			100.		-8.86	844
846																							846
848																							848
850			-1.23					100.			-4.29			100.			-2.13			100.		-7.50	850
852			-1.53					100.			-5.35			100.			-2.94			100.		-9.34	852
854																							854
856			-1.23					100.			-5.05			100.			-2.64			100.		-9.04	856
858																							858
860																							860
861			-1.23					100.			-4.29			100.			-2.13			100.		-7.50	861
864	[illegible]	[illegible]	1.94		17.4	82.6			-5.27		80.7	19.3			-2.22			100.			-9.34	864
866	[illegible]	[illegible]	2.22		17.7	82.3			-4.97		78.7	21.3			-1.96		.1	99.9			-9.04	866
868	[illegible]	[illegible]	[illegible]	[illegible]	[illegible]	[illegible]	[illegible]	[illegible]	[illegible]	[illegible]	[illegible]	[illegible]	[illegible]	[illegible]	[illegible]	[illegible]	[illegible]	[illegible]	[illegible]	[illegible]	[illegible]	[illegible]	868
870	[illegible]	[illegible]	[illegible]	[illegible]	[illegible]	[illegible]	[illegible]	[illegible]	[illegible]	[illegible]	[illegible]	[illegible]	[illegible]	[illegible]	[illegible]	[illegible]	[illegible]	[illegible]	[illegible]	[illegible]	[illegible]	[illegible]	870
872	[illegible]	[illegible]	[illegible]	[illegible]	[illegible]	[illegible]	[illegible]	[illegible]	[illegible]	[illegible]	[illegible]	[illegible]	[illegible]	[illegible]	[illegible]	[illegible]	[illegible]	[illegible]	[illegible]	[illegible]	[illegible]	[illegible]	872
874	[illegible]	[illegible]	2.26		19.2	80.8			-4.96		80.5	19.5			-1.95		.1	99.9			-9.04		874
876	[illegible]	[illegible]	2.37		1.2	98.8			-2.57		20.9	79.1			-.75			100.			-4.33		876

Table B-2. (Continued)

USERS MODEL II-2

TIME (SEC)	LIQUID WATER CONTENT (G/CC) PARTICLE DIAM(MICRON) <3	3 -46	47 -470	>470	TOTAL	MASS CONCENTRATION (G/M**3) PARTICLE DIAM(MICRON) <3	3 -46	47 -470	>470	TOTAL	(LOG)	EXTINCTION COEFFICIENT (1/KM) PARTICLE DIAM(MICRON) <3	3 -46	47 -470	>470	TOTAL	(LOG)	RADAR REFLECTIVITY FACTOR ((MM**6)/(M**3)) PARTICLE DIAM(MICRON) <3	3 -46	47 -470	>470	TOTAL	(LOG)	TIME (SEC)
	(PERCENTAGE)					(PERCENT OF TOTAL)						(PERCENT OF TOTAL)						(PERCENT OF TOTAL)						
878	2.34	-.49	-5.51		2.34	.6	81.3	18.1		-2.36		16.4	79.7	3.9		-.68		9.3	90.7		-2.80	878
880	2.53	-.12	-5.29		2.53	.3	3.3	96.4		-1.52		34.4	28.5	37.1		-.52			100.		-.02	880
882	2.99	.53	-2.64		2.99	1.1	38.5	60.5		-1.39		32.1	60.4	7.4		.17		.1	99.9		-.17	882
884	3.43	1.46	-1.17		3.44	.4	72.7	26.5		-.60		15.4	79.5	5.2		1.12		.6	99.4		-.17	884
886	3.51	1.66	-.93	-4.89	3.51	1.2	74.4	23.3	1.1	-.49		19.5	75.6	4.9		1.27		.3	52.0	47.7	.16	886
888	3.34	1.05	-1.43	-4.30	3.34	1.4	69.8	19.8	9.0	-.82		25.9	69.8	4.0	.4	.91		.1	5.8	94.1	.49	888
890	3.22	.73	-1.58	-4.88	3.22	.4	50.6	40.6	8.0	-1.14		21.6	68.1	10.0	.3	.48			8.0	91.9	.28	890
892	3.50	1.75	-1.12	-4.43	3.50	1.1	74.5	22.3	2.1	-.53		18.2	78.0	3.7	.1	1.25		.3	56.9	42.9	.21	892
894	3.48	1.78	-.49	-5.82	3.49	1.0	69.4	19.9	9.7	-.82		16.7	78.4	4.5	.4	1.33		.1	5.7	94.2	.88	894
896	3.48	1.64	-.93	-4.19	3.49	1.1	69.5	23.7	5.6	-.43		19.2	75.5	5.1	.2	1.30		.1	7.2	92.7	.84	896
898	3.46	1.56	-1.07	-3.91	3.47	1.0	56.6	34.9	7.6	-.51		21.0	72.7	6.0	.4	1.16			53.6	46.4	.85	898
900	3.43	1.50	-1.31	-4.61	3.44	1.4	79.6	16.2	2.8	-.77		27.7	68.9	3.2	.1	1.03		.5	21.6	78.0	-.22	900
902	3.24	.44	-2.21	-4.89	3.24	1.4	82.2	4.1	12.0	-1.52		26.7	71.7	1.2	.3	.38				99.9	-.16	902
904	3.36	1.07	-1.14	-4.91	3.36	1.1	56.2	40.9	1.9	-.96		23.0	67.2	9.7	.1	.74		.2	55.1	44.6	-.28	904
906	3.45	1.42	-1.17	-4.00	3.46	1.0	51.2	39.0	8.8	-.66		22.7	69.8	7.1	.5	1.01			42.1	57.9	.68	906
908	3.51	1.74	-.62	-3.54	3.51	.9	57.9	30.1	11.1	-.17		17.6	74.5	7.4	.5	1.47			6.5	93.5	1.43	908
910	3.47	1.60	-.76	-3.76	3.48	1.2	64.2	24.6	10.0	-.35		19.7	74.2	5.7	.4	1.38			4.3	95.6	1.13	910
912	3.48	1.94	-.83	-3.90	3.49	.9	67.7	26.1	5.3	-.20		15.2	78.8	5.8	.2	1.52		.1	8.4	91.5	1.08	912
914	3.45	1.98	-.65	-3.99	3.47	1.2	74.2	19.5	5.1	-.23		16.5	78.6	4.8	.2	1.50		.1	3.4	96.5	.92	914
916	3.45	2.01	-.62	-4.11	3.46	1.0	70.4	25.1	3.6	-.13		14.8	79.8	5.3	.1	1.59		.1	10.6	89.3	1.07	916
918	3.43	1.98	-.49	-3.50	3.45	.8	52.1	20.7	26.4	-.02		15.3	77.3	6.7	.8	1.59			.1	99.9	2.78	918
920	3.43	1.95	-.54	-4.06	3.44	1.0	67.5	28.9	2.6	-.14		16.3	77.1	6.5	.1	1.56		.2	39.1	60.6	.70	920
922	3.44	1.91	-.67	-3.99	3.45	1.4	70.5	22.1	6.1	-.29		19.1	75.3	5.4	.2	1.48		.1	4.2	95.7	.92	922
924	3.41	1.58	-1.24	-4.21	3.42	1.8	61.7	31.4	5.1	-.64		27.1	68.1	4.6	.2	1.15		.1	31.9	68.0	.38	924
926 *	3.25	-.35	-1.44		3.26	1.9	9.3	88.8		-1.98		80.3	19.7			-.01			100.		-4.50	926
928 *	3.06	-1.05	-3.45		3.06	.8	8.1	91.1		-2.14		80.1	19.9			-.77			100.		-5.14	928
930	2.77				2.77	100.				-4.62		100.				-1.25		100.			-10.37	930
932	2.51				2.51	100.				-4.88		100.				-1.55		100.			-10.27	932
934	2.35	-1.15			2.35	22.3	77.7			-4.35		76.2	23.8			-1.59		.2	99.8		-7.78	934
936	2.30	-1.53			2.30	21.9	78.1			-4.48		80.7	19.3			-1.71		.1	99.9		-7.81	936
938	2.28				2.28	100.				-5.30		100.				-1.88		100.			-11.14	938
940	2.26	-1.53			2.26	13.9	86.1			-4.52		76.0	24.0			-1.81			100.		-7.81	940
942	2.23	-1.53			2.23	49.2	50.8			-5.06		90.8	9.2			-1.90		2.3	97.7		-9.35	942
944	2.23	-.95			2.23	23.2	76.8			-4.64		71.5	28.5			-1.79		.9	99.1		-8.73	944
946	2.24	-1.53			2.24	3.7	96.3			-4.09		58.2	41.8			-1.73			100.		-6.85	946
948	2.24	-1.55			2.24	6.4	93.6			-4.22		54.5	45.5			-1.72			100.		-7.50	948
950	2.22	-1.55			2.22	12.5	87.5			-4.82		71.9	28.1			-1.91			100.		-8.86	950
952	2.21	-1.23			2.20	25.7	74.3			-4.92		81.1	18.9			-1.91		.3	99.7		-9.03	952
954	2.22	-1.53			2.22	36.0	64.0			-5.16		89.3	10.7			-1.97		.2	99.8		-9.34	954
956	2.20				2.20	100.				-5.56		100.				-2.02		100.			-11.70	956
958	2.22	-1.23			2.22	33.4	66.2			-4.87		82.7	17.3			-1.87		1.3	98.7		-9.03	958
960	2.21	-1.23			2.21	33.4	66.6			-4.88		82.4	17.6			-1.88		1.2	98.8		-9.03	960
962	2.14	-1.53			2.14	2.7	97.3			-4.10		51.9	48.1			-1.79			100.		-6.85	962
964	2.18	-1.23			2.18	23.5	76.5			-4.94		79.1	20.9			-1.96		1.0	99.0		-9.03	964
966	2.21	-1.53			2.21	57.0	43.0			-4.99		91.1	8.9			-1.89		6.9	93.1		-9.31	966
968	2.14	-1.55			2.14	21.6	78.4			-4.77		73.6	26.4			-1.88		.5	99.5		-8.86	968
970	2.17	-1.23			2.17	2.0	98.0			-3.74		39.5	60.5			-1.62			100.		-6.15	970
972	2.14	-1.23			2.14	29.1	70.9			-4.90		80.8	19.2			-1.92		1.2	98.8		-9.03	972
974	2.14	-1.53			2.14	1.6	98.4			-3.75		36.7	63.3			-1.68			100.		-6.15	974
976	2.15	-1.23			2.15	6.8	93.2			-4.26		52.9	47.1			-1.80		.1	99.9		-7.50	976

Table B-2. (Continued)

MISERS BLUFF II-2

TIME (SEC)	LIQUID WATER CONTENT (G/CC) PARTICLE DIAM(MICRONS) <3	3 -46	47 -470	>470	TOTAL	MASS CONCENTRATION (G/M**3) PARTICLE DIAM(MICRONS) <3	3 -46	47 -470	>470	TOTAL (LOG) (PERCENT OF TOTAL)	EXTINCTION COEFFICIENT (1/KM) PARTICLE DIAM(MICRON) <3	3 -46	47 -470	>470	TOTAL (LOG) (PERCENT OF TOTAL)	RADAR REFLECTIVITY FACTOR ((MM**6)/(M**3)) PARTICLE DIAM(MICRON) <3	3 -46	47 -470	>470	TOTAL (LOG) (PERCENT OF TOTAL)	TIME (SEC)
970	2.17	-1.23			2.17	22.3	77.7			-4.94	78.2	21.8			-1.97	.4	99.6			-9.03	970
972	2.11	-1.53			2.11	30.3	69.7			-5.20	86.3	13.7			-2.07	.3	99.7			-9.34	972
974	2.13				2.13	100.				-5.85	100.				-2.15	100.				-12.72	974
976	2.13				2.13	100.				-5.44	100.				-2.04	100.				-11.19	976
978	2.14				2.14	100.				-5.36	100.				-2.02	100.				-10.87	978
980	2.11	-1.05			2.11	6.9	93.1			-4.43	57.2	42.8			-1.85		100.			-7.78	980
982	2.13				2.13	100.				-5.34	100.				-2.05	100.				-10.47	982
984	2.10	-1.53			2.10	7.5	92.5			-4.55	65.8	34.2			-1.96		100.			-7.81	984
986	2.13				2.13	100.				-5.81	100.				-2.16	100.				-12.51	986
988	2.15	-1.53			2.15	44.8	55.2			-5.10	88.9	11.1			-1.98	2.3	97.7			-9.33	988
990	2.13	-1.05			2.13	1.5	98.5			-3.79	32.1	67.9			-1.61		100.			-6.55	990
992	2.11	-1.53			2.11	28.9	71.1			-5.21	85.9	14.1			-2.09	.2	99.8			-9.34	992
994	2.14				2.14	100.				-5.75	100.				-2.12	100.				-12.13	994
996	2.17				2.17	100.				-5.07	100.				-1.81	100.				-10.62	996
998	2.18	-1.23			2.18	11.5	88.5			-4.47	67.4	32.6			-1.82	.1	99.9			-7.79	998
1000	2.17				2.17	100.				-5.46	100.				-2.01	100.				-11.33	1000
1002	2.16	-1.23			2.16	11.4	88.6			-4.47	64.6	35.4			-1.86	.2	99.8			-7.79	1002
1004	2.15	-1.53			2.15	43.2	56.8			-5.11	89.0	11.0			-1.98	1.0	99.0			-9.33	1004
1006	2.17	-1.53			2.17	17.1	82.9			-4.51	73.8	26.2			-1.84	.2	99.8			-7.80	1006
1008	2.18	-1.05			2.18	9.7	90.3			-4.21	56.1	43.9			-1.71	.1	99.9			-7.50	1008
1010	2.17	-1.53			2.17	44.5	55.5			-5.10	89.0	11.0			-1.98	2.5	97.5			-9.33	1010
1012	2.16	-1.53			2.16	9.2	90.8			-4.55	70.9	29.1			-1.89		100.			-7.81	1012
1014	2.13	-.75			2.13	6.3	93.7			-4.55	51.9	48.1			-1.84		100.			-8.56	1014
1016	2.15				2.15	100.				-5.71	100.				-2.11	100.				-11.93	1016
1018	2.10	-1.23			2.10	14.1	85.9			-4.45	66.3	33.7			-1.84	.1	99.9			-7.79	1018
1020	2.12				2.12	100.				-5.85	100.				-2.16	100.				-12.61	1020
1022	2.14	-.93			2.14	3.1	96.9			-4.20	43.9	56.1			-1.76		100.			-7.49	1022
1024	2.10	-1.53			2.10	21.9	78.1			-5.25	85.1	14.9			-2.11		100.			-9.34	1024
1026	2.13	-1.53			2.13	28.8	71.2			-5.21	86.2	13.8			-2.08	.5	99.5			-9.33	1026
1028	2.13	-1.05	-1.44		2.13	1.5	98.5			-3.79	2.1	4.3	93.5		-.45			100.		-.75	1028
1030	2.66	.72	-2.45		2.66	.9	99.1			-2.00	10.2	84.7	5.1		-.01			.1	99.9	-1.28	1030
1032	2.75	.84			2.76	1.4	98.6			-2.19	18.2	81.8			-.21		100.			-4.14	1032
1034	2.32				2.32	100.				-5.12	100.				-1.77	100.				-10.80	1034
1036	3.28	1.27	-1.60		3.28	1.5	83.8	14.7		-1.32	20.1	76.5	3.4		.61		15.2	84.8		-2.27	1036
1038	3.49	1.57	-1.20		3.49	1.6	83.8	14.7		-.91	20.4	75.9	3.7		.98		18.1	81.9		-2.04	1038
1040	3.47	1.53	-1.41		3.47	2.0	86.2	11.8		-1.00	22.8	74.6	2.6		.93		10.5	89.5		-1.91	1040
1042	3.44	1.51	-1.33		3.45	2.0	85.1	12.9		-.98	23.7	73.2	3.1		.94		22.0	78.0		-2.18	1042
1044	3.42	1.44	-1.15		3.42	1.3	67.8	31.0		-.94	19.7	73.6	6.7		.88		1.0	99.0		-.94	1044
1046	3.52	1.48	-.91	-4.91	3.53	1.6	80.9	16.7	.8	-.61	19.2	76.9	3.9		1.29		.9	11.3	87.8	-.58	1046
1048	3.48	1.71	-1.41		3.49	2.2	86.0	11.8		-.86	23.1	74.8	2.1		1.10		5.5	94.5		-1.64	1048
1050	3.50	1.43	-1.05	-4.89	3.51	1.3	86.0	11.4	1.3	-.56	17.3	79.9	2.8		1.30		.6	4.2	95.2	-.14	1050
1052	3.52	1.92	-.75	-4.91	3.54	1.2	77.1	21.3	.5	-.37	16.9	78.4	4.7		1.44		1.2	49.3	49.5	-.33	1052
1054	3.51	1.83	-.77	-4.11	3.52	1.2	71.3	19.2	8.3	-.38	18.8	76.0	4.9	.2	1.39			.8	99.2	1.30	1054
1056	3.49	1.78	-.82	-4.39	3.50	1.2	71.1	20.5	7.2	-.38	19.2	75.6	5.0	.2	1.37			1.1	98.9	1.48	1056
1058	3.42	1.64	-1.12		3.43	1.0	79.4	19.6		-.67	15.8	80.2	4.1		1.15		1.7	98.3		-.76	1058
1060	3.45	1.66	-1.18		3.46	1.5	78.3	20.3		-.70	20.6	75.6	3.7		1.14		.8	99.2		-.41	1060
1062	3.48	1.68	-1.03		3.48	1.3	76.8	21.9		-.65	19.6	75.7	4.7		1.18		2.3	97.7		-.85	1062
1064	3.47	1.55	-1.28	-4.84	3.47	1.8	74.9	14.4	8.9	-.82	25.5	71.0	3.3	.2	1.03			.3	99.7	.93	1064
1066	3.46	1.45	-1.29		3.46	1.6	84.8	13.6		-.96	21.9	74.7	3.4		.92		15.1	84.9		-1.91	1066
1068	3.42	1.17	-1.94		3.43	2.1	92.0	5.9		-1.36	25.8	72.7	1.4		.61		52.9	47.1		-2.99	1068

Table B-2. (Continued)

CASES CODE 11=2

TIME (SEC)	NUMBER CONCENTRATION (#/CC) PARTICLE DIAM(MICRON) <3	3 -46	46 -470	>470	TOTAL (LOG)	MASS CONCENTRATION (G/M**3) PARTICLE DIAM(MICRON) <3	3 -46	46 -470	>470	TOTAL (LOG)	PARTITION COEFFICIENT (1/KM) PARTICLE DIAM(MICRON) <3	3 -46	46 -470	>470	TOTAL (LOG)	RADAR REFLECTIVITY FACTOR ((MM**6)/(M**3)) PARTICLE DIAM(MICRON) <3	3 -46	46 -470	>470	TOTAL (LOG)	TIME (SEC)
1084	3.55	1.32	-1.93		3.33	1.7	80.9	17.4	-1.44	25.2	71.4	3.4	.47		10.8	89.2	-2.26	1084
1086	3.24	1.10	-2.03		3.28	1.6	90.2	8.1	-1.55	20.3	77.8	1.9	.42		48.9	51.1	-3.06	1086
7 1088	3.46	1.31	-1.83		3.47	1.6	89.9	9.6	-1.01	23.0	75.4	1.7	.85		4.7	95.3	-1.38	1088
1090	3.32	.94			3.32	1.7	98.3		-1.36	24.5	75.5		.52		100.		-2.90	1090
1092	3.21	.88			3.21	1.6	98.4		-1.55	21.9	78.1		.39		100.		-3.44	1092
1094	3.15	.90			3.15	1.7	98.3		-1.60	25.7	74.3		.26		100.		-3.28	1094
→1096	2.65	-1.53			2.65	48.1	51.9		-4.30	92.2	7.8		-1.32	.7	99.3		-7.80	1096
1098	2.58				2.58	100.			-4.95	100.			-1.67	100.			-10.48	1098
1100	2.24	-1.53			2.24	35.9	64.1		-4.39	84.2	15.8		-1.65	.5	99.5		-7.80	1100
1102	2.21	-1.23			2.21	12.2	87.8		-3.93	62.8	37.2		-1.51		100.		-6.80	1102
1104	2.14				2.14	100.			-5.47	100.			-2.01	100.			-11.61	1104
1106	2.20	-1.23			2.20	16.4	83.6		-4.44	70.6	29.4		-1.78	.2	99.8		-7.79	1106
1108	2.18	-1.53			2.18	66.8	33.2		-4.87	91.7	8.3		-1.86	14.1	85.9		-9.27	1108
1110	2.16	-1.53			2.14	49.0	51.0		-5.06	89.6	10.4		-1.95	2.8	97.2		-9.32	1110
1112	2.15				2.15	100.			-5.76	100.			-2.12	100.			-12.15	1112
1114	2.17				2.17	100.			-5.04	100.			-1.91	100.			-10.02	1114
1116	2.19				2.19	100.			-5.52	100.			-2.01	100.			-11.72	1116
1118	2.16	-1.23			2.16	.5	99.5		-3.18	18.9	81.1		-1.30		100.		-5.30	1118
1120	2.22	-1.53			2.22	40.3	59.7		-4.36	86.1	13.9		-1.57	.6	99.4		-7.80	1120
1122	2.19	-1.53			2.19	11.3	88.7		-4.54	72.6	27.4		-1.86		100.		-7.81	1122
1124	2.17	-1.53			2.17	63.2	36.8		-4.92	92.2	7.8		-1.83	4.6	95.4		-9.32	1124
1126	2.13	-1.53			2.13	45.0	55.0		-5.09	88.6	11.4		-1.99	2.3	97.7		-9.33	1126
1128	2.09	-1.23			2.10	.8	99.2		-3.39	24.3	75.7		-1.43		100.		-5.57	1128
1130	2.11				2.10	100.			-5.33	100.			-2.02	100.			-10.85	1130
1132	2.08	-1.23			2.08	8.4	91.6		-4.25	56.4	43.6		-1.76		100.		-7.50	1132
1134	2.07	-1.23			2.07	24.1	75.9		-4.93	76.6	23.4		-2.00	.6	99.4		-9.03	1134
1136	2.05	-1.23			2.05	2.5	97.5		-3.80	34.1	65.9		-1.63		100.		-6.55	1136
1138	2.10	-1.53			2.10	59.4	40.6		-4.96	90.4	9.6		-1.92	5.3	94.7		-9.31	1138
1140	2.09	-1.23			2.09	33.9	66.1		-4.87	80.1	19.9		-1.93	1.8	98.2		-9.03	1140
1142	2.09	-1.53			2.09	42.2	57.8		-5.12	88.0	12.0		-2.01	.9	99.1		-9.33	1142
1144	2.10	-.93			2.10	17.4	82.6		-4.67	65.2	34.8		-1.88	.6	99.4		-8.73	1144
1146	2.06	-1.53			2.06	10.2	89.8		-4.54	67.3	32.7		-1.94		100.		-7.81	1146
1148	2.09	-1.23			2.09	5.7	94.3		-4.49	58.9	41.1		-1.92		100.		-7.79	1148
1150	2.09	-1.53			2.09	.6	99.4		-3.48	26.5	73.5		-1.56		100.		-5.60	1150
1152	2.09	-1.53			2.09	38.4	61.6		-5.14	87.4	12.6		-2.04	.8	99.2		-9.33	1152
1154	2.09	-1.53			2.09	33.7	66.3		-5.17	87.0	13.0		-2.05	.3	99.7		-9.34	1154
1156	2.07	-1.23			2.07	19.7	80.3		-4.42	68.9	31.1		-1.80	.3	99.7		-7.79	1156
1158	2.12	-1.53			2.12	40.8	59.2		-5.13	88.4	11.6		-2.00	.8	99.2		-9.33	1158
1160	2.14	-1.53			2.14	9.0	91.0		-4.55	67.7	32.3		-1.94		100.		-7.81	1160
1162	2.10	-1.53			2.10	4.8	95.2		-4.09	52.8	47.2		-1.78		100.		-6.85	1162
1164	2.11	-1.53			2.11	47.8	52.2		-5.07	89.5	10.5		-1.96	.9	99.1		-9.33	1164
1166	2.10				2.10	100.			-5.56	100.			-2.08	100.			-11.46	1166
1168	2.08				2.08	100.			-5.33	100.			-2.03	100.			-10.84	1168
1170	2.08	-.75			2.08	.9	99.1		-3.25	16.9	83.1		-1.26		100.		-5.67	1170
1171	2.09				2.09	100.			-5.21	100.			-1.97	100.			-10.65	1171
~~1184~~	~~2.08~~	~~-.93~~			~~2.08~~	~~2.6~~	~~97.4~~		~~-3.97~~	~~35.5~~	~~64.5~~		~~-1.63~~		~~100.~~		~~-7.20~~	~~1182~~
~~1184~~	~~2.07~~				~~2.07~~	~~100.~~			~~-5.35~~	~~100.~~			~~-2.04~~	~~100.~~			~~-10.87~~	~~1184~~
~~1186~~	~~2.12~~	~~-1.23~~	~~-1.53~~		~~2.12~~		~~.4~~	~~99.6~~	~~-2.69~~	~~4.4~~	~~2.7~~	~~92.7~~	~~-.74~~			~~100.~~	~~-2.70~~	~~1186~~
~~1188~~	~~2.14~~		~~-1.83~~		~~2.16~~	~~.1~~		~~99.9~~	~~-2.39~~	~~8.1~~		~~91.9~~	~~-1.02~~			~~100.~~	~~-3.02~~	~~1188~~
~~1190~~	~~2.08~~		~~-1.91~~		~~2.08~~	~~.1~~		~~99.9~~	~~-2.52~~	~~10.1~~		~~89.9~~	~~-1.14~~			~~100.~~	~~-3.17~~	~~1190~~

Table B-2. (Continued)

MISMS RUDE 11-2

TIME (SEC)	NUMBER CONCENTRATION (#/CC) PARTICLE DIAM(MICRON) <3	3 -46	47 -470	>470	TOTAL (LOGARITHM)	MASS CONCENTRATION (G/M**3) PARTICLE DIAM(MICRON) <3	3 -46	47 -470	>470	TOTAL (LOG) (PERCENT OF TOTAL)	EXTINCTION COEFFICIENT (1/KM) PARTICLE DIAM(MICRON) <3	3 -46	47 -470	>470	TOTAL (LOG) (PERCENT OF TOTAL)	RADAR REFLECTIVITY FACTOR ((MM**6)/(M**3)) PARTICLE DIAM(MICRON) <3	3 -46	47 -470	>470	TOTAL (LOG) (PERCENT OF TOTAL)	TIME (SEC)
1182		-.93			-.93		100.			-3.99		100.			-1.82		100.			-7.20	1182
1184	2.07		-5.54		2.07	.7		99.3		-3.20	54.2		45.8		-1.77			100.		-3.23	1184
1186	2.12	-1.23	-1.59		2.12		.3	99.7		-1.93	3.7	2.2	94.0		-.66			100.		-2.09	1186
1188	2.10		-1.78		2.10			100.		-2.20	6.7		93.3		-.94			100.		-2.05	1188
1190	2.09		-1.86		2.09			100.		-2.11	6.3		93.7		-.93			100.		-1.84	1190
1192	3.31	1.43	-1.31		3.31	1.1	77.2	21.7		-.87	16.8	79.1	4.1		.95		.9	99.1		-.78	1192
1194	3.42	1.42	-1.27		3.43	1.6	82.1	16.4		-.91	21.5	74.6	3.9		.96		10.5	89.5		-1.78	1194
1196	3.37	1.01	-1.25		3.38	1.5	61.9	36.6		-.91	27.7	64.7	7.6		.83		.6	99.4		-.56	1196
1198	3.21	.41	-1.62	-4.91	3.21	1.8	33.1	59.9	5.2	-1.41	40.7	45.6	13.4	.3	.29			23.4	76.6	-.52	1198
1200	3.19	.66	-1.54	-4.91	3.19	.8	37.5	59.6	2.1	-1.02	24.9	62.1	12.8	.2	.52		.1	75.6	24.3	-.02	1200
1202	3.24	.77	-1.42	-4.40	3.24	1.0	45.4	38.3	15.4	-.91	26.6	62.4	10.3	.7	.67			2.1	97.9	.98	1202
1204	3.41	1.49	-.82	-4.60	3.41	1.0	65.4	31.3	2.4	-.63	16.8	74.6	8.4	.1	1.11		.2	13.6	86.2	.03	1204
1206	3.53	1.75	-.74	-4.30	3.53	1.1	71.2	25.3	2.4	-.33	17.8	76.7	5.4	.1	1.41		.2	35.7	64.1	.46	1206
1208	3.51	1.64	-.89	-3.77	3.51	.9	58.6	22.4	18.0	-.32	19.8	74.0	5.6	.6	1.32			.6	99.4	1.99	1208
1210	3.51	1.74	-.71	-4.06	3.52	1.1	70.1	25.3	3.5	-.26	18.0	76.1	5.8	.2	1.46		.2	17.8	82.0	.64	1210
1212	3.50	1.69	-.78	-4.61	3.51	1.4	67.7	29.9	1.0	-.40	21.7	72.1	6.2		1.35		.4	63.1	36.5	.11	1212
1214	3.46	1.66	-1.17		3.47	1.8	82.7	15.4		-.73	22.9	73.6	3.5		1.15		7.3	92.7		-1.47	1214
1216	3.42	1.54	-1.71		3.42	2.4	88.7	8.9		-1.04	25.3	73.2	1.4		.94		4.0	96.0		-1.69	1216
1218	3.39	1.45	-1.41	-4.91	3.39	1.0	82.1	15.1	1.8	-.93	16.5	81.1	2.4	.1	.89		.6	23.8	75.7	-.51	1218
1220	3.52	1.79	-.74		3.53	1.1	76.0	22.9		-.37	17.2	77.6	5.2		1.40		1.8	98.2		-.40	1220
8 1222	3.51	1.79	-.83	-4.91	3.52	1.7	78.6	19.0	.7	-.53	21.9	73.5	4.6		1.32		1.4	19.5	79.1	-.53	1222
1224	3.48	1.74	-1.00		3.48	1.4	85.9	12.6		-.57	19.5	77.2	3.2		1.27		10.2	89.8		-1.29	1224
1226	3.47	1.73	-1.06		3.48	1.5	86.5	12.1		-.63	19.1	77.8	3.1		1.23		18.8	81.2		-1.68	1226
1228	3.52	1.77	-.78	-4.91	3.53	1.8	81.2	16.2	.7	-.56	23.0	73.4	3.6		1.30		1.0	39.1	59.8	-.41	1228
1230	3.49	1.71	-1.16	-4.61	3.49	1.7	81.5	15.2	1.7	-.62	21.9	75.3	2.8	.1	1.24		.5	29.9	69.6	-.17	1230
1232	3.51	1.76	-1.06		3.51	1.7	85.6	12.7		-.58	21.4	75.7	2.9		1.29		9.1	90.9		-1.39	1232
1234	3.45	1.58	-1.40	-4.89	3.45	2.0	86.2	9.5	2.3	-.81	23.7	74.1	2.1	.1	1.09		.3	1.6	98.1	-.15	1234
1236	3.40	1.25	-1.91		3.40	2.2	83.2	14.5		-1.21	28.1	69.9	2.0		.71		2.2	97.8		-1.37	1236
1238	3.40	1.14	-1.69		3.40	1.8	85.1	13.1		-1.19	25.4	71.9	2.7		.70		6.8	93.2		-1.90	1238
1240	3.47	1.36	-1.42	-4.89	3.47	1.9	78.7	15.7	3.8	-1.02	25.4	71.1	3.4	.1	.86		.2	2.6	97.2	-.15	1240
1242	3.51	1.53	-1.21	-4.86	3.51	1.6	83.2	10.4	4.7	-.72	21.6	75.6	2.7	.1	1.14		.1	.5	99.5	.60	1242
1244	3.50	1.65	-1.28		3.51	1.8	83.4	14.7		-.71	23.6	73.7	2.7		1.16		3.9	96.1		-1.09	1244
1246	3.48	1.62	-1.09	-4.28	3.50	1.5	72.2	17.9	8.4	-.61	22.2	73.4	4.1	.2	1.18			1.3	98.7	.83	1246
1248	3.48	1.51	-1.12	-4.59	3.48	1.5	58.8	36.2	3.6	-.66	25.6	68.3	6.0	.1	1.09		.1	40.4	59.5	.52	1248
1250	3.39	1.16	-1.92	-4.91	3.40	2.2	84.5	9.8	3.5	-1.23	27.9	70.1	1.9	.1	.68		.3	2.6	97.1	-.62	1250
1252	3.50	.84	-2.12	-4.91	3.50	3.1	75.8	10.8	10.3	-1.70	35.6	61.9	2.2	.3	.29		.1	.2	99.7	-.63	1252
1254	3.51	1.55	-1.42		3.51	1.6	87.8	10.4		-.74	22.0	76.0	2.0		1.15		5.5	94.5		-1.33	1254
1256 *	3.22		-1.18	-4.91	3.22	1.3		94.2	4.5	-1.39	~~100.~~				~~-.20~~			~~47.9~~	~~52.1~~	~~-.35~~	1256
1258	2.97	-.93			2.87	46.2	53.8			-3.95	90.0	10.0			-1.01		.8	99.2		-7.49	1258
1260	2.57	-1.75			2.57	3.5	96.5			-3.20	50.6	49.4			-1.13			100.		-5.14	1260
1262	2.36				2.36	100.				-4.87	100.				-1.61		100.			-10.55	1262
1264	2.27	-.93			2.27	18.3	81.7			-4.10	65.4	34.6			-1.50		.3	99.7		-7.48	1264
1266	2.20	-1.25			2.20	58.1	41.9			-4.67	88.0	12.0			-1.71		9.9	90.1		-8.99	1266
1268	2.19	-1.53			2.19	81.2	18.8			-4.63	94.7	5.3			-1.66		23.2	76.8		-9.22	1268
1270	2.22				2.22	100.				-4.75	100.				-1.65		100.			-9.99	1270
1272	2.14	-1.75			2.19	4.1	95.9			-3.67	46.3	53.7			-1.47			100.		-6.14	1272
1274	2.14				2.19	100.				-4.83	100.				-1.74		100.			-9.94	1274
1276	2.14	-1.53			2.18	11.6	88.4			-4.05	66.3	33.7			-1.65			100.		-6.85	1276
1278	2.14	-.75			2.14	2.8	97.2			-3.72	30.8	69.2			-1.46			100.		-6.69	1278
1280	2.17	-1.35			2.17	10.0	90.0			-4.02	57.3	42.7			-1.63			100.		-6.84	1280

Table B-2. (Continued)

SISERS RUDER 11-2

TIME (SEC)	NUMBER CONCENTRATION (#/CC) PARTICLE DIAM(MICRON) <3	3 -46	47 -470	>470	TOTAL (LOGSWITM)	MASS CONCENTRATION (G/M**3) PARTICLE DIAM(MICRON) <3	3 -46	47 -470	>470	TOTAL (LOG) (PERCENT OF TOTAL)	EXTINCTION COEFFICIENT (1/KM) PARTICLE DIAM(MICRON) <3	3 -46	47 -470	>470	TOTAL (LOG) (PERCENT OF TOTAL)	RADAR REFLECTIVITY FACTOR ((MM**6)/(M**3)) PARTICLE DIAM(MICRON) <3	3 -46	47 -470	>470	TOTAL (LOG) (PERCENT OF TOTAL)	TIME (SEC)
1282	2.17	-1.23			2.17	11.4	88.6			-4.23	63.5	36.5			-1.69			100.		-7.50	1282
1284	2.17	-1.53			2.17	46.6	53.4			-5.08	89.6	10.4			-1.95	1.3		98.7		-9.33	1284
1286	2.15	-1.05			2.15	29.6	70.4			-4.72	74.2	25.8			-1.87	2.9		97.1		-8.85	1286
1288	2.14	-1.23			2.14	5.8	94.2			-4.06	55.9	44.1			-1.69			100.		-6.85	1288
1290	2.11	-1.23			2.11	1.4	98.6			-3.98	37.6	62.4			-1.73			100.		-6.80	1290
1292	2.12				2.12	100.				-5.59	100.				-2.10	100.				-11.30	1292
1294	2.14	-1.05			2.14	6.0	94.0			-4.43	57.6	42.4			-1.84			100.		-7.78	1294
1296	2.12	-1.05			2.12	2.3	97.7			-4.05	43.1	56.9			-1.75			100.		-6.84	1296
1298	2.15	-.75			2.15	10.8	89.2			-4.27	55.3	44.7			-1.67	.1		99.9		-7.75	1298
1300	2.15	-.93			2.15	2.7	97.3			-3.94	40.2	59.8			-1.63			100.		-6.80	1300
1302	2.14	-1.53			2.14	52.7	47.3			-5.03	90.3	9.7			-1.92	2.7		97.3		-9.33	1302
1304	2.11	-.93			2.11	11.7	88.3			-4.35	57.5	42.5			-1.77	.2		99.8		-7.77	1304
1306	2.12	-1.23			2.12	2.9	97.1			-3.44	36.7	63.3			-1.42			100.		-5.59	1306
1308	2.10	-1.05			2.10	21.2	78.8			-4.48	75.0	25.0			-1.82	.3		99.7		-7.80	1308
1310	2.11	-.83			2.11	3.6	96.4			-3.84	37.4	62.6			-1.55			100.		-6.76	1310
1312	2.08	-1.23			2.08	2.3	97.7			-4.07	43.7	56.3			-1.80			100.		-6.85	1312
1314	2.08	-1.53			2.08	8.1	91.9			-4.07	56.0	44.0			-1.75			100.		-6.85	1314
1316	2.09	-1.53			2.09	31.8	68.2			-5.19	86.4	13.6			-2.07	.6		99.4		-9.33	1316
1318	2.10	-1.05			2.10	14.3	85.7			-4.39	64.5	35.5			-1.77	.1		99.9		-7.78	1318
1320	2.11	-1.23			2.11	3.6	96.4			-4.07	49.3	50.7			-1.75			100.		-6.85	1320
1322	2.09	-1.05			2.09	8.3	91.7			-4.42	58.0	42.0			-1.84			100.		-7.78	1322
1324	2.11	-1.05			2.11	5.8	94.2			-4.43	56.6	43.4			-1.85			100.		-7.78	1324
1326	2.07	-.93			2.07	3.3	96.7			-4.20	42.8	57.2			-1.77			100.		-7.49	1326
1328	2.10				2.10	100.				-5.58	100.				-2.11	100.				-11.03	1328
1330	2.07	-1.05			2.07	8.9	91.1			-4.84	64.2	35.8			-2.01			100.		-8.86	1330
1332	2.11	-1.53			2.11	5.3	94.7			-4.08	54.8	45.2			-1.76			100.		-6.85	1332
1334	2.12	-1.53			2.12	53.6	46.4			-5.02	89.7	10.3			-1.95	4.5		95.5		-9.32	1334
1336	2.13	-1.23			2.14	26.0	74.0			-4.92	79.2	20.8			-1.95	.5		99.5		-9.03	1336
1338	2.15	-.75			2.15	1.5	98.5			-3.56	25.8	74.2			-1.40			100.		-6.35	1338
1340	2.14	-1.23			2.14	7.2	92.8			-4.49	61.0	39.0			-1.90			100.		-7.79	1340
1342	2.15	-1.53			2.15	8.8	91.2			-4.55	68.6	31.4			-1.92			100.		-7.81	1342
1344	2.16	-1.53			2.16	45.4	54.6			-5.09	89.0	11.0			-1.98	2.6		97.4		-9.33	1344
1346	2.16	-.93			2.16	1.0	99.0			-3.63	27.2	72.8			-1.52			100.		-6.13	1346
1348	2.14	-1.53			2.14	6.6	93.4			-4.08	57.4	42.6			-1.74			100.		-6.85	1348
1350	2.15	-1.23			2.15	9.1	90.9			-4.48	65.1	34.9			-1.85			100.		-7.79	1350
1351	2.18				2.18	100.				-5.00	100.				-1.82	100.				-10.17	1351
1369	2.23				2.23	100.				-5.11	100.				-1.86	100.				-10.65	1369
1371	2.25	-1.53			2.25	4.3	95.7			-4.09	56.9	43.1			-1.74			100.		-6.85	1371
1373	2.26				2.26	100.				-5.44	100.				-1.96	100.				-11.37	1373
1375	2.26				2.26	100.				-4.99	100.				-1.82	100.				-10.19	1375
1377	2.25				2.25	100.				-5.15	100.				-1.89	100.				-10.34	1377
1379	2.25				2.25	100.				-5.62	100.				-2.00	100.				-12.19	1379
1381	2.27				2.27	100.				-5.21	100.				-1.89	100.				-10.46	1381
1383	2.27				2.27	100.				-5.07	100.				-1.84	100.				-10.49	1383
1385	2.27				2.27	100.				-5.10	100.				-1.84	100.				-10.34	1385
1387	2.24	-1.53			2.24	63.5	36.5			-4.92	92.6	7.4			-1.81	9.0	91.0			-9.30	1387
1389	2.27	-1.53			2.27	64.3	35.7			-4.91	92.2	7.8			-1.83	10.3	89.7			-9.29	1389
1391	2.27				2.27	100.				-5.21	100.				-1.88	100.				-10.67	1391
1393	2.23		-1.14	-0.01	2.20			95.5	4.5	-1.35	2.1		97.8	.9	-.24				47.6	52.4	-.35	1393
1395	2.24	-1.53			2.29	13.4	86.6			-4.40	66.9	33.1			-1.74	.1		99.9		-7.78	1395

9

Table B-2. (Continued)

MISERS BLUFF II-2

TIME (SEC)	NUMBER CONCENTRATION (#/CC) PARTICLE DIAM(MICRON) <3	3 -46	47 -470	>470	TOTAL (LOGARITHM)	MASS CONCENTRATION (G/M**3) PARTICLE DIAM(MICRON) <3	3 -46	47 -470	>470	TOTAL (PERCENT OF TOTAL) (LOG)	EXTINCTION COEFFICIENT (1/KM) PARTICLE DIA?(MICRON) <3	3 -46	47 -470	>470	TOTAL (PERCENT OF TOTAL) (LOG)	RADAR REFLECTIVITY FACTOR ((MM**6)/(M**3)) PARTICLE DIAM(MICRON) <3	3 -46	47 -470	>470	TOTAL (PERCENT OF TOTAL) (LOG)	TIME (SEC)
1397	3.19	1.32	-2.04		3.19	2.4	89.8	7.8		-1.63	24.3	71.9	1.8		.39		43.0	57.0		-3.36	1397
1399	3.47	1.57	-1.38		3.48	2.2	85.0	12.8		-.94	24.5	73.0	2.5		1.00		4.7	95.3		-1.57	1399
1401	3.49	1.59	-1.21	-4.91	3.50	2.2	75.2	21.3	1.3	-.80	27.7	68.4	3.8		1.04		.5	35.8	63.7	-.44	1401
1403	3.42	1.22	-1.54		3.42	2.1	48.3	49.6		-1.01	35.8	58.0	6.3		.76		.1	99.9		.05	1403
1405	3.12	.58	-3.12		3.12	2.2	93.0	4.8		-2.02	30.7	68.5	.8		-.02		39.8	60.2		-3.50	1405
1407	3.51	1.55	-1.66		3.52	1.9	91.8	6.3		-1.01	21.9	76.6	1.4		.94		41.7	58.3		-2.50	1407
1409	3.48	1.52	-1.49		3.48	2.1	87.3	10.6		-1.02	23.2	74.6	2.2		.94		13.2	86.8		-2.11	1409
1411	3.48	1.52	-1.13	-4.91	3.49	1.5	77.6	19.5	1.3	-.82	21.8	73.5	4.6		1.02		.8	15.1	84.1	-.56	1411
1413	3.49	1.60	-1.15	-4.28	3.49	1.4	72.8	12.7	13.1	-.69	21.0	75.1	3.5	.3	1.12			.1	99.9	1.25	1413
1415	3.47	1.53	-1.38	-4.91	3.48	1.8	82.1	14.7	1.4	-.83	23.1	73.9	3.0		1.03		.7	13.9	85.4	-.56	1415
1417	3.46	1.44	-1.31	-4.89	3.46	1.8	76.3	19.2	2.7	-.88	24.5	71.6	3.8	.1	.97		.2	7.5	92.3	-.13	1417
1419	3.47	1.48	-1.34		3.48	1.9	77.0	21.1		-.96	24.4	71.6	4.0		.93		2.5	97.5		-1.29	1419
1421	3.48	1.48	-1.42	-4.91	3.48	1.8	80.4	15.9	2.0	-.99	23.4	73.3	3.2	.1	.91		.4	9.4	90.2	-.59	1421
1423	3.47	1.35	-1.55		3.47	1.8	86.5	11.8		-1.02	23.6	73.7	2.7		.86		13.9	86.1		-2.01	1423
1425	3.39	1.12	-1.85		3.39	1.8	90.8	7.5		-1.31	23.9	74.2	2.0		.61		45.3	54.7		-2.74	1425
1427	3.34	1.01	-2.02		3.34	1.7	68.1	30.2		-1.38	28.2	68.3	3.5		.45		.3	99.7		-.66	1427
1429	3.21	.41	-2.85		3.21	1.7	59.2	40.1		-1.47	31.5	64.7	3.8		.31		.2	99.8		-.64	1429
1431	3.28	.88	-1.97	-4.43	3.28	1.7	74.5	10.5	13.3	-1.34	29.1	67.9	2.5	.5	.48		.1	.9	99.0	-.15	1431
1433	3.24	.98	-2.21		3.25	1.9	94.4	3.7		-1.49	24.1	74.9	1.0		.45		75.7	24.3		-3.16	1433
1435	3.37	1.16	-1.54	-4.89	3.37	1.1	79.6	15.8	3.5	-.99	19.3	76.9	3.7	.1	.79		.2	4.1	95.7	-.14	1435
1437	3.29	.93	-2.14	-4.88	3.30	2.1	61.7	19.5	16.7	-1.46	33.1	63.6	2.9	.4	.39			1.6	98.4	.25	1437
1439	3.12	.59	-3.27		3.12	1.6	32.3	66.1		-1.70	36.5	57.5	6.0		.01			100.		-.60	1439
1441	2.96	.36	-3.62		2.96	2.0	83.0	15.0		-1.84	29.7	67.6	2.8		.04		10.3	89.7		-2.76	1441
1443	2.87	.22	-2.74	-4.89	2.87	2.1	55.9	9.9	32.2	-1.95	37.7	59.1	2.1	1.1	-.15			.2	99.8	-.16	1443
1445	2.68	-.28	-3.65	-4.91	2.68	1.6	63.6	11.4	23.4	-2.06	38.6	58.1	2.0	1.2	-.38		.1	1.3	98.6	-.63	1445
1447	2.84	.25	-2.05	-4.89	2.84	1.1	38.9	49.4	10.6	-1.47	30.2	58.1	11.1	.6	.12			11.3	88.7	-.11	1447
1449	3.29	.88	-1.31	-4.43	3.29	1.3	62.2	31.2	5.3	-.94	24.9	67.4	7.4	.3	.77		.2	14.4	85.5	-.09	1449
1451	3.27	.75	-1.47	-4.40	3.27	1.3	59.6	19.6	19.5	-1.01	27.7	66.1	5.5	.7	.68			.6	99.4	.96	1451
1453	3.16	.35	-2.13		3.16	2.9	77.2	19.8		-1.55	41.5	55.1	3.4		.32		4.5	95.5		-1.90	1453
1455	2.94	.07	-2.91	-4.91	2.94	1.6	55.0	34.8	8.6	-1.63	33.9	57.8	7.9	.4	.08		.1	14.3	85.7	-.57	1455
1457	3.09	.47	-1.89	-4.12	3.09	.8	27.2	46.6	25.3	-1.12	30.1	57.1	11.0	1.7	.35			14.5	85.5	.60	1457
1459	3.27	.67	-1.67	-3.64	3.27	.7	26.1	30.9	42.3	-.75	30.3	57.9	8.5	3.3	.65			3.2	96.8	1.40	1459
1461	3.35	.87	-1.48	-3.74	3.35	.9	37.0	27.9	34.2	-.72	28.8	62.7	6.6	1.9	.79			3.4	96.6	1.43	1461
1463	3.32	.69	-1.61	-4.20	3.32	1.4	42.9	42.7	13.1	-.97	34.1	57.6	7.6	.7	.65			20.2	79.8	.53	1463
1465	3.18	.13	-1.93	-4.06	3.18	1.1	15.4	44.6	38.9	-1.31	46.6	38.8	11.1	3.4	.10			10.7	89.3	.53	1465
1467	3.14	.77	-1.78	-4.41	3.19	1.0	63.8	19.6	15.6	-1.03	21.6	73.4	4.4	.6	.65			1.3	98.6	.70	1467
1469	3.32	.87	-1.44	-4.43	3.32	1.0	58.7	35.4	4.9	-.81	22.6	70.8	6.3	.3	.84		.1	43.9	56.0	.32	1469
1471 *	3.15	.41	-2.12	-4.91	3.15	.9	91.6	1.8	6.2	-1.48	~~33.0~~	~~66.8~~		.2	~~.36~~		~~.3~~		~~99.7~~	~~-.63~~	1471
1473 *	2.90	-.33	-2.18		2.90	.9	72.6	24.0		-2.11	~~52.0~~	~~48.0~~			~~-.23~~		~~100.~~			~~-3.86~~	1473
1475 *	2.79	.42	-2.52		2.80	2.1	93.0	4.9		-1.91	~~24.8~~	~~35.2~~			~~-.03~~		~~100.~~			~~-3.01~~	1475
1477	2.61	-.34			2.60	3.1	96.9			-2.56	42.2	57.8			-.62		100.			-4.10	1477
1479	2.69	.16			2.69	3.6	96.4			-2.39	34.7	65.3			-.32		100.			-4.58	1479
▶ 1481	2.64	.16			2.64	.8	99.2			-2.03	16.6	83.4			-.23		100.			-3.66	1481
1483	2.36	-1.53			2.36	3.6	96.4			-3.74	54.2	45.8			-1.53		100.			-6.15	1483
1485	2.25	-1.53			2.25	32.2	67.8			-5.18	88.8	11.2			-1.99	.2	99.8			-9.34	1485
1487	2.25	-.93			2.25	3.0	97.0			-3.94	44.3	55.7			-1.60		100.			-6.80	1487
1489	2.27	-1.53			2.27	22.4	77.6			-4.48	77.3	22.7			-1.78	.4	99.6			-7.80	1489
1491	2.24	-1.75			2.24	8.4	91.6			-4.07	52.0	48.0			-1.63	.1	99.9			-7.33	1491
1493	2.25	-1.53			2.25	41.9	58.1			-5.12	89.7	10.3			-1.95	.9	99.1			-9.33	1493
1495	2.23	-1.23			2.23	9.0	91.0			-4.48	65.6	34.4			-1.85	.1	99.9			-7.79	1495

Table B-2. (Continued)

[illegible] II-2

TIME	[illegible] (LOGARITHMS) <3	3-46	47-470	>470	TOTAL	[illegible] CONCENTRATION (PERCENT OF TOTAL) <3	3-46	47-470	>470	TOTAL (LOG)	EXTINCTION COEFFICIENT (1/KM) (PERCENT OF TOTAL) <3	3-46	47-470	>470	TOTAL (LOG)	RADAR REFLECTIVITY FACTOR ((MM**6)/(M**3)) (PERCENT OF TOTAL) <3	3-46	47-470	>470	TOTAL (LOG)	TIME (SEC)
[illegible]	2.23	-1.55			2.23	20.6	79.4			-4.49	76.1	23.9			-1.80	.3	99.7			-7.80	1507
[illegible]	2.21				2.21	100.				-4.87	100.				-1.78	100.				-10.09	1509
1511	2.22	-1.55			2.22	13.7	86.3			-4.52	73.8	26.2			-1.84		100.			-7.81	1511
1513	2.24	-1.55			2.24	10.5	89.5			-4.41	64.2	35.8			-1.77		100.			-7.78	1513
1515	2.25				2.25	100.				-5.86	100.				-2.09	100.				-13.35	1515
1517	2.25	-1.55			2.25	23.0	77.0			-5.24	87.5	12.5			-2.03		100.			-9.34	1517
[illegible]	2.23				2.23	100.				-5.59	100.				-2.03	100.				-11.50	1519
1521	2.24	-1.55			2.24	45.4	54.6			-5.09	90.1	9.9			-1.93	1.3	98.7			-9.33	1521
[illegible]																					1521
[illegible]	2.27		-2.12		2.27	.7		99.3		-3.21	41.7		58.3		-1.61			100.		-4.08	1532
[illegible]	2.28		-2.14		2.28	.2		99.8		-2.74	23.2		76.8		-1.32			100.		-3.12	1534
[illegible]	2.24	-1.23	-2.52		2.24	.7	4.7	94.6		-3.19	37.1	15.9	47.0		-1.51			100.		-4.08	1536
[illegible]	2.26	-1.53			2.26	12.1	87.9			-4.53	73.8	26.2			-1.85	.1	99.9			-7.81	1538
[illegible]	2.3	-1.23			2.31	9.8	90.2			-3.94	60.4	39.6			-1.54		100.			-6.80	1540
[illegible]	[illegible]	[illegible]			2.95	2.1	97.9			-1.82	22.9	77.1			.18		100.			-3.73	1542
[illegible]	[illegible]	.65	[illegible]		2.93	2.1	89.7	8.2		-1.95	26.3	72.2	1.4		.02		18.2	81.8		-3.11	1544
[illegible]	[illegible]	.85	-1.45		3.15	1.8	90.2	8.0		-1.47	26.2	71.6	2.2		.43		43.9	56.1		-2.81	1546
[illegible]	3.3	1.15	-1.36	-4.91	3.31	1.1	70.0	27.2	1.8	-.95	20.2	73.9	5.8	.1	.81		.4	41.5	58.0	-.40	1548
[illegible]	[illegible]	1.42	-1.49		3.41	1.8	79.4	18.8		-.99	24.0	72.4	3.6		.90		4.7	95.3		-1.61	1550
[illegible]	[illegible]	1.17	-1.78		3.30	1.8	83.2	15.0		-1.39	24.0	72.9	3.1		.55		11.5	88.5		-2.43	1552
[illegible]	3.34	1.23	-1.12	-4.91	3.39	1.0	77.2	20.7	1.1	-.73	18.3	76.0	5.7	.1	1.01		1.1	21.9	77.0	-.52	1554
[illegible]	3.5	1.52	-.85	-4.91	3.51	1.2	76.2	22.1	.6	-.47	19.6	74.7	5.7		1.27		1.4	41.9	56.6	-.39	1556
[illegible]	3.54	1.59	-.76	-4.11	3.54	1.3	71.1	21.9	5.6	-.31	20.6	73.9	5.3	.2	1.42		.1	3.2	96.7	.98	1558
[illegible]	3.55	[illegible]	-.75	-4.03	3.54	1.2	70.8	26.7	1.4	-.36	19.3	74.6	6.0	.1	1.39		.5	38.6	60.9	.06	1560
[illegible]	3.53	1.75	-.84	-3.99	3.53	1.4	72.2	20.4	6.0	-.32	21.2	74.0	4.5	.2	1.43		.1	4.5	95.4	.90	1562
[illegible]	3.53	1.61	-.66	[illegible]	3.53	1.5	61.5	33.1	3.9	-.31	24.8	67.4	7.6	.2	1.40		.2	22.3	77.6	.55	1564
[illegible]	3.52	1.58	-.65	-3.76	3.53	1.1	53.7	37.5	7.6	-.23	22.7	68.7	8.2	.4	1.42			22.4	77.6	1.24	1566
[illegible]	3.53	1.53	-.69	-3.79	3.54	.9	59.2	33.7	6.2	-.23	19.4	72.6	7.6	.3	1.41		.1	26.8	73.2	1.02	1568
[illegible]	3.53	1.55	-.74	-4.27	3.53	1.1	58.9	31.5	8.5	-.30	21.1	71.6	7.1	.2	1.36			3.1	96.9	1.74	1570
1572	3.52	1.45	[illegible]	-4.34	3.52	1.6	49.7	28.3	20.4	-.50	30.3	62.0	7.2	.5	1.18			.5	99.5	1.91	1572
[illegible]	3.51	1.62	-.87	-4.12	3.51	1.3	66.3	26.9	5.5	-.50	22.3	71.4	6.0	.2	1.26		.1	11.4	88.5	.58	1574
[illegible]	[illegible]	1.66	-1.02	-4.91	3.50	1.2	70.0	28.1	.7	-.54	20.1	74.6	5.3		1.23		.6	61.7	37.7	-.21	1576
[illegible]	3.52	1.54	-.99	-4.43	3.53	1.7	75.6	19.7	3.0	-.59	23.8	71.9	4.2	.1	1.24		.3	10.1	89.6	.11	1578
[illegible]	3.45	1.42	-1.21	-4.56	3.46	1.6	59.2	26.6	12.6	-.78	27.1	67.3	5.3	.3	.99			2.0	98.0	1.23	1580
[illegible]	[illegible]	[illegible]	[illegible]	-4.41	3.44	1.5	73.7	13.1	11.7	-.83	23.3	73.6	2.9	.3	.99			.4	99.6	.95	1582
[illegible]	3.45	1.41	-1.12	-4.89	3.46	1.4	71.9	24.6	2.1	-.78	22.2	72.3	5.4	.1	1.02		.3	14.0	85.8	-.09	1584
[illegible]	3.45	1.43	[illegible]	-4.61	3.45	1.6	69.0	26.3	3.1	-.89	24.2	69.9	5.7	.1	.94		.3	12.7	87.0	-.27	1586
[illegible]	3.43	1.35	-1.55		3.44	2.0	85.9	12.1		-1.06	25.9	71.5	2.6		.85		14.5	85.5		-2.06	1588
[illegible]	[illegible]	[illegible]	-1.25	-4.91	3.48	1.5	78.1	19.1	1.3	-.81	21.8	74.0	4.1		1.03		.7	16.7	82.6	-.55	1590
[illegible]	[illegible]	1.22	-1.35	-4.91	3.47	1.7	83.7	13.3	1.3	-.81	24.0	72.9	3.0		1.04		1.0	9.0	90.1	-.59	1592
[illegible]	3.35	1.3			3.36	4.3	95.7			-1.58	37.9	62.1			.51		100.			-3.61	1594
[illegible]	[illegible]	.7			[illegible]	3.3	96.7			-1.92	35.5	64.5			.14		100.			-3.74	1596
[illegible]	2.85	-1.23			2.83	68.7	31.3			-4.01	95.3	4.7			-.98	1.9	98.1			-7.78	1598
[illegible]	2.52	-1.53			2.52	84.2	15.8			-4.55	97.1	2.9			-1.41	17.7	82.3			-9.25	1600
[illegible]	2.42	[illegible]	-2.52		2.42	.7	85.1	14.2		-2.37	14.2	86.8			-.55		100.			-4.32	1602
[illegible]	[illegible]	[illegible]	-1.49		[illegible]	1.0	52.4	46.6		-1.55	23.7	76.3			.17		100.			-3.63	1604
[illegible]	[illegible]	[illegible]	-2.39		[illegible]	1.4	94.6	4.0		-1.29	18.6	81.4			.65		100.			-3.14	1606
[illegible]	[illegible]	[illegible]	-2.60		[illegible]	3.1	72.9	24.0		-1.61	34.3	65.7			.38		100.			-3.91	1608
[illegible]	[illegible]	.31	-2.26		2.49	1.6	36.5	61.9		-2.22	34.0	65.1			-.42		100.			-5.22	1610
[illegible]	[illegible]	-1.53	-2.82		[illegible]	8.4	1.3	90.3		-3.48	97.1	2.9			-1.40	26.2	73.8			-9.21	1612

10

Table B-2. (Continued)

TIME (SEC)	LIQUID WATER CONTENT (G/CC) PARTICLE DIAM(MICRON) <3	3 -46	47 -470	>470	TOTAL (LOG)	MASS CONCENTRATION (G/M**3) PARTICLE DIAM(MICRON) <3	3 -46	47 -470	>470	TOTAL (LOG)	EXTINCTION COEFFICIENT (1/KM) PARTICLE DIAM(MICRON) <3	3 -46	47 -470	>470	TOTAL (LOG)	RADAR REFLECTIVITY FACTOR ((MM**6)/(M**3)) PARTICLE DIAM(MICRON) <3	3 -46	47 -470	>470	TOTAL (LOG)	TIME (SEC)
	(G/CUBIC M)					(PERCENT OF TOTAL)					(PERCENT OF TOTAL)					(PERCENT OF TOTAL)					
1614	2.36 -1.63				2.36	52.8	47.2			-5.03	92.7	7.3			-1.80	1.4	98.6			-9.33	1614
1616	2.3				2.3	100.				-5.42	100.				-1.92	100.				-11.35	1616
1618	2.28 -1.23				2.28	1.9	98.1			-3.74	41.8	58.2			-1.60		100.			-6.15	1618
1620	2.28				2.28	100.				-4.86	100.				-1.73	100.				-9.95	1620
1622	2.26 -1.65				2.26	2.2	97.8			-3.62	35.3	64.7			-1.44		100.			-6.37	1622
1624	2.26				2.26	100.				-5.15	100.				-1.86	100.				-10.61	1624
1626	2.25				2.25	100.				-5.24	100.				-1.92	100.				-10.43	1626
1628 *	3.1 .98 -1.39				3.11	1.3	88.0	10.7		-1.46	20.0	80.0			.41		100.			-3.17	1628
1630 *	3.36 1.14 -2.03 -4.91				3.36	2.5	89.0	8.3	5.2	-1.41	29.7	70.3			.56		100.			-3.34	1630
1632	2.45				2.45	100.				-4.20	100.				-1.01	100.				-9.64	1632
1634	2.57 -1.63				2.57	81.9	18.1			-4.61	96.8	3.2			-1.44	18.4	81.6			-9.25	1634
1636	2.41 -1.63				2.41	77.6	22.4			-4.70	95.5	4.5			-1.59	16.5	83.5			-9.26	1636
1638	2.31 -1.63				2.31	14.4	85.6			-4.52	78.0	22.0			-1.77		100.			-7.81	1638
1640	2.31 -1.23				2.31	19.9	80.1			-4.19	73.2	26.8			-1.55	.2	99.8			-7.50	1640
1642	2.26 -1.65				2.26	5.1	94.9			-4.44	60.1	39.9			-1.82		100.			-7.78	1642
1644	2.26				2.26	100.				-5.45	100.				-1.96	100.				-11.38	1644
1646	2.22 -1.63				2.22	5.9	94.1			-4.56	68.3	31.7			-1.93		100.			-7.81	1646
1648	2.23 -1.65				2.23	11.4	88.6			-4.82	70.4	29.6			-1.93		100.			-8.86	1648
1650	2.25 -1.23				2.25	5.6	94.4			-4.49	63.9	36.1			-1.87		100.			-7.79	1650
1652	2.22 -1.63				2.22	7.4	92.6			-4.55	69.8	30.2			-1.91		100.			-7.81	1652
1654	2.20				2.20	100.				-5.72	100.				-2.10	100.				-11.61	1654
1656	2.23 -1.23				2.23	4.1	95.9			-4.50	61.1	38.9			-1.90		100.			-7.79	1656
1658	2.22 -1.63				2.22	25.9	74.1			-5.22	87.1	12.9			-2.05	.1	99.9			-9.34	1658
1660	2.20				2.20	100.				-5.76	100.				-2.10	100.				-12.14	1660
1662	2.20				2.20	100.				-5.72	100.				-2.11	100.				-11.59	1662
1664	2.21 -1.23				2.21	1.7	98.3			-4.08	45.9	54.1			-1.78		100.			-6.85	1664
1666	2.2 -1.23				2.20	15.7	84.3			-4.98	76.3	23.7			-2.01	.1	99.9			-9.04	1666
1668	2.22				2.22	100.				-5.72	100.				-2.08	100.				-11.91	1668
1670	2.19 -1.63				2.19	46.1	53.9			-5.08	88.1	11.9			-2.01	6.4	93.6			-9.31	1670
1672	2.17 -1.63				2.17	39.2	60.8			-5.14	87.2	12.8			-2.04	2.5	97.5			-9.33	1672
1674	2.15				2.15	100.				-5.92	100.				-2.20	100.				-12.26	1674
1676	2.16				2.16	100.				-5.88	100.				-2.18	100.				-12.23	1676
1678	2.15 -1.63				2.15	11.9	88.1			-4.53	69.4	30.6			-1.91	.1	99.9			-7.81	1678
1680	2.16 -1.63				2.16	23.5	76.5			-5.24	85.6	14.4			-2.09	.1	99.9			-9.34	1680
1682	2.17 -1.63				2.17	51.1	48.9			-5.04	89.2	10.8			-1.97	4.2	95.8			-9.32	1682
1684	2.16 -1.63				2.16	8.6	91.4			-4.55	67.9	32.1			-1.93		100.			-7.81	1684
1686	2.13				2.13	100.				-5.65	100.				-2.16	100.				-11.03	1686
1688	2.14 -1.63				2.14	21.6	78.4			-5.25	84.5	15.5			-2.13	.1	99.9			-9.34	1688
1690	2.16 -1.23				2.16	12.7	87.3			-4.99	74.7	25.3			-2.04		100.			-9.04	1690
1691	2.14				2.14	100.				-5.90	100.				-2.18	100.				-12.62	1691
1741																					1741
1743																					1743
1745		-1.63			-1.63		100.			-5.35		100.			-2.94		100.			-9.34	1745
1747																					1747
1749																					1749
1751																					1751
1753																					1753
1755																					1755
1757																					1757
1759																					1759

10

Table B-2. (Continued)

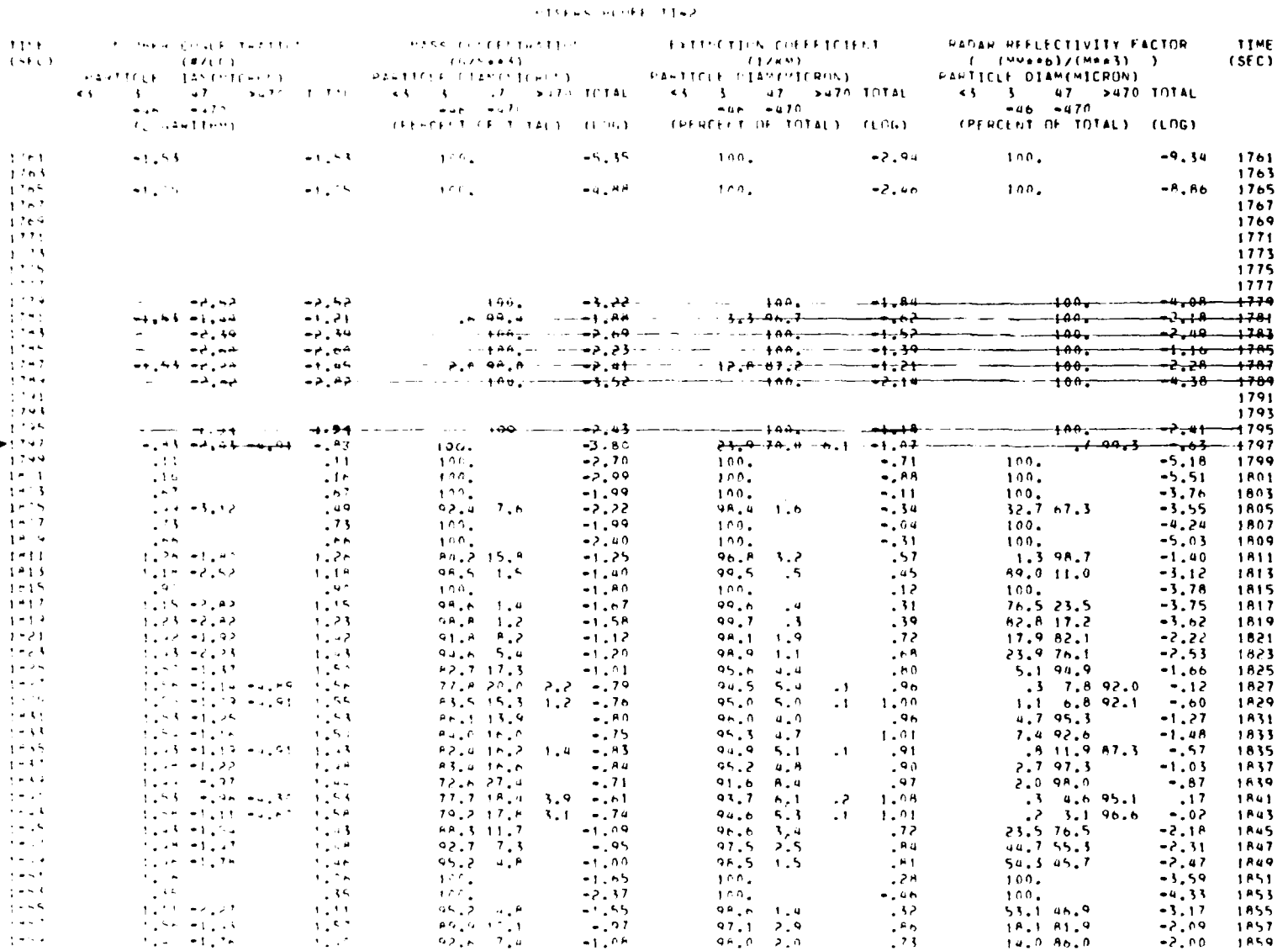

TIME (SEC)	PARTICLE CONCENTRATION (#/LITER) PARTICLE DIAM(MICRON) <.5	.5 -.46	.47 -.470	>.470	TOTAL	MASS CONCENTRATION (GM/M**3) PARTICLE DIAM(MICRON) <.5	.5 -.46	.47 -.470	>.470	TOTAL (LOG) (PERCENT OF TOTAL)	EXTINCTION COEFFICIENT (1/KM) PARTICLE DIAM(MICRON) <.5	.5 -.46	.47 -.470	>.470	TOTAL (LOG) (PERCENT OF TOTAL)	RADAR REFLECTIVITY FACTOR ((MM**6)/(M**3)) PARTICLE DIAM(MICRON) <.5	.5 -.46	.47 -.470	>.470	TOTAL (LOG) (PERCENT OF TOTAL)	TIME (SEC)
1761		-1.53			-1.53		100.			-5.35		100.			-2.94		100.			-9.34	1761
1763																					1763
1765		-1.75			-1.75		100.			-4.88		100.			-2.60		100.			-8.86	1765
1767																					1767
1769																					1769
1771																					1771
1773																					1773
1775																					1775
1777																					1777
1779		-	-2.52		-2.52		100.			-3.22		-	100.		-1.84		100.			-4.08	1779
1781		-1.45	-1.66		-1.21		.6	99.4		-1.84		3.3	96.7		-.62		100.			-2.18	1781
1783		-	-2.46		-2.46			100.		-2.69			100.		-1.52		100.			-2.48	1783
1785		-	-2.04		-2.04			100.		-2.23			100.		-1.39		100.			-1.16	1785
1787		-2.44	-2.24		-1.85		2.0	98.0		-2.41		12.8	87.2		-1.21		100.			-2.28	1787
1789		-	-2.42		-2.42			100.		-3.52			100.		-2.14		100.			-4.38	1789
1791																					1791
1793																					1793
1795		-	-2.34		-2.34			100.		-2.43			100.		-1.18		100.			-2.41	1795
1797		-.41	-2.01	-4.01	-.83		100.			-3.80		23.9	76.0	4.1	-1.87			99.3		-.63	1797
1799		.11			.11		100.			-2.70		100.			-.71		100.			-5.18	1799
1801		.16			.16		100.			-2.99		100.			-.88		100.			-5.51	1801
1803		.67			.67		100.			-1.99		100.			-.11		100.			-3.76	1803
1805		.44	-3.12		.48		92.4	7.6		-2.22		98.4	1.6		-.34		32.7	67.3		-3.55	1805
1807		.73			.73		100.			-1.99		100.			-.04		100.			-4.24	1807
1809		.66			.66		100.			-2.40		100.			-.31		100.			-5.03	1809
1811		1.26	-1.45		1.26		84.2	15.8		-1.25		96.8	3.2		.57		1.3	98.7		-1.40	1811
1813		1.18	-2.52		1.18		98.5	1.5		-1.40		99.5	.5		.45		89.0	11.0		-3.12	1813
1815		.97			.97		100.			-1.80		100.			.12		100.			-3.78	1815
1817		1.15	-2.83		1.15		98.6	1.4		-1.67		99.6	.4		.31		76.5	23.5		-3.75	1817
1819		1.23	-2.82		1.23		98.8	1.2		-1.58		99.7	.3		.39		82.8	17.2		-3.62	1819
1821		1.42	-1.93		1.42		91.8	8.2		-1.12		98.1	1.9		.72		17.9	82.1		-2.22	1821
1823		1.43	-2.23		1.43		94.6	5.4		-1.20		98.9	1.1		.68		23.9	76.1		-2.53	1823
1825		1.53	-1.87		1.53		92.7	17.3		-1.01		95.6	4.4		.80		5.1	94.9		-1.66	1825
1827		1.58	-1.14	-4.69	1.58		77.8	20.0	2.2	-.79		94.5	5.4	.1	.96		.3	7.8	92.0	-.12	1827
1829		1.55	-1.23	-4.01	1.55		83.5	15.3	1.2	-.76		95.0	5.0	.1	1.00		1.1	6.8	92.1	-.60	1829
1831		1.53	-1.26		1.53		86.1	13.9		-.80		96.0	4.0		.96		4.7	95.3		-1.27	1831
11 1833		1.52	-1.14		1.52		84.0	16.0		-.75		95.3	4.7		1.01		7.4	92.6		-1.48	1833
1835		1.43	-1.13	-4.01	1.43		82.4	16.2	1.4	-.83		94.9	5.1	.1	.91		.8	11.9	87.3	-.57	1835
1837		1.48	-1.22		1.48		83.4	16.6		-.84		95.2	4.8		.90		2.7	97.3		-1.03	1837
1839		1.44	-.97		1.44		72.6	27.4		-.71		91.6	8.4		.97		2.0	98.0		-.87	1839
1841		1.53	-.96	-4.35	1.53		77.7	18.4	3.9	-.61		93.7	6.1	.2	1.08		.3	4.6	95.1	.17	1841
1843		1.58	-1.11	-4.01	1.58		79.2	17.8	3.1	-.74		94.6	5.3	.1	1.01		.2	3.1	96.6	-.02	1843
1845		1.43	-1.54		1.43		88.3	11.7		-1.09		96.8	3.4		.72		23.5	76.5		-2.18	1845
1847		1.48	-1.47		1.48		92.7	7.3		-.95		97.5	2.5		.84		44.7	55.3		-2.31	1847
1849		1.46	-1.34		1.46		95.2	4.8		-1.00		98.5	1.5		.81		54.3	45.7		-2.47	1849
1851		.28			1.28		100.			-1.65		100.			.28		100.			-3.59	1851
1853		.36			.36		100.			-2.37		100.			-.46		100.			-4.33	1853
1855		1.11	-2.27		1.11		95.2	4.8		-1.55		98.6	1.4		.32		53.1	46.9		-3.17	1855
1857		1.52	-1.15		1.52		89.9	10.1		-.97		97.1	2.9		.86		18.1	81.9		-2.09	1857
1859		1.46	-1.74		1.47		92.6	7.4		-1.08		98.0	2.0		.73		14.0	86.0		-2.00	1859

Table B-2. (Continued)

USERS GUIDE II-2

TIME (SEC)	NUMBER CONCENTRATION (#/CC) PARTICLE DIAM(MICRON) <3	3-46	47-470	>470	TOTAL	MASS CONCENTRATION (GM**3) PARTICLE DIAM(MICRON) <3	3-46	47-470	>470	TOTAL (LOG) (PERCENT OF TOTAL)	EXTINCTION COEFFICIENT (1/KM) PARTICLE DIAM(MICRON) <3	3-46	47-470	>470	TOTAL (LOG) (PERCENT OF TOTAL)	RADAR REFLECTIVITY FACTOR ((MM**6)/(M**3)) PARTICLE DIAM(MICRON) <3	3-46	47-470	>470	TOTAL (LOG) (PERCENT OF TOTAL)	TIME (SEC)
1861		1.57	-1.52		1.57		92.2	7.8		-.97		97.8	2.2		.88		31.9	68.1		-2.37	1861
1863		1.54	-1.46		1.54		89.6	10.4		-.98		97.2	2.8		.87		15.3	84.7		-2.15	1863
1865		1.57	-2.43		1.57		96.6	3.4		-.97		99.5	.5		.88		8.2	91.8		-1.73	1865
1867		1.64	-1.53		1.69		94.5	5.5		-.91		98.4	1.6		.97		48.7	51.3		-2.59	1867
1869		1.20			1.20		100.			-1.50		100.			.42		100.			-3.56	1869
1871		.88			.88		100.			-1.93		100.			.03		100.			-4.06	1871
1873		-1.05			-1.05		100.			-4.25		100.			-2.06		100.			-7.50	1873
1875		.84			.84		100.			-2.08		100.			-.16		100.			-4.11	1875
1877		.41	-2.82		.84		97.1	2.9		-1.98		100.			.01		100.			-4.41	1877
1879		1.12			1.12		100.			-1.68		100.			.29		100.			-3.91	1879
1881		-.93			-.93		100.			-4.22		100.			-2.01		100.			-7.49	1881
1883		-1.35			-1.35		100.			-4.46		100.			-2.22		100.			-7.78	1883
1885		-1.23			-1.23		100.			-3.81		100.			-1.81		100.			-6.55	1885
1887		-1.53			-1.53		100.			-5.35		100.			-2.94		100.			-9.34	1887
1889																					1889
1891																					1891
1893		-1.53			-1.53		100.			-4.59		100.			-2.43		100.			-7.81	1893
1895																					1895
1897		-1.23			-1.23		100.			-4.52		100.			-2.31		100.			-7.79	1897
1899		-.93			-.93		100.			-4.09		100.			-1.91		100.			-7.32	1899
1901																					1901
1903		-1.53			-1.53		100.			-5.35		100.			-2.94		100.			-9.34	1903
1905		-1.23			-1.23		100.			-4.08		100.			-2.05		100.			-6.85	1905
1907		-1.23			-1.23		100.			-4.52		100.			-2.31		100.			-7.79	1907
1909		-1.53			-1.53		100.			-5.35		100.			-2.94		100.			-9.34	1909
1911		-1.23			-1.23		100.			-5.05		100.			-2.64		100.			-9.04	1911
1913		-1.53			-1.53		100.			-5.35		100.			-2.94		100.			-9.34	1913
1915		-1.53			-1.53		100.			-5.35		100.			-2.94		100.			-9.34	1915
1917		-1.53			-1.53		100.			-5.35		100.			-2.94		100.			-9.34	1917
1919		-1.23			-1.23		100.			-5.05		100.			-2.64		100.			-9.04	1919
1921		-.93			-.93		100.			-4.75		100.			-2.33		100.			-8.74	1921
1923																					1923
1925																					1925
1927																					1927
1929		-1.23			-1.23		100.			-5.05		100.			-2.64		100.			-9.04	1929
1931		-.83			-.83		100.			-3.97		100.			-1.79		100.			-7.20	1931
1933		-1.23			-1.23		100.			-4.52		100.			-2.31		100.			-7.79	1933
1935		-.75			-.75		100.			-3.92		100.			-1.79		100.			-6.80	1935
1937		-1.23			-1.23		100.			-5.05		100.			-2.64		100.			-9.04	1937
1939		-1.53			-1.53		100.			-4.59		100.			-2.43		100.			-7.81	1939
1941																					1941
1943		-1.23			-1.23		100.			-4.52		100.			-2.31		100.			-7.79	1943
1945		-1.23			-1.23		100.			-5.05		100.			-2.64		100.			-9.04	1945
1947		-.93			-.93		100.			-4.75		100.			-2.33		100.			-8.74	1947
1949																					1949
1951		-1.35			-1.35		100.			-4.46		100.			-2.22		100.			-7.78	1951
1953		-1.26			-1.26		100.			-4.88		100.			-2.46		100.			-8.86	1953
1955		-.93			-.93		100.			-4.41		100.			-2.14		100.			-7.77	1955
1957																					1957
1959		-1.23			-1.23		100.			-5.05		100.			-2.64		100.			-9.04	1959

APPENDIX C

THE MISERS BLUFF II-2 AEROSOL ENVIRONMENT

C-1 INTRODUCTION

The presentation of spectral data obtained from the LAS-X instrument (particle size range 0.1 to 6 μm) is being included as an appendix to this document since these particle measurements were not common to both the single and multiple burst dust clouds. The addition of this particular probe to the in-situ sampling instrumentation suite was prompted by an unexpected wavelength sensitivity in lidar backscattering measurements obtained by SRI International during the single burst test. It is hoped that the inclusion of this spectral data obtained from the MBII-2 dust cloud will aid in interpreting the lidar backscatter measurements made at 10.6 μm, 1.06 μm and 0.532 μm during both events. This may be possible since the very small particle environment was probably similar in both dust cloud environments due to the ANFO and silt commonality.

C-2 PARTICLE SIZE DISTRIBUTIONS

To be consistent with Sections 2 and 3 of this report, the size distributions obtained for dust particles ≤6 μm will be presented only for those sampling passes that were made while ascending to the cloud top, i.e., passes 2-11 in the MBII-2 dust cloud. Further, the LAS-X output was not recorded during sampling passes 4, 5, and 11 so pass-averaged size distributions are not available for those three passes.

Figures C-1 through C-7 depict the average size distribution of particles measured by the LAS-X instrument during ascending, MBII-2 sampling passes. The solid circles depict the particle size distributions of particles 5-25 μm in diameter, as measured by the FSSP instrument, and are included only to show the excellent agreement between the two probes. (For various reasons, the solid circles at 5 μm are less reliable - see Reference 2).

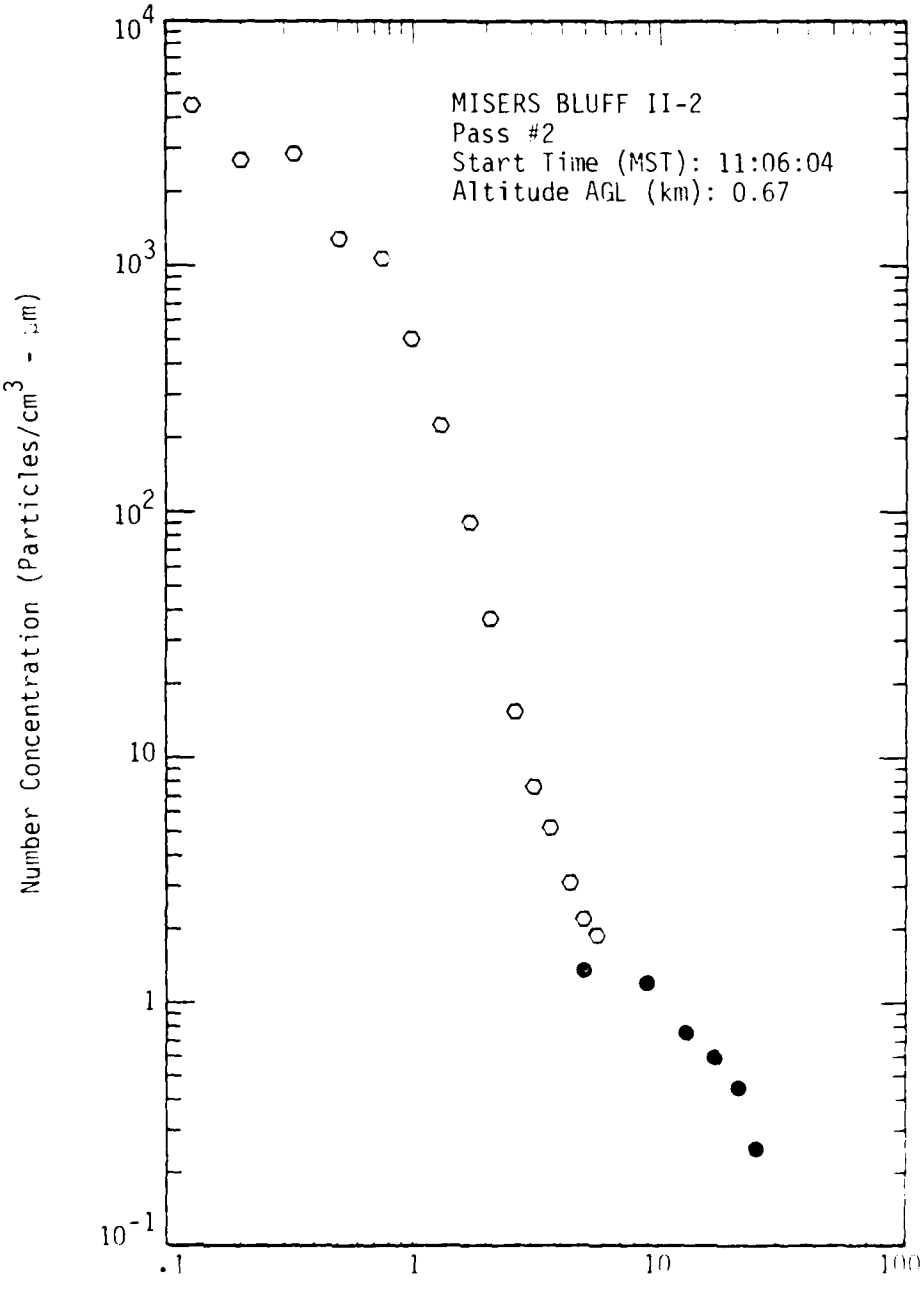

Figure C.1. MISERS BLUFF II-2, Pass 2, Aerosol Particle Size Distribution

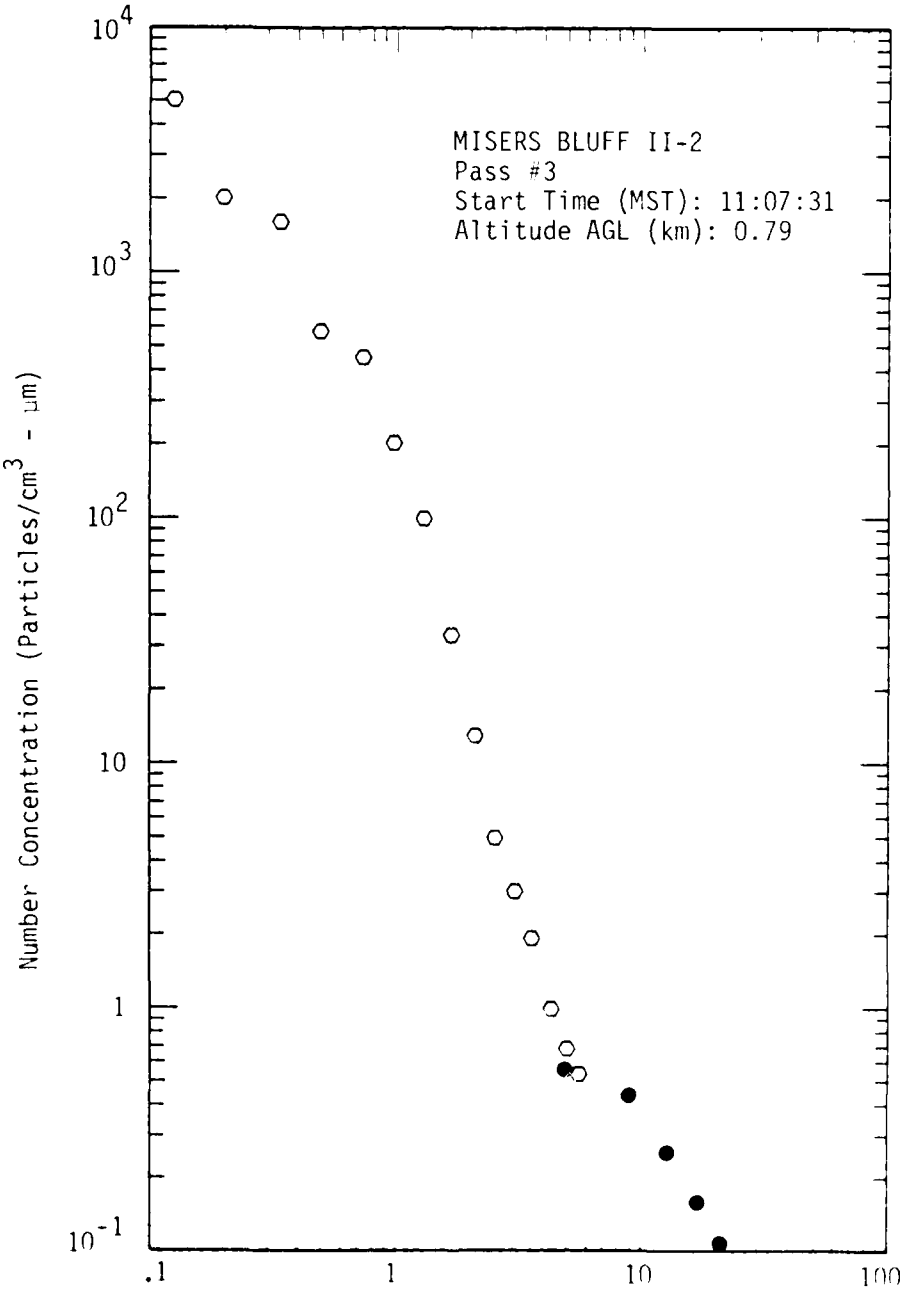

Figure C.2. MISERS BLUFF II-2, Pass 3, Aerosol Particle Size Distribution

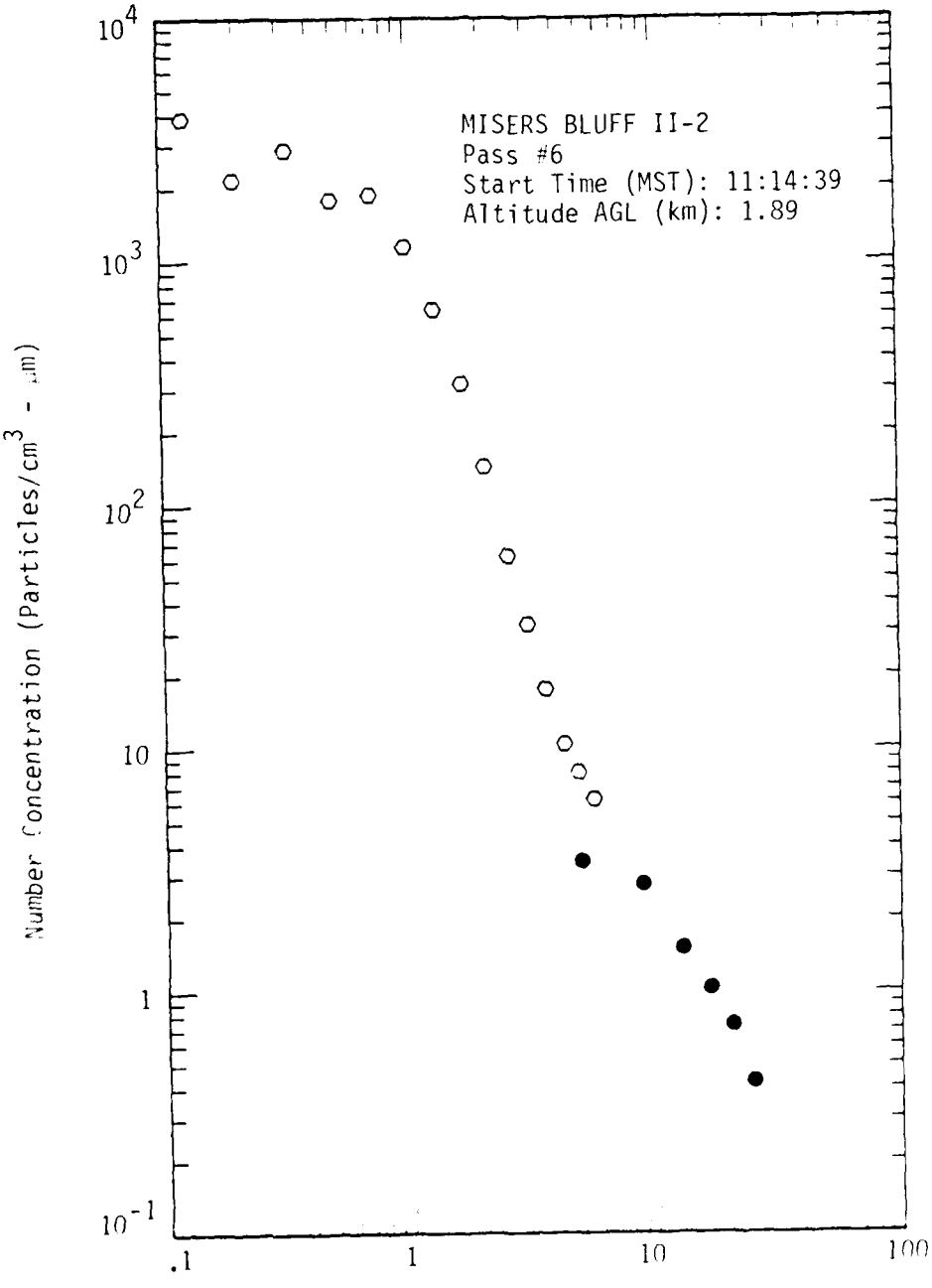

Figure C.3. MISERS BLUFF II-2, Pass 6, Aerosol Particle Size Distribution

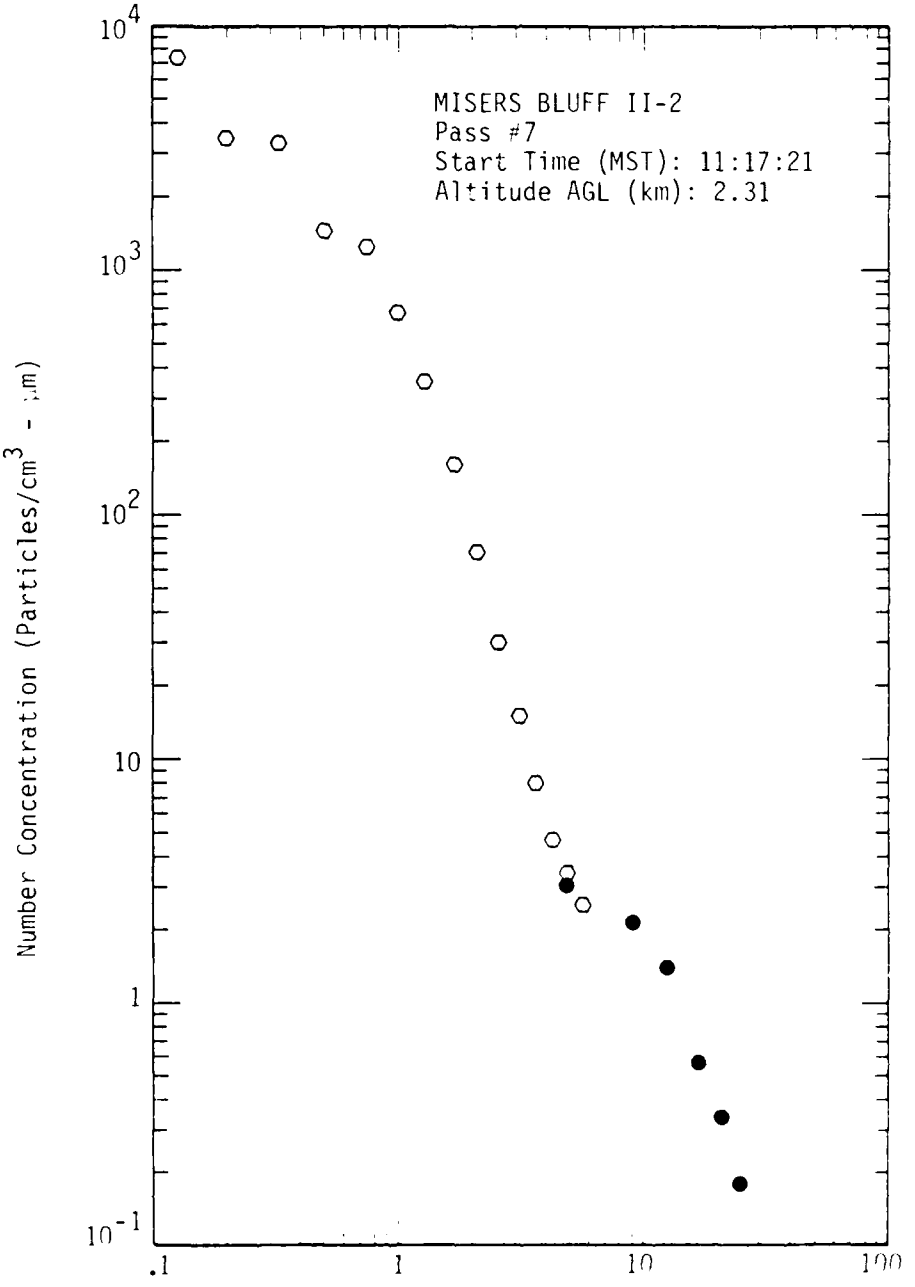

Figure C.4. MISERS BLUFF II-2, Pass 7, Aerosol Particle Size Distribution

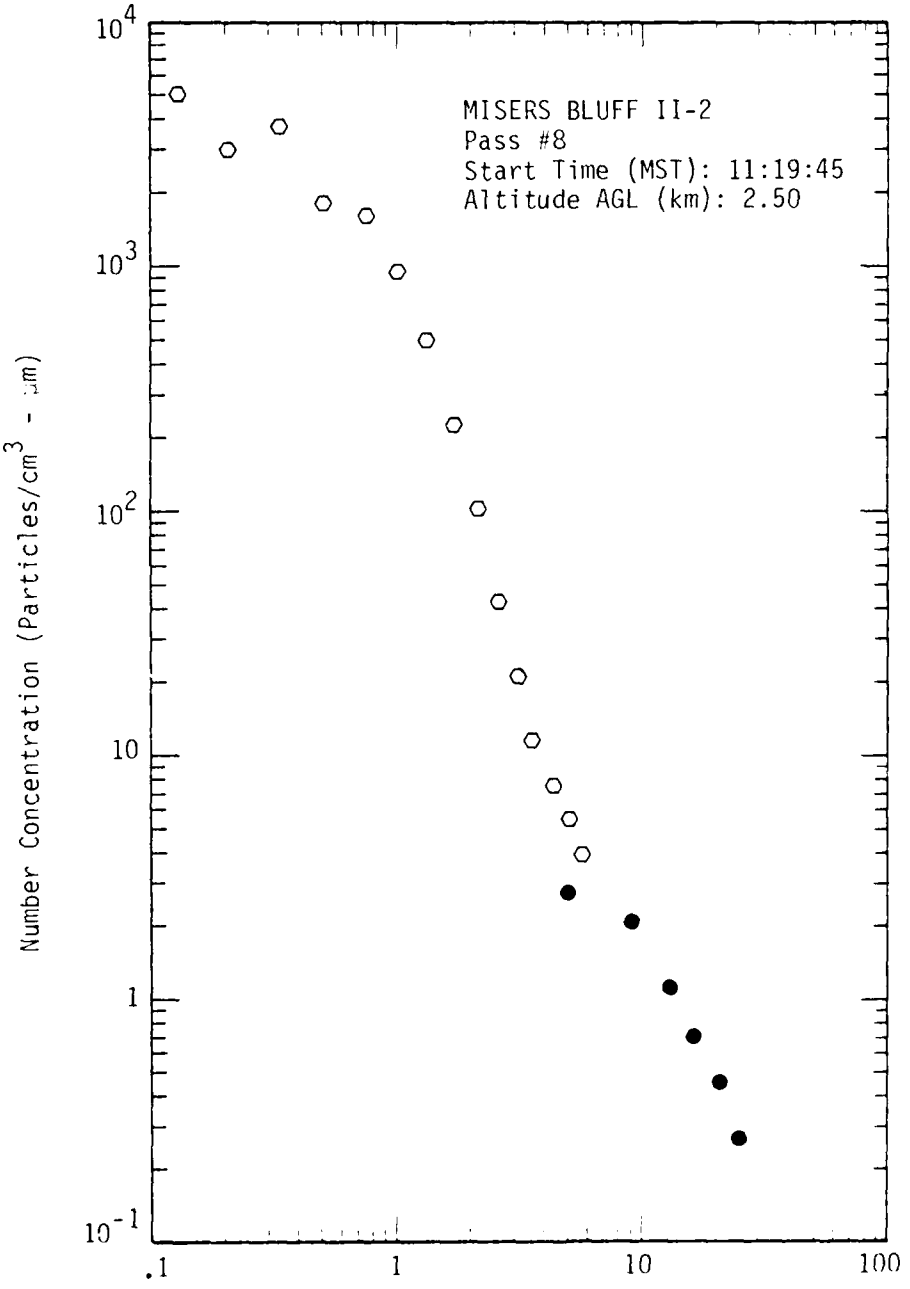

Figure C.5. MISERS BLUFF II-2, Pass 8, Aerosol Particle Size Distribution

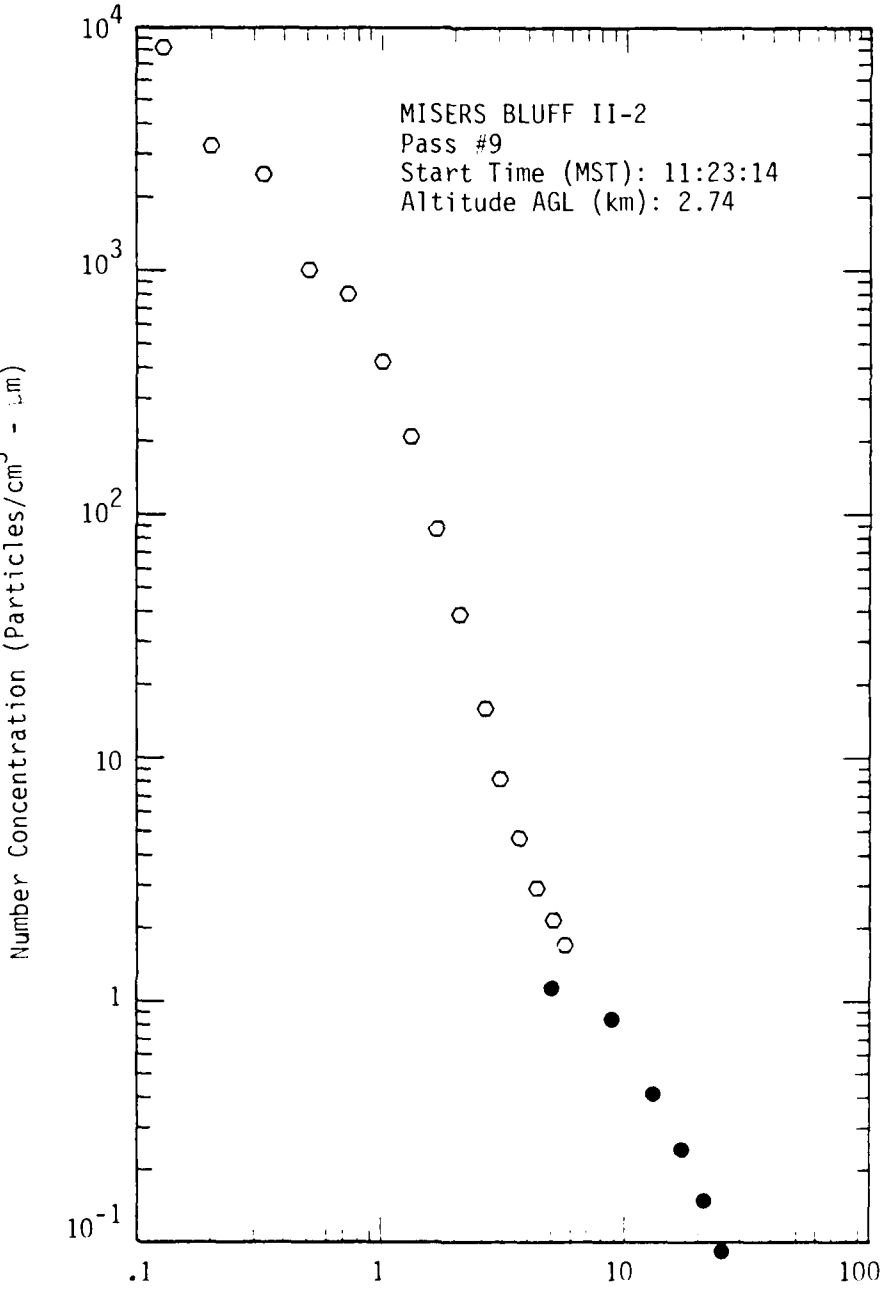

Figure C.6. MISERS BLUFF II-2, Pass 9, Aerosol Particle Size Distribution

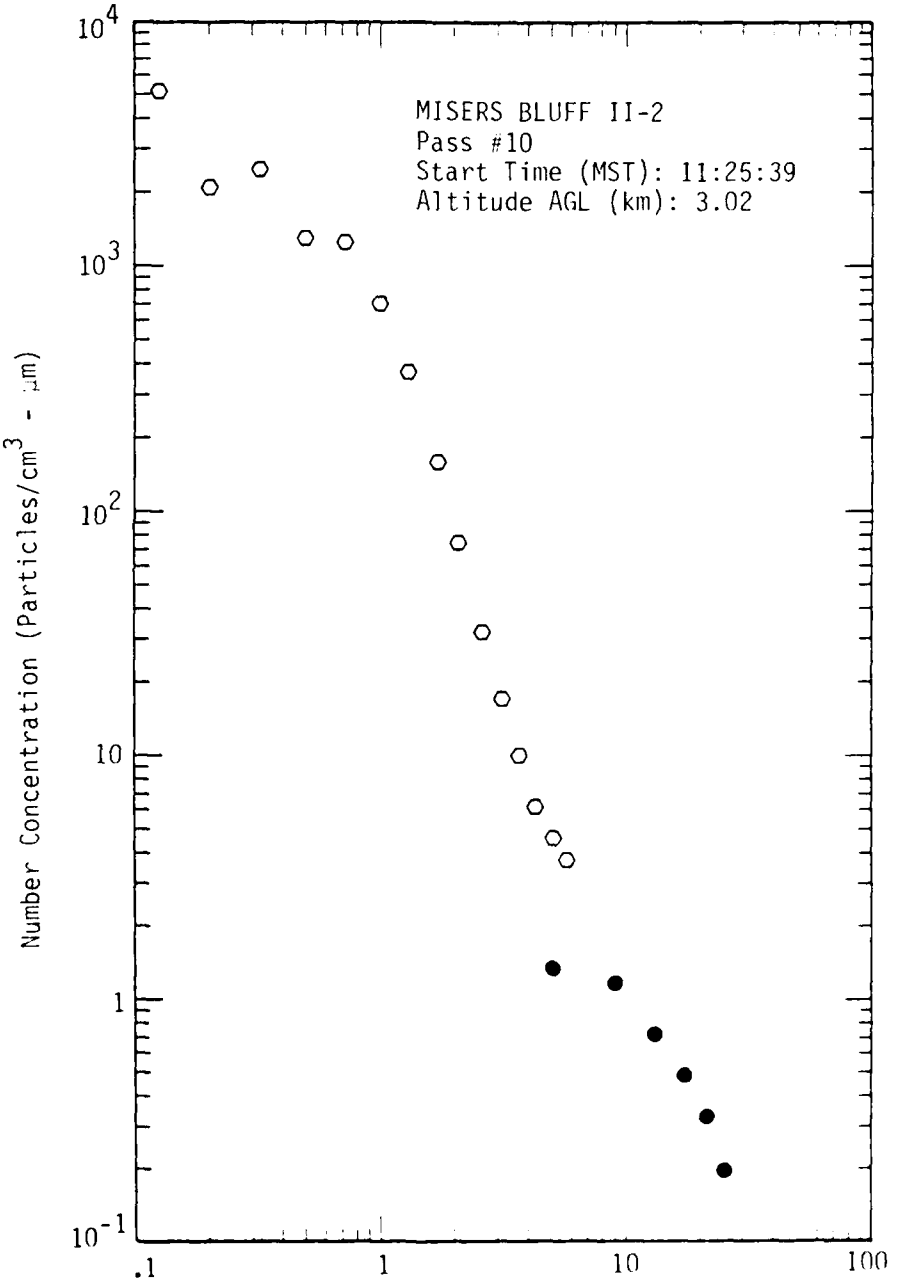

Figure C.7. MISERS BLUFF II-2, Pass 10, Aerosol Particle Size Distribution

For anyone who is focusing on dust particle sizes ≥ 3 μm in their analysis of the MISERS BLUFF II-2 dust cloud, particle number concentrations (#/cc) and calculated mass concentrations (g/m^3), in two-second data intervals (≈400 foot resolution) within the cloud, can be easily extracted from Appendix B (Table B.2) to supplement the size distribution data presented in this appendix.

Since the acquisition of spectral data for particle sizes less than 3 μm was not required for cloud mass loading comparisons, only general comments will be made concerning these size distributions. First, it appears that between 0.1 and 6 μm, the size distribution of these particles cannot be adequately described as either exponential or power law in nature. This fact could affect an analysis of lidar measurements where an assumed particle size distribution was used to calculate backscatter coefficients. Second, there appears to be a "flattening" of the size distributions between ≈0.2 μm and ≈0.7 μm; in fact, most of the pass-averaged distributions indicate a "hump" in the distribution at ≈0.3 μm. This could lead to a significant perturbation in any analysis that assumed the particle size distribution could be represented by a monotonically decreasing function.

APPENDIX D
DUST PARTICLE TERMINAL FALL VELOCITIES

Since much of the analyses of the MISERS BLUFF II dust clouds relied heavily upon assumptions concerning dust particle terminal fall velocities, it was felt a brief appendix pertaining to particle fall velocities was warranted. Although all analyses, for lack of more definitive information on dust particle shapes over the size range of interest, were based on "rough" spherical particles, this appendix also contains terminal fall velocities of circular discs, a shape not totally inconsistent with the "mica flakes" reportedly found by PMS in their aircraft engine filter.

D-1 SPHERICAL PARTICLES

For a spherical particle of mass m falling at its terminal velocity V_t through air of density ρ_a, the force balance is

$$mg = \frac{\rho_p \pi d^3 g}{6} = \frac{\rho_a V_t^2 C_D A_c}{2} \qquad (1)$$

where A_c is the cross-sectional area of a particle with diameter d, ρ_p is the particle density, and C_D is the particle's drag coefficient. The drag coefficient is an empirical function of the Reynolds number Re and is given by

$$C_D = C_1 + (C_2/Re) \qquad (2)$$

where C_1 and C_2 have been experimentally determined for various shaped particles. For "rough" spheres $C_1 = 0.6$ and $C_2 = 36$. By comparison, for smooth spheres, $C_1 = 0.4$ and $C_2 = 24$, which indicates an expected decrease in drag coefficient for a given Reynolds number. The Reynolds number of a particle with diameter d is defined as

$$Re = \rho_a V_t d / \mu \qquad (3)$$

where μ is the dynamic viscosity of air. Substituting (2) and (3)

into (1) and letting $A_c = \pi d^2/4$, we obtain a quadratic in V_t which is given by

$$C_1 V_t^2 + \frac{C_2 \mu V_t}{\rho_a d} - \frac{4\rho_p dg}{3\rho_a} = 0 \qquad (3a)$$

Solving (3a) for the non-negative root of V_t we have

$$V_t = \frac{-C_2\mu + \sqrt{(C_2\mu)^2 + \frac{16}{3}(\rho_p \rho_a g C_1 d^3)}}{2\rho_a C_1 d} \qquad (4)$$

Equation (3a) can be rewritten as

$$C_1 V_t^2 + \frac{C_2 V_t^2}{Re} - \frac{4\rho_p dg}{3\rho_a} = 0$$

which indicates that for large values of Re, (i.e., large particles), the first term in V_t^2 will dominate the equation and V_t can be approximated by

$$V_t = \sqrt{4\rho_p dg/3C_1\rho_a}, \quad d \gtrsim 0.1 \text{ cm}$$

Similarly, for small values of Re, (i.e., small particles), the second V_t^2 term will dominate the equation and V_t will be approximated by

$$V_t = 4\rho_p d^2 g/3C_2\mu, \quad d \lesssim 0.01 \text{ cm}$$

From this equation we note that, for small particles, the density of air through which they are falling has no direct effect on the particles fall velocity.

From the meteorological data obtained during Phase 1 of the MISERS BLUFF II Cloud Sampling Program (see Ref 1), the air density ρ_a for both events as a function of altitude at the test site is given approximately by

$$\rho_a \ (g/cm^3) = 1.128 \times 10^{-3} \exp(-0.02657Z)$$

where Z is the altitude in kft MSL. The dynamic viscosity of air is given approximately by

$$\mu_a \ (g/cm \cdot sec) = (178.7-Z)\times 10^{-6}$$

where, again, z is the altitude in kft MSL.

For the terminal fall velocity calculations performed in connection with the T+10 minute and T+20 minute cloud reconstructions, an average altitude of 5 kft was chosen as being a "representative" altitude at which to compute particle fall velocities. The maximum errors induced by this assumption over the altitude range of interest are typically $\lesssim 10\%$ for the larger particles ($\gtrsim 1$ mm) and much less for the smaller particles ($\lesssim 500$ μm). For the calculations used in the fallout data analysis, the "representative" altitude chosen was 2 kft which, over the range of cloud stem heights, induced much smaller errors.

Another constant used in the terminal fall velocity calculations was:

$$g = 981 \ cm/sec$$

Substituting the constants into (4) we have, for "rough" spherical particles,

$$V_t \ (cm/sec) = \frac{-36\mu_a + \sqrt{1290\mu_a^2 + 3136\rho_p\rho_a d^3}}{1.2\rho_a d} \qquad (5)$$

where d is in cm. All calculations in this report assumed a value of 2.3 g/cm^3 for ρ_p.

D-2 CIRCULAR DISCS

Much of the information presented concerning the fall velocities of circular discs has been extracted from Reference 3. Solving (1) for C_D and multiplying by the square of (3) we obtain

$$C_D(Re)^2 = \frac{2md^2g\rho_a}{A_c\mu^2} = \chi \qquad (6)$$

χ is defined as the Best number (after a person who did much work in this area of physics) and note that it depends only on the particle and its position in the atmosphere - not on speed and drag. For a circular disc falling in a horizontal attitude,

$$m = \rho_p \pi d^2 h/4 \text{ and } A_c = \pi d^2/4 \qquad (7)$$

where h is the thickness of the disc, and hence,

$$\chi = 2\rho_p h d^2 \rho_a g / \mu^2 \qquad (8)$$

Using the same constants as used for the spherical particles, and defining the aspect ratio r of a circular disc as being the ratio of its diameter to its thickness, we obtain

$$\chi = (4.51\text{x}10^3 \rho_a / \mu^2)(d^3/r) \qquad (9)$$

For particles of various shapes, χ and C_D have been experimentally determined, and hence, from (6), the Reynolds number can be determined as a function of the Best number. Over the limited range of Best numbers, $20 \leq \chi \leq 2000$ and drag coefficients $2 \leq C_D \leq 200$, the Reynolds number for a circular disc can be approximated by

$$Re = 0.1 \chi^{0.786} \qquad (10)$$

Substituting (9) into (10) we obtain from (3)

$$V_t \text{ (cm/sec)} = 74.5 \left(\frac{\mu}{\rho_a d}\right)\left[\left(\frac{\rho_a}{\mu^2}\right)\left(\frac{d^3}{r}\right)\right]^{0.786} \qquad (11)$$

which approximates the terminal fall velocity of a circular disc.

Terminal fall velocities for "rough" spheres and circular discs with several aspect ratios have been calculated at an altitude of 5 kft MSL and are presented in Figure D-1. As would be expected, the circular discs fall significantly slower than do the "rough" spheroids with the same diameter and this difference increases with increasing aspect ratios of the circular discs. (In actuality, the curves depicting the fall velocities for circular discs are slightly curved, but due to the Reynolds number being approximated by (10), they appear as straight lines over the range of particle diameters that the approximation is valid.)

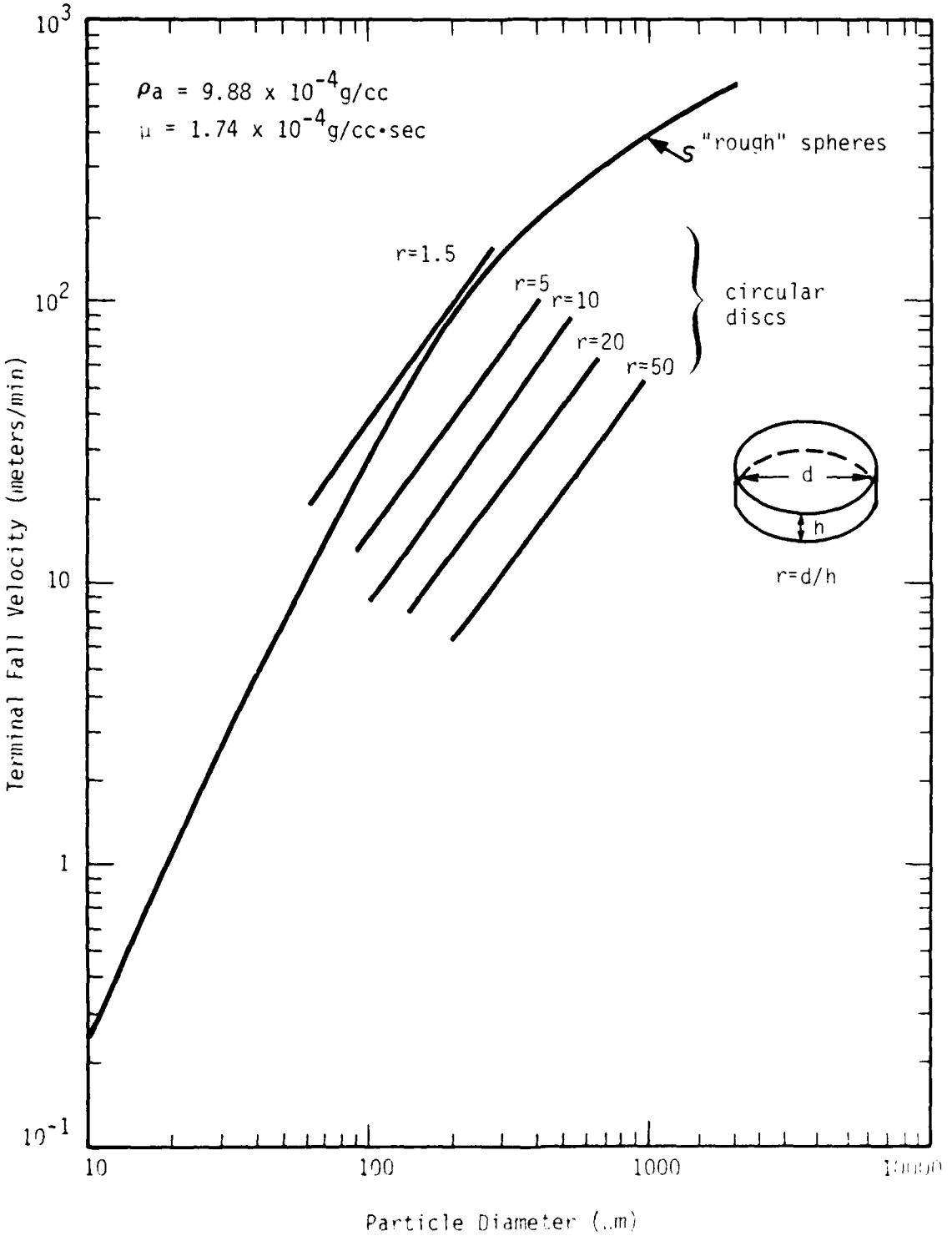

Figure D.1. Terminal Fall Velocities of Various Shaped Dust Particles as a Function of Particle Diameter

DISTRIBUTION LIST

DEPARTMENT OF DEFENSE

Assistant to the Secretary of Defense
Atomic Energy
ATTN: Executive Assistant

Defense Advanced Rsch. Proj. Agency
ATTN: TIO

Defense Communications Agency
ATTN: CCTC

Defense Intelligence Agency
ATTN: DT-2
ATTN: DB-4D
ATTN: DT-1C

Defense Nuclear Agency
ATTN: STSP
ATTN: SPAS
ATTN: SPSS
ATTN: SPTD
4 cy ATTN: TITL

Defense Technical Information Center
12 cy ATTN: DD

Field Command
Defense Nuclear Agency
ATTN: FCTMOF
ATTN: FCTMD
ATTN: FCTMOT
ATTN: FCPR

Field Command
Defense Nuclear Agency
Livermore Division
ATTN: FCPRL

Joint Chiefs of Staff
ATTN: J-5, Nuclear Division
ATTN: SAGA/SSD
ATTN: J-5, Force Planning & Program Div.
ATTN: SAGA/SFD

Joint Strat. Tgt. Planning Staff
ATTN: JLTW-2
ATTN: JPTM
ATTN: JLA

NATO School (SHAPE)
ATTN: U.S. Documents Officer

Undersecretary of Defense for Rsch. & Engrg.
ATTN: Engineering Technology, J. Persh
ATTN: Strategic & Space Systems (OS)

DEPARTMENT OF THE ARMY

BMD Advanced Technology Center
Department of the Army
ATTN: ATC-T, M. Capps

BMD Systems Command
Department of the Army
ATTN: BMDSC-H, N. Hurst

DEPARTMENT OF THE ARMY (Continued)

Deputy Chief of Staff for Ops. & Plans
Department of the Army
ATTN: DAMO-NCZ

Deputy Chief of Staff for Rsch., Dev., & Acq.
Department of the Army
ATTN: DAMA-CSS-N

Harry Diamond Laboratories
Department of the Army
ATTN: DELHD-N-TF
ATTN: DELHD-N-P, J. Gwaltney

U.S. Army Ballistic Research Labs
ATTN: DRDAR-BLT, P. Vitali
ATTN: DRDAR-BLE, J. Keefer
ATTN: DRDAR-BL, R. Eichelberger
ATTN: DRDAR-BLV, W. Schuman, Jr.
ATTN: DRDAR-BLT, J. Frasier
ATTN: DRDAR-BLV

U.S. Army Materiel Dev. & Readiness Command
ATTN: DRCDE-D, L. Flynn

U.S. Army Missile Command
ATTN: DRDMI-XS
ATTN: DRSMI-RKP, W. Thomas
ATTN: DRDMI-TRR, B. Gibson

U.S. Army Nuclear & Chemical Agency
ATTN: Library

U.S. Army TRADOC Systems Analysis Activity
ATTN: ATAA-TDC, R. Benson

U.S. Army Material & Mechanics Rsch. Ctr.
ATTN: DRXMR-HH, J. Dignam

DEPARTMENT OF THE NAVY

Naval Research Laboratory
ATTN: Code 6770, G. Cooperstein
ATTN: Code 2627
ATTN: Code 7908, A. Williams

Naval Sea Systems Command
ATTN: SEA-0352, M. Kinna

Naval Surface Weapons Center
ATTN: Code R15, J. Petes
ATTN: Code F31
ATTN: Code F06, C. Lyons

Naval Weapons Evaluation Facility
ATTN: P. Hughes
ATTN: L. Oliver

Office of Naval Research
ATTN: Code 465

Office of the Chief of Naval Operations
ATTN: OP 604C14, R. Blaise
ATTN: OP 65
ATTN: OP 604C3, F. Frasca

DEPARTMENT OF THE NAVY (Continued)

Strategic Systems Project Office
Department of the Navy
ATTN: NSP-272
ATTN: F. Wimberly

DEPARTMENT OF THE AIR FORCE

Aeronautical Systems Division
Air Force Systems Command
2 cy ATTN: ASD/ENFTV, D. Ward

Air Force Flight Dynamics Laboratory
ATTN: FXG

Air Force Geophysics Laboratory
ATTN: LY, C. Touart
ATTN: A. Barnes

Air Force Materials Laboratory
ATTN: MBC, D. Schmidt
ATTN: MBE, G. Schmitt
ATTN: LLM, T. Nicholas

Air Force Rocket Propulsion Laboratory
ATTN: LKCP, G. Beale

Air Force Systems Command
ATTN: SOSS
ATTN: XRTO

Air Force Weapons Laboratory
Air Force Systems Command
ATTN: DYS
ATTN: DYV
ATTN: DYV, A. Sharp
ATTN: DYT
ATTN: SUL
ATTN: HO, W. Minge
ATTN: NTESIS, K. Filippelli
ATTN: NTES, G. Ganong
2 cy ATTN: NTO

Arnold Engineering Development Center
Air Force Systems Command
ATTN: Library Documents

Ballistic Missile Office
Air Force Systems Command
ATTN: MNNR
2 cy ATTN: MNNXH, Capt Blankinship

Deputy Chief of Staff
Operations, Plans and Readiness
Department of the Air Force
ATTN: AFXOOSS

Deputy Chief of Staff
Research, Development, & Acq.
Department of the Air Force
ATTN: AFRD
ATTN: AFRDQSM

Foreign Technology Division
Air Force Systems Command
ATTN: TQTD
ATTN: SDBS, J. Pumphrey
ATTN: SDBG

DEPARTMENT OF THE AIR FORCE (Continued)

Headquarters Space Division
Air Force Systems Command
ATTN: DYS

Headquarters Space Division
Air Force Systems Command
ATTN: RSS
ATTN: RST
ATTN: RSSE

Headquarters Space Division
Air Force Systems Command
ATTN: AFML, G. Kirshner

Strategic Air Command
Department of the Air Force
ATTN: DOXT
ATTN: XPFS
ATTN: XPQM
ATTN: XOBM

DEPARTMENT OF ENERGY

Department of Energy
ATTN: OMA/RD&T

DEPARTMENT OF ENERGY CONTRACTORS

Lawrence Livermore National Laboratory
ATTN: L-125, J. Keller
ATTN: L-92, C. Taylor
ATTN: L-262, J. Knox
ATTN: L-24, G. Staihle

Los Alamos National Scientific Laboratory
ATTN: J. Taylor
ATTN: J. McQueen
ATTN: R. Thurston
ATTN: R. Skaggs
ATTN: R. Dingus

DEPARTMENT OF DEFENSE CONTRACTORS

Acurex Corp.
ATTN: C. Nardo
ATTN: R. Rindal
ATTN: C. Wolf

Aeroject Solid Propulsion Co.
ATTN: R. Steele

Aerospace Corp.
ATTN: W. Barry
ATTN: R. Crolius
ATTN: H. Blaes
ATTN: J. McClelland

Analytic Services, Inc.
ATTN: J. Selig

APTEK
ATTN: T. Meagher

AVCO Research & Systems Group
ATTN: J. Gilmore
ATTN: Document Control
ATTN: J. Stevens
ATTN: W. Broding

DEPARTMENT OF DEFENSE CONTRACTORS (Continued)

Battelle Memorial Institute
ATTN: E. Unger
ATTN: M. Vanderlind

Boeing Co.
ATTN: B. Lempriere
ATTN: R. Holmes

California Research & Technology, Inc.
ATTN: K. Kreyenhagen
ATTN: M. Rosenblatt

Calspan Corp.
ATTN: M. Holden

Effects Technology, Inc.
ATTN: R. Wengler
ATTN: R. Parisse
ATTN: J. Carlyle

General Electric Co.
ATTN: G. Harrison
ATTN: C. Anderson
ATTN: D. Edelman

General Electric Co.
ATTN: P. Cline

General Electric Company—TEMPO
ATTN: DASIAC

Hercules, Inc.
ATTN: P. McAllister

Institute for Defense Analyses
ATTN: J. Bengston
ATTN: Classified Library

Kaman Sciences Corp.
ATTN: J. Keith
ATTN: D. Sachs
ATTN: F. Shelton
ATTN: J. Hoffman

Lockheed Missiles & Space Co., Inc.
ATTN: F. Borgardt

Lockheed Missiles & Space Co., Inc.
ATTN: R. Walz

Martin Marietta Corp.
ATTN: J. Potts
ATTN: G. Aiello
ATTN: L. Kinnaird

Martin Marietta Corp
ATTN: E. Strauss

McDonnell Douglas Corp.
ATTN: H. Berkowitz
ATTN: L. Cohen
ATTN: E. Fitzgerald

National Academy of Sciences
ATTN: D. Groves

Pacific-Sierra Research Corp.
ATTN: G. Lang
ATTN: H. Brode

DEPARTMENT OF DEFENSE CONTRACTORS (Continued)

Physics International Co.
ATTN: J. Shea
ATTN: D. Guthrie

Prototype Development Associates, Inc.
ATTN: J. McDonald
ATTN: J. Dunn

R & D Associates
ATTN: F. Field
ATTN: P. Rausch
ATTN: W. Graham, Jr.
ATTN: C. MacDonald
ATTN: J. Carpenter

Rand Corp.
ATTN: J. Mate

Rockwell International Corp.
ATTN: G. Perrone

Science Applications, Inc.
ATTN: D. Hove
ATTN: J. Warner
ATTN: G. Ray

Science Applications, Inc.
ATTN: G. Burghart

Science Applications, Inc.
ATTN: W. Layson
3 cy ATTN: J. Cockayne
5 cy ATTN: C. Thomas

Science Applications, Inc.
ATTN: A. Martellucci

SRI International
ATTN: D. Curran
ATTN: G. Abrahamson
ATTN: H. Lindberg
ATTN: P. Dolan

System Planning Corp.
ATTN: F. Adelman

Systems, Science & Software, Inc.
ATTN: R. Duff
ATTN: G. Gurtman

TRW Defense & Space Sys. Group
ATTN: D. Baer
ATTN: T. Williams
ATTN: W. Wood
ATTN: P. Brandt
ATTN: G. Arenguren
ATTN: T. Mazzola
ATTN: M. Seizew
ATTN: A. Zimmerman
ATTN: R. Bacharach

TRW Defense & Space Sys. Group
ATTN: V. Blankenship
ATTN: W. Polich
ATTN: L. Berger

Thiokol Corp
ATTN: W. Shoun

DEPARTMENT OF DEFENSE CONTRACTORS (Continued)

Terra Tek, Inc.
ATTN: S. Green

DEPARTMENT OF DEFENSE CONTRACTORS (Continued)

Teledyne Brown Engineering
ATTN: R. Snow


DATE
LMED
80